Hygrothermal conditioning and fatigue behaviour of high performance composites.

Jones, Christopher J.

Award date:
1985

Awarding institution:
University of Bath

HYGROTHERMAL CONDITIONING AND FATIGUE BEHAVIOUR OF HIGH PERFORMANCE COMPOSITES.

submitted by

Christopher J Jones

for the degree of Ph.D

of the University of Bath

C. J. Jones

February 1985 C J JONES

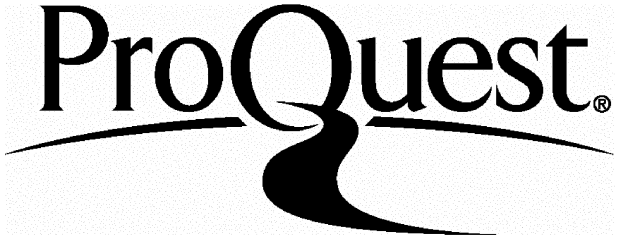

ABSTRACT

The static and fatigue properties of advanced epoxy-based composites reinforced with carbon, glass or aromatic polyamide (Kevlar-49) fibres have been measured for a range of different loading and environmental conditions. Cross-plied laminates were tested in tension in the 0/90 and ±45° orientations and also under flexural loading. The laminates were similar, except for the type of fibre. The effects of environmental exposure were assessed by preconditioning test specimens to equilibrium by either drying at 60°C, storage at 65%RH at ambient temperature or boiling in water.

Moisture absorption was through the resin alone for CFRP and GRP and by additional absorption by the fibres for KFRP. Fatigue testing revealed that the tensile performance in the 0/90 orientation is strongly dependent on the level of cyclic strain. 0/90 CFRP has excellent fatigue and environmental resistance but GRP exhibits a steep fatigue curve and the static and low cycle fatigue strengths are both reduced by boiling. The fatigue strength of 0/90 KFRP is reduced by drying, more so than by boiling, and in all conditions the stress/log-life curves are characterised by a downward curvature or 'knee'. Tensile preloads do not significantly affect the residual fatigue properties or the equilibrium levels of moisture uptake, although extensive damage involving cracking in both longitudinal and transverse plies may lead to increased absorption rates.

A tendency for Kevlar fibres to split or 'defibrillate' plays an important role in most failures of KFRP. It limits the shear strength and causes flexural failures to occur at the compression surface at low stress levels. 0/90 CFRP also fails at the compression surface in flexure but GRP fails at the tensile surface, the environmental fatigue performance resembling that under axial tensile loading. The ±45° tensile and low cycle fatigue strengths are sensitive to the effects of conditioning, all laminates exhibiting optimum performance after conditioning at 65%RH, although generally these effects become insignificant at long lives.

ACKNOWLEDGEMENTS

The author would like to thank the many people who helped in this research programme.

In particular,
T Adam, Professor B Harris and H Reiter for their continued guidance and encouragement throughout the period of the research.

Also,
the technicians of the School of Materials Science for their technical support, especially P Dicken for his assistance in the cutting of the laminate sheets.

R F Dickson for his enthusiasm and invaluable assistance.

Drs P Curtis, G Dorey and J Sturgeon of the Royal Aircraft Establishment, Farnborough for their helpful advice and discussions.

The work was sponsored by the Procurement Executive of the Ministry of Defence under Agreement Number 2112/034 XR/MAT. The electron optics facilities were financed by the Science and Engineering Research Council.

CONTENTS

CHAPTER 1

INTRODUCTION

1.1 INTRODUCTION

Advanced composites have gained recognition as viable alternatives to steels and alloys in structural and engineering applications where high strength and modulus to weight ratios, impact resistance and long term durability are important. They usually consist of high volume fractions of continuous glass, carbon and/or Kevlar-49 (aramid) fibres embedded in high quality polymer matrices, often epoxies. Despite considerable research during the last 10-20 years, funded mainly by the aerospace and defence industries where the most immediate needs for such materials exist, the general level of understanding regarding many aspects of their use and performance still falls short of that for metals. This must be improved if composites are to become more widely accepted by both designers and engineers. Of particular interest and concern for aerospace use is the detailed performance under fatigue loadings and hostile environments and this forms the subject of the investigations reported here.

1.2 GENERAL USE OF COMPOSITES

Although still not common in everyday use, high performance composites are gaining widespread and increasing importance in applications where their advantages over conventional engineering materials outweigh the relatively high initial material costs (which, for example, may be typically 2-5 times greater than those of comparable metals on a strength/weight basis (1)). These applications include aircraft, missiles, spacecraft (e.g. the space shuttle orbiter), sports goods and motor racing (2,3,4).

In particular, composites are used widely in both military and commercial aircraft, including control surfaces and door and cowl assemblies. In recent years the trend has been for each new generation of aircraft to make increasing use of composites and manufacturers have predicted that in the foreseeable future composites will comprise over 50% of aircraft structural components, bringing savings of 10 to 20% in weight and reduction in cost (3,4).

Of the actual and potential advantages of composites, it is their high strength and stiffness (both in ultimate terms and perhaps more importantly on the basis of material weight) and the associated opportunity to tailor the structural properties in different directions that are the most important, making possible weight reductions that lead directly to improved fuel efficiency and higher payload capacity. For instance, it has been estimated that 1 kg weight reduction on a DC-10 airliner can save over 2900 litres of fuel per year (5). The airframe of the Lear Avia Lear Fan 2100 executive aircraft actually contains 70% by weight of carbon and Kevlar/epoxy, providing a weight saving of approximately 45% over a conventional aluminium structure and predicted savings in operating costs (if the plane ever goes into service) of the same order (2,3).

The material's anisotropy means that new design procedures must be adopted if composites are to reach their full potential. In comparison to metals this has often put composites at an

initial disadvantage.

Weight savings are not the only benefits to be gained from using composites however. They offer good impact resistance and are insensitive to electric or magnetic fields. Looking towards the future, composites offer potential savings in manufacturing (both fabrication and finishing) (2,3,5) and this, together with falling material costs makes them attractive to mass producers such as the automobile industry (2,6). Already General Motors are fitting glass/epoxy composite springs to some of their models in the United States (2).

Advanced composites are commonly produced in the form of laminate sheets consisting of bonded unidirectional plies, the numbers and orientations of which are determined by the loads predicted for the specific application.

1.3 PROBLEM OF ENVIRONMENTAL AND FATIGUE LOADINGS

A prime reason for using high performance composites is their reputed resistance to long term environmental and fatigue exposures. The possibility of failure as a consequence of repeated loadings has always been a major problem when designing aircraft, and since fatigue loadings are unavoidable in such applications, it is essential that the fatigue properties of both materials and structures are fully characterised. Also, depending on application, location, season and time of day, components in service are likely to experience a wide range of temperatures (from -40° to 70°C for helicopters and civil aircraft and up to 130°C for supersonic jet fighters) and relative humidities (from 0 to 100%)(7).

While moisture in the atmosphere can lead to corrosion of metal components, fibre reinforced plastics actually absorb moisture as well as being sensitive to temperature and solar radiation. Surface coatings cannot always be relied upon to give total protection and may themselves degrade.

Although there is now a considerable amount of information available concerning the separate effects of environment (particularly moisture) and fatigue loadings, as reviewed in Chapter 2, far less is known about the interaction between these two. Clearly, any effect of environment on the static strength will not necessarily reflect the sensitivity to fatigue loading. For example, composites can sustain considerable secondary damage without suffering a significant drop in strength. It is possible however that such damage could allow enhanced penetration by moisture and thus affect the subsequent fatigue life. Such effects are not easy to predict.

Unfortunately, fatigue performance is dependent on a large number of variables, in particular the loading conditions, the type and properties of the reinforcing fibres and the laminate geometry. Further, the environment is likely to affect each of the components-fibres, matrix and interface-differently. The problem lies not only in relating test data to real structures but also in the range of systems and testing techniques used to obtain such data. This has sometimes led to confusion and has certainly made general comparisons between composites difficult. For a systematic and comparative investigation of

environmental fatigue performance to be successful, it is clearly necessary for the number of variables to be kept as low as possible. Since there are certain advantages and disadvantages associated with each of the main types of reinforcing fibres in current use (Chapter 2) there is an obvious need for a clear understanding of the contribution made by the fibre type to the environmental fatigue properties in order that the optimum choice of fibre or fibres may be made for specific applications.

1.4 GENERAL OUTLINE AND OBJECTIVES OF THE RESEARCH

The basic objective of the work was to determine the effect of environmental conditioning, primarily the sensitivity to moisture content, on the fatigue properties of high performance composites (in this case laminates) representative of those used by and of interest to the aerospace industry. An important and perhaps unique aspect of the investigation was that the carbon, glass and Kevlar fibre reinforced polymer (CFRP, GRP and KFRP) laminates tested were nominally identical except for the type of fibre. This meant that direct and valid comparisons could be made between the laminates. For the same reason, details of the testing and conditioning procedures were kept similar and relatively simple.

Comparison of the results for the different laminates should help to give some insight into the damage mechanisms operating in each case. Clearly the differences in the three types of fibres mean that damage is not necessarily similar or dependent on moisture in the same way. However, the success or failure of existing models in accounting for the results should

give an indication of the general relevance or applicability of these models and also highlight any significant abnormalities in the fatigue behaviour for any of the laminates or conditions.

To keep the test programme within manageable bounds, fatigue testing was confined to the pure tension and the flexural modes (all the tests involved constant rather than variable amplitude cycling). Cross-plied laminates were chosen for the work. Thus by testing with the fibres either orthogonal or aligned at ±45° to the load direction, both fibre dominated and matrix-interface dominated properties could be measured under tensile loading. Characterisation of the ±45° performance was just as important as the 0/90 since in real structural applications secondary off-axis stresses (such as torsional and shear) are often unavoidable. Also, ±45° plies are usually present in quasi-isotropic laminates.

Flexural loading involves combinations of tensile, compressive and sometimes shear stresses and is commonly encountered in aerospace applications. The flexural fatigue testing arrangement was such that the specimens experienced only tensile and compressive stresses. Testing in this mode allowed direct comparison of the tensile and compressive fatigue strengths and the relative sensitivity of these to environment. In static bending, various loading geometries were used so that the shear mode and the effect of moisture on the shear strength could also be studied. The aim was to compare these results with the ±45° tensile data.

The technique chosen for the investigation of the effect of environment was to precondition specimens to known equilibrium moisture contents, sometimes using elevated temperatures to reduce the conditioning times, and to confine all testing to room temperature and the laboratory environment (taking steps to prevent significant moisture loss or gain during cycling). Thus the characterisation of the basic moisture absorption-desorption behaviour and the static mechanical properties (and the effect of environmental conditioning upon these) was necessary to establish a range of standardised equilibrium conditioning exposures and was an essential preliminary step before fatigue testing. It was also necessary to determine any sensitivity of the laminates to the rate of loading, so that valid comparisons between static and fatigue data could be made.

Static preloads were used to establish the effect of moisture on the build-up of secondary crack damage in each of the 0/90 laminates prior to failure. The possibility was investigated that such damage, which in practical situations might occur as a result of static or fatigue loading, affects the moisture absorption characteristics of the laminates and also the subsequent residual fatigue properties (both before and after environmental exposure).

CHAPTER 2

LITERATURE REVIEW :

COMPOSITES, ENVIRONMENTAL AND FATIGUE EFFECTS

2.1 COMPONENTS OF THE LAMINATES

2.1.1 Fibres

a) Glass

Glass fibres are the most long established and popular of the reinforcing fibres used for composites. This is because they are relatively cheap and easy to manufacture and with coupling agents applied to their surface form strong bonds with a wide variety of resin systems. The fibres are based on silica (SiO_2) and are made by drawing from the molten state at temperatures in excess of 750°C. They cool rapidly into an amorphous structure that consists of a 3-dimensional covalently bonded network of linked SiO_4 polyhedra. Normally various oxides are added to the melt in order to control the properties of the glass both before and after vitrification.

E-glass is the most widely used glass for composites. It is an alumino-boro-silicate glass and is favoured because it draws well and compared to many glasses it has good strength, stiffness and resistance to environmental degradation. The main constituents of E-glass are SiO_2 (approximately 54% by weight), Al_2O_3 (14.5%), CaO (17.5%), B_2O_3 (8%) and MgO (4.5%).

The strength of freshly drawn, undamaged fibres is around 3.5 GPa. However, glass fibres are brittle and in practice their strength and failure strain are much lower due to fine, random flaws on the surface caused by unavoidable abrasion during manufacture and handling and interaction with water vapour and dust particles,

Table 2.1. The fibres are usually sprayed with a protective size coating to help minimise such damage.

The main drawbacks of glass fibres in addition to a poor resistance to moisture are their high density and fairly low Young's modulus. This has led to the increasing use of the more recently developed, but also more expensive, carbon and Kevlar fibres. As shown in Table 2.1 these are stiffer, lighter and in practice stronger than glass fibres and they also show far superior resistance to degradation by water. The failure strains (ε_f) are lower for these fibres however and they also possess relatively poor transverse properties.

b) Carbon

Production of Courtaulds carbon fibres involves the conversion of polyacrylonitrile (PAN) precursor fibres into turbostratic graphite by means of a complicated series of high-temperature treatments, during which the fibres are kept under tension to provide alignment of the molecular chains along the fibre axis required for high strength and stiffness. The structure of turbostratic graphite is similar to that of graphite single crystals, except that there is no regular packing of the layer planes and the interlayer spacing is slightly increased (8,9).

In carbon fibres, the turbostratic graphite is in the form of small crystallites with their layer planes aligned roughly parallel to the fibre axis. The high modulus of the fibres derives from the strong covalent bonding of the hexagonal ring structure

of carbon atoms within the layer planes. However, the weak van der Waals forces between the layers means that the radial properties of the fibres are poor.

The mechanical properties of the fibre depend on the final heat treatment temperature. 1500°C is used for HT-S (Type II) fibres, since this is found to give the optimum tensile strength. Higher temperatures produce fibres with increased moduli but reduced strengths and this has been attributed to changes in the structure involving the formation of larger and better aligned crystallites (9,10,11). The fibre structure is inhomogeneous and far from perfect, containing voids and flaws, both at the surface and within the fibre volume. These act as stress raisers and limit the tensile strength.

c) Kevlar

Kevlar is the trade name given by Du Pont to their aromatic polyamide fibres. Specifically these are a highly crystalline and oriented form of poly p-phenyleneterephthalamide which has the chemical structure shown in Figure 2.1a (12,13). Kevlar-49, the high modulus version of the fibre, is the only organic reinforcing fibre to have gained wide acceptance for use in high performance composites. This has been achieved by virtue of its high specific tensile strength (which is greater than that of carbon fibres - Table 2.1) and modulus, allied to reasonable cost and environmental stability.

Kevlar fibres are produced from solution by an extrusion and spinning process that includes a stretching and drawing treatment to improve the tensile properties (9,12). Their high tensile strength and modulus derive from alignment of the covalently bonded polymer chains with the fibre axis and the fact that the aromatic ring structure causes these chains to be rigid and in an extended form (12, 13). The polymer chains are held together by hydrogen bonding in rigid planar sheets (Figure 2.1b). It is believed that these are arranged radially within the fibre and are wrinkled or pleated along their length (Figure 2.1c) (14). The bonding between the sheets is weak and consequently the fibres have poor resistance to transverse, shear and compression loadings (12,15,16). In flexure the fibres do not fracture in a brittle manner like carbon and glass fibres but deform plastically on the compression side by the formation of characteristic deformation or kink bands (Figures 2.1d-e).

Kevlar fibres are known to contain an extensive internal network of defects (14,17). These include microcracks and voids, mainly oriented at small angles to the fibre axis (17), and clusters of molecule end groups which form planes of weakness transverse to the fibre direction (18). Such flaws limit the tensile strength of the fibres. Some ductility and necking is shown in axial tensile tests before failure (9) and the fracture surfaces are characterised by longitudinal fragmentation and splintering into subfilaments (fibrillation) (12). There is evidence that Kevlar-49 fibres have a duplex structure, with the core of the fibre exhibiting far greater crystallinity than the skin (18).

The weak bonding in the transverse direction means that splitting and skin peeling occur quite easily (Figure 2.1e-h) leading to low abrasion resistance (16) and significant tensile weakening (18). Unlike the inorganic fibres, Kevlar suffers genuine, if slight degradation during cyclic tensile loading (19,20,21). Fibre splitting appears to be the primary mode of damage.

Typical properties of the fibres are summarised in Table 2.1. All the fibres actually show significant variability in strength. In each case the stress-strain curves are approximately linear.

2.1.2 Interface

A strong interface depends primarily on the formation of chemical bonds, although physical or mechanical bonding may also be important.

a) Glass

Coupling agents are usually applied to glass fibres to improve the bonding between the fibres and the resin and also to help protect the fibre surface and interfacial bond from attack by moisture. Organic silanes are commonly used although the detailed structure of these coatings and the nature of the bonding is not fully understood and in practice is very complex (22, 23).

One end of the silane molecule is organic and may form covalent bonds with the resin during the laminate cure (9,23). At the other end, the bonding to the glass surface is believed to involve both strong covalent oxane bonds (Si-O-M where M represents Si, Al, Fe) and hydrogen bonding between hydroxyl groups of the silonal

(Si-OH) and the glass surface (M-OH)(22,23). Siloxane bonds (Si-O-Si) formed between adjacent silanol molecules give the coating a coherent structure.

b) Carbon

Carbon fibres are surface treated to obtain good bonding with resin matrices. This normally involves an oxidation treatment, commonly immersion in nitric acid, to produce active functional groups such as carboxylic ($C O_2H$), hydroxyl (C-OH) and carbonyl (C=O) groups on the surface of the fibre (10,24,25). The strong interfacial bonding results from the formation of chemical bonds (primarily hydrogen bonds) between these groups and polar groups in the resin (24). Light acid etching may lead to increased microroughness of the fibre surface, with a corresponding increase in the sites available for chemical bonding (9). Secondary or van der Waals forces may also contribute to the bonding as a result of close contact between the fibre and resin (26).

c) Kevlar

In contrast to the other two materials, little information is available regarding the interfacial bonding between Kevlar fibres and epoxy resins. Although the interface is relatively weak, some adhesion is known to occur (12, 18,27,28). This presumably involves van der Waals forces and possibly hydrogen bonding. It is of note that a high interfacial bond strength is not necessarily beneficial for KFRP, owing to the low transverse strength of Kevlar fibres (18,27).

2.1.3 Epoxy Resin Matrix

The role of the matrix resin is mainly to transfer loads to and from the fibres and to hold the fibres together in a solid rather than as just a loose bundle. The matrix also helps to protect the fibres from any damaging effects of the environment.

Epoxies are the most widely used thermosetting resins for advanced composites. They have good strength and stiffness properties below their curing temperature and generally show good resistance to environmental and chemical degradation. A major advantage of epoxy resins is their ease of processing. They form good bonds with most fibres, exhibit low shrinkage during cure and can be made into flexible prepregs with a long shelf life. Disadvantages include their cost, high viscosity before cure and a requirement for long cure cycles.

The resin used in this work, Code 69, is a proprietary epoxy resin system produced by Fothergill and Harvey Ltd for use as a high performance matrix material for advanced composites in the aerospace industry. In common with most other 175°C cure epoxies (such as Fiberite 934 and Narmco 5208) the main constituent of Code 69 is tetraglycidyl 4,4' diaminodiphenyl methane (TGDDM) epoxy, cured with diaminodiphenylsulphone (DDS) hardener. The structures of the unreacted TGDDM epoxide and DDS amine monomers are illustrated in Figure 2.2. In addition to small amounts of other materials (usually added to improve the handling characteristics of the prepreg) a boron trifluoride-monoethyl amine complex BF_3 MEA

is used as an accelerator since the cure tends to be sluggish even at quite high temperatures. This 'catalyst' is not active at room temperature (29). TGDDM-DDS epoxies form rigid, highly cross-linked networks and the cross-link density tends to increase when BF_3 catalysts are used (30).

The actual structure of the resin depends on the chemical composition and cure conditions. In practice it tends not to be homogeneous but to consist of highly cross-linked regions embedded in a less highly cross-linked matrix (31). As well as the covalent bond network formed during cure, polar groups on adjacent molecular segments within the structure may also bind together via hydrogen bonding. In normal use, epoxy resins are in a non-crystalline glassy state, well below their apparent glass transition temperature range (Tg) which occurs at about 200 to 230°C for typical BF_3 catalysed TGDDM-DDS resin systems (19,32,33).

Typical properties of Code 69 resin are given in Table 2.1. The tensile stress-strain curve is non-linear, but at room temperature there is only a small reduction in modulus as the strain is increased and the resin behaves in an essentially elastic manner (34). Non-linearity and viscoelastic behaviour become more marked at higher temperatures and over long periods of time, although the highly cross-linked structure of Code 69 means that it is less sensitive than many other epoxy resins (35).

Tensile tests on pure resin specimens show Code 69 to be a particularly brittle resin system (34). Plastic yielding is

suppressed in tensile loading since failure tends to initiate prematurely at flaws in the resin or on the specimen surface(9). It is therefore probable that the strength and failure strain values for the resin given in Table 2.1 are inferior to the actual values in a composite where for high fibre volume fractions the resin exists in the form of very thin films or fillets for which the stress state, surface conditions and resin quality will not be the same as the bulk resin(34,35).

Epoxy resins are degraded under cyclic loading (36,37). As for metals this involves the initiation and propagation of fatigue cracks (38) and is mainly a problem where viscoelastic flow occurs that is not recovered upon unloading (9,37). Crack initiation is thus most likely in regions of high stress concentration, at internal flaws or voids for instance, or in composites, at debonds or broken fibres or where the fibre packing is high.

The ratios of the important constituents of Code 69 are roughly as follows (35)

TGDDM (Ciba-Geigy MY720)	100 parts
DDS (Ciba-Geigy Eporal)	30 parts
BF_3MEA (BF_3 400)	1 part

TGDDM is a liquid at room temperature while DDS is a crystalline powder which melts at around 162°C.

2.2 MOISTURE ABSORPTION

Epoxy resins are hygroscopic and absorb moisture directly from humid environments. Typically the moisture content of resins similar to Code 69 may reach a maximum of about 6% by weight for water immersion (32, 39). In contrast, inorganic fibres such as carbon and glass are impervious to moisture and consequently the resin dominates the absorption characteristics of composites reinforced with these fibres. Kelvar fibres do contribute to the absorption process however, absorbing up to 5-6% water themselves (12,40, 41,42,43).

2.2.1 Epoxy resins

The detailed mechanisms of absorption have not yet been fully established. Generally the water, in the form of free molecules or groups of molecules, forms hydrogen bonds with polar groups in the resin. It is believed that the primary sorption sites within TGDDM-DDS epoxies are the hydroxyl, sulphonyl and primary and secondary amine groups (30). By bridging polar groups on adjacent molecular segments the water molecules may effectively be regarded as part of the glassy structure (44). In addition to these strongly bound molecules, it has been suggested that water may also exist as weakly or unbound molecules in the free volume of the polymer.

Disruption of the interchain hydrogen bonding by the water causes the resin to swell (47,48). This is associated with a progressive but reversible resin plasticisation (softening) and lowering of the glass transition temperature, Tg. Most recent results indicate

that 100% RH saturation reduces Tg by approximately 50 to 60°C for highly cross-linked resins such as Code 69 (19,33,48) and that reductions in strength and modulus due to moisture tend to be small at room temperature but become more important as the temperature is raised (31,49).

2.2.2 Equilibrium moisture contents

The equilibrium moisture content of a composite will depend on both the relative humidity (defined as the partial vapour pressure of water relative to the saturated pressure of pure water) of the environment to which it is exposed and the chemistry, structure and state of cure of the resin. Moisture content is usually found to be approximately proportional to the relative humidity (50-54), although there is sometimes a positive deviation from this behaviour, especially at high humidities (39,53,55). Absorption by fibres such as Kevlar and the accumulation of water molecules at debonded fibre/matrix interfaces, voids or cracks may, where applicable, also contribute to the moisture uptake. For most purposes moisture content can be regarded as being independent of temperature, although in some cases there is evidence of very small increases in moisture content over broad ranges of increased temperature (53).

2.2.3 Diffusion

Since composite materials are not isotropic and are inherently inhomogeneous, the details of their moisture uptake are not necessarily the same as those of the resin phase alone. The absorption behaviour is best understood by first considering the effect of this on diffusion in the resin matrix, and secondly,

by looking at the applicability of simple diffusion theory to epoxy resins and their composites in general. For a well made, undamaged laminate containing inorganic fibres, absorption is predominantly by diffusion through the resin matrix.

a) Non-isotropic effects in composites

Composites are not isotropic materials and consequently, they cannot be described by single diffusion coefficients. Since diffusion of moisture occurs only in the resin phase, the diffusivity is less than that of the resin alone and varies for different directions in the composite depending on the matrix volume fraction and the orientation of the fibres to the direction in question. Diffusion is greatest in the direction parallel to the fibres, where it is proportional to the resin volume fraction, and is least perpendicular to the fibres, where for very high volume fractions (in which all the fibres are touching) it is reduced to zero. For most moisture uptake coupons, there is significant moisture absorption at the specimen edges as well as at the top and bottom surfaces. Shen and Springer (56) have developed expressions which, when given the lay-up, volume fraction and dimensions of a composite specimen, allow for the three-dimensional diffusion resulting from edge absorption and are quite successful in predicting the overall 'apparent' diffusivity in terms of the diffusion coefficient of the matrix resin. This will be discussed further in Chapter 4.

b) Ficks Law and Non-Fickian diffusion

Fick's Second Law of Diffusion has generally been found adequate to describe the absorption behaviour of TGDDM-DDS epoxy resins. The rate of absorption for the one-dimensional case (diffusion through the thickness of a semi-infinite plate) is as follows:-

$$\frac{\partial c}{\partial t} = D_x \frac{\partial^2 c}{\partial x^2} \qquad (2.1)$$

where c is the moisture concentration at a distance x from the laminate surface after a time t. D_x is the diffusion coefficient in the x direction, normal to the surface, and is assumed constant in this form of the equation. It is assumed that the moisture concentration at the surface does not vary and remains equal to the equilibrium moisture content for the environment throughout the exposure.

The actual rate of moisture absorption depends on the value of the diffusion coefficient. It tends to be very low at ambient temperatures and for thick laminates the equilibrium moisture content may not be reached during a components lifetime. Under conditions of varying atmospheric humidity, the overall moisture content will reflect the average state of the environment over a considerable time period, with only the material close to the surface showing any short term variations. The diffusivity rises with increasing temperature however, following a simple Arrhenius relationship (which should be the only dependence shown by D_x)(44,47,50,52,53,55,57,58).

Solutions of Fick's Law are available (with the appropriate boundary conditions) that can model the distribution of moisture in epoxy resins and their composites by predicting the moisture profiles as a function of time in a specific environment (59,60). For a semi-infinite flat plate of thickness d absorbing moisture through both surfaces the total amount of absorbed moisture M_t at any time t during the exposure can be determined by integrating such solutions over the material thickness. The most widely used equation for predicting the moisture uptake based on simple Fickian diffusion is given below

$$\frac{M_t}{M_m} = \frac{4}{\sqrt{\pi}} \left(\frac{Dt}{d^2}\right)^{\frac{1}{2}} \qquad (2.2)$$

where M_m is the maximum, equilibrium moisture uptake.

The right hand side of Equation 2.2 is the first term in a series which converges rapidly at short times. This relationship is suitable up to around 0.6 M_m, above which the error introduced by using only the first term becomes large. Up until then interaction between moisture absorbed at the two opposing surfaces is not significant (61,62). At high moisture uptakes, above 0.5 M_m, the rate of absorption decreases and the moisture level approaches the equilibrium uptake asymptotically (Figure 2.3). Equation 2.2 is very useful, since it allows the apparent diffusion coefficient to be calculated simply from the initial linear slope of the weight gain against $\sqrt{t}$ plot, provided that M_m is known.

For simple Fickian diffusion Equation 2.2 should apply for absorption and desorption and these should both proceed at the same rate and be independent of previous environmental conditioning. The time to reach equilibrium moisture content should be insensitive to all aspects of the environment, except temperature, and there should be no net changes upon re-equilibrating a conditioned specimen to its original moisture content.

In practice, few composites behave in a truly Fickian manner(44,46, 52,63,64,65) although systems based on high cross-link density resins such as Code-69 appear to be less susceptible to anomalous behaviour than most. Thus Fick's Law provides a convenient, if only approximate description of the absorption behaviour, with Equation 2.2 yielding a pseudo or 'apparent' diffusion coefficient which can be used as a means of quantifying the initial rate of moisture uptake for a particular specimen in a particular environment (44,46,51,52,58,63,64,65).

Deviations from simple Fickian diffusion may take several forms and depend strongly on the specific nature of the composite and environment. Normally they are more likely to occur or are more severe for higher exposure temperatures and humidities(65) and are also common in specimens possessing an environmental 'history' (32,44,58,63,64,66). Anomalous behaviour may be attributed to a number of phenomena associated either with the resin itself or with the composite as a whole. It may result simply from concentration or swelling effects in the resin (9,58,61),

or may reflect irreversible damage in the form of debonding (32), matrix microcracking (64,67),chemical degradation (31,66) or loss of low molecular weight constituents from the resin (42,66,68). The presence of stress, whether applied externally or resulting from transient internal thermal or moisture gradients (64) or constraints imposed by the fibres (58), can influence all of these.

2.3 EFFECT OF MOISTURE ON FIBRES AND INTERFACES

The effect of moisture on the epoxy matrix has already been discussed. However, composite performance is also dependent on the response of the fibres and interface.

2.3.1 Fibres

a) Carbon

Carbon fibres are chemically inert in the operating range of epoxy resins (up to 170°C). They are resistant to attack by water and exhibit excellent stress-rupture properties (8,69).

b) Glass

Glass fibres are susceptible to corrosion by moisture which irreversibly breaks down the surface of the fibres. This has been associated with the presence of hygroscopic alkali metal oxides, in particular Na_2O, in the glass (70). These do not form part of the covalent glass network but are held interstitially by ionic bonding to adjacent oxygen atoms and are able to diffuse to the fibre surface. The basic corrosion mechanism, in both liquid water and water vapour, involves the exchange of these metal ions in the glass

with hydrogen ions (70).

$$[\equiv Si - O(Na) + H_2O] \longrightarrow [\equiv Si\text{-}OH] + Na^+ + OH^- \qquad (2.3)$$

The volume changes involved in this reaction produce tensile stresses in the fibre surfaces which weaken the fibres since they are independent of any applied external stress (71). Thus, even in the unloaded state, the attack on the glass may be regarded as stress corrosion. Break-up of the glass network involves the subsequent rupture of the strong covalent silicon-oxygen bonds under attack from the OH^- ions.

The content of alkali metal oxide in E-glass fibres is kept low, below 1%, to minimise corrosion damage. Even so, E-glass fibres have been shown to lose up to 60% of their strength after immersion in water at 96°C for just one day, although at room temperature attack is much slower with a corresponding strength drop of only 10% (20% after 3 weeks exposure) (71). In very dry atmospheres or at low temperatures corrosion is simply slowed down and failure is delayed (70,71).

Degradation is accelerated under applied tensile stress. Donnet and Ehrburger (10) have reported that E-glass fibres are weakened by 21% after 3 months in an atmosphere of 65% RH and 20°C and that the strength loss rises to 36% if the fibres are subjected to a load equal to 10% of their tensile strength under the same conditions. Slow or sub-critical crack growth is believed to occur, eventually

leading to 'delayed' or 'stress-rupture' failure if the stress level or time is great enough (71,72). It follows that the strength of glass fibres is dependent on the rate of loading in tensile tests. As the load-rate is increased, the time to reach a particular load level, and thus the amount of sub-critical crack growth that can occur, is reduced. Consequently the fibres become stronger and the amount of corrosion cracking at failure (observed as a mirror zone on the fracture surface) is diminished (71,72). Only where sub-critical or corrosion crack growth causes flaws larger than the original surface flaws should the glass exhibit rate dependence.

c) Kevlar

It is believed that moisture penetrates Kevlar fibres via the extensive defect structure of microvoids and cracks and accumulates within the fibres by interrupting the weak interfibrillar bonding (73). This causes the fibres to swell radially (Table 2.1) and reduces the radial strength and modulus so that there is increased likelihood of internal fibre splitting and core-skin debonding (73). The tensile axial properties are not greatly reduced by moisture or temperature within the service range of epoxy resins however, presumably due to the stability of the stiff covalently bonded polymer chains in the fibre direction (12, 13,43). Similarly, the tensile properties are little affected by load-rate (12) and compared to glass fibres the stress-rupture performance is good (69,74). The actual morphological or chemical changes controlling the stress-rupture lifetimes have apparently not been fully characterised. A major weakness is that the

fibres are susceptible to ultraviolet radiation, and in sunlight for instance this leads to discoloration and degradation (12). In composites, surface coatings can be used to prevent such problems.

2.3.2 Interface

Good bonding and close contact between the fibres and resin are essential requirements if the interface is to exhibit good environmental resistance. The effect of diffusion of moisture to the interface will depend very much on the nature of the particular interface concerned and the severity of the exposure. This has contributed to a certain lack of understanding regarding the degree and reversibility of any damage. Generally degradation is accelerated as the exposure temperature and humidity are increased. Thus boiling water must be regarded as a severe hygrothermal exposure that, given time, is likely to break down the interfacial bonding of most composites.

The interface of CFRP is reported to show good resistance to attack by moisture (7,75). Although moisture does progressively displace the resin at active sites on the fibre surface, the strong hydrogen bonding is not usually destroyed completely (76). As long as the environment is not too severe and debonding does not occur, the effects of moisture should be mainly reversible (26,75).

The resistance of the interface in GRP depends very much on the compatibility of the silane coupling agent with the fibre-resin system. Attack normally involves hydrolysis of the bonds between the

coupling agent and the glass and although suitable coupling agents may slow this down (and thus slow down the attack on the fibres themselves) they cannot totally prevent it (7,9,22,23,77). There is evidence that a small proportion of the (covalent) bonds remain resistant to quite severe exposures so that in some cases degradation can be reversed by drying (which removes the water competing with the coupling agent for the bonds at the glass surface) (22,77,78).

It is reported that moisture disrupts the weak interfacial bonding of Kevlar/epoxy composites (28,73), normally irreversibly (79,80). However, the absorption and accompanying radial swelling of the fibres themselves complicates the situation.

The greater contraction of the resin compared to the fibres upon cooling from the cure temperature leads to a complex residual stress distribution at the interface (81,82). The matrix contraction tends to compress the fibres along their axis, which can be a particular problem in the case of Kevlar fibres.

Residual compressive stresses might be expected normal to the interface, but at high volume fractions these may actually be tensile in some directions and will vary around the fibre circumference (9,82). The problem of tensile normal stresses is greatest for Kevlar fibres since these have a very large radial expansion coefficient (Table 2.1).

Since absorbed water causes the resin to swell, it should (simplistically) tend to relax the normal interfacial stresses. Whether or not debonding occurs will depend on the complex stress state, the compliance of the matrix and the extent of any reduction in interfacial bond strength caused by the moisture. Debonding is more likely where the composite is under applied external stress. Where debonding does occur and the local fibre-matrix alignment is disturbed, reformation of chemical bonds at the interface may not be possible (76,83) and any apparent recovery may simply be due to restoration of relaxed compressive radial stresses around the fibres (84,85).

2.4 GENERAL SENSITIVITY OF COMPOSITES TO ENVIRONMENTAL AND FATIGUE LOADINGS

The mechanical properties of a composite are governed by the properties of the fibres, matrix and interface and also by its anisotropy (Table 2.2). This is true for the basic static performance and for the resistance to environmental and fatigue loadings. Thus composite lay-up and mode of loading have a considerable effect on the damage and failure modes (37,38,39,42,49,68,77, 79,81,86-101).

In fibre controlled situations - where all or a large proportion of the fibres are in the direction of the load, as in the axial loading of a unidirectional laminate - the composite exhibits good strength and stiffness. Generally, unless the load bearing fibres themselves are degraded, there is little if any obvious reduction in properties resulting from moisture absorption

(even at elevated temperatures) and the tensile fatigue resistance tends to be good (68,81,90,94,96).

In matrix-interface controlled situations however - where there are no or only a very small proportion of fibres in the load direction - the overall performance tends to be worse and to show greater environmental/fatigue sensitivity. This is because the weaker and more easily degraded matrix and interfaces are carrying most of the load. This is the case for transverse tensile loading of a unidirectional composite and also for shear loading, including ±45° laminates loaded in tension (90,102,103) and interlaminar shear tests (104,105). Here failure is not dependent on fibre fracture. Increasing amounts of absorbed moisture are usually found to degrade the mechanical properties, often mirroring the effect on the resin alone (7,49) and this is generally made worse (or possibly for high performance resins like Code 69, may only occur) when the testing temperature is raised (9,49,84,106).

Compression properties also depend strongly on the matrix and interface, which provide support for the fibres against microbuckling, and consequently (in contrast to metals) they are often inferior to the equivalent fibre dominated tensile values in both monotonic and fatigue loading, Figure 2.4 (9,81,95,107,108). This is reflected in flexure where failure tends to occur at the compression surface, at least for CFRP (36,68,96,109,110) and KFRP (19,111) despite the presence of stresses of similar magnitude at the tensile surface. With combinations of tension and compression fatigue stresses, the

fatigue resistance is usually reduced with increasing compressive component. Clearly moisture can degrade the compressive (and the flexural) performance of a laminate even in cases where the tensile properties are unaffected.

Generally, the performance in a particular environment depends on the extent of moisture induced degradation and the contribution made by the degraded phase (fibre, matrix or interface) to the particular composite property dominating the mechanical response. It cannot be assumed that there is a simple relationship between the effect of moisture on the static properties and on the response under cyclic loading.

2.5 FATIGUE DAMAGE AND FAILURE UNDER TENSILE LOADING

Static and fatigue failures of metals usually occur by the nucleation and growth of a single dominant flaw. The appearance of the first detectable crack in fatigue signifies the rapid onset of failure. In the period before this, which occupies most of the fatigue life, the crack has negligible effect on the component or specimen. The crack propagates in a well defined manner with respect to the applied stress and the remaining life before failure can be adequately predicted using fracture mechanics. The bulk of the material remains undamaged.

Composites behave differently. They tend to be more damage tolerant than metals, so that random fibre-matrix debonding, resin cracking or fibre fractures may begin to occur at low stress levels or early in the fatigue life, perhaps even on the first loading cycle,

and throughout the entire loaded volume. Stress transfer through the matrix via the interfacial bonding means that early, individual fibre breaks are not critical and initially the damage may not necessarily have any significant effect on the strength. However, it may cause deterioration in other properties such as the modulus or resistance to moisture penetration and may leave the composite more susceptible to subsequent environmental attack. Thus it is important to define 'failure' since, unlike metals, composites may become unsuitable for a specific application long before final fracture.

The exact processes leading to composite failure have not been fully characterised and depend strongly on the details of the composite concerned. They involve the continued build-up of resin cracking, debonding and/or fibre fractures. In fibre controlled situations, which are where the benefits of composites lie, failure can only occur as a result of fibre fracture. The formation of critical 'cracks' consisting of multiple adjacent fibre breaks (which lead to local overloading in the composite) are thought to play an important role in initiating failures in these cases (89, 101,112,113). Often the failures consist of sub-bundles (of several fractured fibres) limited by shear failure between them (112). In fact, the mode of failure is strongly affected by the fibre-matrix adhesion. If this is too low, isolation of fibre breaks in the longitudinal direction becomes less effective and 'brush' type failures tend to occur. If it is high, the stress concentration at individual fibre breaks is large and localised and this leads to a characteristic planar fracture surface with little or no fibre pullout.

In order for failure to occur in fatigue loading the damage must reduce the strength of the composite to the level of the maximum applied cyclic stress (Figure 2.5). Only that damage occurring in fatigue over and above that in normal static loading can be responsible for reduction in the residual strength. Furthermore, the lower the stress level at which failure occurs, the greater this damage must be.

The relative fatigue resistance of composites is best compared after normalising the data to the appropriate static strengths. Often the S-logN curves are approximately linear for much of their range and can be represented by a relationship of the form

$$\sigma = \sigma_f - B \log N_f \qquad (2.4)$$

where σ is the maximum stress during each cycle, σ_f is the static strength (measured at the appropriate loading rate), N_f is the fatigue life and B is the slope of the fatigue curve in units of stress per decade of cycles. The ratio $\frac{B}{\sigma_f}$, the fractional loss of strength per decade, gives a comparative measure of the degradation rate in fatigue loading (87,114,115) and is often in the range 0.6 to 0.12 (101).

2.5.1 Unidirectional laminates

Interpretation of the static and fatigue properties of practical, multiplied laminates requires an understanding of the performance of the individual unidirectional plies. Only tensile loading is considered here.

a) Axial loading

When a unidirectional composite is loaded in the fibre direction the strength and modulus are determined primarily by the properties and volume fraction of the fibres. The relative fatigue performance depends strongly on the working strain of the reinforcing fibres(36,98). Where this is low, as in the case of Type I or HM carbon fibres (ε_f = 0.5%), the axial fatigue properties are extremely good and the slope of the S-logN curve is almost flat. As the failure strain is increased however (falling fibre modulus) the fatigue curve becomes increasingly steep(93). For glass fibres, which have the highest failure strains ($\varepsilon_f \sim 3\%$) of the fibres in common use, the fatigue resistance is relatively poor, with a value of $\frac{B}{\sigma_f}$ of about 0.1(87,116). The correlation between the slope of the fatigue curve and the failure strains is illustrated in Chapter 7 (Figure 7.19). Dharan (36), and later Talreja (98), have shown that this relationship can be explained by the fact that composite failure is initiated by fatigue induced microcracking in the resin. The importance of the fibre strain is to limit the fatigue strains in the resin(98,117). By conducting fatigue tests under strain rather than load control, Dharan demonstrated that the performance of unidirectional GRP was independent of fibre volume fraction (V_f) and that the fatigue curves tended towards a limiting strain similar to that for pure epoxy specimens. Talreja has suggested that the fatigue curve for a unidirectional composite can generally be divided into three regions (Figure 2.6a).

At high cyclic strains, within the fibre fracture scatter band, the performance is limited by the failure strain of the fibres.

'Fatigue' failure occurs by time rather than cycle dependent mechanisms that are similar to those operating in stress-rupture tests. The accumulation of damage involves local stress re-distributions permitted by small viscoelastic movements in the resin. These lead to, or may be caused by, random fibre breaks which in turn cause local overstressing of adjacent unbroken fibres(36, 86,118,119).

At low cyclic strain levels, below the level required to initiate progressive fatigue damage in the matrix, composite failures do not occur, irrespective of the type of fibre (unless the fibre failure strain happens to be exceeded)(36,98).

True fatigue failures, associated with progressive fatigue cracking in the matrix, only occur at cyclic strains between these limits(98). As cycling progresses, resin cracks (growing normal to the load initially) multiply and interconnect. Where they intersect the fibres, debonding or fibre fracture may occur, either of which can lead to weakening of the composite. It is probably safe to assume that near the end of the fatigue life there is a localisation of damage and an acceleration in the rate of fibre breaks. The higher the working strain then the more rapid the build-up of fatigue damage.

When the static failure strain of the fibres (i.e. composite) is reduced, in moving from GRP to CFRP for instance, so the range of strain for progressive fatigue failures becomes smaller and the fatigue curve becomes flatter, indicating a less fatigue sensitive material. Susceptibility to degradation by moisture may also be

reduced, since the matrix and interface will be less heavily loaded for the lower strain/higher modulus composite (94).

b) Off-axis loading

The strength, modulus and failure strain of unidirectional composites are reduced as the angle of loading to the fibre direction (θ) is increased, reaching minimum values when loading is normal (i.e. at 90°) to the fibres (e.g. Figure 2.7). The failure mode also changes from one involving fibre fracture at low angles to shear failure parallel to the fibres or a mixed shear-transverse tensile mode at intermediate angles and transverse tensile fracture at high angles (9,77). These latter modes involve only fibre-matrix interfacial failure and resin cracking and are therefore more sensitive to environmental effects. Which mode occurs first depends on the resolved components of the applied load and the relative magnitudes of the longitudinal, transverse and shear strengths.

Shear and transverse tensile failures are usually initiated at the relatively weak fibre-matrix interfaces. The transverse debonding stress-strain depends on the strength of the interfacial bond, the fibre spacing (i.e. V_f) and the mismatch in the radial fibre modulus and the resin modulus (82,120). For most fibre-resin combinations, the fibres have the higher modulus and this results in a high concentration of strain in the resin layers between the fibres in the load direction. It has been suggested that for $V_f = 0.6$ this strain magnification may reach a value of 20 in GRP, but only 4 in CFRP owing to the lower transverse modulus of carbon fibres (120). Final failure occurs by the growth and coalescence of the debonds, which form initially perpendicular to the load, via cracking in

the matrix between them. Fibre splitting is often observed for KFRP in addition to debonding(73). This is explained by the low radial strength and modulus of Kevlar fibres.

Talreja(98) has demonstrated that the limiting strain below which no fatigue damage occurs is reduced as the loading moves away from the fibre direction (Figure 2.6b). The minimum value is at 90° to the fibres, where the limiting fatigue mechanism is transverse fibre debonding, at a strain level below the normal limit for matrix fatigue cracking. The occurrence of debonding in fatigue at levels below those in monotonic loading has been attributed to strain concentration effects arising from plastic flow in the resin close to the interfaces (9). Subsequently, transverse cracks in the resin are induced by the slight debond opening and closing on each cycle (34).

2.5.2 0/90 laminates

a) Transverse ply cracking

When a 0/90 or quasi-isotropic laminate is subjected to tensile loading, the individual laminae fail successively as the load or fatigue cycles are increased. The first signs of damage are normally in the 90° plies in the form of transverse fibre debonding (Figure 2.8a)(81,83,120,121). These debonds lead to the subsequent formation of transverse ply cracks which spread across the full width and thickness of the plies, normal to the load, partly along the weak interfaces and partly through the matrix (Figure 2.8b). Since most of the load is carried by the 0° plies, it is more informative to consider the behaviour of the constrained off-axis plies in terms of applied strain rather than stress. Clearly the damage suffered by these plies is limited by the ultimate failure strain of the 0° laminae.

Cooling a well bonded 0/90 laminate from the cure to room temperature causes residual stresses and strains in each ply, tensile in directions normal to the fibres and compressive in directions parallel to the fibres (85,120,122). These arise from the mismatch in the transverse and longitudinal thermal expansion coefficients of the plies (the transverse contraction upon cooling being by far the larger) and act to pre-stress the laminate, effectively reducing the transverse ply cracking threshold. The transverse tensile strains for CFRP and KFRP may amount to a significant fraction of the failure strain of the transverse plies but they tend to be lower for GRP since the mismatch in transverse and longitudinal expansion and stiffness coefficients is smaller for this material.

The absorption of water is actually beneficial in that resin swelling causes the plies to expand, primarily normal to the fibres, and thus reduces the previous residual thermal strains(85, 122). At high moisture contents the strains may be eliminated or even change sign(122). Furthermore, any resin plasticisation should reduce the stress concentrations in the resin that initiate the cracking.

Thus, the strains at which debonding and transverse ply cracking occur depend on the temperature and moisture content in addition to the properties of the fibres, matrix and interface and also the lay-up and ply thickness(83,120,123,124). Generally the strains tend to be low and are reduced under fatigue loading(34,81,121). However, the effect of increasing temperature or moisture content is to raise these levels.

b) Characteristic damage state

The first transverse ply cracks occur randomly and at a high rate. However, with increasing strain, the average crack spacing is reduced and fewer new cracks are formed. Eventually a limiting and fairly uniform distribution is reached with a spacing of the order of the ply thickness(120,123). This has been referred to as 'the characteristic damage state'(CDS) of the laminate and is important because it depends simply on the characteristics of the particular laminate concerned rather than on the load history or environmental effects(101,125). Thus the CDS should be the same whether attained in static or fatigue loading.

The build-up of transverse ply cracking in fatigue depends on the relative magnitude of the cyclic strain with respect to the transverse ply cracking strain. If cycling is above this level, then transverse ply cracks appear on the first cycle, in proportion to the amount by which it is exceeded. Where the CDS is not attained on the first cycle, the crack density rapidly increases upon cycling until the CDS is reached, usually still very early in the fatigue life(101,121). Where cycling is below the transverse ply cracking strain, transverse ply cracks may still form (being fatigue induced), but not on the first cycle (34,121,126).

Longitudinal cracks or splits may form in the 0° plies at high strain levels. They are similar in nature to transverse ply cracks (and thus may also be induced by fatigue cycling) and result from the large mismatch between the longitudinal and transverse Poisson's ratios and Young's moduli which cause transverse tensile strains in the 0° plies upon loading(89,120,121,127,128).

Figure 2.8c is a schematic representation of a cross-ply laminate containing a regular array of transverse ply cracks and also isolated longitudinal splits.

c) Deterioration in longitudinal properties

The major danger of damage in the 90° plies is that it may affect the ultimate failure of the longitudinal plies. The formation of transverse ply cracks causes local increases in the load, and thus strain, in the adjacent longitudinal plies and this results in an apparent reduction in composite modulus. Thus the build-up of transverse ply cracking is often observed as a characteristic 'knee' in the stress-strain plot for 0/90 laminates(128). Provided the interlaminar bonding remains sound, the transverse plies continue to carry their share of the load away from the cracks however.

Since the CDS should be the same for both static and fatigue loading, transverse ply cracking during fatigue should not affect the residual strength. However, as cycling proceeds, delaminations may be initiated at the tips of the transverse ply cracks, induced by local interlaminar tensile normal and shear stresses (100,101,129) and often associated with longitudinal splitting(121,127) (Figures 2.8d and 2.9). In static loading such damage is only observed at very high strains if at all. Thus, the growth of the delaminations (which is usually most significant fairly close to failure) has been identified as the first distinctive feature separating fatigue damage from normal monotonic loading damage. The importance of the delaminations with respect to the laminate strength is that, in the localised delaminated regions, the 0° plies are no longer constrained laterally by the transverse plies and they

therefore act independently, with no load transfer, under completely uniaxial stress. Ultimately the strength is reduced locally to the load capacity of the 0° plies alone, with the transverse plies making no contribution at all. Reifsnider et al(101) have shown that such effects alone are sometimes large enough to account for the strength losses necessary for failure under long-term cycling, without even considering fatigue damage in the longitudinal plies. Furthermore, there is evidence that the stress concentrations in the longitudinal plies adjacent to the transverse ply cracks can result in preferential localisation of fibre damage in these regions, increasing the likelihood of a critical 'crack' in the form of multiple adjacent fibre fractures(101, 127). Fortunately, actual propagation of the transverse ply cracks into the longitudinal plies is rarely a problem in 0/90 laminates.

Talreja(98) has pointed out that the fatigue limit for a composite represents the minimum cyclic strain required to initiate the lowest energy damage mechanism. It should be added that this clearly refers to a mechanism that leads to actual weakening of the composite. Thus, transverse fibre debonding will only lower the fatigue limit and reduce the fatigue resistance if it ultimately leads to ply delamination or some other form of damage to the longitudinal plies.

2.5.3 ±45° laminates

A single intralaminar shear crack, parallel to the fibres, will result in the failure of a single 45° ply. Such a crack in a ±45° laminate leads only to an increase in local stress and a reduction in modulus. Failure in this case must also involve delamination at the interfaces between the +45° and -45° plies (interlaminar shear). This is illustrated for two adjacent plies in Figure 2.10.

Damage is initiated by fibre-matrix debonding and this is the mechanism limiting failure under fatigue loading(98). Where the alternating plies are well dispersed, the failures are progressive and characterised by localised multiple cracking(34), observed during cycling as irrecoverable creep(130-134). Delamination, which occurs fairly close to failure, is initiated by the intralaminar cracks. A major problem with finite width ±45° laminates is that, under load, out-of-plane stresses occur in the vicinity of the edges (the interlaminar shear stress being the most important). These may initiate failure and lead to a dependency of strength on specimen width(9,77,135). The edge effects tend to dominate failure of very narrow specimens, but as the width is increased they become less important and the strength approaches a value representative of the true shear strength(9). The affected boundary layer is usually fairly narrow, equivalent to a width of less than the laminate thickness(135). Thus, when investigating ±45° laminates, there is a clear need to determine the effect of width on strength to ensure that the specimens used provide a realistic measurement of the shear properties.

Davis and Sundsrud(136) have shown, for GRP, that the fatigue properties of ±45° laminates are far more sensitive to differences in the resin, cure or interfacial bonding (coupling agents in their tests) than to the fibres themselves.

2.5.4 Observed Strength Degradation During Cycling

The term 'wear-out' is used to describe the situation where the composite strength is reduced by a small amount each cycle throughout the fatigue life. The random nature of the damage accumulation means that

the variability in residual properties compared to the undamaged material is increased as cycling proceeds. Alternatively, 'sudden-death' can be used to characterise situations where there is no significant change in the residual strength until just before failure, as is the case for metals. In reality the behaviour of most composites falls somewhere between these two extremes. Laminates containing high modulus, low failure strain fibres, such as carbon, with a high proportion of fibres or plies in the load direction, tend towards the 'sudden-death' type of behaviour, whereas those with lower modulus, high strain fibres, such as glass, tend to exhibit earlier and more progressive degradation during cycling and are therefore closer to the 'wear-out' behaviour(77). Despite these differences, a catastrophic loss in strength leading to final fracture appears to be common to all composites(87).

2.5.5 Summary of Factors Affecting Fatigue Performance

The fatigue performance of a composite depends on a large number of factors. These include material variables such as the type of fibres and resin, fibre or ply orientation, volume fraction of fibres and interface properties, and also loading variables, such as the cyclic stress range, mode and frequency of loading, environment, and for testing, specimen design. As a general approximation, the lower the fibre modulus or proportion of plies (or fibre volume fraction) in the loading direction then the more sensitive the composite will be to fatigue loading and also to moisture degradation, since for a particular stress level, the strain in the matrix and associated stresses at the interfaces will be greater. At deviations from the load direction, the fibres are less effective in carrying the load and the fatigue performance is undermined by the effect of the off-axis stresses on the matrix and interface.

CHAPTER 3

MATERIALS, EXPERIMENTAL

3.1 MATERIALS

3.1.1 Materials and Laminate Production

The fibre reinforced resin composites investigated were chosen for their relevance to the aerospace industry and contained nominally 60% by volume of either HT-S carbon, E-glass or Kevlar-49 fibres in the same epoxy resin matrix, Code 69 (see Chapter 2). Care was taken that the fibre volume fraction and details of manufacture were as nearly identical as possible in each case. Unidirectional prepreg sheets supplied by Rotorway Composites Limited of Cleveland, Somerset and made from a single batch of Code 69 resin were used to produce eleven ply symmetric laminates. The Kevlar fibres were oven dried, as recommended by the manufacturer prior to prepregging. Further details of the prepreg sheet specifications are given in Table 3.1.

The 1 metre by 0.5 metre sheets were laminated in the Materials Department autoclave at Royal Aircraft Establishment, Farnborough, following the manufacturer's recommended schedule for resin cure(106). Basically this involved heating under vacuum to 130°C and holding for 20 minutes, followed by application of a pressure of 550 - 700 kPa and increasing the temperature to 175°C for 60 minutes. Although Fothergill and Harvey recommend removal from the autoclave once the laminate has cooled to 100°C, pressure was maintained until the laminates were cold in order to avoid the possibility of thermal contraction cracking. The schedule did not require the laminates to be postcured.

After laminating the sheets were examined for quality by ultrasonic C-Scan at RAE. No specimens were cut from any parts of the sheets which appeared to be of poor quality, either from the C-Scan traces

or from visual inspection.

The thickness of the laminates was consistently in the range 2.7 to 2.8mm. Typically 30mm of scrap had to be removed from around the edges of the sheets where they began to taper away.

3.1.2 Laminate Lay-Up, Coding

In the 0/90 (i.e.$[(0/90)_2/0/\overline{90}]_s$) lay-up adjacent unidirectional plies were arranged orthogonally such that when testing the laminate with the surface plies in the load direction (referred to here as tests on 0/90 specimens) there were six (load bearing) plies with their fibres aligned parallel to the load (i.e. in the 0° or longitudinal direction) and only five plies normal to the load (90° or transverse plies), Figure 3.1. Most of the work reported is for specimens of this type, since in practice laminates with 90° surface plies are not selected for component design. In some instances however, it proved informative to conduct tests on 90/0 specimens, where the outer plies were transverse to the load direction.

For the ±45°(i.e. $[(\pm45)_2/+45/-\overline{45}]_s$) specimens, to minimise material wastage and facilitate cutting, laminates with the prepreg sheets laid-up at 45° to the sides of the laminate plate were produced. These were otherwise identical to the 0/90 material.

3.1.3 Laminate Cutting

For specimen production, the laminates were cut into strips (normally 10mm wide) using a dry diamond impregnated slitting wheel rotating at high speed on a milling machine. While the slitting wheel produced good quality cuts for the CFRP and GRP, it was unsuitable for the KFRP where the best results were obtained using a high speed steel side and face cutter. Specimen heating in the latter case was prevented by mounting the laminate on a metal sheet, indirectly cooled by liquid nitrogen, during cutting. Occasionally the cut edges of the KFRP strips had a slightly 'fuzzy' appearance and for the moisture uptake specimens in particular it was necessary to clean up the edges using fine grade carborundum paper.

3.1.4 Determination of Density and Fibre Volume Fractions

The mean laminate densities, shown in Table 3.2,were estimated by weighing and measuring 8 specimens of each material. The true volume fractions, also shown in Table 3.2, were measured using a point counting technique in which photomicrographs were overlaid with a fine grid pattern. Fibre volume fractions were determined by counting the proportion of grid intersections under which there were fibres.

3.2 MOISTURE ABSORPTION STUDIES

3.2.1 Conditioning Environments

Before genuine comparisons of moisture content could be made, coupons had to be conditioned to standardised equilibrium states. It was assumed that these were reached when the weight of the coupons had stabilised. The conditioning environments used were as follows:-

a) Storage in an air-circulating drying oven at 60°C over silica gel desiccant.

b) Exposure to an atmosphere of 65% RH at room temperature, produced by a saturated solution of sodium nitrite in a sealed chamber.

c) Immersion in water (distilled) at room temperature, about 23°C.

d) Immersion in boiling water in a reflux system.

Boiling water was the most severe of the environmental exposures and must be considered as a hygrothermal exposure rather than simply a means of accelerating the moisture uptake. Degradation occurring in boiled samples cannot necessarily be assumed to occur in specimens conditioned in water at 23°C. The 100°C conditioning temperature was however well below the saturated glass transition temperature of 140 to 150°C representative of resins similar to Code 69(19,33).

Some specimens were subjected to combinations of the standard exposures. For example, weight gain in boiling water was measured for specimens from the following equilibrium states:- 65% RH; dried; dried, boiled and redried.

3.2.2 Measurement Techniques

The 0/90 lay-up was used for the majority of the work. The coupon dimensions were 90mm x 10mm unless stated otherwise. To ensure reproducible moisture uptake measurements, the specimens were usually conditioned to 65%RH before subsequent exposures.

Changes in moisture content were recorded as weight gains or losses. These were monitored periodically by removing coupons from the chosen environment and weighing immediately. Specimens conditioned in water were dried with tissue paper to remove any surface moisture before weighing.

3.2.3 Standard Conditioning Treatments

On the basis of the results to be reported in Chapter 4, three different conditioning treatments were adopted as standards for the mechanical testing. These were (from 'as-received').

1) Drying at 60°C over desiccant for at least 4 weeks ('dried')
2) Holding in an atmosphere of 65% RH at room temperature for at least 4 months ('65%RH').
3) Exposure to boiling water for 3 weeks, followed by storage in water at room temperature until test ('boiled').

Exposures 1) and 2) bound the range of moisture contents expected in normal service (e.g. ref.84). Although somewhat extreme, exposure 3) gives a useful indication of the ultimate hygrothermal stability of the laminates.

3.3 STATIC TENSILE TESTING

3.3.1 Specimen design

The tensile monotonic and fatigue specimen dimensions were standardised at 200mm long by 10mm wide, with a total uniform central gauge section of 100mm, the latter in order to accommodate both an extensometer and an acoustic emission transducer which was used for some of the monotonic tests. A small number of tests were also carried out on

selected specimens with non-standard widths (mainly 20mm). Plane sided specimens were used throughout, since not only did this design allow easier specimen preparation and the retention of the excellent surface finish to the cut edges, but also avoided the problems of stress concentrations due to specimen curvatures. Increased susceptibility to failure in the vicinity of the grips is an acknowledged drawback of this design however, and to minimise grip initiated damage and also prevent specimen slippage, soft aluminium end-tabs (50mm x 13mm) were bonded to the specimen ends under low pressure. To ensure good bonding the specimens were lightly abraded and the end-tabs grit-blasted and degreased before being glued together using Araldite AV138/HV998 adhesive. This adhesive cured at room temperature and maintained its integrity even after 6 months in boiling water.

3.3.2 Testing Programme

The tensile mechanical properties of the 0/90 and ±45 laminates in the standard environmental conditions were measured using a screw driven Instron 1195 machine at a constant cross-head speed of 0.5mm/minute and also at much higher loading rates, equivalent to those used in the fatigue test programme, using an Instron 1332 servo-hydraulic machine under load control. Both machines were of 100kN capacity and had wedge action grips (hydraulic in the case of the Instron 1332).

In the 'slow' tests it took from between 3 and 15 minutes for the specimens to fail. The average effective stress and strain rates in these tests are given in Table 3.3 for each of the materials and

conditions. Strain was measured using an Instron dynamic knife-edge extensometer over a 12.5mm gauge-length. The load-rates quoted for the ±45° laminates are average rates up to the (initial) peak load because these materials exhibited strongly non-linear stress-strain curves and consequently constant strain-rate and constant load-rate tests are not strictly comparable.

The properties were also measured for a limited number of specimens that had been subjected to non-standard exposures. These were:-

a) exposure to 100°C in air for 3 weeks prior to testing.
b) immersion in water at room temperature (23°C) for 2 years.
c) redried at 60°C after the standard boiling water exposure.
d) immersion in boiling water for 6 months.

These treatments were intended to help isolate the causes of any changes in the mechanical properties resulting from the standard boiling water exposure. Exposures a) and b) were chosen to help determine whether any effects of boiling water could be attributed to the high temperature conditioning or the presence of moisture alone, while c) should indicate the reversibility of any such effects.

For the reasons explained in Section 3.5.1, the load-rates used in the 'fast' tests were 200kN/s (7.2 GPa/s) for the 0/90 CFRP, 100kN/s (3.6 GPa/s) for the 0/90 GRP and KFRP and 25kN/s (0.9 GPa/s) for the ±45° laminates. These are around 3 to 4 orders of magnitude greater than the rates in the equivalent slow tests. Additional tests were performed on the three 0/90 laminates in the 65%RH condition (using

the Instron 1332) at load-rates of 10, 1.0, 0.1 and 0.01 kN/s to determine the nature of any changes in strength with increasing load-rate. It should be emphasised that all tests using the servo-hydraulic machine were conducted under load control and consequently are referred to in terms of loading rate for the standard 10x2.75mm cross-section specimens. The testing rates are also shown as rates of stress application (in brackets). This is actually the important parameter and where wider than standard specimens were tested the load-rate was adjusted so as to maintain the original rate of stress application. An oscilloscope was used to monitor the load-time traces to ensure that the demanded load-rates were actually achieved throughout the high speed tensile tests. Despite the use of a dynamic extensometer, strain measurements were not very reproducible and because of the short testing times a minicomputer (DEC MINC-11) was required to collect the load-deflection data. The slow tests were therefore essential for the acquisition of accurate strain and modulus data.

All tests were performed under laboratory conditions immediately after removal from the conditioning or storage environment. The build-up of secondary crack damage in both longitudinal and transverse plies was assessed by visual observation, sectioning and polishing of preloaded specimens and acoustic emission monitoring.

Preliminary investigations indicated that exposure to UV radiation for 2500 hours (in a Heraeus Suntest cabinet) had no measurable effect on the tensile properties of any of the laminates.

3.3.3 Preloading

a) Prior to moisture absorption measurements

0/90 specimens were preloaded to different fractions of the failure loads so that the effect of damage on the moisture absorption characteristics in boiling water could be investigated. Most preloads were applied at 0.1 GPa intervals using an Instron 1195 machine (0.5mm/minute cross-head speed). The maximum applied stress ranged from 0.2 to 0.8 GPa for the CFRP and 0.1 to 0.6 GPa for the KFRP and GRP. These were chosen so that the lowest loads did not produce any visible cracking whilst the highest loads induced the greatest amount of damage in the specimens without causing failure.

Full sized 100mm gauge-length tensile specimens preconditioned at 65% RH were used to apply the preloads, with the moisture uptake coupons being cut from the gauge-lengths prior to the boiling water exposure. The coupon dimensions were limited to approximately 50x10mm since transverse and longitudinal sections were also taken for microscopic examination of the damage (Section 3.3.2).

In addition, the GRP was loaded at the much higher rate of 100kN/s (as used in the fatigue test programme) in an Instron 1332 servo-hydraulic machine (under load control). Since the tensile strength of GRP increases with testing load-rate (Chapter 5) this provided the unique opportunity to investigate GRP specimens that had undergone preloads and therefore secondary crack damage greater than at failure in slow loading. Overshoot meant that it was more difficult to control the maximum load in these tests and as a result, the increments of preload up to the maximum of 0.79GPa were not evenly distributed.

b) Prior to fatigue testing

Groups of specimens were also preloaded and subsequently tested in fatigue until failure, either immediately (at stresses below the preload level) or after 3 weeks conditioning in boiling water (in which case the monotonic strengths were also measured). The fatigue testing procedures followed those described in Section 3.5. The prestress levels were 0.7 GPa for the CFRP (representing about 75% of the tensile strength), 0.6 GPa for the KFRP (84%) and 0.4 GPa and 0.7 GPa for the GRP (68% and 80%). The preloads were applied under 'slow' loading except for the 0.7GPa GRP which was applied at 100kN/s. In this case stress is quoted as a percentage of the 100kN/s tensile strength The preloads were chosen so as to introduce extensive amounts of secondary crack damage into the specimens in a controlled manner. This damage consisted primarily of high densities of transverse ply cracks and, in addition, considerable longitudinal ply splitting in the 0.7 GPa GRP.

3.4 BEND TESTING

Bend testing was confined to 10mm wide 0/90 specimens. An Instron 1195 was used for the ILSS, 4-point and 3-point bend tests. The cross-head speed was 1, 5 and 10mm per minute respectively.

3.4.1 Interlaminar Shear Strength (ILSS) Tests

The ILSS of 20mm coupons was measured in the three standard environmental conditions. A short beam 3-point bending jig (Figure A2.1) with a 14mm span was used for the tests. This gave a span (S) to specimen thickness (d) ratio of 5 to 1 which was low enough to produce 'shear' rather than flexural failures. 3mm loading rollers were used to prevent excessive indentation or crushing damage of the specimens.

As far as possible the experimental details conformed to those in BS2782: Part 3: Method 341A:1977.

3.4.2 4-Point Bend Tests

90mm long specimens were tested in a standard, symmetrical Hounsfield 4-point bending jig (Figure A2.2). The inner load point spacing was equal to half the outer load point span (S) of 63.5mm (2.5 inches). This gave an overall value for $^{S}/_{d}$ of 23 to 1.

Specimens were tested after the three standard exposures and also after non-standard periods of immersion in boiling water ranging from 1 hour to 4 weeks.

3.4.3 3-Point Bend Tests

A standard Instron bending attachment (load-roller diameters of 5mm) was used for 3-point bend tests, which were confined to specimens in the 65% RH condition (and the boiled condition for the KFRP). To ensure a true flexural mode of failure, a high value of $^{S}/_{d}$ of $^{40}/_{1}$ was used (S = 109mm; 180mm specimens). The deflections at failure for the GRP specimens were very large and comparative tests were therefore run with $^{S}/_{d} = {}^{30}/_{1}$ for this material (S = 84mm; 120mm specimens).

3.4.4 Avery Flexure Tests

Specimens (90mm) were tested in the 65%RH and boiled conditions. The Avery (Type 7305) machine, which produced pure bending stresses and is described in Section 3.6, was operated by hand.

3.5 TENSILE FATIGUE TESTING

3.5.1 Dynamic Fatigue Tests

The tensile fatigue tests were conducted using the 1332 servo-hydraulic machine operated in load control. Unless stated otherwise, a stress ratio R (minimum stress/maximum stress) of 0.1 was used.

The tests were performed at constant average rates of applied loading rather than at constant frequency in order to minimise any load-rate or hysteretic heating effects. The advantages of constant load-rate tests have been explained by both Sims and Gladman(114) and Mandell(87). A benefit is that it means higher frequencies are used at lower stress amplitudes, thus reducing the time taken to failure in the high cycle regime. In all the tests, the point of failure was taken as final specimen separation.

The load-rate used for the fatigue testing of the 0/90 GRP and KFRP laminates was 100kN/s, for which the resultant frequencies ranged from about 2Hz (for cyclic stresses of 0.8 GPa) to 19Hz (0.1 GPa). This rate was necessarily a compromise between being high enough to give a reasonably productive testing rate and low enough to prevent large autogenous heating effects in the specimens. Temperature rises of up to 30°C were measured using a surface mounted thermocouple for the KFRP at the higher stress levels, but no heating was observed for the GRP using this method.

A testing rate of 200 kN/s was used for the 0/90 CFRP, since the lower strains and conduction by the fibres reduce the heating effects for this material. The ±45° laminates were all tested at the much lower rate of

25 kN/s, which was consistent with their lower strengths and resulted in a range of cycling frequencies similar to those used for the 0/90 laminates.

The load-rates quoted are average values because the wave-form used for the tests was actually sinusoidal. Thus the instantaneous load-rate varied from a maximum at the mean load level to zero at the maximum and minimum loads. A series of fatigue tests were performed on the 0/90 GRP (65%RH) using a triangular wave-form to determine whether this affected the fatigue performance. Steps were taken to prevent large changes in moisture content of conditioned specimens during testing in case this affected the outcome of the fatigue tests. Boiled specimens were prevented from drying out by surrounding the gauge-length with moist tissue paper and plastic film during the tests. The dried specimens were also wrapped in plastic film to minimise any absorption of moisture. These precautions were considered adequate in view of the fact that all fatigue tests were conducted at room temperature (at which the diffusion rates were relatively low - Chapter 4) and that the tests seldom lasted for longer than 1 week.

3.5.2 Stress-Rupture Tests

A limited number of stress-rupture tests on 65% RH specimens were performed using the Instron 1332.The initial rate of loading in these tests was approximately 4 kN/s.

3.6 FLEXURAL FATIGUE TESTING

The flexural fatigue performance of the 0/90 laminates in the 65% RH and boiled conditions was measured using an Avery dynamic fatigue machine (Type 7305). The testing arrangement is shown in Figures A2-3a and b.

For testing, the specimens (90x10 mm) were clamped between two sets of grips such that the clear span (42mm) to specimen thickness ratio was 15 to 1. In this arrangement, the mid-span was subjected to pure bending stresses, always maximum tensile at one surface and maximum compression at the other, while the clamped outer spans experienced neither bending nor shear stresses. The loads were imposed at one end of the specimen by movement of the grip attached to an oscillating spindle driven by means of a connecting rod, crank and double eccentric. The grip holding the other end of the specimen was firmly attached to a torsion bar dynamometer, the amount of twist in which was measured by a dial gauge pre-calibrated to enable determination of the bending moment and hence the apparent maximum surface stress.

The fatigue tests were carried out over a range of initial surface stress levels under constant cyclic angular deflection in one direction only (such that one surface experienced only tensile stresses and the other only compressive stresses). This enabled direct comparison of the relative tensile and compressive fatigue performance. The magnitude of the first cycle surface stress range was determined by the laminate flexural modulus (and thickness) and the pre-set angular

setting on the eccentric. The latter was limited to only 24° in fatigue and this meant that the GRP and KFRP laminates (which had lower moduli than the CFRP) could only be tested in the high cycle fatigue regime. Minimum angular deflections were kept slightly positive to prevent the possibility of reversed bending.

Fatigue damage sustained by the specimens was indicated by decreasing stiffness which was monitored periodically during each test (at durations not exceeding one decade of cycles) by stopping the machine and moving the eccentric by hand to take each reading. Except for the first 100 cycles, which were applied by hand comparatively slowly to allow representative readings to be taken in this range, the cyclic frequency was 8.2Hz, the machine's slowest speed. There was no obvious increase in specimen temperature during cycling, the greatest stresses being at the surfaces where heat was most easily dissipated. Boiled specimens were prevented from drying out by surrounding them with wet tissue paper kept moist during testing using a capillary action technique.

CHAPTER 4

MOISTURE ABSORPTION STUDIES

4.1 MOISTURE ABSORPTION AND DESORPTION

4.1.1 Exposure to 65% RH

In the 'as-received' condition specimens had been exposed to the laboratory environment (approximately 23°C; 35% to 55% relative humidity, with occasional excursions beyond this) for varying periods of time. These specimens absorbed moisture when exposed to the 65% RH environment, Figure 4.1. Absorption was relatively slow at ambient temperatures, with over four months being required for the moisture contents to even approach the equilibrium level for 65% RH. The evidence of other weight gain curves at 23°C (see later) indicates that in fact the final equilibrium moisture content may not have been attained for a considerable time. Past 4 months however, the absorption was very slow and probably insignificant as far as conditioning for mechanical testing was concerned. One benefit of this was that specimens already preconditioned at 65% RH could be tested in the normal laboratory atmosphere without the need to maintain humidity at 65% RH.

4.1.2 Drying

Figure 4.2 shows that all three laminates required at least 4 weeks in the drying oven to reach a stable weight, which was taken as nominally 0% moisture content. For consistency, the test coupons were preconditioned to 65% RH before exposure. All weight losses were attributed to loss of absorbed moisture alone, since the fibres and Code 69 resin should not have been affected by the 60°C drying temperature, at least over the relatively short time periods involved(19,60,106).

Drying curves were also obtained for 20mm, 40mm and 200mm coupons. These were basically similar to those reported except that the results for the shortest specimens showed greater scatter.

As for the as-received specimens (Figure 4.1), fully dried coupons re-exposed to 65% RH at room temperature absorbed moisture very slowly (Figure 4.3).

4.1.3 Water at 23°C

Figure 4.4 shows that specimens immersed in water at 23°C absorbed moisture very slowly, which was to be expected in view of the previous results at room temperature. This effectively precluded the use of water at 23°C as a standard preconditioning environment for mechanical test specimens and highlighted the need to employ an accelerated conditioning technique using elevated temperature to reach saturation over realistic periods of time.

4.1.4 Boiling Water

a) 0/90 laminates

The absorption rates were very much greater when specimens were immersed in boiling water, with the weight gains stabilising after about 3 weeks exposure. This was the case for both 65% RH and fully dried specimens (Figures 4.5a and b).

Discoloration of the water and weight losses indicated irreversible degradation for exposures longer than 3 to 4 weeks. This was confirmed by redrying specimens that had previously been boiled for 5 weeks from dry (Figure 4.6, ref. Figure 4.5b). The weight losses were presumably due to the loss of small quantities of leachable

resin constituents, such as low-molecular weight material or residual monomer or catalyst. Some additional effects, probably associated with the fibres themselves, must account for the larger weight loss for the KFRP (approximately 0.7% cf. 0.1-0.2% for the CFRP and GRP). Polished sections revealed significant cracking in specimens boiled for 6 months, although there was no such damage after only 3 weeks exposure (Figures 4.7 and 4.8).

Accurate measurement of moisture uptake in boiling water was not possible. Not only was there the problem of material losses, but also the specimens began to lose moisture as soon as they were exposed to the laboratory atmosphere for weighing. This was a particular problem for the KFRP (although it probably accounted for no more than 0.2 to 0.3% of the coupon weight at most) and the difficulty in achieving a good reproducible surface finish to the cut edges may have added to the scatter in weight gain measurements for this material. To help reduce moisture losses during weighing, the specimens were held in water at room temperature except when actually on the balance. Surprisingly, all the laminates gained in weight slightly as a result (over a period of one week for instance, the CFRP and GRP gained up to 0.2% in weight and the KFRP up to 0.5%). This may reflect the regain of moisture initially lost from the hot surface of the specimens or may simply be a manifestation of the reverse thermal effect noted by Adamson(45).

Weight gain curves for 20mm, 40mm and 200mm long specimens were generally similar to those in Figure 4.5 for 90mm coupons. The only exception was for the 20mm KFRP specimens, which showed substantially

higher moisture uptake rates early on. As in the case of the drying curves (Section 4.1.2) the results for the shorter specimens were generally more scattered, probably due to the increased influence of weighing errors in these tests.

b) Effect of voids

The CFRP and KFRP laminates were generally free from voids, but the quality of the GRP was more variable with significant voidage in some regions, e.g. Figure 4.9. Voids were present in both 0° and 90° plies and were usually non-spherical in shape, being elongated in the direction of the fibres. They were often associated with ply interfaces and varied greatly in size, extending sometimes up to 5mm in length and typically 0.05 to 0.15mm in cross-section. The semi-transparent nature of the GRP laminates meant that the voids were clearly visible to the naked eye and this was used to screen the specimens so that poor quality material could be eliminated from the testing programme.

The effect of the voids on the weight gain of the GRP in boiling water is shown in Figures 4.5a and 4.5b, where specimens of quality more similar to that of the CFRP and KFRP, containing few voids, are compared with much poorer quality samples in which the void concentration was significantly higher. Both figures show that the weight gain for specimens containing high void concentrations is typically about 0.4% greater than the gain for low void content material. For oven drying at 60°C from 65% RH (Figure 4.2) there was little or no effect of void content on weight change however.

Taking 0.4% as the additional weight gain of the void containing material and making the assumption that this is entirely due to filling of the voids with liquid water during the boiling water immersion, then a rough estimate of the void content can be made

$$\frac{W_w}{W_c} = \frac{\rho_w V_w}{\rho_c V_c} = 0.004 \qquad (4.1)$$

where W_w, ρ_w and V_w are the weight, density and volume of the water contained in the voids and W_c,ρ_c and V_c are the corresponding terms for the composite. Taking values of $2.01 \times 10^3 kgm^{-3}$ for ρ_c (Table 3.2) and $1.0 \times 10^3 kgm^{-3}$ for ρ_w, Equation 4.1 yields a value of about 0.8% by volume for the excess void content $\left(\frac{V_w}{V_c}\right)$ of the poor quality GRP.

c) ±45° laminates

Although most moisture absorption studies were conducted on specimens in the 0/90 orientation, weight gains in boiling water were also measured for ±45° coupons to see if the change in fibre orientation at the cut edges (which constituted 24% of the total surface area for the standard 90 x 10mm coupons) affected the uptake rate. As Figure 4.10 shows, absorption rates and times to saturation were similar for both lay-ups.

4.1.5 Swelling

Table 4.1 shows the results of measurements of specimen swelling caused by moisture absorption during immersion in boiling water for up to six months. The measurements were limited to six 0/90 specimens (200x10mm) for each laminate.

As expected, in each case swelling was substantially greater through the thickness than within the plane of the laminate, there being no fibres to constrain the swelling in this direction. The greater swelling for the KFRP was due to the fact that the Kevlar fibres absorb moisture themselves, with quoted axial and radial swelling coefficients of 0.06 - 0.09% strain per % moisture uptake and up to 1.0% per % respectively (Table 2.1). The swelling coefficient of the resin is probably of the order of 0.2-0.3% per %.

The increased swelling, particularly in the plane of the laminate, after 6 months boiling cannot be due to changes in moisture content. It most likely results from a degree of relaxation in the constraining effect of the fibres due to the resin cracking observed after this prolonged exposure.

4.2 EQUILIBRIUM MOISTURE CONTENTS AND STANDARD ENVIRONMENTAL CONDITIONS

On the basis of the results reported in Section 4.1, the following exposures provided specimens with near equilibrium moisture contents approximating to the 'dried','saturated' and '65% RH' conditions.

1) storage in a drying oven at 60°C over desiccant for at least 4 weeks.
2) immersion in boiling water for 3 weeks
3) exposure to an atmosphere of 65% RH at room temperature for not less than 4 months.

The corresponding weight gains relative to the dried state are summarised in Table 4.2. Ranges rather than single values are quoted because of the scatter in measured weight changes, particularly for the KFRP laminate. The results are presented in two ways, firstly as percentage weight increases over the dry condition and secondly in terms of weight gain per unit volume. Problems arise with the first, more traditional method when trying to compare composites with different components or fibre volume fractions (or fibre types, as here) because of their different initial densities. For otherwise identical specimens absorbing equal amounts of moisture, the percentage weight gains are less for a laminate containing denser fibres, for example glass fibres instead of carbon. It is more informative therefore to quote weight gains per unit volume of composite. In the case of inorganic fibre composites, if the weight gain is assumed to be due simply to moisture absorption by the resin, then for equal fibre volume fractions, the weight gains should be independent of laminate density. Percentage weight gains have been converted to weight gains per unit volume of material (kg m^{-3}) by multiplying by the dry laminate density (kg m^{-3}) as indicated below

$$\text{Weight gain/unit volume} = \frac{\text{Total weight gain}}{\text{Original dry weight}} \times \text{Dry laminate density} \qquad (4.2)$$

The dry laminate densities used in these calculations were as follows:

CFRP : $1.49 \times 10^3 kgm^{-3}$

GRP : $2.00 \times 10^3 kgm^{-3}$

KFRP : $1.32 \times 10^3 kgm^{-3}$

An overall view of the relative absorption behaviour of the three laminates is shown in Figure 4.11 where the saturation moisture contents (kgm^{-3}) from Table 4.2 are plotted as a function of the relative humidity of the conditioning environment. Moisture content is roughly proportional to relative humidity over most of the range except for the boiling water treatment, where the weight gains are larger than expected. This could indicate that additional absorption mechanisms are acting in boiling water. However, TGDDM-DDS epoxy resin systems commonly show positive deviations from linearity on this type of plot at high humidities(39,55). Edge(84) and Long(47) have shown that water immersion tends to give higher equilibrium moisture uptakes than predicted from relative humidity data and that this is true for room temperature conditioning(47) as well as exposure to boiling water(84). Long showed that the effect is associated with the resin matrix rather than the composite as a whole. This is in accord with the results here, since close comparison between the curves for the three laminates shows that the effect is present in each but is less pronounced for the KFRP, presumably because of the greater scatter and overall higher weight gains for this material.

The specimens immersed in water at 23°C for 2 years had not reached saturation and it is hard to estimate what their final equilibrium moisture uptakes would have been.

The weight gains for the inorganic fibre composites are approximately similar, confirming that moisture uptake is confined to the resin which is the same in each case. The slightly higher gains for the CFRP reflect the higher measured volume fraction of the resin for this material. The boiled weight gains are somewhat anomalous, indicating a marginally greater moisture uptake for the GRP in this condition. This may have been due to liquid water in the voids which were present in even the better quality GRP specimens selected for testing. It has already been shown in Section 4.1.4b that void content markedly affects the moisture uptake of the GRP laminates. An initial voidage of around 0.4% in the nominally 'void-free' GRP specimens could explain the discrepancy. Quantitative analysis of several polished microsections (using a microscope fitted with a grid in the eyepiece to allow point counting) confirmed that the void content of the GRP was typically of this order. Up to 1% void content is usually considered acceptable for well-fabricated laminates.

Assuming that the resin has a density of $1.268 \times 10^3 kgm^{-3}$ (35) and an equilibrium moisture content in boiling water of 6%, maximum moisture uptakes for the inorganic fibre laminates can be estimated in terms of the volume fractions of the absorbing resin phase. For Code 69, a 6% weight gain is equivalent to an increase in weight of about 76kg per $metre^3$ of resin. The composite weight gain is equal to the weight gain of the resin fraction of the laminate and in cases where the fibres absorb moisture, the weight gain of the fibre fraction as well. The predicted moisture uptakes for the carbon and glass/epoxy laminates are thus 31.9 kgm^{-3} and 27.4 kgm^{-3}

respectively. These are of the order of the boiled values in Table 4.2.

Moisture contents are generally 2 to 3 times higher for the KFRP than for the other two laminates. In this case the absorption by the fibres must also be considered. Assuming that the fibre gain in boiling water is 5% (41) and that the fibre density is $1.45 \times 10^3 kgm^{-3}$, the predicted weight gain for the composite is 73.8 kgm^{-3}, which is within the measured scatterband. The measured weight gains are generally representative of those reported in the literature for similar composites and environmental conditions.

4.3 MEASUREMENT OF DIFFUSION RATES

4.3.1 Fick's Law Plots and Apparent Diffusivities

The curves of weight change with time for the various exposures shown in Figures 4.1 to 4.5a are re-plotted against the square root of time in Figure 4.12. One of the requirements of simple Fickian diffusion is that such curves should be linear up to around 60% of the total weight gain (Chapter 2). This generally appears to be the case for the CFRP and GRP laminates for all the exposures, but the KFRP tends to show non-linearity much earlier, indicating strongly non-Fickian behaviour for this material. This has been observed by other investigators (19,43) and is to be expected. Although the fibres and resin both absorb moisture (and there is evidence that weight gain in Kevlar fibres can also be represented by a Fick's Law plot (43)), the rates and manner in which they do so are quite different(41,43).

There is no reason to suppose a priori that the absorption by the inorganic fibre composites is fully described by Fick's Law, despite the characteristics of such behaviour shown in Figure 4.12. It was not the aim of the work to fully characterise the absorption/desorption behaviour of the laminates over the full range of environments, temperatures and hygrothermal histories used. However, evidence of small overall weight losses upon re-drying and increased uptake rates on secondary boiling water exposures (Section 4.4) do indicate that none of the laminates behaved in a truly Fickian manner.

It is useful to have a means of comparing the initial rates of moisture absorption for the various laminates and conditions used and to have an indication of how well they follow the initial $\sqrt{t}$ relationship characteristic of Fickian diffusion. Here, absorption data in each case have been fitted to a Ramberg-Osgood type curve. Such analytical curves are traditionally used to fit stress-strain data or similar load-deflection data for metals in the elastic-plastic range and are of the form

$$x = Ay + By^n + C \qquad (4.3)$$

where A is the effective linear slope

By^n is the trend away from the linear and C may be the experimental offset.

For the relationship between $\frac{M_t}{M_m}$ and $\sqrt{t}$ the Ramberg-Osgood equation is written as

$$\sqrt{t} = A\left(\frac{M_t}{M_m}\right) + B\left(\frac{M_t}{M_m}\right)^n + C \qquad (4.4)$$

The apparent diffusion coefficient for each specimen can thus be determined from Equation 2.2 rewritten in the form

$$D = \frac{d^2\pi}{16}\left(\frac{M_t}{M_m}\Big/\sqrt{t}\right)^2 \qquad (4.5)$$

since initially $\left(\frac{M_t}{M_m}\Big/\sqrt{t}\right)$ is equal to A^{-1} in the Ramberg-Osgood equation.

For each separate set of data, the values of A, B, C and n for Equation 4.4 were obtained using a least squares best fit method , Appendix 1. The curves thus generated are plotted in Figure 4.12.

An advantage of the Ramberg-Osgood analysis is that there is no assumption that the absorption is Fickian. This avoids the normal requirement that all the data points up to 0.5-0.6 M_m be included in a conventional straight line data fit. Obviously this last method would be unsuitable for the KFRP and could result in inclusion of inappropriate data points for the other laminates if these showed early deviations from linearity. This would include situations where the specimen geometry is such that absorption through the edges is significant.

A further advantage of the Ramberg-Osgood analysis is that an indication of the relative 'strength' of the linear portion can be gained from the magnitude of the parameter $\frac{B}{A}$. A comparatively large value of $\frac{B}{A}$ indicates a strong trend away from linearity and consequently a greater deviation from Fick's Law.

In practice, although the Ramberg-Osgood analysis was found to be excellent for determining the initial slope and the apparent diffusion coefficient there were sometimes too few data points for accurate curve fitting in the non-linear region.

The apparent diffusion coefficients have been calculated for the different exposures and are presented in Table 4.3. No values are quoted for conditioning at 65% RH from 'as-received' since accurate data for the equilibrium weight changes were not obtained in these tests. The diffusivities are meant only as a rough guide. For example, inconsistences can arise as a result of the relatively small numbers of specimens tested, scatter in weight gain data, differences in specimen dimensions and resultant edge effects, and errors in estimating M_m (especially at the lower temperatures). Values for KFRP are quoted merely to indicate that absorption rates were higher for this material (the $\sqrt{t}$ uptake curves were generally non-linear, leading to considerable errors in the determination of the initial slope).

4.3.2 Edge Corrections

Apparent diffusivities calculated using Equation 2.2 can only be compared when specimens are of the same dimensions and lay-up since the test coupons do not approximate to semi-infinite plates and consequently some absorption occurs through the cut-edges. This is particularly important where the fibres or fibre/resin interfaces contribute to moisture transport through the laminate.

Provided that the diffusion is limited to the resin and remains Fickian and that the volume fraction, lay-up and dimensions of the specimen are known, expressions developed by Shen and Springer(56) can be used to predict the apparent diffusivity in terms of the diffusion coefficient of the resin, D_r. Their expression for the diffusivity normal to an exposed surface (along the x-axis say) is

$$D_x = D_r[(1-V_f)\cos^2\alpha+(1-2\sqrt{\frac{V_f}{\pi}})\sin^2\alpha] \qquad (4.6)$$

where V_f is the fibre volume fraction and α is the fibre orientation with respect to the x-axis. This assumes square array fibre packing but nevertheless is often found to be satisfactory. As one might expect, Equation 4.6 indicates a reduction in diffusion coefficient as the fibres diverge from the normal to the surface.

The early interaction free diffusion coefficient of a composite can be estimated by considering the diffusion at each surface independently, so that for a multi-layer laminate consisting of N plies, all with their fibres in the same plane i.e. parallel to the top and bottom surfaces, the following expression can be used to determine the overall diffusivity (56):

$$D = D_r(1-2\sqrt{\frac{V_f}{\pi}})\left[1+\frac{h}{l}\sqrt{\frac{(1-V_f)\sum_{j=1}^{N}h_j\cos^2\beta_j}{(1-2\sqrt{V_f/\pi})\sum_{j=1}^{N}h_j}+\frac{\sum_{j=1}^{N}h_j\sin^2\beta_j}{\sum_{j=1}^{N}h_j}}+\frac{h}{n}\sqrt{\frac{(1-V_f)\sum_{j=1}^{N}h_j\sin^2\beta_j}{(1-2\sqrt{\frac{V_f}{\pi}})\sum_{j=1}^{N}h_j}+\frac{\sum_{j=1}^{N}h_j\cos^2\beta_j}{\sum_{j=1}^{N}h_j}}\right]^2 \qquad (4.7)$$

In this equation, h_j is the thickness of the jth ply, while l, n and h are the specimen length, width and total thickness respectively. β is the angle between the fibres in each ply and the length axis. V_f is assumed to be the same in each ply. The first term in the expression refers to the diffusion through the top and bottom surfaces, where the fibres are parallel to the surface, while the latter terms refer to diffusion through both pairs of cut edges. It is assumed that there are no diffusion discontinuities across the ply interfaces and that diffusion does not occur through the fibres, interfaces or any cracks in the resin. The equation is therefore not valid for KFRP.

Substituting the appropriate values for the standard 90 x 10mm specimens used in this work into Equation 4.7, together with V_f = 0.6, yields diffusivities of 0.26 D_r for both the 0/90 and ±45° specimens. Despite the limitations of Equation 4.7, the predicted similarity in the absorption rates for both lay-ups is consistent with the experimental results (Figure 4.10). Equation 4.7 predicts that edge effects cause the diffusivity for the standard specimens to be double that for absorption through the upper and lower surfaces alone (0.13 D_r), while for 20x 10mm specimens the diffusivity is raised to 0.32 D_r. In the latter case the proportion of edge to total surface area is significantly increased. Unfortunately, the inherently greater scatter in results for the smaller coupons meant that it was not possible to detect this increase in diffusivity experimentally for the inorganic fibre composites.

The increase in initial uptake rate noted for the KFRP on moving to smaller specimens can be explained by the more significant effect of absorption through the cut edges for this laminate. Moisture is known to diffuse rapidly along the axis of Kevlar fibres and Allred and Lindrose(41) have shown that for KFRP laminates the diffusion coefficient parallel to the fibres may be up to two orders of magnitude greater than that of the pure resin, which is in turn, several times greater than the diffusivity in a direction perpendicular to the fibres.

Assuming that absorption is through the resin phase only and that the diffusion coefficient for Code 69 resin at 23°C is typically $8.95 \times 10^{-10} cm^2 s^{-1}$(59,65) then Equation 4.7 predicts an apparent diffusivity for the standard specimens at room temperature of $2.33 \times 10^{-10} cm^2 s^{-1}$, which is of the order of the experimentally measured values in Table 4.3. This, together with the similarity in absorption rates between the 0/90 and ±45° specimens and the absence of any large increase in rate on moving to shorter 0/90 specimens (in contrast to KFRP) suggests that diffusion through the resin rather than wicking up the fibre-matrix interfaces is the primary mechanism of moisture absorption for the carbon and glass fibre reinforced laminates. This does not necessarily discount the possibility of degradation of the fibre/matrix interfacial bonding however.

Equation 4.7 is very sensitive to the values of V_f. Using the measured volume fractions instead of the nominal value of 0.6, yields apparent diffusivities for the standard specimens of 0.30 D_r

for CFRP (V_f = 0.58) and 0.22 D_r for GRP (V_f = 0.64). A trend to higher diffusivities for CFRP was indeed exhibited for most of the environmental exposures.

4.4 SECONDARY BOILING WATER EXPOSURES

Figure 4.13 shows that the absorption rates for specimens that had been previously boiled for 5 weeks and then redried were increased for secondary exposures. The weight gains tended towards the original saturated values during the second boil, but on redrying the weight losses were even greater than before. Compared to the original dried weight, the losses on redrying were around 0.3% for the CFRP and GRP specimens and around 1.1% for the KFRP. The corresponding losses after the first boil were only 0.1 to 0.2% and 0.7%. Once again the weight loss for the KFRP was greater than that for the inorganic fibre composites. If this irreversible behaviour was due to further loss of material, then the moisture uptake for the second boil was greater than for the first boil.

Thus, while it appears that initially at least most moisture entered the CFRP and GRP by diffusion through the resin, the greater absorption rates recorded for secondary exposures to boiling water indicate that in this case moisture was entering by mechanisms that were different from or additional to the original ones. These must result from changes to or degradation of the interface or matrix. Increased absorption rates for secondary moisture exposures have been commonly observed in the past and do not necessarily depend on immersion or high exposure temperatures (32,44,58,64,66,137). The effect is evidently due to changes occurring during

the first exposure rather than as a result of environmental cycling, since the rate for the initial desorption is also reported to be increased(44,51,58,64,66). Since optical microscopy revealed no significant resin cracking after 4 weeks in boiling water, it must be assumed that the accelerated absorption was due either to wicking facilitated by prior degradation of the interfaces, as has been observed by Kaelble(32), or to some irreversible change in the matrix. The latter could, for example, have involved microvoid formation caused by the leaching out of unattached low molecular weight material(31,64,66). This would correlate with the increased weight losses upon drying. Fibre damage, in the form of internal splitting or debonding, could explain the very high secondary absorption rates for the KFRP. However, no direct evidence was obtained to substantiate these suggestions.

4.5 EFFECT OF PRELOAD ON MOISTURE ABSORPTION

The weight gains in boiling water for the preloaded specimens are compared in Figures 4.14 to 4.16 with the results for the standard,undamaged material (taken from Figure 4.5a). The difference in dimensions and resulting edge effects between the standard and preloaded coupons means that the curves are not directly comparable. However, the saturated moisture uptakes are independent of such effects and furthermore, the analysis of Shen and Springer (56) indicates that differences in absorption rates should be small(less than 5%, Section 4.3.2).

Predamaging the specimens might be expected to affect the moisture absorption in two ways, by increasing the saturated moisture content and also by increasing the rate of uptake.

4.5.1 Equilibrium Weight Gains

a) GRP

The curves for GRP (Figures 4.14a and 4.14b) suggest that there is no regular pattern of behaviour to reveal the effect of preloading. (The large scatter in uptakes for undamaged GRP was attributed to the presence of voids in the specimens - Section 4.1.4b).

The equilibrium weight gains, taken from Figure 4.14 after 4 weeks in boiling water, are plotted as a function of preload in Figure 4.17a. Contrary to expectation, the damage caused by prestressing at either the low or high rate did not obviously increase the water taken in , despite the presence of large amounts of fibre debonding, transverse ply cracking and (for the high load-rate tests) longitudinal splitting in the samples preloaded to close to failure.

Figure 4.18a shows the overall weight losses when the GRP specimens, preloaded and then boiled for 4 weeks, were dried to constant weight at 60°C (for 15 weeks). Since the specimens were dried to the 0% RH condition, the weight losses were greater than the original gains from 65% RH. Unlike the data in Figure 4.17a, they are also independent of any material losses incurred during boiling or any small differences in moisture content between specimens originally conditioned to (nominally) 65% RH. The results simply represent the amount of moisture lost during drying i.e. the moisture contents of the boiled specimens. It is clear from Figure 4.18a that within the sensitivity of the measurements, this was independent of damage due to preloading (at either load-rate).

It is concluded that, in the absence of a load, the cracked areas did not accommodate large quantities of moisture as might be supposed. Presumably the cracks were tightly closed. The relief of any residual thermal contraction or curing stresses present in the laminate upon moisture absorption would tend to close transverse ply cracks in a 0/90 laminate.

The sensitivity of the weight gain measurements was approximately 0.01%, representing 2.5×10^{-4}g of water for a typical 2.5g sample of 50mm gauge-length. Since 6×10^{23} (Avogadro's number) water molecules weigh 18g, the limit of sensitivity represents around 8×10^{18} water molecules. Transverse ply cracking reached a saturation level for high preloads with a spacing of the order of the ply thickness or 0.25 mm (actually the spacing was slightly greater than this). Over a 50mm gauge-length this gives $^{50}/_{0.25}$ cracks per ply and a total crack area in all five transverse plies of 2500mm^2 (assuming an area of 10x0.25mm for each transverse ply crack). Making the further assumption that the diameter of a water molecule is of the order of 3×10^{-10}m(138), it follows that a 'theoretical' monomolecular layer of water in all the transverse ply cracks would amount to about 3×10^{17} molecules, which is significantly below the sensitivity of the weighing experiments. Thus, although based on a number of assumptions which tend to oversimplify the true situation, this calculation clearly indicates that substantial quantities of water can in fact accumulate at damage such as transverse ply cracks without being detected by simple weighing measurements. Such water could affect the properties of the composites, for example by causing localised degradation of the reinforcing fibres. The effect on the fatigue properties of preloading to a known

damage state prior to boiling water conditioning is investigated in Chapter 7.

b) CFRP

There was no obvious effect of preload on the weight gain curves for the CFRP, Figure 4.15. The influence of preload is not clear from the maximum weight gains (Figure 4.17b) but the re-drying results in Figure 4.18b show that the overall moisture contents were similar for all the boiled specimens and were unaffected by preload. Although further, more detailed tests are required in order to confirm these findings, it appears that, as in the case of the GRP, the moisture content of the boiled CFRP was not measurably altered by the presence of transverse ply cracks.

c) KFRP

The large scatter in the weight gain curves for both standard and preloaded KFRP samples (Figure 4.16) is associated with difficulties in obtaining reproducible uptake measurements for this material in boiling water (Section 4.1.4a). Weight gains from 65% RH appeared to be independent of preload (Figure 4.17c) as did the saturation moisture contents after 4 weeks boiling indicated by the drying curves in Figure 4.18c. Overall weight changes were larger for KFRP, owing to absorption by the fibres as well as the resin, and this served to hinder identification of any possible effects of preloading.

4.5.2 Apparent Diffusivities

Although the damage caused by preloading did not produce any consistent, measurable increase in the overall water uptake for any of the laminates, there remains the possibility that such damage

could alter the absorption characteristics of the coupons. Cracking might be expected to increase the apparent diffusion coefficient and also reduce any correspondence to Fick's Law. This can be investigated by analysing plots of weight gain against $\sqrt{t}$ for immersion in boiling water. In this Section the slopes and 'strengths' of the initial linear portions of the plots are compared using the Ramberg-Osgood curve fit analysis outlined in Section 4.3.1.

Apparent diffusion coefficients for the standard preloaded specimens were calculated using Equation 4.5 from values of A obtained in the Ramberg-Osgood curve fit. The apparent diffusivities for the GRP and CFRP are plotted as a function of preload in Figure 4.19.

The effect of preload on the diffusion coefficient for CFRP appears to be slight up to the maximum preload of 0.8 GPa. GRP also appears to be unaffected at or below 0.45 GPa, but above this the data points are more scattered and show a definite trend towards higher diffusivity. At 0.79 GPa preload (fast loading) the apparent diffusivity has risen to about $9 \times 10^{-8} cm^2 s^{-1}$ compared to $2 \times 10^{-8} cm^2 s^{-1}$ originally. The situation is shown more clearly in Figure 4.20 in which the diffusion coefficient is plotted against the prestrain corresponding to the appropriate preload. Strain gives a better indication of the damage suffered by the composite and allows direct comparison between laminates since the damage inflicted by a particular preload depends very much on the modulus of the load bearing fibres. The absence of any change in diffusivity for CFRP is not surprising in view of the fact that even at 0.8 GPa the strain is still well below that which causes an increase for

GRP ($\sim$ 2.0% ε).

The saturation density of transverse ply cracks is approached in both laminates without any change in the apparent diffusivity. It is not until the onset of longitudinal ply splitting (which occurs only in the GRP) that increases in diffusivity are observed. Although the increases might be associated with general damage in the resin at these strain levels, the correlation with the longitudinal splitting suggests that the two could be related. No resin damage was actually observed under the microscope and Morgan, O'Neal and Fanter(30) have shown that diffusion in epoxy resins similar to Code 69 is not affected by preloads (unless there are permanent dilatational changes, as caused by crazing close to failure).

Except after very high preloads for GRP, the longitudinal plies, including those at the top and bottom surfaces of the specimens, are undamaged. The fibres running parallel to the surface limit the diffusion and as a result the cut edges, which have a much lower surface area, play a significant role in absorption of moisture (Section 4.3.2.). Transverse ply cracks come into direct contact with liquid water only at the edges and in an orientation (parallel to the fibres) where absorption rates are already high. When longitudinal splits are formed, those in the outer plies intersect the top and bottom surfaces. They also intersect the cracks in the transverse plies forming a network of interconnecting transverse ply cracks and longitudinal splits through the specimen thickness. A thin film of water spread throughout this network could provide a plausible explanation for the observed results. Although not great enough in itself to affect the weight gains of the specimens within the sensitivity of the measurements, the film could nevertheless allow more rapid penetration of water into the

interior of the specimen by capillary flow and increase the surface area for absorption (by up to 5-6 times for the 50x10mm specimens).

The ratio of $\frac{B}{A}$ in the Ramberg-Osgood curve fit gives an indication of the strength of the deviation from the initial linear slope (from which the apparent diffusion coefficient was measured) and as such can be used to indicate trends away from Fick's Law. The plots of $\frac{B}{A}$ against preload for CFRP and GRP (Figure 4.21) are generally similar to those for the diffusion coefficients, with the only strong effect occurring for GRP above 0.45 GPa, where the values of $\frac{B}{A}$ increase and become more scattered. The increased non-linearity in the weight gain against $\sqrt{t}$ plot indicates that different or additional absorption mechanisms are operating, and is consistent with the mechanism for increased diffusivity discussed above. There is no reason to expect the diffusion to remain 'Fickian' in these circumstances. The rate of preload itself had no observed effect on the absorption characteristics.

The apparent diffusion coefficients for the KFRP specimens are plotted as a function of preload in Figure 4.22 and the corresponding prestrain in Figure 4.23. The generally higher diffusivity for the preloaded specimens is most likely due to a greater proportion of cut edges to total surface area compared to the standard coupons. The absorption by the fibres has a strong effect on the diffusion characteristics of this material, the diffusivities being an order of magnitude greater than for the CFRP and GRP. Figure 4.23 shows that increases in rate of absorption occur at lower strains than for the inorganic fibre composites. This could substantiate later suggestions (Chapter 5) that in addition to normal transverse ply cracking, damage

also occurs in the longitudinal plies at low stress levels, possibly involving fibre splitting. The greater nonlinearity in the initial $\sqrt{t}$ plot for the KFRP, associated with the absorption by the fibres, is reflected in higher $\frac{B}{A}$ ratios with values of 2 to 2.5 compared to about 1 for CFRP and GRP. These help to account for the greater scatter in measured diffusivity for this material. The $\frac{B}{A}$ ratio shows a general rise with increasing preload (Figure 4.22), up to a value of about 7 for 0.6GPa, mirroring the increased absorption rates.

4.5.3 Support for Observed Effects

It is important to draw a distinction between the results reported here, in which a preload was applied and the moisture absorption measured afterwards in the unloaded state, and those where the uptake is measured for material actually under load. The presence of applied external load, whether static or cyclic, is usually found to increase both rates and levels of moisture uptake in composites(42,102,139). Often such increases do not become significant until a certain critical level of stress or strain is reached. This has usually been found to correlate with some form of damage, such as transverse ply cracking in 0/90 laminates(57,139), and the effect is therefore greatest where the failure strain is high or a large proportion of the fibres or plies are angled away from the load(140). It is likely that tensile loads 'hold open' debonds and resin cracks, allowing moisture to penetrate the composite by capillary action. It has been suggested that there may also be a contribution arising from an increase in free volume in the resin under volumetric strain. Although any damage will remain when the load is removed, a reduction in moisture uptake under

these circumstances is not surprising.

The absence of any large changes to the equilibrium moisture content and (for most preloads) the apparent diffusion coefficient is supported by recent results of Curtis and Moore(141), who found no significant changes in the absorption characteristics of a $[0_2/-45_2/90_2/+45_2]_2$ CFRP laminate in a 70°C/95% RH environment after various compression fatigue loadings, despite cracking in the 90° and 45° plies and in some instances limited delamination between these, but notably no damage to the outer 0° plies. There is some corroboratory evidence that diffusivity may be increased where crack or debond damage is excessive, as is likely to be the case for preloaded woven cloth reinforced laminates for instance. McGarry(142) observed a three-fold increase in the moisture absorbed by a cross-laminated glass/epoxy composite after preloading to 75% of the failure stress and subsequent immersion for 1 day in water at room temperature (this was a measure of uptake rate since equilibrium moisture content would not have been reached in this short time) and was able to correlate moisture uptakes for various preloads with the area of transverse ply cracks formed.

CHAPTER 5

STATIC TENSILE TESTS

The monotonic tensile properties of the laminates, after various environmental exposures, are presented in Tables 5.1 to 5.4. The main emphasis was placed on testing at the 'slow' loading rate for which a comprehensive set of data for the full range of conditions (as defined in Chapter 3) was obtained (Tables 5.1 and 5.2). The 'fast' tensile properties (Tables 5.3 and 5.4) correspond to those conditions used in the fatigue test programme (Chapter 7). For practical reasons the strain and moduli data in Table 5.3 are based on single test results only.

5.1 INFLUENCE OF ENVIRONMENT ON TENSILE STRENGTH OF 0/90 LAMINATES

5.1.1 CFRP

Tables 5.1 and 5.3 show that the tensile properties of the 0/90 CFRP were not significantly affected by any of the standard environmental exposures. This can be attributed primarily to the resistance of the carbon fibres to temperature and moisture but also to the relative environmental stability of the Code 69 epoxy matrix. Moisture did affect the formation of secondary crack damage but this did not alter the strength and is discussed further in Section 5.2.

The only degradation observed for the CFRP laminate was a 10% loss of strength after 6 months in boiling water. This was a very severe hygrothermal exposure for the epoxy resin and caused crack damage in both longitudinal and transverse plies (Figure 4.8) and deterioration in strength in all three laminates. Similar losses in strength for CFRP have been observed during temperature/humidity cycling (with 12 hours at 2°C and 0% RH alternating with 12 hours at 85°C and 100% RH) after about 350 cycles (1 year) and these were also accompanied by large amounts of cracking in the laminate.

The failure appearance, shown in Figure 5.1, was similar for all conditions and involved extensive damage which usually occurred over most of the gauge-length, even when initiating close to the Instron grips (no results are reported for any specimens where failure actually occurred at the grips). The damage included extensive splitting and delamination of the longitudinal plies and frequent delamination and loss of the transverse plies close to the specimen surface.

5.1.2 GRP

The 0/90 GRP showed strong load-rate dependence (Section 5.4) and this means that the data obtained in the fast and slow load-rate tests (Tables 5.1 and 5.3) are not directly comparable. Nevertheless, each set of data is self-consistent and the basic effects of environmental conditioning are the same in each case. The strength and failure strain were similar in the dried and 65% RH conditions, but 3 weeks immersion in boiling water reduced both to less than one half of their original values. The rate of loss of strength of the GRP in boiling water decreased with time, as shown in Figure 5.2, in this case for fast loading although the trend was similar for slow loading. Prolonged boiling for 6 months resulted in further weakening, reducing the strength and failure strain to approximately one third of the 65% RH values.

Little if any of the strength and failure strain were recovered on redrying the laminate, which indicates that the damage caused by the boiling water exposure was irreversible and most likely involved degradation of the glass fibres themselves. The deleterious effect of water was confirmed by the fact that exposure to high temperature alone

(100°C for 3 weeks) had little effect on the laminate properties, and may actually have caused a slight increase in strength and failure strain for both the GRP and CFRP laminates.

Immersion in water at 23°C for two years caused a 10% loss in strength and failure strain for the GRP. The specimens had not quite reached saturation but the degradation was still much less than expected for a similar weight gain in boiling water. It would appear that as well as accelerating the rate of moisture uptake, the elevated temperature of the boiling water exposure led to increased corrosion of the glass fibres, presumably facilitated by localised breakdown of the interfacial bonding and silane coupling agent.

An attempt was made to discover more about the nature of the fibre degradation after 3 weeks in boiling water by examining the fracture surfaces using a scanning electron microscope (SEM). As Figure 5.3 shows, the fibre surfaces were smooth and free from the type of extensive pitting damage observed by Ashbee and Farrar (143) for fibres in E-glass/polyester specimens that had been immersed in boiling water for 400 hours and by Ishai(139) for fibres in E-glass/epoxy after 864 hours immersion at 80°C. This would indicate that in the present work the coupling agent provided relatively good protection for the glass fibres.

The failure appearance of 65% RH and dried GRP specimens (Figure 5.4) was basically similar to that for the CFRP, although damage tended to be more extensive with increased longitudinal splitting, notably for the faster loading rate tests (Figure 5.5). Failures of specimens that had been boiled were generally much more localised with less extensive

delamination or longitudinal ply damage. The fracture surfaces were quite flat, with cracks passing directly from weakened fibre to weakened fibre along the main crack plane.

The stiffness of the GRP laminate was not significantly affected by any of the environmental exposures despite the reported large changes in strength and failure strain. This is not unexpected in view of the fact that the modulus of the glass fibres is an intrinsic property of the glass and corrosion damage affects only the fibre surface. The fibre strength and failure strain are controlled by surface flaws and this explains their sensitivity to the environment.

5.1.3 KFRP

The 0/90 KFRP showed only a moderate reduction in strength after 3 weeks exposure to boiling water. This is not unexpected in view of the environmental stability of the fibres. Strength losses of 2%(12) and 18%(13) have been reported for Kevlar fibres themselves after immersion in boiling water for 4 to 7 days. The strength loss of the composite after boiling for 6 months was much more serious and presumably reflected damage to the matrix in addition to further degradation of the fibres. This was an extremely severe hygrothermal exposure however.

The increase in strength after 2 years in water at 23°C is somewhat surprising, although it is comparable to the 10 to 15% increase reported by Roylance(19,144) for a unidirectional KFRP composite immersed in water at 50°C for 2-3 weeks (saturation). Roylance attributed the

strengthening to the relief of residual thermal stresses or possibly to improved alignment of the fibres under load facilitated by limited plasticisation of the resin (Fiberite 934). Alternatively, the effect could be due to optimisation of the interfacial bonding.

The absence of any degradation in water at room temperature and the similarity in the strength reduction after 3 weeks immersion in boiling water and after exposure to air at 100°C for the same length of time (Table 5.1) could suggest that it is the high temperature alone that causes the weakening of the Kevlar fibres rather than the combined action of water and temperature. However, there is no evidence in the literature of any substantial reduction in room temperature strength for fibres previously exposed to air at 100°C, although exposure at 160°C is known to cause some degradation(9,13,43). Furthermore, the resin matrix should help to protect the fibres from oxidation(43).

Drying at 60°C caused a reduction in the tensile strength and failure strain of the KFRP laminate. This behaviour was not expected and contrasts with that of the other two materials. Such drying does however account for the reduced properties of the specimens conditioned for 3 weeks at 100°C. Furthermore, redrying the 3 weeks boiled specimens did not lead to recovery (despite the reported reversible effects of moisture and temperature on Kevlar fibres themselves(43)) but instead resulted in a further substantial reduction in strength. Allred(79) also found that saturated KFRP composites did not recover their original strength (in flexure) upon redrying although he did not observe any additional degradation below the wet strength.

Since Kevlar fibres themselves should not be significantly affected by prolonged exposures to temperatures up to 60°C, it must be assumed that the degradation caused by the drying is associated with the interface and the loads imposed on the fibres via the interface. It is interesting to note that while the 65%RH tensile strengths for the CFRP and GRP were close to the values expected from typical fibre and unidirectional ply properties (Tables 2.1 and 2.2), based on a simple mixture rule, the strength of the KFRP falls somewhat below the predicted values. This discrepancy could be associated with the strength of the interfacial bond. While some degree of bonding is essential for shear load transfer, excessive bond strength can lead to reduced tensile strength as a result of transverse or shear loadings on the radially weak fibres (18,27).

Drying increases the residual stresses present in 0/90 laminates and the high radial contraction of the Kevlar fibres, which is 0.5-1%/% moisture loss compared with around 0.27%/% for the resin (Table 2.1), means that there is a tendency for the fibres to shrink away from the matrix. It therefore seems likely that the strength reduction is due to damage resulting from increased tensile stresses transverse to the fibres. This damage, in the form of fibre debonding and/or fibre splitting and fibre skin-core debonding, will impair load transfer within both the composite and the fibres themselves. It may occur immediately, during the cool down from the drying temperature or subsequently during tensile loading. Since the tensile failure of Kevlar fibres occurs by the propagation of cracks at a small angle to the fibre axis, involving the splitting of successive bundles of fibrils(20), transverse tensile stress might be expected to aid this process. The initial high concentration

of water in the boiled specimens, and the degradation that this causes, should promote increased damage of the type discussed above upon drying.

The failure appearance of the KFRP specimens was generally similar to that for the CFRP and GRP except that it involved extensive internal splitting of the fibres in addition to the normal damage modes (Figures 5.6 and 5.7).

As in the case of the CFRP, temperature/humidity cycling for periods in excess of one year reduced the strengths of both the GRP and KFRP below the three weeks boiled values to the level of the 6 month boiled laminates. Both exposures caused environmental cracking in the laminates.

5.2 EFFECT OF ENVIRONMENT ON THE BUILD-UP OF TRANSVERSE PLY CRACKS AND LONGITUDINAL SPLITS IN 0/90 LAMINATES

The tensile stress-strain curves for the 0/90 CFRP and KFRP laminates were basically linear to failure for all environmental conditions, Figure 5.8. Close examination sometimes showed an increasing modulus with increasing strain for CFRP. This has commonly been observed with fibre controlled carbon reinforced plastics and has been associated with preferential reorientation (straightening) of the fibres (145).

The 0/90 GRP exhibited a reduction in modulus during loading (by up to 35%, Table 5.1) mainly at the characteristic 'knee' in the stress-strain curve, Figure 5.8. This was due to the formation of transverse ply cracks which were clearly visible to the naked eye and were also observed by sectioning and polishing preloaded specimens (Figure 5.9a). The latter technique confirmed the occurrence of transverse ply cracks in the CFRP and KFRP laminates (Figures 5.9b-c), although the much lower contribution of the transverse plies to the overall stiffness negated any significant change in modulus for these laminates.

The build-up of transverse ply cracks and longitudinal splits (where applicable) in the GRP and CFRP is shown in Figures 5.10a-b. The data were obtained by counting the cracks in polished 10mm transverse and longitudinal sections taken from preloaded specimens and viewed under an optical microscope. The general form of the damage accumulation curves follows the predictions of Garrett and Bailey (123) and Bailey et al (120) for transverse ply cracking in 0/90 laminates.

Damage accumulation was also monitored by recording acoustic emission (AE) output from specimens during loading. Typical graphs of AE event counting rate against stress (with the top curves giving the total count rates in each test and the lower curves representing successively higher amplitude events as indicated) are presented in Figures 5.11 to 5.13 for each of the laminates and environmental conditions. Only the general AE patterns are of interest here. Full details of the technique and

analysis of the results have been presented elsewhere (146, P1,P4, P5). Comparisons between the AE plots and the curves in Figures 5.10a-b indicate correlations between crack formation and AE count rates. These become clearer if the slopes of the crack density curves (i.e. the rates of crack formation) are plotted as a function of stress, e.g. Figure 5.10c. Clearly the initial peaks in the AE plots (for the CFRP and GRP) are associated with transverse ply cracking while the secondary peaks for the drier GRP are due to longitudinal ply splitting. A characteristic common to all the AE plots is a rapid upturn in emissions at high stress levels that signals the onset of the high damage rate leading to failure and includes AE resulting from fibre fractures.

The AE plots confirm that the onset of transverse ply cracking occurred at different stress/strain levels for each laminate and that these levels were raised with increasing moisture content. While the drier GRP underwent both transverse ply cracking and longitudinal splitting, the boiled GRP and the CFRP, with much lower failure strains, exhibited only transverse ply cracks. In fact, transverse ply cracking occurred so close to failure for the boiled GRP that the saturation crack density was not reached (even in the 100kN/s tests where the failure strain and thus crack density were greater) and the emissions were swamped by the overall acoustic activity in this region. Generally, where longitudinal splitting occurred, the density of the cracks remained well below the levels observed in the transverse plies (e.g. Figure 5.10a).

Figure 5.10a indicates that transverse ply cracking and longitudinal splitting showed a slight sensitivity to load-rate, although this was far less than the effect on the ultimate strength of the 0/90 GRP. For a given stress level, the crack density was greater at the higher rate and this was also reflected in the saturation crack densities. This presumably indicates a 'stiffer' response in the direction transverse to the fibres, dominated by the resin.

The early onset of AE for the 0/90 KFRP (Figure 5.13) can be attributed to the lateral weakness of the Kevlar fibres and to the comparatively poor interfacial bonding, which together lead to transverse ply cracking at low stress levels. Split Kevlar fibres associated with transverse ply cracking can be observed in Figure 5.9c. Unlike the other laminates, the emissions did not fall away again with increasing stress but continued until the characteristic rise approaching failure. This may indicate fibre damage (in the form of fibre tearing or splitting) in the longitudinal load bearing plies at quite low stresses, as suggested previously to explain the relatively low strength of the composite compared to that expected from the bare fibre strength. This may also help to explain the disappointing high cycle tensile fatigue performance outlined in Chapter 7.

5.3 TENSILE STRENGTH OF ±45° LAMINATES

5.3.1 Influence of Environment

In theory, the laminates tested were not ideal for ±45° shear strength measurements since they were not balanced and were therefore free from shear coupling stresses only when tested in the orthogonal directions. Where the laminate consists of a

large number of plies this is not usually found to be a problem however(147). For instance, of the eleven plies making up the ±45° laminates tested here, there is a net total of just one ply that is not balanced.

The laminates were much weaker and were generally more sensitive to the conditioning exposures when tested in the ±45° orientation. This reflects the domination of the matrix and interface, which are subjected to maximum shear loading, and the relatively small effect of the fibres in this orientation. The stress-strain curves were all non-linear, exhibiting a rapidly falling modulus with increasing stress (Figure 5.14). This results from the non-linearity of the resin and progressive cracking in the 45° plies, parallel to the fibres, under shear deformation. This cracking, often initiated at the specimen edges, became visible in the outer plies as the peak load was approached, confirming that the laminates retained substantial stress and strain capability beyond the onset of damage. Final failure involved delamination along the ply interfaces, commonly initiated at the specimen edges at the tips of 45° cracks. Once the delamination damage became excessive in one particular region, the specimen became unstable and the strain became concentrated in that region (Figures 5.15 to 5.17).

The 65% RH GRP was unique in that it exhibited a characteristic double peak in the load-extension curve (Figure 5.14). After the initial peak, which was accompanied by cracking in the outer 45° plies and occurred at about 1.8% strain (close to the peak for the CFRP), the load fell only slightly and with increasing strain

rose to a second, higher level peak before final failure. By this time the specimen had undergone extensive ±45° cracking and delamination. The failure strain, which was far higher than for any of the other laminates, is indicative of large shear displacements for this material(148).

The strengths of the GRP and CFRP were quite similar and these two were significantly stronger than the KFRP under all conditions. The latter showed considerable damage in the form of fibre splitting or tearing (Figures 5.17 and 5.18a) indicating that the shear strength in this case was limited by the poor shear and transverse properties of the fibres themselves rather than by the matrix or interface as for the inorganic fibre composites. Indeed, the strength was actually quite high compared with the values reported for other ±45° KFRP laminates (147), confirming that in relative terms the interfacial bonding was good.

All three laminates exhibited optimum strength in the 65% RH condition and were weakened by either drying or boiling water exposure (Tables 5.2 and 5.4 and Figure 5.19). Although moisture is normally expected to reduce the matrix-interface dominated properties of a composite, in cross-plied laminates there is the additional effect of a reduction in the residual thermal stresses (Section 5.2) which may lead to a limited improvement in shear behaviour. The latter effect appears to dominate between 0% RH and 65% RH, which presumably reflects a relatively minor (and at low moisture levels probably beneficial) plasticising effect of moisture on the resin at 23°C. Boiling water however does reduce the strength,

although this is a more severe, hygrothermal exposure which is also more likely to lead to weakening of the interfacial bonding, particularly for GRP and KFRP, and degradation of the glass and Kevlar fibres. In fact, the amount of moisture in the fibres probably made a major contribution to the performance of the KFRP in all the conditions investigated, although no obvious differences in fibre damage with moisture content were observed.

The trend with increasing moisture content was generally towards a more progressive, less sudden mode of failure and an increase in failure strain, consistent with reduced residual stresses and limited resin plasticisation. The only exceptions were the boiled GRP and KFRP both of which showed a reduction in failure strain which was presumably associated with fibre weakening. The involvement of the fibres in the failure of the boiled GRP is illustrated in Figures 5.16 and 5.18b. Broken fibres remained a dominant feature of the fracture upon redrying, where the laminate strength was not recovered, confirming that the degradation was irreversible. As in the 0/90 tests, prolonged boiling caused a further small reduction in strength.

The drier GRP and the CFRP did not exhibit broken fibres in the fracture surfaces (Figures 5.15, 5.16 and 5.18c-d). The CFRP actually showed most clearly the effects of conditioning on the load-deflection curve. While drying from 65% RH caused failure to occur in a more brittle manner, at reduced failure strain, without altering the curve to any great extent, boiling tended to lower

and flatten the curve. For all the laminates, the main effect of drying boiled specimens was to reduce the failure strain. The fact that in this condition the CFRP was weaker than the dried laminate indicates that at least some of the degradation caused by boiling water was irreversible.

The scanning electron micrographs of the fracture surfaces in Figure 5.20 clearly show considerable localised plastic flow of the matrix despite the fact that Code 69 is normally regarded as a brittle resin. This is the case for all the conditions, including fully dried, and is presumably a reflection of the way in which the resin properties are modified under the complex 3-dimensional stresses in high fibre volume fraction composites.

5.3.2 Effect of Specimen Width

In view of the fact that the failure modes in ±45° laminates are complicated by edge effects, a limited investigation was made into the effect of specimen width on the tensile strengths and failure strains of the laminates (under slow loading). The results for 65% RH CFRP, shown in Figure 5.21, suggest a slight increase in both strength and failure strain over a range of widths from 5mm to 21mm. There was also a change in failure mode from sudden, catastrophic failures for the 5mm specimens to much more progressive failures, with a gradual load drop, for the wider coupons. The GRP and KFRP laminates (in both the 65% RH and boiled conditions) behaved in a similar manner to the CFRP, showing a small increase in strength and failure strain (Table 5.5) and a tendency towards a more progressive failure past the peak

load for the wider specimens. Although not shown in the table, the strain and stress level of the initial load peak for the 65% RH GRP were not altered by increasing the specimen width. The excessive increase in failure strain observed for the boiled KFRP was due primarily to strain after the peak load. At the peak, the strain was a more reasonable 2.8%.

The relatively weak dependence of strength and failure strain on the specimen width may be explained by the fact that the edge effects are quite low for ±45° laminates in comparison to laminates with lower fibre angles(9,130). Certainly the strengths and failure strains of the 65% RH 10mm specimens are fully representative of values reported in the literature(34,130, 147,148),revealing no unexpected shear weaknesses for any of the laminates. The standard 10mm wide specimens were therefore judged as acceptable for the fatigue test programme. The only doubt concerned the KFRP laminate which did show a somewhat greater sensitivity to specimen width than the other two laminates. A limited number of comparative fatigue tests were therefore run on 20mm wide 65% RH KFRP specimens to assess the importance of the edge effects on measured fatigue life. These results are reported in Chapter 7.

5.4 SENSITIVITY TO LOAD-RATE

It is clear from Tables 5.1 to 5.4 that the tensile properties of some of the composites were sensitive to the rate of loading. Figure 5.22 shows that while the strengths of the 65% RH CFRP and KFRP 0/90 laminates were basically unaffected by varying the loading rate over 4 orders of magnitude, the GRP laminate exhibited a strong rate dependence of about 75 MPa per decade of testing speed over this range. This is equivalent to a strength increase of 9 to 13%

(depending on the reference strength) per decade. Although not shown, the modulus was not significantly altered since the failure strains were also increased with load-rate.

Table 5.6 summarises the effects of loading rate on the tensile strengths for all the laminates and standard environmental conditions reported in Tables 5.1 to 5.4. Changes in strength are assumed to be proportional to the logarithm of load-rate as indicated by the 65% RH GRP laminate in Figure 5.22. The 0/90 CFRP and KFRP remain insensitive to testing rate, irrespective of environmental conditioning. Although the strength increase for the boiled GRP is only about one half of that for the 65% RH and dried material, the values are similar when expressed as percentages of the respective strengths.

The rate-dependence of reinforced plastics is often associated with the resin matrix. However the fact that the CFRP and KFRP were not significantly affected by testing speed indicates that the increase in strength for the 0/90 GRP is due primarily to the properties of the fibres which control the behaviour in this lay-up and, as explained in Chapter 2, are known to be rate sensitive, unlike carbon and Kevlar fibres.

The rate-dependence of E-glass fibres results from their susceptibility to stress corrosion damage at the surface (Section 2.3.1b) and has been reported by Metcalfe and Schmitz(71) to be about 300MPa per decade over the appropriate range of strain-rates. This represents about 10% of the strength of their fibres, which were very strong.

They also observed that strength effects in individual fibres due to corrosion damage were proportional to the fibre strength. A limited study at Bath into the rate-dependence of single glass fibres (50mm gauge-length) taken from rovings of commercial Silenka E-glass and with strengths more representative of those used in the laminates, has indicated a strength gain of 104 MPa per decade, about 7% of the fibre strength.

These fibre values compare well with the percentage strength increases for the 0/90 GRP laminates and also with those for fibre controlled GRP composites reported elsewhere(99,114,149).

Any direct contribution made by the resin to the composite rate-dependence should be negligible(31,149) and well within the tensile strength scatter bands of the 0/90 laminates.

The ±45° laminates showed a moderate increase in strength with testing speed. The increases for the GRP were generally no greater than those for the other laminates, indicating presumably that the effect was due primarily to the matrix rather than the fibres in this orientation.

5.5 COMPARISON OF SPECIFIC PROPERTIES

Since high performance composites are of primary importance in situations where weight must be kept to a minimum, the measured tensile strengths and moduli for both the 0/90 and ±45° laminates (65% RH, slow loading) are compared in Table 5.7, after normalising for their different specific densities. Some values for typical

engineering materials are also included. It is clear that even in the cross-plied lay-up, the specific properties of the CFRP and KFRP laminates are excellent, although only in the main fibre directions. The lower specific properties and lower cost of the fibres makes GRP something of a compromise choice where weight saving is not of the utmost importance.

CHAPTER 6

STATIC FLEXURE TESTS

The results for the static bend tests are reported in this Chapter. Short beam shear was used to measure the effect of environment on the ILSS. Flexural strengths (required for comparison with the Avery flexural fatigue data) were obtained in 4-point bending, 3-point bending and Avery flexure, although only the 3-point bending actually produced flexural failures for all of the laminates.

6.1 SHORT BEAM INTERLAMINAR SHEAR TESTS

The ILSS data, calculated from the measured failure loads using the simple beam theory equation for 3-point loading (Appendix 2, Equation A2.3), are presented in Table 6.1 and Figure 6.1. (The data provide a qualitative guide to the shear properties rather than absolute values of the shear strength).

Drying from 65% RH caused significant reductions in the ILSS of all the laminates (Table 6.1). Furthermore, the GRP and KFRP were both weakened by boiling water exposure, although the CFRP was little affected. Despite the difference in failure modes, the results tend to confirm the observation made for the ±45° tensile tests that the optimum shear strength occurs in the intermediate condition.

The lay-up plays an important role in the interlaminar shear failure of 0/90 laminates since it results in a different, more complex failure mode to that exhibited by unidirectional composites and this makes interpretation of the results difficult. A typical failure is shown in Figure 6.2 (for 65% RH CFRP). In addition to the expected delamination at ply interfaces, the failure exhibits cracks in the 90° plies, but unlike

the transverse ply cracks in normal tensile tests these cracks are formed at an oblique angle to the 0° plies. Such a failure mode is characteristic of interlaminar shear failures in cross-plied laminates(81,107, 109,150,151). Morris(150), who worked on an eleven ply carbon/epoxy laminate of identical lay-up and thickness to that used here, demonstrated that the oblique cracks can be accounted for by the position and orientation of the maximum principal stress in the layers and that it is these cracks that initiate failure. The shear, and thus the resolved tensile stress component, is greatest through the central ply. In other plies, the flexural stresses are non-zero and therefore affect the angle of the cracks such that they remain orthogonal to the resolved tensile stresses in the ply. The ILSS reported in Table 6.1 are generally lower than the values expected of unidirectional material, where cracking is confined to the shear mode parallel to the fibres. This can be explained by the low strength of the plies transverse to the fibre direction (Table 2.2). This is particularly poor in the case of KFRP where fibre splitting can also occur.

As for the ±45° tests, the effect of moisture on the strength depends on a number of factors, including resin plasticisation, changes to the residual thermal stresses, degradation of the interfacial bonding and, in some instances, fibre weakening. On the basis of the failure mode, it would appear that factors affecting the strength of the transverse plies should be particularly important. Drying tends to increase the residual thermal stresses (Chapter 5) and might therefore be expected to lower the load required for the formation of the oblique transverse ply cracks. In KFRP debonding or fibre splitting may occur as a result of the mismatch in fibre and resin swelling coefficients. Drying also tends to make the resin

more brittle, less compliant. While immersion in boiling water causes a relaxation in the residual thermal stresses, other mechanisms must be acting which weaken the composites. Any resin plasticisation should reduce the strength of the ply interfaces and also increase the importance of any weakening of the fibre-matrix interface (or the fibres). It may be that since the principal tensile stresses are not parallel to the neutral plane, any drop in transverse strength is reflected more directly than in normal tensile loading (where the high modulus longitudinal plies limit the stresses in the transverse plies). The retention of ILSS by the CFRP during boiling may indicate that the fibre-matrix interface is less susceptible to degradation than for the other two materials. It also indicates that degradation of the matrix properties, whether by plasticisation or, more permanently, by resin cracking or chemical breakdown, is not great. This is in accord with the 4-point bend test and Avery flexure results that follow.

6.2 4-POINT BEND TESTS

Under 4-point bending, the CFRP and KFRP failed in a shear mode and the GRP in a flexural mode, irrespective of environmental conditioning. The 'apparent' flexural strengths (Table 6.2) and shear strengths (Table 6.3) were calculated using Equations A2.2 and A2.3. Only the maximum flexural stresses survived are reported for the CFRP and KFRP. The effect of moisture content on the 4-point bend strengths for each of the laminates must be considered separately according to the failure mode (Figures 6.3 and 6.4).

It should be noted that only those specimens tested at the two lowest moisture levels (dried and 65%RH) and the highest level (boiled for 4 weeks) had been brought to equilibrium with their conditioning environments. The others (boiled for 2 weeks or less) had non-uniform moisture distributions, with falling moisture concentrations moving away from the surface into the specimen.

Typical load-deflection curves for all three laminates (65%RH) are presented in Figure 6.5.

6.2.1 Shear Failures - CFRP and KFRP

a) Failure mode

The CFRP and KFRP laminates failed by interlaminar shear in the highly consistent pattern shown schematically in Figure 6.6. The mode was basically similar to that in the ILSS tests (Section 6.1) and involved oblique transverse ply cracking in the 90° plies (initiated just outside the central span) and delamination along the adjacent 0/90 ply interfaces. Often these modes were not confined to single events or just one side of the specimen as depicted in the figure. The interlaminar shear cracks usually propagated into the region between the inner load points and along the full length of the specimen. The location of the oblique cracks, close to one of the central load points and in the second 90° ply from the tensile surface (rather than in the mid-ply where the shear stresses were greatest) indicates that the tensile flexural stress, which was quite large in this region (but zero along the mid-plane) influenced the failure. This was substantiated by a steeperangle to the oblique cracks.

Further evidence indicating the importance of the flexural stresses is provided by the fact that the 4-point bend shear strengths reported here are lower than the short beam ILSS values. Ideally the shear strength should not be affected by loading span (Equation A2.3). However, Figure 6.7 shows that the calculated ILSS (for 65%RH CFRP) falls as the S/d ratio (and thus the magnitude of the flexural stresses) is increased and that the 4-point bend shear strength is similar to the ILSS provided that the equivalent span is based on the outer sections only (S = 31.75mm).

The usual reservations apply to the calculated 4-point bend test data, particularly since failure did not actually occur at the neutral or mid-plane nor in a truly interlaminar shear mode. Also, while the flexural load-deflection curves for the CFRP (Figure 6.5) were basically linear to sudden failure, the KFRP showed non-linear response above about one half of its maximum load and the specimens were permanently deformed after bending to large deflections, unlike the other two laminates. This can be explained by the known poor non-linear compressive behaviour of this material(79,111,152), caused by fibre buckling or kinking which was most prominent under the central (compression) load points. This damage, illustrated in Figure 6.8, was noticeable mainly after the peak load (upon which the calculation of the shear strength was based) and might therefore be expected to have influenced the strength measured. Indeed, it could be argued that the specimens had already failed in a flexural mode at the compression surface by fibre microbuckling prior to shear failure. No similar damage was observed for the CFRP.

b) Influence of Environment

It is difficult to draw any firm conclusions about the effect of moisture on the strength of the laminates from Figure 6.3.

The data for CFRP show a great deal of scatter, although there is an indication that the mean strength was slightly higher at intermediate moisture contents, corresponding to short periods in boiling water (less than 24 hours, at which the moisture was not evenly distributed throughout the specimen). The KFRP exhibited far less scatter but was not significantly affected by drying or boiling water except for a small reduction in strength close to saturation (after 2 weeks conditioning). The extremely complex failure mode inhibits analysis of the data, and while the effect of moisture appears to be basically consistent with the interlaminar shear test results, it is much less pronounced. This may reflect the increased importance of the flexural stresses in these tests. The lack of any significant effect of moisture on the flexural strength is in agreement with the observations of Allred(79) for a quasi-isotropic $[\pm 45,0/90]_6$ KFRP laminate, although his results suggest that there may be a significant reduction in strength at elevated temperature (150°C).

6.2.2 Flexural Failures - GRP

a) Failure Modes

The GRP, which failed in a flexural mode, showed a much greater dependence of strength on moisture content in 4-point bending than the CFRP and KFRP laminates. At low moisture contents, failure occurred progressively by cracking and delamination (into thin strips)

of the surface ply on the compression side, initiated at the two load points and confined to the region between them. Often random multiple interlaminar shear failure occurred before total failure of the outer ply was complete.

At higher moisture contents the mode changed and tensile surface ply cracking became evident such that compression and tension surface failures initiated almost simultaneously at about 0.9% moisture (corresponding to 24 hours in boiling water). Above this, only tensile failure occurred, by progressive cracking and strip delamination within the central span of the outer ply. At or near saturation (2-4 weeks in boiling water) failures were sudden and much more localised, usually adjacent to one of the central load points. There was little longitudinal cracking.

b) Influence of environment

Since failure was dominated by two different modes, Figure 6.4 has been divided into two parts, each with a distinctly different slope, and separate straight lines have been drawn through the two sets of data, crossing at the point where compression and tension ply failures were initiated simultaneously.

The failures indicate that at low moisture contents the effective compression strength was below the tensile value, causing failure to occur at the compression surface. The results show a gradual reduction in compression strength with increasing moisture content. This was presumably due to reduced support provided by the matrix against fibre microbuckling - associated mainly with interfacial

degradation rather than increased resin compliance since the flexural strength of the CFRP in boiling water was hardly affected (Section 6.4) - and reduced buckling strength of the fibres themselves. Also, it must be assumed that the compression performance was influenced by the stress concentrations or damage at the inner load points, since failure for the 65%RH 3-point bend test and Avery fatigue test specimens (Section 6.3 and Chapter 8) occurred at the tensile surface. In Chapter 5 it was shown that while drying had little or no effect on the tensile strength of the 0/90 GRP, boiling was much more damaging. This is reflected by the slope for the tensile failure mode in Figure 6.4, which is more severe than that indicated for the compression mode. Thus failure occurred at the tensile surface when the tensile strength had fallen below the effective compression value, which was for moisture contents above about 0.9%.

6.3 3-POINT BEND TESTS

The 3-point bend strengths, calculated using the simple beam theory Equation A2.1, are given in Table 6.2 for the 65% RH condition. While all failures occurred under the central load point in the flexural mode, the details differed for each laminate.

The CFRP failed by cracking (and subsequent delamination) of the outer ply on the compression surface. By contrast, the GRP failed by jagged fracture (accompanied by extensive cracking parallel to the fibres and delamination) of the outer tensile ply. Initially, failure for the KFRP appeared to be at the tensile surface,

but close examination showed buckling and cracking of the outer compression ply also. Damage in boiled KFRP was confined to the compression surface.

Fracture at the tensile surface for GRP and the compression failures for CFRP and KFRP correspond to the modes normally reported for these materials and as such, reflect the relative magnitudes of their tensile and compressive strengths. Although the values reported in Table 6.2 are useful, the simplified analysis used in their calculation means that they bear little resemblance to the 'true' flexural strengths and are not strictly comparable. This is highlighted by the GRP, where the shorter span reduced the non-linearity in the load-deflection curve (which was common to all the laminates) and increased the calculated strength.

6.4 AVERY FLEXURE TESTS

Table 6.2 includes 65%RH bend strength data for specimens tested in static flexure using the Avery machine.

The tests were performed primarily to obtain static flexural strength data for comparison with the flexural fatigue results obtained using the same machine. The surface stresses were calculated using simple isotropic beam theory as explained in Appendix 2.

The CFRP failed in compression by cracking initiated in the outer ply at both grip points and delamination at or close to the first ply interface. The angle of flexure at failure for the three specimens tested was within the range 28° to 31°.

The stresses quoted in Table 6.2 for GRP and KFRP are the maximum attained, since the flexural failure strains of these laminates were outside the range of the machine which was limited to flexural angles of about 50° in static bending (and only 24° in fatigue). This necessitated the use of independent 3 and 4-point bend tests (Sections 6.3 and 6.2) to enable estimation of the bend strengths.

The flexural stress noted for KFRP is only very approximate. The material showed significant creep effects such that the flexural surface stress at constant deflection decayed even over a period of a few minutes (Figure 6.9). Also the flexural load-deflection curves were non-linear, presumably due to the non-linear compressive behaviour of this material resulting from low stress level kinking or buckling of the Kevlar fibres as occurred also in 3 and 4-point bending.

The CFRP and GRP showed no such creep and their load-angular deflection curves were basically linear throughout.

Preconditioning in boiling water for 3 weeks slightly increased the flexural strength of the CFRP from 0.9 to 1.0 GPa (mean of 3 tests), although the failure mode was not altered.

6.5 EFFECT OF $^{S}/_{d}$ RATIO

The results in Sections 6.1 to 6.3 show clearly the trend from shear to flexural failures as $^{S}/_{d}$ and thus the ratio of flexural to shear stresses is increased. It can be shown that the flexural stresses in the surface plies at shear failure in the short beam shear tests ($^{S}/_{d}$ = $^{5}/_{1}$) were well below the longitudinal strengths shown in Table 2.2. Similarly, the predicted shear stresses at flexural failure in the 3-point flexure tests ($^{S}/_{d}$ = 30 or 40/1) were much lower than those that caused shear failure in the other bend tests. For the intermediate $^{S}/_{d}$ ratio of the 4-point bend tests ($^{S}/_{d}$ = 23/1 which is equivalent to 11.5/1 in 3-point bending) the ratios of flexural stress to flexural strength and shear stress to shear strength were more evenly matched. The different failure modes can be accounted for by the different ratios of flexural to shear strength for each of the laminates. This is evidently lower for the GRP than for the CFRP.

The use of different bend tests and geometries makes comparison of the flexural strengths difficult and also inhibits comparison with the longitudinal tensile strengths. This is because flexural loading gives greatest weight to the material at or near the surface and, additionally, simple beam theory underestimates the flexural stresses for the 0/90 laminates tested (by up to 35% for the CFRP and KFRP). The results from the 3-point, 4-point and Avery flexure tests are discussed further in Chapter 8 in conjunction with the flexural fatigue results.

CHAPTER 7

TENSILE FATIGUE TESTS

The tensile fatigue results are presented in the form of S-logN (cyclic stress versus log cycles to fail) curves. The static tensile strengths, taken from Tables 5.3 and 5.4, are plotted conventionally at one half-cycle and represent the strengths of the laminates in monotonic loading when tested at the load-rates used in the relevant fatigue tests. This approach is particularly important for materials, such as the GRP, where the strength variation with load-rate is large.

S-logN curves for the laminates in the 3 standard environmental conditions form the basis of the results reported in this Chapter. Additional fatigue tests are reported where they help in the interpretation of previous results or are of particular interest.

7.1 TENSILE FATIGUE PERFORMANCE OF 0/90 CFRP

Figure 7.1a shows that the tensile fatigue performance of the 0/90 CFRP was not significantly affected by any of the standard environmental exposures. The fatigue resistance is generally excellent with a reduction in fatigue strength of only 3-4% per decade of cycling. Although the results exhibit some degree of scatter this is not unexpected in view of the relatively flat nature of the S-logN curves. There is a tendency for the fatigue curves to flatten slightly upon extrapolation to the tensile strength scatter bands. Such behaviour is not uncommon and as explained for the GRP and KFRP laminates (Sections 7.2 and 7.3) reflects the importance of static rather than dynamic failure mechanisms at low cycles. The data show no clear sign of a fatigue limit at 10^7 cycles.

It appears that (as reported elsewhere (68,81,94,96))the environmental and fatigue insensitivity of the carbon fibres in the 0° plies dominates the fatigue performance and that any environmental degradation of the matrix, interfaces or changes in the residual and transverse ply cracking stresses are of little importance. It may be that the impact of any such effects is limited also by the low working strains of this composite.

The appearance of fractured specimens was generally similar to that in monotonic loading, although splitting of the longitudinal plies tended to be more extensive in the high cycle regime.

A characteristic of the high cycle tests in particular was the formation of strip type delaminations in the surface plies during cycling. These formed early on (usually within the first third of the total life) and multiplied and grew progressively along the gauge-length as cycling continued until failing at the end-tabs, commonly well before final specimen fracture. Although neither longitudinal ply splitting nor delamination were observed in normal monotonic tests (Chapter 5) it is known that this type of damage can be induced by fatigue loadings(34,101,127). Jamison et al(127) have shown that longitudinal splits are often nucleated at the tips of transverse ply cracks and accompanied by local delamination at the ply interface. They suggest that this is due to the transverse tensile stress component generated at the crack tip and that delamination is caused by the out-of-plane tensile stress components of both the transverse ply cracks and the longitudinal splits which are additive and therefore greatest where the cracks intersect.

A series of fatigue tests were carried out on 65% RH CFRP in the 90/0 lay-up to see if the presence of 90° plies on the outside improved the fatigue performance by shielding the inner 0° load bearing plies from stress concentrating effects associated with the glued-on end-tabs at the grips and also by preventing strip delamination of the type observed in the outer plies of the 0/90 laminate. As Figure 7.1b shows, the fatigue results for the 90/0 specimens lie within the scatter of the 0/90 data when normalised to account for the lower tensile strength in this orientation, indicating that the above mentioned effects do not significantly alter the fatigue performance of this material.

7.2 TENSILE FATIGUE PERFORMANCE OF 0/90 GRP

7.2.1 Influence of Environment

The tensile fatigue curves for the 0/90 GRP, shown in Figure 7.2a, indicate that boiling causes a large reduction in the low cycle fatigue strength of this material. However, there is no observable difference in the fatigue resistance of specimens in the dried condition compared to those conditioned at 65% RH. This reflects the similarity in monotonic properties and, as in the case of the CFRP, indicates that differences in the residual thermal stresses and moisture content of the matrix are of little importance with regard to the ultimate fatigue resistance of the laminate in these conditions and orientation.

The fatigue curves for the GRP in the 65% RH and dried conditions are non-linear, becoming flatter at very high stress levels (for the extrapolation to the monotonic strength) and also at very low stress levels where there is a tendency towards a fatigue

limit at about 0.1 GPa. Since the load-rate was the same in all the tests and heating effects should not have been important at the 100kN/s load-rate used(114), it appears that in this case the non-linearity in the S-logN curves is genuine and cannot be accounted for by inconsistences in the testing conditions in the manner proposed by Sims and Gladman(114) and Mandell(87). The S-shape of the curve is in fact very similar to that presented by Dharan(36) for a unidirectional glass/epoxy laminate. Dharan's tests were also conducted under constant (low) loading rate conditions to ensure against rate and heating effects, and like the results in Figure 7.2 do not support the view that the S-logN curves for GRP composites are invariably linear with no sign of a fatigue limit. In fact, as Figure 7.3 shows, the fatigue results (excluding the static strength) closely follow a power law relationship and the fatigue life (N_f) can be predicted quite accurately using the following expression

$$\log N_f = 22-7 \log\sigma$$

where σ is the maximum stress per cycle (in MPa). Dharan's(36) fatigue results also produced a linear logS-logN plot.

The fact that the monotonic tensile strength falls below a linear extrapolation of the S-logN curve at high stress levels, despite the use of similar loading rates, is not surprising since it is shown in Section 7.2.2 that stress-rupture or creep damage (i.e. damage that occurs under constant load as opposed to that caused by actually cycling the load) plays an increasingly important part in

limiting the strength at high stress levels. At 590 MPa, the 'slow' static strength, the fatigue life is approximately 100-200 cycles.

The S-logN curve for the boiled GRP shows greater linearity than for the 65% RH and dried laminates. The slope of the curve is also less steep indicating a slower build-up of fatigue damage. Although the shallower slope might be expected because of the much reduced monotonic strength and the corresponding reduction in fatigue strength at shorter lives, what is surprising is the fact that the curves cross so that for cyclic stress levels below about225MPa (i.e. for fatigue lives greater than 10^5 cycles) the boiled material actually survives more fatigue cycles than the drier laminates.

Figure 7.4, which shows the fatigue curves after normalising to the appropriate tensile failure stresses for the different preconditioned states, indicates that the relative fatigue resistance of the boiled GRP is superior to the drier laminates over the full range of lifetimes investigated and that in the work reported here the differences in fatigue performance cannot simply be resolved in terms of reduced monotonic strength.

Because the common S-logN curve for the drier GRP laminates is non-linear, it is not possible to characterise the slope by a single value of the ratio $\frac{B}{\sigma_f}$ (as defined in Chapter 2). However, a value for $\frac{B}{\sigma_f}$ of 0.16 (i.e. a 16% strength loss per decade of cycles) gives a good indication of the slope for the initial

part of the curve (before the curve deviates towards the fatigue limit) while the ratio is closer to 0.13 if all the fatigue data points are considered. By contrast, the value for the boiled laminate is only 0.074. These values differ quite significantly from the ratio of 0.1 proposed by Mandell and his co-workers (87,116) for a wide variety of glass fibre reinforced composites. Far from the degradation rate being constant and independent of factors such as the interfacial bond strength and the matrix, the large reduction in the normalised slope of the fatigue curve suggests that boiling water conditioning results in significant changes in the mechanisms of damage build-up during cycling.

In absolute terms fatigue lifetimes approaching those of unconditioned specimens have been reported previously for weakened moisture conditioned GRP specimens at low cyclic stress levels(115,153,154). For example, Sims and Gladman(115) have presented results for a finely woven 0/90 glass/epoxy laminate which showed that while the monotonic tensile strength was reduced by 24% after immersion in boiling water for 64 hours, the long life (above 10^4 cycles) fatigue results were indistinguishable from those for unconditioned specimens. Boiling caused a reduction in the slope of the normalised S-logN curve (i.e. rate of degradation) although not to the same extent as that shown in Figure 7.4. However the authors gave no indication of the variation in strength and moisture content with immersion time and it is likely that both the magnitude of the reduction in monotonic strength and the effect on the slope of the fatigue curve would have been greater if the period of boiling had been longer. Sims and Gladman found that conditioning in water at room

temperature for 100 days caused only a minor (5%) loss in strength and that the slope of the normalised S-logN curve was unaltered.

The reason for the reduced fatigue sensitivity of the GRP laminate after boiling water conditioning is not totally clear. There is no reason to expect the mechanisms governing the development of fatigue damage in the composite, and thus the relative importance of the fibres, resin and interface in controlling this, to be the same as those governing the monotonic tensile strength, which depends primarily on the strength of the fibres. Thus, if the properties of the components of the composite are altered, as in boiling, a reduction in the monotonic tensile strength does not necessarily mean that there is a corresponding fall in the relative fatigue resistance. That the rate or mechanisms of damage accumulation and/or the state of damage causing final fracture are altered by boiling, as indicated by the superior lifetimes of the boiled material, is confirmed by the difference in shape of the residual strength curves presented in Section 7.5.

A number of effects may contribute to the superior fatigue resistance of the boiled laminate. It is possible that resin plasticisation by moisture may improve the crack growth resistance and long life fatigue strain of both resin and composite(37). However, the lack of any notable effect of moisture content on the fatigue response of the CFRP laminate and the GRP in the drier conditions suggests that matrix plasticisation, which is probably small for Code 69 at room temperature, is of little importance by itself.

Similarly, the relaxation of residual thermal stresses by resin swelling and plasticisation (Chapter 5) appears to have little direct influence on the fatigue performance. Boiling may be expected to weaken the interfacial bonding, thus reducing the stress transfer capacity of the interface. Consequently stress concentrations in the vicinity of resin microcracks or broken fibres should be reduced. The range of fibre strengths is also altered by boiling. In conclusion, the improved fatigue performance probably derives from a combination of the effects mentioned above. One possibility is that the 'critical crack nucleus' size for failure is larger in the boiled condition (or the rate of growth is lower). Such concepts have been discussed in Reference P1, including comparisons with the CFRP. The relative fatigue performance is discussed further in Section 7.7.

The failure appearance in fatigue was generally similar to that in monotonic loading. There was again a tendency towards more localised failures for the boiled specimens. In the high cycle tests the accumulation of damage, in the form of localised delaminated regions with central cracks of obvious fibre damage, was often observed well before final specimen fracture. However, none of the specimens exhibited the outer ply strip delamination characteristic of the CFRP (and KFRP) laminates. This presumably derived from the smaller mismatch in transverse and longitudinal ply properties for the GRP.

7.2.2 Stress-Rupture Tests

The dependence of the tensile strength of the 0/90 GRP laminate on load-rate indicates that time under load has a strong effect

on the performance of this material. The stress-rupture curve for 65% RH specimens confirms this (Figure 7.5). There is an approximately linear drop in strength with the logarithm of time of about 6% per decade over the range investigated. It has been shown that such strength losses can be explained by stress corrosion weakening of the load bearing glass fibres(69,87,116), although there may also be a minor contribution from viscoelastic relaxation effects in the matrix(119).

Figure 7.5 also includes the dynamic fatigue data (R = 0.1) for the 65% RH GRP laminate. These data points are the same as those in Figure 7.2a except that each has been divided by the appropriate testing frequency in order that it can be plotted on a time to failure basis. It should be noted that for these results the stress represents the peak stress per cycle rather than a constant stress level as in the stress-rupture tests and that the time spent at or close to the peak is actually far less than the total time to failure. Bearing this in mind, some interesting observations can be made.

It is clear that for most stress levels cycling the load causes failure over much shorter time periods than continuous exposure to the peak load. Generally the mechanisms of stress-rupture appear to be much less damaging than those of cyclic loading and time under load appears to have little effect on the fatigue life. Harris(86) drew the same conclusion from tests on a unidirectional glass/polyester composite using AE monitoring. Under constant load, AE activity died out rapidly while for fatigue cycling to the same

stress level, emissions continued at a rapid rate.

Figure 7.5 indicates that the fatigue life exceeds that in stress-rupture only at very high stress levels. Thus raising the peak load should be expected to increase the influence of creep damage (and thus dependency on frequency and waveform shape). This presumably explains the deviation of the fatigue curve at high stress levels to the monotonic tensile strength since this is determined by the time-dependent mechanisms that also control the stress-rupture strength rather than those mechanisms dominating the cyclic response.

7.2.3 Differences Between Static and Dynamic Fatigue Degradation. A number of experimental observations confirm the differences between static and dynamic loading and the small effect of time under load on the fatigue resistance of the GRP laminates.

1) The fatigue lives in tests using a triangular waveform were no greater than in the sinusoidal tests (Figure 7.2b) despite the fact that in the latter the load-rate and thus the instantaneous tensile strength varied throughout the cycle, with relatively long periods under high loads and low loading rate. For the sine wave, the maximum rate of loading is at the quarter cycle (i.e. at one half of the peak load) where it is about 50% greater than the average value (of 100 kN/s). The rate falls to zero as it approaches the peak load and the situation is reached where the instantaneous strength falls below the current stress level. Specimen failure does not necessarily follow however, since the rate-dependence of strength

actually depends on the growth of corrosion damage in the glass fibres with time under load and in the fatigue tests, particularly at lower peak stress levels, there is insufficient time per cycle for significant damage of this type to occur.

2) Figure 7.2b shows that increasing the minimum stress level in the fatigue tests to one half of the peak value (so that the stress ratio R = 0.5) whilst maintaining the rate of loading at 100kN/s, had little effect on the fatigue performance of the 65% RH GRP laminate. There is a small increase in fatigue life (by a factor of the order of 2-3 at all stress levels) but the shape of the curve and the degradation rate ($\frac{B}{\sigma_f}$) are not altered significantly. Thus, despite the increase in the average load levels and time close to the peak load, lifetimes continued to be dominated by dynamic fatigue mechanisms. This is in agreement with the results of Mandell et al (87,116), who found that there was very little change in the normalised slope of the fatigue curve for stress ratios between 0.1 and 0.7. For stress ratios above this (i.e. as the alternating stresses became even smaller and the average stress level approached the peak value) the slope fell rapidly, ultimately to the value for the stress-rupture curve (plotted at R = 1). This correlates well with the results reported here. The fall in slope marks a change in the dominant damage mechanisms from those operating in dynamic fatigue, which become less important as the alternating stresses are reduced, to those controlling the creep-rupture strength. Mandell attributed the effect of increasing the R value to reduced abrasion damage to the fibres caused by interfacial movements during cycling.

3) The fatigue life was generally insensitive to cycling frequency within the range 1 to 25Hz.

4) Prior creep damage had no effect on the fatigue life even in cases where specimens had been preloaded for times within the stress-rupture scatter band (Figure 7.6).

Instantaneous tensile preloads as high as 0.7 GPa (80% of the monotonic tensile strength) did not alter the residual fatigue lives of the GRP laminate in the 65%RH condition (Section 7.4.1). It was therefore of interest to determine whether damage sustained under constant load for various proportions of the stress-rupture life affected the residual fatigue performance. The tests were limited to 2 stress levels, 0.53GPa (Figure 7.6a) and 0.58GPa (Figure 7.6b), which gave stress-rupture and fatigue failures over fairly short time periods. Specimens were subjected to the chosen static creep load for different periods of time (indicated by the x-axis in the figures) and then fatigue tested (R = 0.1) to the same stress level until failure (indicated by the y-axis). The residual fatigue lives for the predamaged specimens were all close to the values for the undamaged material (plotted at zero time under preload).

The results highlight differences between the damage sustained under static and fatigue loading. Metcalfe and Schmitz (71) have shown that glass fibres themselves exhibit no reduction in strength for most or nearly all of their stress-rupture lives. While the composite stress-rupture strength is controlled by the fibres, fatigue damage is initiated in the resin or at the interfaces and

involves progressive weakening of the composite on each cycle. Thus, although the GRP can sustain preloads very close to the static strength or for a high proportion of the stress-rupture life without the fatigue performance being significantly affected, both residual monotonic strength (Section 7.5) and stress-rupture life (Figure 7.6c) are reduced by prior fatigue cycling.

7.3 TENSILE FATIGUE PERFORMANCE OF 0/90 KFRP

7.3.1 Influence of Environment

The fatigue curves for the 0/90 KFRP were non-linear in all three standard environmental conditions (Figure 7.7a). The data points show considerable scatter although the trend is clear (and similar) in each case. At higher stress levels (within 10 to 20% of the tensile strength) the fatigue performance is excellent, if somewhat unpredictable owing to the scatter in strength, with a very flat S-logN curve extrapolating to the appropriate tensile strength scatter band. However, at lower stress levels, corresponding to fatigue lifetimes beyond about 10^4 cycles, there is a drastic reduction in fatigue resistance as indicated by the sharp downturn or 'knee' in the fatigue curves.

Over most of the stress range the 65%RH laminate appears to have the best fatigue performance and the dried laminate the worst. The fatigue data are replotted in Figure 7.7b after normalising to the respective tensile strengths for each condition. All the data fall within the same fairly wide scatter band indicating that environmental conditioning does not affect the basic mechanisms of fatigue damage or the downturn in the S-logN curve. The differences in the curves simply

reflect the effect of conditioning on the tensile strength.

The 'knee' in the S-logN curve is particularly unfortunate in view of the fact that the low cycle fatigue performance is superior to that of the other laminates. It also places serious doubt on the future usefulness of KFRP laminates in primary structural applications where large alternating loads are expected and illustrates the dangers involved when extrapolating fatigue data from short lifetimes. It is clearly important to try to identify the cause of the rapid increase in degradation rate and to confirm that the effect is not simply due to the testing arrangement or particular testing conditions used.

7.3.2 'Knee' in S-logN Curves

a) Possibility of damage to surface plies or autogenous heating associated with test techniques

It has generally been recognised that unidirectional KFRP possesses excellent fatigue performance, with a linear S-logN curve approaching that of CFRP (77,87,155). Such behaviour is not consistent with the results reported here however. In appearance the fatigue failures resembled (but were possibly more extensive than) those in monotonic loading and exhibited considerable splitting of the broken fibres. There were no obvious differences (Figure 7.8a) that could be associated with the change in slope and environmental conditioning did not significantly alter the fracture mode. However, longitudinal strip delaminations were observed in the surface plies early in the tests at low stresses. These were similar to those which formed in the

CFRP specimens and continued to grow as cycling progressed.

In order to investigate the possibility that the delamination damage was responsible for the poor high cycle fatigue performance, a series of fatigue tests were carried out on 65%RH samples in the 90/0 orientation i.e. with the fibres in the surface plies angled at 90° to the load direction. These were similar to the tests performed on the 90/0 CFRP (Section 7.1). The results are included in Figure 7.7b where all data are normalised to the appropriate tensile strengths. As for the CFRP, the data points all fall within the scatter band of the 0/90 laminate. The outer 90° plies were seen to eliminate the delamination mode of damage and effectively shielded the 0° plies from any stress concentrations or abrasion damage near the end-tabs and grips. Since the 'knee' in the fatigue curve is still present, these factors clearly did not affect the overall fatigue performance.

Another possibility is that the high cycle fatigue performance was limited by hysteretic heating effects causing the composite to deteriorate prematurely. Such effects have been well documented for GRP(114). Cycling to 0.6GPa at 3Hz caused surface temperature rises of up to 30°C in the fatigue tests on the 65%RH material. The higher frequencies used for the lower stress levels could have led to even greater temperature increases, although the use of a constant average rate of loading should have helped to avoid any serious problems of this kind since even at 0.3GPa (the lowest cyclic stress level tested for this laminate) the frequency was only 6.2Hz.

Roylance (19) has published results which lend support to the view that hysteretic heating did not influence the fatigue performance at the cycling rates employed here. She found that increasing the test frequency from 4.5 to 10Hz had no measurable effect on the fatigue lifetimes of a unidirectional Kevlar/epoxy composite (V_f = 0.7) cycled to high stress levels (1.1 GPa), despite an increase in the surface temperature from 40°C to over 100°C. This is presumably explained by the excellent thermal stability of the fibres and also the resin, which was of a type similar to Code 69. Miner et al (156) found that increasing the frequency from 10 to 30Hz however can lead to reductions in the fatigue life of unidirectional KFRP.

Bunsell(21) has shown that after the first loading cycle Kevlar fibres themselves behave elastically with almost no creep or hysteresis, and that internal heat generation is negligible even at 50Hz. Roylance(19) has suggested that (in addition to the contribution made by the resin) hysteretic heating results from the rubbing together of the internal fracture surfaces of the Kevlar fibres which sustain longitudinal splitting damage during cycling. In this case the autogenous heating would appear to occur as a result of the fatigue degradation rather than to be a cause of it.

b) Support for 'Knee' in the literature

Having concluded that the 'knee' in the S-logN curve is genuine, and not simply a consequence of the testing techniques used, its cause still needs to be established. Furthermore, the discrepancy with the linear S-logN curves normally reported for KFRP needs

to be accounted for. In fact, surprisingly few original data actually appear to have been published concerning the tensile fatigue performance of KFRP. The earliest and most widely quoted results are those of Miner et al (156), for a unidirectional Kevlar/epoxy laminate (V_f = 0.63, R = 0.1) tested at the rather high cycling rate of 30 Hz. The fatigue curve, which included run-outs at 10^7 cycles, exhibited a strength reduction of approximately 4-5% per decade of cycles (which predictably is greater than that for Kevlar yarn) but showed no sign of a downward curvature similar to that reported here. However, the authors also presented limited fatigue data for a Kevlar fabric reinforced/epoxy laminate in the same paper. The results are reproduced in Figure 7.9. Although the tensile strength was not reported, it is clear that the data might be better represented by a curve of the type shown in Figure 7.7 rather than the straight line used by Miner et al.

More recently, Roylance(19) fitted a straight line to her quite extensive tensile fatigue data for a unidirectional Kevlar/epoxy laminate cycled at 10Hz (R = 0.1) in both dry and wet conditions. The strength loss was approximately 6.5% per decade of fatigue cycling in both cases. Straight sided specimens were used, as in the work of Miner et al, although to fit the linear extrapolation of the fatigue data the monotonic strengths of the normal specimens were considered to be too low and higher values obtained using special 'streamline' specimens of different design were plotted instead. The results for the dry specimens (straight sided only) are replotted in Figure 7.9. The points clearly indicate a downward

curvature similar to that reported here. The wet specimens (not shown) exhibited a similar trend although they reflected the higher tensile strength previously noted for Roylance's material in this condition (Chapter 5). Roylance (19) concluded that the fatigue resistance, which was lower than predicted, resulted from abrasion damage to the fibres caused by fretting not only at the internal surfaces of split fibres but also at the fibre/matrix interfaces.

Further support for the 'knee' in the fatigue curve is provided by the recent results of Hahn and Chin (90,157,158) which also show an increase in the slope of the S-logN curve below about 80% of the tensile strength (typically for fatigue lives greater than 10^5 cycles). These tests were performed at 4Hz on a unidirectional composite (V_f = 0.65, R = 0.1) at both room temperature and at 75°C, the latter having little effect on the fatigue performance. Increases in surface temperature of up to 15°C were recorded but were not considered to be a problem.

Thus, the majority of published data tend to confirm the downward curvature of the tensile fatigue curve for KFRP, although this is not always clear from the presentation of results. It appears that the effect derives from the load bearing 0° plies rather than as a consequence of the cross-plied lay-up.

c) Stress-rupture (time-dependent) effects

The increase in slope at the 'knee' of the S-logN curve suggests a change in mechanism governing the fatigue life. Figure 7.10 shows the 65%RH fatigue data plotted on a time to failure basis.

Also included in this figure are the results from stress-rupture tests in which 0/90 KFRP specimens were held under constant load until failure (or the test was terminated). The KFRP exhibited very good resistance to creep-rupture with only a very small reduction in strength over the time span investigated. This can be attributed to the known good resistance of Kevlar fibres themselves(69,74) and contrasts markedly with the far inferior performance of the 0/90 GRP laminate under similar conditions (Figure 7.5).

For lifetimes before the knee in the fatigue curve (i.e. below 10^4 - 3 x 10^4 seconds) there is relatively little difference between the fatigue and stress-rupture data. Beyond this however the curves diverge rapidly with the creep failures showing no sign of a downward trend similar to that in fatigue loading. Since the time under load in the stress-rupture tests is much greater than the effective time at an equivalent load in the cyclic tests, the poor fatigue resistance of the KFRP at lower stress levels cannot be attributed to creep damage. Creep is far more likely to be important in the high stress region of the fatigue curve where the slope and thus fatigue sensitivity are low.

d) Effect of minimum cyclic stress (R - ratio)

For a stress ratio R of 0.1, the fatigue performance of the KFRP may be summarised as follows. At high stresses, before the knee, the fatigue strength seems to be limited by mechanisms closely related to those which determine the monotonic strength. These presumably depend primarily on the initial defects and the stress-rupture behaviour and their comparative insensitivity to load cycling is

reflected in the relatively shallow slope of the fatigue curve in this region. The specimens apparently survive too few cycles for progressive fatigue damage to cause failure. Beyond the knee however, the cycle dependent mechanisms dominate, as indicated by the much steeper slope to the S-logN curve. Failure now occurs in too short a time period for the previous, much less severe static mechanisms to be important. In many ways the situation is comparable to the competing stress-rupture/fatigue mechanisms operating at high stress levels in GRP.

It can be inferred from the preceding discussion that the fatigue performance should be sensitive to the cyclic stress ratio. A small number of fatigue tests were therefore performed with the minimum stress level raised to one half of the peak, i.e. R = 0.5. The results, Figure 7.7c, show a dramatic improvement in high cycle fatigue life, far greater than that shown by the GRP under the same circumstances (Figure 7.2b). The effect on the fatigue curve appears to be an extension of the flat upper region. There is no sign of a 'knee' over the limited stress range investigated, fatigue lives at 0.6GPa being raised by a factor or 10 or more. Since the loading rate was maintained at 100kN/s, the high fatigue lives confirm that autogenous heating at the higher frequencies is not deleterious to the fatigue performance.

e) Influence of environment

It is somewhat surprising that environmental conditioning had no obvious effect on the position of the 'knee' in the fatigue curves. However, the scatter in results could mask any small effects and since

the change in slope occurs gradually it is hard to define the knee accurately in any case. The fact that the normalised data overlap may indicate that the low stress, cycle dominated damage occurs earlier in the dried and boiled conditions, as might be expected. However, since the damage caused by both environmental conditioning and fatigue loading is complex and not fully understood, it is difficult to predict how the two should interact and their subsequent effect on the fatigue curve.

7.4 EFFECT OF PRELOADING DAMAGE ON RESIDUAL FATIGUE PERFORMANCE OF 0/90 LAMINATES

7.4.1 Effect of Preload Only

Only the GRP and KFRP were tested in the 65%RH condition after preloading. As Figures 7.11a, b and c show, there does not appear to be any significant effect of preload on the residual fatigue performance of either laminate. This is in general agreement with results reported elsewhere (115,159,160) for fibre dominated laminates preloaded at up to 90% of their static strength.

Secondary damage similar to that in monotonic loading, such as transverse ply cracking and longitudinal ply splitting, occurs at lower stress levels in fatigue (34,101,121,126,127) and it has been suggested that such damage may lead to weakening of the load bearing plies during cycling(101,127). Transverse ply cracking was observed early in the fatigue life for the GRP and presumably also for the other laminates, at all stress levels investigated, and this most likely explains the absence of any effect of preload. For the fatigue loading of undamaged specimens, a level of damage equivalent to that produced

by preloading should be reached after relatively few cycles and these should be insignificant on a logarithmic life plot. Alternatively, the results may indicate that secondary crack damage has little or no effect on the fatigue performance.

7.4.2 Effect of Preloading and Boiling

The fatigue lives for the preloaded and boiled CFRP and KFRP specimens are similar to those for the undamaged samples (Figure 7.11c and d). Although the data points for the preloaded CFRP fall largely near the bottom of the scatterband for the undamaged material, it had been necessary to cut these samples from a laminate sheet that was slightly weaker than the others and one that was not used for any other tests.

The arguments put forward in the previous Section are also applicable here, except that since moisture tends to relax the residual stresses in the laminate, fatigue induced secondary cracking might be expected to build up at a lower rate in these boiled specimens. Even if access of moisture to the load bearing fibres in the longitudinal plies were increased by preloading damage, any effect should be limited since the carbon fibres are not degraded by moisture and the Kevlar fibres are already rapidly saturated.

The fatigue results for the GRP preloaded to 0.4GPa prior to boiling fall on the curve for specimens boiled without preload (Figure 7.11a). As in the case of the CFRP and KFRP, preloading damage did not lead to an increase in the damage (weakening) resulting from subsequent boiling water exposure, presumably because cracking was confined to the non load-bearing transverse plies.

The GRP specimens preloaded to 0.7GPa did suffer extra damage during boiling however, as indicated in Figure 7.11b. Both the monotonic strength (Table 5.3) and the S-logN curve fall substantially below those of the composite boiled without preload, although the two curves converge at the lower stress levels (long lifetimes). The reduced performance must derive from damage introduced into the longitudinal plies during the preload. In particular the longitudinal splitting and fibre-matrix debonding should expose the load bearing glass fibres to increased attack by water. It was shown in Chapter 4 that such damage results in an enhanced rate of moisture uptake in the composite whereas when damage is confined to the transverse plies alone as in the case of the 0.4 GPa preload, the rate of water ingress is little affected. There is also the possibility of matrix cracks in the longitudinal plies transverse to the load direction at such high strains although microstructural examination did not reveal significant damage of this type.

It appears that the lower fatigue strength of the preloaded specimens is simply a reflection of the degraded tensile strength and that the mechanism controlling the long-life fatigue resistance of the boiled laminate is independent of preload.

7.5 INFLUENCE OF FATIGUE LOADING ON THE RESIDUAL STRENGTHS OF 0/90 LAMINATES

An assessment of the strength loss as a function of cycles endured can provide useful information regarding the mechanisms and build-up of fatigue damage. This section summarises the results from a limited investigation that involved the measurement of the residual monotonic strengths of 0/90 specimens that had been cycled to various stress levels

and proportions of the predicted lives. The loading rate was the same as that used in the fatigue tests.

A full presentation and analysis of the residual strength results is given in References P1 and 146. Clearly, strength losses can only occur between the monotonic strength at one half-cycle (σ_f) and the cyclic stress level (σ). Thus the residual strength ratio can be defined as

$$r = \frac{(\sigma_R - \sigma)}{(\sigma_f - \sigma)}$$

where σ_R is the residual strength measured after n cycles. Since these losses occur between one half-cycle and the fatigue life (N_f) corresponding to σ, the cycle (or log-time) ratio can be defined similarly

$$t = \frac{(\log n - \log 0.5)}{(\log N_f - \log 0.5)}$$

For each material/condition examined it was found that the shapes of the residual strength against cycles endured (σ_R vs logn) curves were basically similar and could be superposed if the above normalising procedures were adopted to account for the stress-dependence of the rate of damage accumulation. All residual strength data could be presented by single interaction curves of the general form

$$r^y + t^x = 1$$

where x and y are curve fitting parameters and are unique to each material.

These curves and the appropriate values for x and y are shown in Figure 7.12.

There appear to be important differences in the mechanisms of fatigue degradation for all three laminates and for the boiled and drier GRP, but in each case the basic response is little affected by stress level. The GRP shows the classic 'wear-out' behaviour expected of this material, with early reductions in strength accelerating as cycling (plotted logarithmically) continues. Boiling appears to delay the onset of significant degradation however. The strength of the CFRP remains unaffected by cycling until just before failure, when there is a sudden rapid loss of strength. The KFRP shows wear-out behaviour similar to the GRP.

7.6 TENSILE FATIGUE PERFORMANCE OF ±45° LAMINATES

The fatigue results for the ±45° laminates in the three standard environmental conditions are presented in the S-logN curves shown in Figures 7.13 to 7.15. It is clear that the ±45° laminates were much weaker in fatigue than their 0/90 counterparts. This reflects the differences in monotonic strengths (Chapter 5) and the fact that in the ±45° orientation the performance is limited by the resin and interface rather than by the much stronger and stiffer fibres. The fibre type therefore had much less influence on the fatigue properties than in the 0/90 orientation.

The failures were localised and generally similar to those in monotonic loading, although there was a tendency towards more extensive secondary

damage, in the form of debonding and cracking parallel to the fibres away from the fracture surface, particularly for the high cycle tests.

7.6.1 CFRP

Compared to the 0/90 laminate, fatigue cycling was far more damaging in the ±45° orientation. Furthermore, while the fatigue properties of the 0/90 CFRP were unaffected by environmental conditioning, the ±45° laminate was weakened both by drying and boiling water exposure (Figure 7.13).

Figure 7.13 shows that the effect of conditioning was only significant at short lives, where the performance reflected directly the relative tensile strengths. At long lives, the fatigue curves merged, indicating that changes to the residual stress state, matrix plasticisation (or interfacial bonding) brought about by environmental conditioning were of little importance in this range. When normalised to the appropriate tensile strengths all three curves show a slope of approximately 7 to 7.5% loss in strength per decade of cycles (compared to a value of only 3-4% for the 0/90 CFRP). Thus it appears that the basic mechanisms of fatigue damage are not affected by environmental exposure.

It is worthy of note that, allowing for small differences in the overall strengths, the results for the 65%RH condition compare closely with those reported previously by Sturgeon for 40mm wide 8-ply ±45° HT-S/epoxy specimens(130,131,133).

7.6.2 GRP

As in the case of the CFRP, the fatigue results for the ±45° GRP (Figure 7.14) reflect the domination of the resin in this orientation. The 65%RH results for the ±45° CFRP and GRP are compared in Figure 7.16, where it can be seen that the two sets of data overlap. This reflects the similarity in tensile strengths and also the strains to the (initial) peak load for these two materials and emphasises the fact that the fibres, with their very different mechanical properties, are of secondary importance.

Drying had little or no effect on the fatigue properties of the GRP. Although this contrasts with the reported deterioration for the CFRP, it is consistent with the relatively small reduction in the monotonic tensile strength. Boiling, on the other hand, reduced not only the tensile strength but also the fatigue properties throughout the stress range so that even at long lifetimes the boiled performance was inferior to that for the drier conditions. Thus, when the data are normalised to the appropriate tensile strengths, the slope of the S-logN curve for the boiled specimens is slightly steeper than the slopes for the dried and 65%RH samples ($\frac{B}{\sigma_f}$ = 0.09 compared to 0.08 for the drier laminates). This indicates that the fatigue degradation mechanisms are more severe in the boiled condition, presumably due to the fact that the fibres themselves are involved in the failures. For the CFRP, where the fibres were not degraded by boiling, the normalised slope of the fatigue curve was unaffected. Thus fibre fractures appear to be associated with a lowering of the fatigue limit in the ±45° orientation. However, it should be emphasised that fibre degradation is much less important than in the 0/90 GRP, particularly at shorter lifetimes.

It is interesting to compare the normalised fatigue performance of the ±45° GRP with that of the 0/90 GRP, since the latter was found to be weakened by fatigue loading to a far greater extent than the 0/90 CFRP. Figure 7.4 confirms that in the 65%RH and dried conditions the fibre controlled 0/90 GRP is actually more fatigue sensitive than the ±45° laminate. Of course, for a specific load level, the 0/90 laminate has superior life and in fact the tensile strength of the ±45° specimens is below 150MPa, the lowest stress level for which fatigue failures in the 0/90 orientation were recorded.

The normalised ±45° curves actually correlate well with the 0/90 GRP in the boiled condition, for which the slope of the fatigue curve $(\frac{B}{\sigma_f})$ is 0.074. This could be interpreted as an indication that the resin/interfaces play dominant roles in the fatigue response of the boiled 0/90 laminate whereas the fibres are more important in the drier conditions since they allow the composite to attain high strain levels and thus a steep slope to the S-logN curve. The curves for the ±45° and boiled 0/90 laminates are certainly less steep than would be expected from the value of $\frac{B}{\sigma_f} = 0.1$ predicted by Mandell(87,116) for fatigue failures dominated by the glass fibres.

7.6.3 KFRP

The fatigue performance of the ±45° KFRP, shown in Figure 7.15, was inferior to that of the other two materials in all three standard environmental conditions. This is highlighted in Figure 7.16 for the 65%RH laminates. The lower fatigue strength can be attributed to the lateral and shear weakness of the Kevlar fibres themselves, as indicated by the split or torn fibres in the fracture surfaces. This

was also the cause of the poor monotonic strength (Chapter 5). In the ±45° orientation, the fatigue performance is dominated by the weakest or most fatigue sensitive part of the composite. Normally this is the resin or interface. However, for the KFRP (and presumably the GRP in the boiled condition) it appears that the fibres are so weak that they initiate or accelerate the damage leading to failure. That the fatigue curves do not show the characteristic 'knee' of the 0/90 KFRP is explained by the fact that the stresses and damage mechanisms are completely different in the ±45° orientation.

The KFRP exhibited its best fatigue resistance in the 65%RH condition, with the drying and boiling water treatments both reducing the low cycle performance by roughly similar amounts. Presumably this is related to the effect of moisture on both the epoxy matrix and the fibres as discussed for the monotonic tensile results. At high lifetimes the three fatigue curves converge, as in the case of the CFRP but at a lower stress level consistent with the fibre damage mode, indicating that the main effect of conditioning is on the monotonic strength rather than the basic fatigue mechanisms and level of the 'fatigue limit'.

As for the monotonic tests, shear cracking and delamination damage tended to initiate at the specimen edges as a result of the out-of-plane stresses in these regions. This presents the possibility that fatigue life could show a dependence on specimen width. Figure 7.15 includes a small number of results for 20mm wide KFRP specimens in the 65%RH condition. Within the scatter of the data, which is generally greater for the KFRP than for the other two materials, there appears to be no obvious effect of specimen width on the fatigue strength.

7.7 FURTHER COMPARISONS OF FATIGUE PERFORMANCE OF 0/90 LAMINATES

7.7.1 Comparison of Slopes of Fatigue Curves

The 65%RH fatigue data for the 0/90 CFRP and GRP laminates are compared in Figure 7.17 with typical fatigue curves for unidirectional composites reinforced with the three common types of carbon fibre(93) and with E-glass fibres(87). The curves are directly comparable since differences in strength have been eliminated by normalising to the monotonic strengths. Thus it is reasonable to assume that any effect of the transverse plies, and associated damage, on the fatigue resistance and accumulation of damage in the 0° plies would result in a deviation of the 0/90 data away from the unidirectional fatigue curve for the same fibre type.

Most of the data points for the CFRP lie fairly close to the unidirectional HT-S (Type II) line (and well above the transverse ply cracking stress level in monotonic loading,Figure 5.10b), indicating that mechanisms operating in the longitudinal plies only, presumably matrix fatigue cracking, control the fatigue behaviour. However, close examination of the results shows that at longer lives there may be a tendency for the 0/90 data to fall below the unidirectional curve. Such behaviour might be expected if stress concentrating effects of the transverse ply cracks or delamination at the crack tips accelerate the rate of accumulation of critical fibre damage in the longitudinal plies, in the manner proposed by Talreja(98) and Reifsnider and his co-workers (101,127). The behaviour would indicate a change in the way in which the critical level of damage in the longitudinal plies is built up, with that initiated by the transverse plies becoming dominant after large numbers of cycles. It could after all indicate an effect of the characteristic outer ply

delamination observed in the high cycle tests and in any case highlights the dangers associated with the extrapolation of fatigue curves from data obtained at short lifetimes only. It should be emphasised though that the effect (if present) is small.

The results for the 0/90 GRP fall below the unidirectional curve (plotted with a slope $\frac{B}{\sigma_f} = 0.1$, after Mandell (87,116)) throughout the range tested, indicating a much stronger effect of the transverse plies in this case. Presumably the stress-rupture sensitivity of the fibres and differences in the local stress system compared to the CFRP lead to accelerated localisation of fibre damage in the longitudinal plies adjacent to the transverse ply cracks. Figure 7.18 presents photomicrographs showing possible evidence of such an effect. The behaviour is consistent with Reifsnider's model (101,127) rather than that of Mandell(87,116) where the normalised fatigue performance should not be affected. The data for the boiled GRP fall somewhere between the lines for the unidirectional GRP and XA-S CFRP in Figure 7.17. The problem with Figure 7.17 is that it takes no account of the cyclic strains, although these actually control the fatigue response.

The normalised slopes of all the curves are compared by plotting against the static failure strains in Figure 7.19. The strains for the unidirectional composites are assumed to be similar to those measured for the 0/90 laminates. There appears to be a simple linear relationship for the unidirectional composites, and the 0/90 CFRP falls on this line. The linear relationship might be expected from the critical strain model of Talreja, which indicates that the slope is

governed by the range of working strain above the fatigue limit. It follows that there is actually no reason to expect the line drawn through the points in Figure 7.19 to pass through the origin. The 65%RH and boiled 0/90 GRP both lie above the line, confirming that for this material the slope and thus the degradation rate is increased by the presence of the transverse plies.

7.7.2 Importance of Cyclic Strain

To examine the effect of cyclic strain on the fatigue performance in more detail, the S-logN curves for the laminates in the three standard environmental conditions are plotted in Figure 7.20 against maximum strain rather than stress. Of course, under load control as in these tests, any reduction in modulus during cycling causes an increase in the alternating strain. Previous authors, such as Dharan(36) and Talreja(98), have tended to ignore this when plotting their data. Consequently the strains given in Figure 7.20 are only meant as a guide. They were calculated using the modulus as given by the monotonic strength divided by the failure strain for each of the laminates and conditions. Thus, for 65%RH GRP, which shows a distinct drop in modulus after failure of the transverse plies in monotonic loading, the calculated strain at a particular stress level is generally somewhat higher than that obtained in a normal monotonic test. Since transverse ply cracking builds up rapidly early in the fatigue life at all the stress levels tested, the secondary modulus gives a better indication of the average cyclic strain.

a) GRP and CFRP

The curves in Figure 7.20 confirm the importance of cyclic strain on the fatigue performance. They can be interpreted according to Talreja's(98) critical strain theory, falling from the tensile strain scatter bands down through the region of fatigue failures to limiting strains at high cycles which, although generally similar, appear in detail to depend on the actual laminate and environmental condition. It is not possible to be certain of these limiting levels because of the uncertainty regarding the true cyclic strains at long lives (for example, although the drier GRP laminates show the lowest limiting strain, they should also exhibit the greatest reduction in modulus during cycling). However, on the basis of the curves shown, some observations can be made.

None of the composites exhibited failures below 0.6% strain, which was the limiting strain for the drier GRP laminates. This coincides with the fatigue limit proposed by Dharan(36) and Talreja(98) for cracking in the epoxy matrix and hence for fatigue failure of unidirectional composites. However, it was suggested in Section 7.7.1 that the critical damage in the longitudinal plies of the GRP is that caused by the cracking in the transverse plies, initiated by transverse fibre debonding. The fatigue limit for transverse debonding has been quoted at around 0.1% strain(81,98) although this value actually depends on a number of factors, including the interfacial bond strength, the modulus of the resin, the transverse modulus of the fibres, the fibre volume fraction and any residual strains present. Talreja has noted that where failure for 0/90 laminates is induced by 90° debonding and delamination, the fatigue limit is commonly around 0.46%ε. This

should also be sensitive to the factors mentioned above and additionally to the actual way in which the longitudinal plies are weakened. Thus it seems more likely that the CFRP, which appeared not to be greatly affected by the transverse plies, gives a better indication of the fatigue limit for the resin, at approximately 0.8% strain. No fatigue data for Code 69 resin are available, but in view of the high rigidity of Code 69 compared to Dharan's resin, Shell Epon 815, this value seems reasonable. Curtis and Moore(117) have quoted a limiting fatigue strain of 0.8 to 1% for unidirectional glass and carbon (XA-S) reinforced composites using Ciba-Geigy type BSL913 epoxy resin.

The observation that extensive preloading damage (transverse ply cracks, longitudinal ply splits) does not affect the residual fatigue lifetimes, even at very low cyclic stress levels (Section 7.4) confirms that the initiation of such damage is not in itself critical. The cracks only become important if they develop during cycling in a way that is deleterious to the strength of the composite. Even in the case of the GRP, preloaded to 0.7GPa and then boiled, degradation can be attributed to the reduced static properties, the high cycle fatigue performance and limiting fatigue strain remaining unaffected.

Generally, the GRP possesses superior lifetimes to the CFRP, indicating a greater tolerance of matrix fatigue damage. This is primarily due to the higher strain capacity of the glass fibres. Only at low levels, where the different limiting fatigue strains become important, does the CFRP survive more cycles.

Figure 7.20 shows that the limiting strain for fatigue failures in the boiled GRP is above that for the drier laminates, which is consistent with the cyclic stress plots (Figure 7.2a). Previously it was suggested that this could indicate an effect of moisture on the build-up of fatigue crack damage in the 0° plies and a change in the size of the 'critical nucleus' of fibre breaks precipitating fracture. The analysis presented in this section suggests an additional mechanism. Boiling reduces the level of residual thermal stresses (thus increasing the transverse ply cracking strain, Chapter 5), and weakens the interlaminar bonding (Chapter 6) and might therefore be expected to reduce the stress concentrating effects of the transverse ply cracks on the longitudinal plies. The limiting fatigue strain, although higher, is still below the level for the CFRP, supporting the supposition made from Figure 7.19 that the transverse ply cracks continue to influence the fatigue performance of the 0/90 GRP in the boiled condition. The CFRP, being far less sensitive to transverse ply cracking, is not affected by moisture. This could indicate that moisture actually has little effect on the fatigue cracking in the resin (in the longitudinal plies). Tests on unidirectional composites, otherwise identical to the 0/90 laminates, would indicate more clearly the importance of transverse ply crack damage and help to differentiate between effects due to this and effects confined to the longitudinal plies alone.

The trend towards higher limiting strains, from the drier GRP to the boiled GRP to the CFRP, corresponds to the trend away from wear-out towards sudden-death type failures. It also reflects the trend towards lower normalised slopes to the S-logN curves and reduced ranges of cyclic strain in which fatigue failures occur. It should be noted that the limiting cyclic strains discussed above are those at 10^6-10^7

cycles rather than true fatigue limits. Thus, it is possible that the curve for the CFRP may fall to the level for the GRP, but after very many more cycles consistent with the lower rate of damage accumulation in this material.

b) KFRP

The 0/90 KFRP does not follow the pattern of behaviour set by the other laminates. The slopes before the 'knee' of the S-logN curves are shallower than predicted both when normalised to the monotonic strengths and in terms of working strains. The strain-log life plots in Figure 7.20 illustrate the resistance of the KFRP to fatigue. The curves extend beyond those for the drier GRP, despite the higher ultimate failure strain of the latter, and even at 10^6 cycles, which is well beyond the 'knee' in the fatigue curves, the KFRP survives higher cyclic strains than either the CFRP or GRP. The accumulation of fatigue damage in the matrix should depend on cyclic strain but not fibre type. Thus the Kevlar fibres appear to have a greater tolerance of matrix fatigue cracking and debonding, both in the longitudinal and the transverse plies, than the brittle glass and carbon fibres. It was suggested in Section 7.3.2 that the increase in the slope of the fatigue curve past the 'knee' indicates a general change in the mechanisms controlling the fatigue life, the transition apparently being from predominantly time-dependent to cycle-dependent failures. The nature of the mechanisms operating in the cycle-dependent region are far from clear however. The superior tolerance of cyclic strains indicates significant differences compared to the CFRP and GRP, for which the high cycle performance was evidently limited by fatigue cracking in the matrix. Unlike carbon and glass fibres, Kevlar is known to suffer damage and weakening under tensile cyclic loading(19,20,21,161).

The damage is reported to occur by the development of splits along the fibre length, at very small angles to the fibre axis. These splits, initiated at surface or internal flaws, weaken the fibre by gradually reducing the load bearing cross-sectional area(20,21). Inevitably such splitting is more extensive than in normal static loading (Figure 7.21(20)). Konopasek and Hearle(20) suggest that cycling causes a general 'loosening' of the weak interfibrillar bonds, which facilitates the formation of the splits. Thus the fatigue performance of the KFRP should be strongly dependent on the build-up of fatigue damage in the fibres themselves.

A number of authors have reported fatigue data for single Kevlar fibres. It has generally been found that fibre weakening is relatively small under tensile fatigue loading (19,20,21,161). Roylance(19) has reported a strength loss of approximately 1.7% per decade of cycles, and there is no sign of a 'knee' in the S-logN curve similar to that exhibited by the KFRP composites. Clearly therefore the performance of the laminate cannot be explained by the tensile fatigue properties of the fibres alone. In the composite the fatigue life may be undermined by off-axis loading of the fibres or fatigue damage associated with the matrix.

Internal fibre damage, in the form of splitting or skin/core debonding is likely under tensile loading. Transverse tensile stresses in the radially weak fibres will result from Poisson mismatch effects. Although no data are available in the literature, it is likely that the properties of the fibre skin, in particular the elastic, thermal expansion and moisture expansion characteristics, differ from those

of the fibre core. This will lead to the formation of residual stresses within the fibres themselves and under tensile loading it is unlikely that the stress distribution through the fibres will be uniform and free from shear. In Chapter 5 it was suggested that such effects lead to transverse fibre damage at relatively low stress levels in normal monotonic loading. In fatigue more extensive damage would be expected. There is also the possibility of fretting damage during cycling, caused by relative movement both within the fibres and, where debonding has occurred, at the fibre-matrix interfaces. Roylance(19) proposed that such abrasion damage accelerates the deterioration of the fibres. It is known that surface damage can lead to a reduction in fibre strength(18) and that in contrast to glass and carbon fibres, Kevlar is particularly sensitive to surface abrasion(16).

Consider also the effect of matrix fatigue cracking, specifically a crack whose plane is normal to the applied load meeting a fibre which is parallel to the load direction (Figure 7.22). Not only is there an intensification of the applied stress at the crack tip (σ_1), tending to cause fibre fracture, but there is in addition an associated transverse tensile stress (σ_2) in the plane of the crack (which is at a maximum just ahead of the crack tip) and a shear stress (τ) parallel to the fibre(9). These latter stresses, which depending on the relative values of the longitudinal tensile, transverse tensile and shear strength may cause debonding, will also tend to promote defibrillation and fibre splitting in the KFRP. While such damage will absorb strain energy and relax the stress concentration in the fibres, making complete transverse fibre fracture less likely and thus reducing the relative sensitivity of this laminate to matrix fatigue cracking, it will nevertheless tend to reduce the fatigue strength of the fibres themselves (fibre

splitting being the major damage mode).

The substantial increase in the fatigue life obtained by raising the stress ratio (i.e. raising the minimum stress for a given maximum stress) is far greater than that reported for the 65%RH GRP. Over the range R = 0.1 to R = 0.5 the high cycle fatigue life of the KFRP is more sensitive to the cyclic amplitude than to the level of maximum stress whereas for the GRP the reverse is true. There is insufficient data to be certain of the actual extent of the improvement in fatigue life. However, it is probable that the effect simply reflects the response of the fibres to the reduced amplitude of oscillation. Bunsell(21,161) found that increasing the stress ratio resulted in appreciable improvements in the fatigue life in tests on individual Kevlar fibres. His data indicated that only for stress ratios below about R = 0.3 did accelerated failures occur which could be reasonably attributed to true fatigue mechanisms (internal fibre fretting was suggested, in support of Roylance) rather than to simple creep. Thus Bunsell's fibre results are consistent with the increased lives reported here for the composites.

In addition to the reduced cyclic amplitudes, there is also the possibility that the effect of increasing the R-ratio reflects the absence of more serious damage caused by cycling to low stress levels. Konopasek and Hearle(20) tested single Kevlar fibres in tensile fatigue and found a reduction in performance in tests where the fibres were allowed to go slack at the bottom of each cycle. Similarly, Hearle and Wong(16) have shown that the tensile strength of Kevlar fibres is

reduced by up to 25% in cases where the fibres have suffered kinking damage as a result of repeated buckling. In both cases, the compression stresses appeared to initiate or accelerate axial fibre splitting and defibrillation, the major damage modes in tensile fatigue. Thus, in the composite, the possibility that the fibres experience compression or bending at the bottom of each cycle (and that this no longer occurs when the stress ratio is raised to 0.5) must be considered. How these compression stresses could arise under purely tensile fatigue loading is not clear however. For the drier laminates, they could involve the original residual compressive thermal stresses induced in the fibres during the cool down from the cure temperature. The problem is that increasing moisture contents did not alter the basic fatigue response, even though swelling should have relieved the residual stresses.

Alternatively, they could occur as a result of relaxation effects within the composite, especially after large numbers of cycles. Significant tensile creep in the fibres at high stress levels, over and above any similar effects in the resin, could lead to fibre unloading or buckling at the bottom of each cycle. However, data published by Bunsell(21) for single fibres suggest that Kevlar fibres creep very little in fatigue, perhaps up to 0.2% plastic strain during the first few cycles but no more. Localised creep might occur within the fibres themselves though, especially in view of the weak interfibrillar bonding.

It is not possible to be certain of the shape of the fatigue curves for the 0/90 KFRP beyond 2-3 x 10^6 cycles, the highest level for which

fatigue data are available, without further testing. However, data points in Figure 7.7a do indicate that there may be a tendency for the curves to begin to level off at very low stress levels, although in view of the preceding discussion it cannot be assumed that the KFRP possesses a fatigue limit determined by cracking in the matrix or transverse plies, as for the other two laminates.

A very careful study would be required in order to confirm the mechanisms of fatigue damage in KFRP. As already noted, there were no obvious features of the fracture surfaces that could be positively attributed to differences in fatigue life or stress-ratio, since extensive splitting was common to all failures (Figure 7.8).

c) ±45° laminates

It is interesting to note that, based on the first cycle stress-strain relationship, the limiting cyclic strain for the 65%RH ±45° GRP and CFRP at 10^6 cycles is in the region of 0.4 - 0.45%, compared to strains of approximately 0.7% and 0.9% for the corresponding 0/90 laminates. The ±45° KFRP, being dominated by the fibre splitting mode, has a limiting strain below those of the other laminates. Since it is likely that the true strains are increased most in the ±45° laminates during cycling, and least in the 0/90 CFRP, it is possible that the actual values are much closer together. However the difference in stress states and failure modes between the 0/90 and ±45° laminates makes it hard to substantiate any proposal that the same mechanisms limit the fatigue failures in each case.

CHAPTER 8

FLEXURAL FATIGUE TESTS

Although fatigue testing of composites has been concentrated mainly on the axial tensile mode, an important feature of fibre reinforced plastics, in contrast to metals, is their relative weakness under compressive loading. In service, compressive fatigue stresses frequently occur as a result of flexural loadings and can result in increased sensitivity of the composite to moisture. Consequently flexural testing is not only a useful but also an important method for assessing the effects of compressive fatigue damage.

This part of the investigation is concerned with establishing the flexural fatigue behaviour of the 0/90 laminates and the effect of environmental conditioning upon this.

8.1 PRESENTATION AND ANALYSIS OF RESULTS

8.1.1 Variation in Flexural Stiffness with Cycles Endured

Figures 8.1 to 8.3 show the maximum surface stress as a function of number of cycles endured. Since the tests were conducted under conditions of constant cyclic angular deflection these smoothed curves represent the change in stiffness with number of cycles.

The basic form of the curves is a period of initial stability in which changes in flexural stiffness were small, followed at some critical stage by relatively rapid (or at high stress levels quite sudden) reduction in stiffness. Similar curves have been reported by other workers for constant deflection flexural and torsional cycling (68,80,109,162,163,164). The loss of stiffness, which generally occurred earlier at higher cyclic stresses, was caused by the onset of significant amounts of cracking and delamination

associated with one of the surface plies, although the actual mode depended on the laminate concerned. Complete specimen fracture or total separation did not occur in these deflection controlled tests and the cyclic stress level stabilised at the much reduced level carried by the inner undamaged plies. The CFRP and KFRP generally failed at the compression surface and the GRP at the tensile surface. The outer 90° plies on the tensile side exhibited extensive transverse ply cracking for all three laminates.

The initial stable portions of the stiffness-cycles curves show some interesting features. They are near horizontal for the GRP. Reductions in flexural stiffness due to observed transverse ply cracking are small, as might be expected in view of the through the thickness stress distribution in bending. The curves for the CFRP are very similar to the GRP at high cyclic stresses, close to the failure level. One specimen, whose strength was actually above the statistical mean, shows a quite rapid loss of stiffness from the outset and this must be associated with actual surface ply damage and delamination. At low stress levels however, the tendency is towards a slight increase in stiffness before serious damage occurs. Such cyclic strengthening or stiffening has been reported elsewhere for CFRP and is normally attributed to small improvements in alignment of the load bearing fibres(86,164), which in this case are mainly in the surface plies.

The response of the KFRP is complicated by non-linear time-dependent behaviour associated with damage at the compression surface involving fibre kinking or buckling. The static Avery flexure tests (Chapter 6) showed that this becomes significant at around 40% of the estimated flexural strength. The build-up of such damage may explain the

progressive loss of stiffness for 65% RH specimens cycled at stresses above this level (Figure 8.3a). The initial 100 cycle flat portions are probably due to the lower cycling rate here, which implies that an extrapolation back to the surface stress axis (at ½ cycle) should give an indication of the maximum surface stress in the case where little or no relaxation has occurred. At low cyclic stress levels the corresponding changes in stiffness are very much smaller, indicating that the stresses here are too low to cause significant buckling or damage at the compression surface.

The curves for the boiled KFRP are basically similar to those for the 65% RH specimens at high stress levels. They all show significant reductions in stiffness with increasing cycles in the 'stable' region. Although further curves at lower cyclic stress levels would be informative, it appears that the compressive 'yield' strength is reduced by the boiling water exposure. As discussed in Section 8.4 this is most probably due to weakening of the fibres themselves rather than to any effects of resin plasticisation .

The calibration plots in Figure 8.4 show that environmental conditioning did not affect the flexural stiffness (i.e. maximum surface stress on the first cycle for a particular angle of flexure) of the CFRP and GRP, but boiling caused a reduction in the stiffness of the KFRP. Unfortunately interpretation of the flexural results for this material is complicated by the non-linear time-dependent behaviour.

8.1.2 S-logN Plots

a) Failure criterion

Relative fatigue performance is most easily compared in the form of stress-life (S-logN) curves. Since the flexural fatigue tests did not result in specimen fracture or total separation, it was necessary to use an alternative criterion for failure based on changing specimen stiffness. Logically this would have been the upper knee on the stiffness-cycles curve, but its position appeared to be somewhat erratic. Therefore, an objective criterion for the life, shown schematically in Figure 8.5, was chosen as the number of cycles to the point at which the stiffness (maximum surface stress) had fallen to 85% of its original, first cycle value. This ensured that 'failure' occurred at a point on the curve where observable damage was causing rapid stiffness loss. This was especially important in the case of KFRP where there were significant stiffness reductions long before this. Similar criteria have commonly been used in the analysis of fatigue data in constant cyclic deflection tests in both torsion and flexure(36,68,109,163,165) and are clearly relevant to composite applications where the component stiffness is the primary design requirement (for example, in leaf springs or rotor blades).

In the S-logN curves shown in Figure 8.6, specimen life (as defined above) is plotted as a function of first cycle maximum surface stress. The results appear to show a greater scatter than those obtained in the axial fatigue tests, presumably because of the more complex failure modes and the greater problems associated with establishing 'failure'. The limited angular deflection of the Avery machine and the relatively low flexural moduli of the GRP and KFRP meant that failures were only

obtained after large numbers of cycles for these laminates.

b) Static flexure strengths

It is customary to include the static strengths on S-logN plots, usually at one half cycle when the loading is in one sense only. This facilitates comparison between the fatigue performance (and in these tests the effect of moisture on this) and the relative static strength. Since static failures using the Avery machine could only be obtained for CFRP, it is necessary to use alternative flexural strength data for the GRP and KFRP. Although flexural strength is sensitive to test geometry, the 3 and 4-point bend test results reported in Chapter 6 can be used to provide an approximation of the Avery flexure strength.

The 4-point bend test geometry is closest to, but not quite equivalent to that of the Avery test. The mid-spans are quite similar (32 mm compared to 42mm for the Avery) and both theoretically experience pure bending moment. However the major difference is in the gripping arrangement and the fact that in the 4-point test, there are bending and in particular shear stresses present outside the central span, whereas for the Avery, deflection is restricted by the grips. This limits the usefulness of the 4-point bend tests.

As explained in Chapter 6, true flexural failures in 4-point loading were only obtained for the GRP-failures for the CFRP and KFRP were initiated by the shear stresses outside the central span. Thus, in Figures8.6a and b, the static flexural strengths measured in the Avery are plotted for the CFRP while for the GRP the 4-point bend strengths are used. Although the failures for GRP in Avery fatigue were at the

tensile surfaces for both environmental conditions, in static 4-point bending only the boiled material showed a similar mode of failure since damage in the 65% RH specimens occurred at the compression surface initiated at the inner load points. While the change in failure mode for GRP in 4-point bending gave an indication of the changing relative compressive and tensile strengths of this laminate with exposure to boiling water, such behaviour is not absolute since it depended on the loading geometry and damage or stress concentration effects at the inner load points. Failure in 3-point bending was at the tensile surface and it is therefore probable that the failure mode would have remained tensile in static flexure if greater deflections of the Avery machine had been possible. Consequently, tensile 4-point bend strengths have also been plotted. These were estimated from an extrapolation of the results for the tensile surface failures shown in Figure 6.4 to the moisture content at 65% RH.

3-point bend strengths are plotted for the KFRP in Figure 8.6c since flexural static failures were not obtained in either 4-point bending or the Avery machine. The standard boiling water conditioning lowered the mean bend strength from 427MPa to 356MPa and caused the specimens to fail at much reduced deflections. Similar strength losses in 3-point bending have been reported by Smith (43) for Kevlar fabric reinforced epoxy specimens after exposure to 95% RH at 82°C for 21 days.

Although failure occurred at the compression surface as for the high deflection Avery fatigue tests, the two flexure tests have quite different loading geometries. 3-point bending tends to give higher 'flexural strengths' as evidenced by the results for the CFRP and GRP. The strengths plotted are therefore meant only as a rough guide.

c) Rate - effects

No attempt has been made to account for the fact that the maximum surface strain-rates in static bending were much lower than those in the flexural fatigue tests. The use of different bend tests to measure the static and fatigue properties of the GRP and KFRP meant that comparisons would be subject to considerable errors anyway. In the case of the GRP, the difference in rates was about three orders of magnitude - in fact similar to the difference in rates between the 'slow' tensile tests (Instron 1195) and the tensile fatigue tests (Chapters 5 and 7).

8.2 FLEXURAL FATIGUE PERFORMANCE OF CFRP

The failure modes for the 65% RH and boiled CFRP specimens were similar for both static and cyclic flexural loading. Localised transverse cracking in the outer compression surface ply, initiated near one or both grip points and delamination at or close to the first ply interface (which effectively blunted the crack, preventing further propagation towards the neutral plane) led to reduction in stiffness. Sometimes longitudinal cracking in the outer compression ply occurred. Initiation of failure at the compression surface can be attributed to the fact that the axial compressive strength of unidirectional HTS-Code 69 at room temperature is only about $\frac{2}{3}$ of the tensile value (Table 2.2).

The fibre micro-buckling mode is common to compressive failures of most carbon/epoxy composites and is due to the relatively low shear moduli of the supporting resins currently used for these systems(108). At the high volume fractions associated with modern advanced composites, the fibres tend to buckle 'in-phase' and usually along two planes in the form of kink zones with fibre rotation between the planes(9). In fatigue, these zones propagate by fibre buckling followed by fibre fracture (for carbon and also glass fibres but not Kevlar) and matrix shearing. However the transverse plies in cross-plied laminates can, as reported here, prevent the buckling damage from extending into the specimen beyond the first ply (initially at least) by diverting the crack along the ply interface as a delamination(166). The broken fibres in the compression zones have been shown to exhibit the fracture morphology of a single fibre broken in bending i.e. brittle fracture in the tensile region and crushing or shear failure in the compressive region of each fibre(9,36).

Fatigue failures occurred quite suddenly and without a more sophisticated method to enable constant monitoring of stiffness, it was not possible to stop a test and examine a specimen in the important period of rapidly falling modulus. Polished microsections of specimens taken in the prior stable region showed no evidence of compression surface damage, although an accumulation of transverse ply cracking near the tensile surface was observed (Figure 8.7). Localised delamination at the first ply interface could well have precipitated buckling failure of the sub-sequently unsupported surface ply in a manner similar to that reported by Bader and Johnson(110) for a unidirectional multiplied laminate. Similarly, Owen and Morris(167) found axial static and fatigue

compression failures occurred by splitting along the ply interfaces and buckling of the individual plies. Conners et al(168) have noted a similarity between the normalised slopes to their compressive S-logN curves for 0/90 glass and carbon/epoxy laminates and those reported by Owen(81) for interlaminar loading and suggest that for these systems compression fatigue could be governed by interlaminar performance.

The 65%RH CFRP showed good fatigue resistance in flexure, with a fatigue strength at 10^6 cycles of approximately 65% of the static flexural value (Figure 8.6a). This compares well with the 60% recorded by Bevan and Sturgeon(109) for a carbon (II)/epoxy laminate of similar lay-up in 4-point bending fatigue. The effect of boiling water exposure on the subsequent flexural fatigue performance is not clear owing to the considerable scatter in the results for the boiled specimens. Although more results are required in order to make positive conclusions, there does appear to be a trend towards a small increase in life at long lifetimes and in static flexure. The reason for this is uncertain since no such strengthening was observed in any of the axial tests and, if anything, moisture would be expected to reduce the compressive strength by reducing the matrix stiffness (and thus support for the fibres against microbuckling) via plasticisation and perhaps by weakening the fibre-matrix interfacial bonding.

While there is some evidence that moisture reduces the compressive fatigue strength of fibre controlled CFRP laminates(169), mainly by promoting delamination damage(94), a large number of authors have, in practice, found moisture to have little or no significant effect on the static and fatigue properties in either axial compression(141,168) or

flexure(49,68,96). Gillat and Broutman(57) noted a small increase in flexural strength for cross-plied CFRP. They suggested that this may have been due to a relaxation in the residual thermal stresses (set up by differential contractions during cooling from the cure temperature) caused by the absorbed moisture. Specifically the small compressive residual stresses in the longitudinal plies and the balancing tensile stresses in the transverse plies are reduced with increasing moisture content and may even change sign. Such a mechanism could help to explain the effect observed here. Presumably matrix plasticisation and degradation of the interfacial bonding is limited.

8.3 FLEXURAL FATIGUE PERFORMANCE OF GRP

Flexural fatigue damage in the GRP was confined to the tensile side of the specimen. In contrast to CFRP, GRP has often been found to possess superior static and fatigue properties in compression than in tension (9,168,170,171), as illustrated by the constant life diagrams in Figure 2.4. This has been attributed to the lower tensile strength of glass compared to carbon fibres, which brings the uniaxial composite tensile strength down below the compressive value. The latter, being controlled substantially by matrix shear stiffness, should be fairly similar to that for CFRP.

For 65% RH specimens, 'failure' occurred away from the grips by the progressive growth of small random longitudinal delaminated strips containing central cracks. These coalesced until sufficiently large as to cause fracture of the outer ply which delaminated into thin strands. The damage appeared to be initiated at transverse ply cracks,

which were clearly visible in the adjacent 90° plies, possibly at intersections with longitudinal splits in the surface ply. The general form of the damage was very similar to that observed for the axial tensile fatigue tests at long lifetimes and is discussed further in Chapter 7. Generally the damage occurred earlier and at a faster rate for higher angular deflections.

Figure 8.8 is a micrograph showing typical damage near the tensile surface in flexural fatigue loading. This particular specimen had experienced 10^6 cycles at an initial maximum surface stress level of 300MPa.

Damage was more localised for the boiled specimens, with ply fracture close tothe grips a common mode especially at high stress levels where strand delamination was much reduced (presumably as a consequence of the shorter lifetimes). A tendency towards this type of failure was shown by the 4-point bend test GRP specimens after prolonged boiling, with damage in this case initiated adjacent to the inner load points, and a more localised mode of failure was also observed for boiled specimens in axial tension (Chapter 7).

Figure 8.6b shows that boiling water conditioning reduced the flexural fatigue life of the GRP laminate at higher cyclic deflections but at lower levels the life was not affected or may even have been increased slightly. On the basis of the fatigue results alone, the performance appears to be good with fairly flat S-logN curves and a much less drastic effect of boiling water than in axial tensile fatigue loading. However, since testing constraints meant that failures could only be obtained in the high cycle regime, the fatigue results alone give a distorted view of the laminate performance.

The static flexural strength (4-point bending) was severely reduced by boiling water exposure, with the boiled specimens exhibiting only approximately one half of the strength of the 65% RH material. This approaches the strength losses shown by the GRP in monotonic tensile loading (and is again explained by weakening of the glass fibres). The absence of any effect of the water boil treatment on the flexural modulus (Figure 8.4b) is in agreement with the axial tensile results. Extrapolating the fatigue curves back to the static flexural strengths gives an indication of the low cycle behaviour and a new perspective to the overall flexural fatigue performance. Comparison with Figure 7.2a shows clearly that the fatigue response in flexure and the effect of boiling water conditioning mirrors closely that in axial tensile loading, as is to be expected in view of the failure mode. The rate of degradation appears to be less severe in flexure though, probably because these tests were under constant cyclic deflection rather than load and different failure criteria were used in each case.

8.4 FLEXURAL FATIGUE PERFORMANCE OF KFRP

Whereas compressive buckling failures of carbon and glass fibres involve brittle fibre fracture, Kevlar fibres yield and deform plastically with the formation of buckling or kink bands on the compression surface. Such damage is illustrated in Figures 2.1d-e. The stability of the fibre is limited by weak interfibrillar bonding, which allows viscous relaxation to occur under applied compressive stress(15). Such deformation of the fibres rather than the matrix explains the time dependent non-linear load-deflection response of the KFRP in flexural loading (Chapter 6) since similar effects were not observed for the CFRP and GRP. Similarly, the increase in flexural compliance at large deflections after moisture

conditioning must also be attributed to the fibres (where absorbed moisture reduces the radial and shear properties) since the other laminates were unaffected, ruling out any direct contribution of resin plasticisation. Allred(79) and Roylance(19) accounted for comparable reductions in flexural strength and stiffness of KFRP in a similar way.

All KFRP specimens had a slight permanent set after flexural testing. Figure 2.1e illustrates intra-fibre splitting in buckled Kevlar fibres.

The results in Figure 8.6c show that the boiling water exposure caused a small reduction in fatigue strength. This reflects the reduced static bend strength and the fact that moisture lowers the flexural fatigue performance of Kevlar fibres themselves(16). The different test geometries and stress distributions in the Avery and 3-point bend tests mean that the fatigue results (which could only be obtained in the high cycle regime) cannot be expected to extrapolate back to the static 3-point bend strengths.

Comparison with Figure 7.7 indicates that the fatigue performance of KFRP in flexure is very different from that in axial tensile loading. In particular, the S-logN curves do not show the characteristic downturn exhibited in tensile cycling. This can be explained by the different failure mode in flexure which is compression dominated.

At high deflections, above the flexural (compression) yield point and into the non-linear section of the load-deflection curves where compression damage (presumably fibre microbuckling) was occurring from

the outset, 'failure' of 65% RH KFRP was initiated at the compression surface via a transverse crack within the outer ply gauge-length. After prolonged cycling this crack gradually propagated towards the neutral plane of the specimen, often together with local delamination at the ply interfaces.

In contrast, at low deflections damage often originated at the tensile surface, normally near one of the grips, accompanied by progressive strip delamination of the outer ply and reduction in stiffness. The change in mode may have been due to the noted poor tensile fatigue performance at high cycles (Chapter 7) or possibly to wear damage at the grips over the long lifetimes of these specimens. The boiled KFRP failed in the compression mode, in accordance with the lower lifetimes and reduced compressive yield strength in this condition.
Figure 8.9 shows a typical compression surface failure for KFRP. This specimen was in the boiled condition and the micrograph was taken after 10^6 cycles at a maximum initial surface stress of 300MPa. The micrograph clearly illustrates the importance of plastic fibre buckling.

Failure criteria involving loss of stiffness are especially important for KFRP in flexure since the bending fatigue resistance of the fibres themselves is good (16) and substantial damage and losses in flexural stiffness can occur through plastic fibre buckling which does not necessarily involve actual fibre fracture. Cycling may cause such damage to propagate through the specimen, effectively moving the neutral plane towards the tensile surface. In such cases, 'failure' may be attributed to fibre fracture at the tensile surface rather than the prior compressive buckling damage(17).

In relative terms the fatigue performance of the KFRP is superior to that of the 65% RH GRP (Figure 8.6b) but not as good as the CFRP (Figure 8.6a). At 10^5-10^6 cycles, the fatigue strengths of the KFRP and GRP, in terms of modulus reduction, are very similar. Clearly the KFRP has poor fatigue strength in flexure (i.e. compression) and this severely limits the potential usefulness of composites reinforced with Kevlar fibres alone. However, the weakness apparently derives from the low static bend strength rather than any disastrous effect of actual cycling.

CHAPTER 9

CONCLUSIONS

9. CONCLUSIONS

The static and fatigue properties of advanced epoxy-based composites reinforced with different types of fibres have been measured and compared for a range of different loading and environmental conditions.

It was confirmed that the static tensile properties of 0/90 laminates are governed by the respective properties of the carbon, glass and Kevlar fibres, and that in the ±45° orientation laminates are much weaker, failure occurring in shear dominated by the matrix and interfaces. Failures of KFRP, unlike the other two materials, are characterised by a fibre splitting mode of damage which is associated with the fibrillar structure and radial weakness of the Kevlar fibres. Tests showed that this mode of damage undermines the performance of KFRP in all situations where the loading is not tensile and confined to the direction of the fibre axis. Thus the ±45° tensile strength of KFRP falls below that of the other laminates and in 0/90 flexure tests failure occurs at low stresses at the compression surface, associated with buckling of the Kevlar fibres themselves. Flexural failure of CFRP also occurs at the compression surface, although in this case at relatively high stress levels. GRP fails at the tensile surface, which is consistent with the lower tensile strength of this material.

Under tensile fatigue loading the performance of 0/90 CFRP and GRP can be accounted for by consideration of the levels of cyclic strain (rather than the applied cyclic stresses). CFRP has a relatively flat S-logN curve. The low working strains limit the fatigue damage

compared to GRP for which the working strains and thus the slope to the fatigue curve are much greater. Compared to unidirectional composites, the presence of transverse plies is detrimental to the fatigue performance of GRP, and apparently lowers the fatigue limit, but hardly affects CFRP. Significantly, the ultimate fatigue performance and the limiting fatigue strains are independent of damage induced by tensile preloads. The S-logN curves for GRP are non-linear, tending to flatten out at long lifetimes (towards a fatigue limit) and at very short lifetimes (towards the static strength). This is the only laminate to exhibit considerable weakening as a function of time under load, which is associated primarily with the fibres and is also reflected in a dependence of monotonic strength on rate of loading. Under cyclic loading there are clear differences between degradation due to the accumulation of time-dependent damage and that associated with progressive fatigue damage which dominates at all but very high cycling levels.

0/90 KFRP differs markedly from inorganic fibre composites in its response to tensile fatigue loading. It exhibits superior lifetimes at all levels of cyclic strain (with a remarkably flat S-logN curve at short lifetimes) and is characterised by a downturn or 'knee' to the S-logN curve which is consistent with a transition from creep to fatigue dominated failures. 'Defibrillation' or splitting damage within the fibres themselves may effectively 'delay' fatigue failure of these composites. An observation of importance to potential users of KFRP is that the high cycle fatigue lives are vastly improved when the fatigue stress ratio R is increased from 0.1 to 0.5, an effect that has previously been observed for Kevlar fibres themselves.

In contrast to 0/90 laminates, the tensile fatigue performance in the ±45° orientation is relatively little affected by fibre type. The fatigue strength of KFRP is consistently below that of the other materials, reflecting the lower static strength and the fibre splitting damage which leads to a lower limiting stress for fatigue failure. In flexure, fatigue failures occur at the tensile surface for GRP and at the compression surface for CFRP and KFRP, as in the static tests. These tests show the compression fatigue performance of CFRP to be good with a relatively flat S-logN curve. As in the ±45° tensile tests, KFRP no longer exhibits a knee to the fatigue curve. This is a reflection of the different failure modes and the direct shear/compressive loading of the fibres. The flexural fatigue performance of GRP generally resembles the 0/90 tensile behaviour.

Three different treatments were chosen to assess the effects of environmental exposure (involving accelerated conditioning to predetermined moisture contents) on the static and fatigue properties of the laminates. These involved conditioning to equilibrium by drying at 60°C, storage at 65%RH at ambient temperature and boiling in water. It was found that the rates of initial moisture gain or loss and the equilibrium moisture contents for CFRP and GRP in the different environments are basically similar and can be approximated by 'Fickian' diffusion through the resin phase. For KFRP additional absorption by the fibres means that both the rates and levels of water uptake are appreciably higher than those for the inorganic fibre composites and that the diffusion is non-Fickian. In fact, irreversible effects occur during boiling for all the laminates, as indicated by small overall weight losses upon redrying and more rapid

non-Fickian moisture uptake for secondary water exposures.

In the fibre controlled 0/90 orientation the tensile monotonic and fatigue performance of CFRP is relatively insensitive to environmental exposure. The much weaker GRP is little affected by drying but immersion in boiling water reduces the strength and failure strain irreversibly, by over 50% for saturation. This is attributed to damage of the glass fibres. The lower range of working strains results in reduced relative fatigue damage for the boiled GRP, as indicated by a flatter slope to the normalised S-logN curve, in accordance with the critical strain model noted previously. The high cycle fatigue lifetimes are actually improved by boiling, possibly due to a reduction in the damaging effect of transverse ply cracking on the fatigue performance of the longitudinal plies. Very high tensile preloads (sufficient to cause extensive transverse ply cracking and longitudinal splitting) prior to boiling can cause a further reduction in the static and low cycle fatigue strength but the high cycle performance and thus presumably the ultimate fatigue mechanisms are unaffected. 0/90 KFRP is weakened by boiling and to a slightly greater extent by drying, although in both cases the strength losses are small, less than 10%. These effects are evidently associated with the absorption/desorption of moisture by the fibres themselves. The fatigue performance and the characteristic 'knee' are unaffected by conditioning except for differences in the positions of the S-logN curves which reflect the relative static strengths.

Generally tensile preloads have no observable effect on the moisture absorption characteristics in boiling water or the subsequent residual fatigue properties except in the notable case of the GRP mentioned above where the initial rate (but not the overall level) of moisture uptake is also increased.

In the ±45° orientation all the laminates are sensitive to environmental conditioning. The tensile monotonic and short term fatigue strengths of the 65%RH laminates are reduced both by boiling water exposure and by drying. This can be attributed to changes in the residual thermal stresses, limited plasticisation of the resin and, where applicable, degradation of the fibres and interfacial bonding. Conditioning generally has little effect on the high cycle fatigue performance however, except in the case of GRP where boiling causes a change in failure mode to one involving fibre fracture and reduces the performance at all stress levels. Fibre splitting continues to limit the strength of the conditioned KFRP.

The effect of conditioning on the non-fibre dominated properties is confirmed by short beam interlaminar shear tests where the relative strengths and the sensitivity to moisture generally follow the ±45° tensile behaviour. In this mode of loading delamination failure is initiated by oblique cracking in the transverse plies. This involves transverse fibre splitting in KFRP which (as in the case of the ±45° tensile tests) leads to a lower strength for this material. In fact the low ILSS of KFRP and the relatively high stress levels required to cause flexural failure for CFRP mean that these laminates are prone to shear failure in bending.

Boiling causes a small reduction in the compressive flexural static and fatigue strengths of 0/90 KFRP, compared to a slight strength increase for CFRP. Moisture presumably reduces the buckling resistance of the Kevlar fibres. The effect of environment on the flexural fatigue performance of GRP resembles that of the 0/90 laminates in tensile loading, the failure modes being very similar despite the different stress conditions and failure criteria.

REFERENCES

1. B Harris, AGARD Lecture Series No.124, 1982, pp.1.1-1.5.
2. Mechanical Engineering, 1981, 24-56.
3. R Hadcock, AGARD Lecture Series No.124, 1982, pp.12.1-12.13.
4. J R Vinson, 'Composite Materials', Proceedings of Japan- U.S. Conference, Tokyo, 1981, pp.353-361.
5. C Zweben,Composites, 12, 1981, 235-240.
6. J Bell, New Scientist, 1984, 8-13.
7. G Dorey, AGARD Lecture Series No.124, 1982, pp.10.1-10.13.
8. D M Riggs, R J Shuford, R W Lewis, 'Handbook of Composite Materials', Ed. G Lubin, Van Nostrand Reinhold, New York, 1982, pp.197-271.
9. D Hull, 'An Introduction to Composite Materials', Cambridge University Press, Cambridge, 1981.
10. J B Donnet and P Ehrburger, Carbon, 15, 1977, 143-152.
11. W N Reynolds and R Moreton, Phil Trans R Soc Lond, A294, 1980, 451-461.
12. C C Chiao and T T Chiao, 'Handbook of Composite Materials', Ed. G Lubin, Van Nostrand Reinhold, New York, 1982, pp.272-317.
13. W B Black, Annual Review of Materials Science, 10, 1980, 311-362.
14. M G Dobb, D J Johnson and B P Saville,Phil Trans R Soc Lond, A294, 1980, 483-485.
15. J H Greenwood and P G Rose, J Materials Science, 9, 1974, 1809-1814.

16. J W S Hearle and B S Wong, J Materials Science, 12, 1977, 2447-2455.

17. M G Dobb, D J Johnson, A Majeed and B P Saville, Polymer, 20, 1979, 1284-1288.

18. C O Pruneda, W J Steel, R P Kershaw and R J Morgan, Composites Technology Review, 3, 1981, 103-104.

19. M E Roylance, PhD Thesis, Dept of Civil Engineering, Massachusets Inst of Technology, 1980.

20. L Konopasek and J W S Hearle, J Applied Polymer Science, 21, 1977, 2791-2815.

21. A R Bunsell, J Materials Science, 10, 1975, 1300-1308.

22. E P Plueddemann, International Journal of Adhesion and Adhesives, 1981, 305-310.

23. W D Bascom, J Adhesion, 2, 1970, 161-183.

24. E Fitzer, K-H Geigl, W Huttner and R Weiss, Carbon, 18, 1980, 389-393.

25. L M Manocha, J Materials Science, 17, 1982, 3039-3044.

26. N C W Judd, Aeronautical Research Council Paper ARC 37818, 1978.

27. N A Mumford, P C Hopkins and B A Lloyd, AIAA Paper 82-1069, 1982.

28. D J Vaughan, Proc 11th National SAMPE Techn Conf., November 13-15, 1979, pp.593-600.

29. L S Penn and T T Chiao, 'Handbook of Composite Materials', Ed G Lubin, Van Nostrand Reinhold, New York, 1982, pp.57-88.

30. R J Morgan, J E O'Neal and D L Fanter, J Materials Science, 15, 1980, 751-764.

31. R J Morgan and J E O'Neal, Polymer-Plast. Tech Eng , 10, 1978, 49-116.

32. D H Kaelble, 'Resins for Aerospace', American Chemical Society, 1980, Paper 29, pp.395-417.

33. P J Dynes and D H Kaelble, 'Composite Materials: Testing and Design (Fifth Conference)', ASTM STP 674, Ed S W Tsai, American Society for Testing and Materials, 1979, pp.566-577.

34. R P Harrison and M G Bader, Final Report under Agreement A93B/25, 1981, University of Surrey.

35. D B S Berry, B I Buck, A Cornwell and L N Phillips, Handbook of Resin Properties, Part A : Cast Resins.

36. C K H Dharan, J Materials Science, 10, 1975, 1665-1670.

37. R W Hertzberg and J A Manson, 'Fatigue in Engineering Plastics', Academic Press, New York, 1980.

38. D Dew-Hughes and J L Way, Composites, 4, 1973, 167-173.

39. W W Wright, Composites, 12, 1981, 201-205.

40. C Gourdin, 'Proceedings of the Third International Conference on Composite Materials', Volume 1, Pergamon Press, 1980, pp.497-513.

41. R E Allred and A M Lindrose, 'Composite Materials: Testing and Design (Fifth Conference)', ASTM STP 674, Ed. S W Tsai, American Society for Testing and Materials, 1979, pp.313-323.

42. T J Martin, R M Hunt and G Duff, The Reinforced Plastics Congress 80, The British Plastics Federation Reinforced Plastics Group, 1980.

43. W S Smith, SPE Technical Conference, Los Angeles, California, December 4-6, 1979, Paper A-34.

44. Y A Tajima, SAMPE Quarterly, 11, 1980, 1-9.

45. M J Adamson, J Materials Science, 15, 1980, 1736-1745.

46. H G Carter and K G Kibler, J Composite Materials, 12, 1978, 118-131.

47. E R Long, Jr., NASA Technical Paper 1474, 1979.

48. P Peyser and W D Bascom, J Materials Science, 16, 1981, 75-83.

49. C E Browning, G E Husman and J M Whitney, 'Composite Materials: Testing and Design (Fourth Conference)', ASTM STP 617, American Society for Testing and Materials, 1977, pp.481-496.

50. E L McKague, J D Reynolds and J E Halkias, ASME Transactions Series H-, J Engineering Materials and Technology, 98, 1976, 92-95.

51. C D Shirrell, 'Advanced Composite Materials - Environmental Effects', ASTM STP 658, Ed J R Vinson, American Society for Testing and Materials, 1978, pp.21-42.

52. P Bonniau and A R Bunsell, J Composite Materials, 15, 1981, 272-293.

53. A C Loos and G S Springer, J Composite Materials, 13, 1979, 131-147.

54. F W Crossman, R E Mauri and W J Warren, 'Advanced Composite Materials - Environmental Effects', ASTM STP 658, Ed J R Vinson, American Society for Testing and Materials, 1978, pp.205-220.

55. R DeIasi and J B Whiteside, 'Advanced Composite Materials - Environmental Effects', ASTM STP 658, Ed J R Vinson, American Society for Testing and Materials, 1978, pp.2-20.

56. C-H Shen and G S Springer, J Composite Materials, 10, 1976, 2-20.

57. O Gillat and L J Broutman, 'Advanced Composite Materials - Environmental Effects', ASTM STP 658, Ed J R Vinson, American Society for Testing and Materials, 1978, pp.61-83.

58. J M Whitney and C E Browning, 'Advanced Composite Materials - Environmental Effects', ASTM STP 658, Ed J R Vinson, American Society for Testing and Materials, 1978, pp.43-60.

59. P T Curtis, RAE Technical Memorandum Mat 375, 1981.

60. S M Copley, RAE Technical Report 82010, 1982.

61. G T Van Amerongen, Rubber Chemistry and Technology, 37, 1964, 1065-1152.

62. J Crank, 'The Mathematics of Diffusion', 2nd Edition, Oxford University Press, 1975.

63. B Dewimille and A R Bunsell, Composites, 14, 1983, 35-40.

64. H T Hahn and R Y Kim, 'Advanced Composite Materials - Environmental Effects', ASTM STP 658, Ed J R Vinson, American Society for Testing and Materials, 1978, pp.98-120.

65. G S Springer, 'Developments in Reinforced Plastics -2', Ed G Pritchard, Applied Science Publishers, London, 1982, pp.43-65.

66. W J Mikols, J C Seferis, A Apicella and L Nicolais, Polymer Composites, 3, 1982, 119-124.

67. C D Shirrell and F A Sandow, 'Proceedings of 4th Conference on Fibrous Composites in Structural Design', Ed E M Lenoe, D W Oplinger and J J Burke, Plenum Press, 1978, pp.795-808.

68. P W R Beaumont and B Harris, 'Carbon Fibres, their Composites and Applications', Plastics Institute, London, 1971, pp.283-291.

69. J Aveston, A Kelly and J M Sillwood, 'Proceedings of the Third International Conference on Composite Materials', Volume 1, Pergamon Press, 1980, pp.556-568.

70. R J Charles, J Applied Physics, 29, 1958, 1549-1560.

71. A G Metcalfe and G K Schmitz, Glass Technology, 13, 1972, 5-16.

72. R W Davidge, J R Mclaren and G Tappin, J Materials Science, 8, 1973, 1699-1705.

73. R E Allred and D K Roylance, J Materials Science, 18, 1983, 652-656.

74. T T Chiao and R L Moore, Composites, 4, 1973, 31-33.

75. N L Hancox, J Materials Science, 16, 1981, 627-632.

76. D H Kaelble, P J Dynes, L W Crane and L Maus, 'Composite Reliability', ASTM STP 580, American Society for Testing and Materials, 1975, pp.247-262.

77. B D Agarwal and L J Broutman, 'Analysis and Performance of Fibre Composites', Wiley-Interscience, New York, 1980.

78. D J Vaughan and E L McPherson, Composites, 4, 1973, 131-133.

79. R E Allred, J Composite Materials, 15, 1981, 100-116 and 117-132.

80. D C Phillips, J M Scott and N Buckley, 'Proceedings of the Second International Conference on Composite Materials', 1978, pp.1544-1559.

81. M J Owen, 'Composite Materials, Volume 5, Fracture and Fatigue', Ed L J Broutman, Academic Press, New York, 1974, pp.313-340, 341-369.

82. C C Chamis, 'Composite Materials, Volume 6, Interfaces in Polymer Matrix Composites', Ed. E P Plueddemann, Academic Press, New York, 1974, pp.32-77.

83. J E Bailey and A Parvizi, J Materials Science, 16, 1981, 649-659.

84. E C Edge, AGARD Conference Proceedings No 288, 1980, pp.1.1-1.17.

85. B L Lee, R W Lewis and R E Sacher, 'Proceedings of the Second International Conference on Composite Materials', 1978, pp.1560-1583.

86. B Harris, Composites, 8, 1977, 214-220.

87. J F Mandell, 'Developments in Reinforced Plastics-2', Ed G Pritchard, Applied Science Publishers, London, 1982, pp.67-107.

88. M J Salkind,'Composite Materials: Testing and Design (Second Conference)', ASTM STP 497, American Society for Testing and Materials, 1972, pp.143-169.

89. H T Hahn, 'Composite Materials, Testing and Design (Fifth Conference)', ASTM STP 674, Ed S W Tsai, American Society for Testing and Materials, 1979, pp.383-417.

90. H T Hahn, 'Proceedings of 3rd Riso International Symposium on Metallurgy and Materials Science', RISO Press, 1982, pp.19-35.

91. C-H Shen and G S Springer, J Composite Materials, 11, 1977, 2-16 and 250-264.

92. A W Cardrick, RAE Technical Report 73022, 1973.

93. J B Sturgeon, RAE Technical Report 75135, 1975.

94. J J Gerharz and D Schutz, RAE Translation 2045, Volume 1, Royal Aircraft Establishment, 1980, pp.72-99.

95. J J Gerharz, AGARD Lecture Series No.124, 1982, pp.7.1-7.20.

96. M J Owen and S Morris, Modern Plastics, 47, 1970, 158-169.

97. R B Pipes, 'Composite Materials: Testing and Design (Third Conference)', ASTM STP 546, American Society for Testing and Materials, 1974, pp.419-432.

98. R Talreja, Proc R Soc Lond, A378, 1981, 461-475.

99. J M Lifshitz, 'Composite Materials, Volume 5, Fracture and Fatigue', Ed L J Broutman, Academic Press, New York, 1974, pp.249-311.

100. W W Stinchcomb and K L Reifsnider, 'Fatigue Mechanisms', ASTM STP 675, Ed J T Fong, American Society for Testing and Materials, 1979, pp.762-787.

101. K L Reifsnider, K Schulte and J C Duke, 'Long-term behaviour of Composites', ASTM STP 813, Ed T K O'Brien, American Society for Testing and Materials, 1983, pp.136-159.

102. M Watanabe, 'Composite Materials: Testing and Design (Fifth Conference)', ASTM STP 674, American Society for Testing and Materials, 1979, pp.345-367.

103. C Y Lundemo and S Thor, J Composite Materials, 11, 1977, 276-284.

104. L G Bevan, Composites, 8, 1977, 227-232.

105. A K Green and P L Pratt, Composites, 6, 1975, 246-248.

106. Carboform, Technical Data Sheet, Fothergill and Harvey Ltd., 1976.

107. J W Johnson, Phil Trans R Soc Lond A294, 1980, 487-494.

108. K F Port, RAE Technical Report 82083, 1982.

109. L G Bevan and J B Sturgeon, Proc 2nd International Conference on Carbon Fibres, The Plastics Institute, London, 1974, Paper 32.

110. M G Bader and M Johnson, Composites, 5, 1974, 58-62.

111. C Zweben, J Composite Materials, 12, 1978, 422-430.

112. M Fuwa, A R Bunsell and B Harris, J Materials Science, 10, 1975, 2062-2070.

113. B W Rosen, AIAA Journal, 2, 1964, 1985-1991.

114. G D Sims and D G Gladman, Plastics and Rubber: Materials and Applications, 1978, 41-48.

115. G D Sims and D G Gladman, Plastics and Rubber: Materials and Applications, 1980, 122-128.

116. J F Mandell, D D Huang and F J McGarry, Composites Technology Review, 3, 1981, 96-102.

117. P T Curtis and B B Moore, RAE Technical Report 82031, 1982.

118. A R Bunsell, AGARD Lecture Series No.124, 1982, pp.3.1-3.10.

119. J M Lifshitz and A Rotem, Fibre Science and Technology, 3, 1970, 1-20.

120. J E Bailey, P T Curtis and A Parvizi, Proc R Soc Lond, A366, 1979, 599-623.

121. L J Broutman and S Sahu, Proc 24th Annual Conference, Plastics/Composites Inst., SPI, 1969, Paper 11-D.

122. P T Curtis, RAE Technical Report 80045, 1980.

123. K W Garrett and J E Bailey, J Materials Science, 12, 1977, 157-168.

124. A Parvizi, K W Garrett and J E Bailey, J Materials Science, 13, 1978, 195-201.

125. D O Stalnaker and W W Stinchcomb,'Composite Materials: Testing and Design (Fifth Conference)', ASTM STP 674, Ed S W Tsai, American Society for Testing and Materials, 1979, pp.620-641.

126. M G Bader and L Boniface, Proc Conf on 'Testing, Evaluation and Quality Control of Fibre Composites', Surrey, Butterworths Press, 1983, pp.66-75.

127. R D Jamison, K Schulte, K L Reifsnider and W W Stinchcomb, Presented at ASTM Symposium on 'Effects of Defects in Composite Materials', San Francisco, California, 1982.

128. J Aveston and A Kelly, Phil Trans R Soc Lond, A294, 1980, 519-534.

129. P T Curtis, RAE Technical Report 80054, 1980.

130. J B Sturgeon, RAE Technical Memorandum Mat 228, 1975.

131. J B Sturgeon and F S Rhodes, RAE Technical Report 80115, 1980.

132. J B Sturgeon, RAE Technical Report 80151, 1980.

133. J B Sturgeon, J Materials Science, 13, 1978, 1490-1498.

134. M E Roylance, W W Houghton, G E Foley, R J Shuford and G R Thomas, AGARD Conference Proceedings No.355, 1983, pp.7.1-7.14.

135. R B Pipes, AGARD Lecture Series No.124, 1982, pp.5.1-5.11.

136. J W Davis and G J Sundsrud, 'Composite Materials: Testing and Design (Fifth Conference)', ASTM STP 674, Ed S W Tsai, American Society for Testing and Materials, 1979, pp.137-148.

137. A C Loos and G Springer, J Composite Materials, 13, 1979, 17-33.

138. R S Berry, S A Rice and J Ross, 'Physical Chemistry', John Wiley and Sons, New York, 1980.

139. O Ishai, Polymer Engineering and Science, 15, 1975, 486-499.

140. G Marom and L J Broutman, Polymer Composites, 2, 1981, 132-136.

141. P T Curtis and B B Moore, Composites, 14, 1983, 294-300.

142. F J McGarry, 'Fundamental Aspects of Fiber Reinforced Plastic Composites', Ed R T Schwartz and H S Schwartz, Interscience, New York, 1968, pp.63-87.

143. K H G Ashbee and N Farrar, 'Proceedings of the (First) International Conference on Composite Materials', Volume 1, AIME, New York, 1975, pp.771-782.

144. M E Roylance, Proc 11th National SAMPE Tech Conf., November 13-15, 1979, pp.601-613.

145. D Schutz and J J Gerharz, Composites, 8, 1977, 245-250.

146. R F Dickson, PhD Thesis, Dept of Materials Science, University of Bath, 1984.

147. C C Chiao, R L Moore and T T Chiao, Composites, 8, 1977, 161-174.

148. A Rotem and Z Hashin, J Composite Materials, 9, 1975, 191-206.

149. E Pink and J D Campbell, J Materials Science, 9, 1974, 658-664.

150. S Morris, PhD Thesis, University of Nottingham, 1970.

151 J W Johnson, Composites, 14, 1983, 107-114.

152. C Zweben, W S Smith and M W Wardle, 'Composite Materials: Testing and Design (Fifth Conference)', ASTM STP 674, Ed S W Tsai, American Society for Testing and Materials, 1979, pp.228-262.

153. K H Boller, Modern Plastics, 41, 1964, 145-188.

154. A W Thompson, Trans Plastics Inst., 30, 1962, 39-50.

155. M J Owen, Phil Trans R Soc Lond., A294, 1980, 535-543.

156. L H Miner, R A Wolffe and C H Zweben, 'Composite Reliability', ASTM STP 580, American Society for Testing and Materials, 1975, pp.549-559.

157. H T Hahn and W K Chin, Composites Technology Review, 3, 1981, 27-31.

158. H T Hahn and W K Chin, Proc 37th Annual Conference, Reinforced Plastics/Composites Inst., SPI, 1982, Paper 24-C.

159. A S D Wang, P C Chou and J Alper, 'Fatigue of Fibrous Composite Materials', ASTM STP 723, American Society for Testing and Materials, 1981,116-132.

160. J N Yang and M D Liu, J Composite Materials, 11, 1977, 176-203.

161. M H Lafitte and A R Bunsell, J Materials Science, 17, 1982, 2391-2397.

162. L C Cessna, J A Levens and J B Thomson, Proc 24th Annual Conference, Reinforced Plastics/Composites Inst., SPI, 1969, Paper 1-C.

163. B D Agarwal and S K Joneja, Composites Technology Review, 4, 1982, 6-13.

164. H T Sumsion, AIAA Paper 75-771, 1975.

165. H T Sumsion and M J Adamson, 'Methods for Predicting Material Life in Fatigue', American Society of Mechanical Engineers, New York, 1979, pp.265-274.

166. S C Kunz and P W R Beaumont, 'Fatigue of Composite Materials', ASTM STP 569, American Society for Testing and Materials, 1975, pp.71-91.

167. M J Owen and S Morris, 'Carbon Fibres, their Composites and Applications', Plastics Institute, London, 1971, pp.292-301.

168. J D Conners, J F Mandell and F J McGarry, Proc. 34th Annual Conference, Reinforced Plastics/Composites Inst., SPI, 1979, Paper 4-A.

169. S V Ramani, 'Proceedings of the Second International Conference on Composite Materials', 1978, p.1602 (Abstract only).

170. H C Kim and L J Ebert, Fibre Science and Technology, 14, 1981, 3-20.

171. C Zweben and M W Wardle, Polymer Composites, 2, 1981, 61-67.

172. E Popov, 'Mechanics of Materials', 2nd Edition, Prentice/Hall International, New Jersey, 1978.

173. J M Whitney and G E Husman, Experimental Mechanics, 18, 1978, 185-190.

174. J Cook and J E Gordon, Proc. Roy. Soc. London., A282, 1964, 508-520.

PUBLICATIONS

P1 Environmental fatigue of reinforced plastics
R F Dickson, C J Jones, T Adam, H Reiter and B Harris,
Final Report under Agreement 2112/034XR/MAT, July 1983.

P2 Les effets de l'environnement sur la fatigue de divers materiaux composites,
C J Jones, R F Dickson, T Adam, H Reiter and B Harris
Comptes Rendus des Troisiemes Journees Nationales sur les Composites, JNC3, Ed A Corvino et al, Editions Pluralis, 1982, pp.77-88.

P3 Environmental fatigue of reinforced plastics
C J Jones, R F Dickson, T Adam, H Reiter and B Harris,
Composites, 14, 1983, 288-293.

P4 Effects of moisture on high performance laminates
R F Dickson, C J Jones, B Harris, T Adam and H Reiter
Proceedings of 'First International Conference on Acoustic Emission from Reinforced Composites', San Francisco; SPI, New York, 1983, Paper A4: 1-14.

P5 Effects of moisture on high performance laminates
R F Dickson, C J Jones, B Harris, H Reiter and T Adam,
Proceedings of 'Fibre Reinforced Composites '84', Liverpool; Plastics and Rubber Institute, London, 1984, Paper 30: 1-11.

P6 Environmental tensile fatigue of reinforced plastics
C J Jones, R F Dickson, T Adam, H Reiter and B Harris,
Proc Int Conference, 'Fatigue '84', Birmingham, September 1984.

P7 The environmental fatigue behaviour of reinforced plastics
C J Jones, R F Dickson, T Adam, H Reiter and B Harris,
Proc Roy Soc Lond, A396, 1984, 315-338.

APPENDIX 1

A standard least squares best fit method (developed by Mr T Adam of the School of Mechanical Engineering, University of Bath), run on a Hewlett Packard 9810A programmable calculator and plotter, was used to calculate the values of A,B,C and n for the Ramberg-Osgood Equation 4.4 and hence generate curves of moisture uptake as a function of √time. Some of these curves (for undamaged specimens) are reproduced in Figure 4.12. Values of A, B, C and n for the various exposures are tabulated below.

65%RH, 23°C (from 'as-received')

Laminate	A	B	C	n
CFRP	9.01	1.83	0.01	5.74
GRP	12.22	0.05	0.06	3.31
KFRP	5.75	5.13	0.04	2.89

Drying, 60°C (from 65%RH)

Laminate	A	B	C	n
CFRP	4.47	3.04	-0.15	10.28
CFRP	4.41	4.55	0.01	5.40
GRP	3.61	3.89	-0.04	4.01
GRP	3.58	4.21	0.01	4.00
GRP (voids)	3.82	2.31	0.00	7.62
KFRP	2.42	0	-0.07	12.04
KFRP	3.69	0	0.01	18.11

65%RH, 23°C (from dry)

Laminate	A	B	C	n
CFRP	26.12	2.24	-0.447	9.89
GRP	29.70	0	-0.799	1.00
KFRP	15.64	16.33	-0.029	2.66

Boiling water (from 65%RH)

CFRP	Preload, GPa	A	B	C	n
	0	12.96	13.37	0.07	10.50
	0	13.16	13.22	0.02	11.05
	0	13.56	12.75	0.01	8.61
	0	13.22	13.03	0.10	5.76
	0	12.29	14.17	-0.01	9.45
	0	12.86	13.63	-0.04	12.09
	0.1	12.96	14.18	-0.20	12.81
	0.2	12.16	14.91	-0.14	7.70
	0.3	12.72	14.47	-0.27	8.30
	0.4	12.49	14.55	-0.09	8.23
	0.5	12.19	15.04	-0.30	14.80
	0.6	12.13	15.00	-0.19	19.18
	0.7	11.71	15.40	-0.18	17.33
	0.8	12.06	14.90	-0.01	16.18

KFRP	Preload, GPa	A	B	C	n
	0	8.16	0	-0.53	12.29
	0	7.57	1.85	-0.53	25.00
	0	5.61	12.70	-0.05	10.34
	0	7.24	0	-0.32	14.36
	0	9.05	0	-0.65	24.00
	0.1	5.51	21.25	-0.11	4.02
	0.2	6.06	33.21	0.10	2.09
	0.3	5.57	32.52	0.03	1.75
	0.4	4.10	22.76	0.08	4.94
	0.5	5.88	20.87	-0.17	6.79
	0.6	3.24	23.75	0.01	6.16

GRP	Preload, GPa	A	B	C	n
	0	13.95	12.32	0.14	5.59
	0	9.25	17.14	-0.14	3.23
	0	14.18	12.54	-0.39	6.01
	0	14.84	11.57	-0.02	8.40
	0	14.17	12.27	-0.06	8.27
	0	15.59	11.01	-0.23	5.97
Slow load-rate	0.1	13.36	12.59	-0.06	4.13
	0.2	13.20	12.95	-0.33	6.97
	0.3	14.44	11.81	-0.44	5.84
	0.4	12.69	13.46	-0.34	5.34
	0.5	9.89	16.03	-0.03	3.68
	0.6	10.43	15.46	-0.03	4.09
Fast load-rate	0.1	14.10	12.03	-0.30	4.84
	0.24	13.39	12.63	-0.21	3.85
	0.28	13.42	12.75	-0.38	5.31
	0.40	14.46	11.69	-0.33	5.21
	0.46	13.03	13.00	-0.16	11.26
	0.54	7.99	17.85	0.04	3.27
	0.67	9.81	16.08	0.26	4.00
	0.79	6.82	18.94	-0.07	3.29

Water, 23°C (from 'as-received')

Laminate	A	B	C	n
CFRP	88.26	53.40	1.27	5.91
GRP	119.89	31.01	2.81	14.79
KFRP	26.19	127.23	-0.16	2.90

APPENDIX 2

Bend testing offers the opportunity to apply combinations of tensile, compressive and interlaminar shear stresses and to control the relative magnitudes of these by simple changes to the test geometry. The geometries of the most common methods, 3 and 4-point bending, are shown schematically in Figures A2.1 and A2.2. The rectangular cross-section specimen is supported close to its ends and load applied via a single, central loading roller (3-point bending) or by two symmetrically spaced inner loading rollers (4-point bending). This produces both flexural and shear stresses within the specimen gauge-length.

In 3-point bending, the flexural stress varies linearly from zero at the outer supports to a maximum at the central load point. The situation in 4-point bending is similar, with the addition of a constant, maximum bending moment in the region between the inner load points. The in-plane shear stress is uniform along the specimen length but of opposite sense either side of the central load point. In 4-point loading there are no shear stresses between the inner load points and this section of the specimen should experience pure bending moment.

Through the specimen thickness, the flexural stress varies in response to a linear variation in strain that is maximum at the lower surface, equal maximum at the upper surface and zero along the neutral plane xx'. The shear distribution varies parabolically through the thickness such that it is zero at the surfaces and a maximum at

the mid-plane. For non-isotropic materials such as laminated composites, the resultant flexural and shear stresses do not necessarily resemble the uniform strain distributions since there are discontinuities at the ply interfaces and the effective modulus changes with the ply orientation through the specimen thickness.

For isotropic materials, the maximum surface flexural stress is given by the simple beam theory equations (172,173).

$$\sigma_{max} = \frac{3PS}{2bd^2} \quad \text{for 3-point loading} \qquad \text{(A2.1)}$$

and

$$\sigma_{max} = \frac{3PS}{4bd^2} \quad \text{for 4-point loading} \qquad \text{(A2.2)}$$

where P is the applied load, S is the span or distance between the outer load points and b and d are the specimen width and thickness respectively. Similarly, the maximum (interlaminar) shear stress along the mid-plane is given by

$$\tau_{max} = \frac{3P}{4bd} \qquad \text{(A2.3)}$$

These equations are normally adequate for the analysis of the stresses in unidirectional composites and can also be applied to laminates which are symmetrical about the mid-plane, such as the cross-plied laminates tested in this work. However, the 'apparent' strengths calculated thus are valid for qualitative comparisons only. For laminates containing significant proportions of off-axis plies or for composites such as KFRP where the compressive proportional limit is

known to be much lower than the tensile strength (with yielding at the compression surface effectively shifting the neutral plane away from the mid-plane towards the tensile surface (79,111)), non-linear stress/strain behaviour will reduce the validity of the above expressions. In general the state of stress is far more complex than that predicted from simple beam theory, especially in regions close to the loading points.

It is evident from Equations A2.1-3 that increasing the span results in higher ratios of flexural to shear stresses within the specimen and consequently a greater likelihood of failure occurring in a flexural rather than a shear mode. Material inhomogeneity means that the first ply failure of a laminate in bending does not necessarily occur at the outer surfaces (in flexure) or at the mid-plane (by shear). It will instead depend on the lay-up and stiffnesses of the various plies, and the variation in shear and flexural strength with respect to the stresses through the specimen thickness. These can be analysed using Laminated Plate theory with stiffness matrices calculated for the laminates concerned. An example of such an analysis has been presented by Morris(150).

In the Avery flexure test (Figure A2.3) the specimen is assumed to be free from shear stress. The maximum surface stress, constant along the gauge-section, is given by the standard flexure formula for beams (172)

$$\sigma_{max} = \frac{Mc}{I} \qquad (A2.4)$$

where M is the bending moment, I is the moment of inertia of the

specimen cross-section about the neutral plane and c is the distance from the neutral plane to the specimen surface (in this case one half of the beam thickness, i.e. $\frac{d}{2}$). For beams of rectangular cross-section (and of width b), the moment of inertia is given by

$$I = \frac{bd^3}{12} \qquad (A2.5)$$

$$\text{Hence } \sigma_{max} = \frac{6M}{bd^2} \qquad (A2.6)$$

Equation A2.6 also provides the basis for the simple 3-point and 4-point bend test Equations A2.1-3.

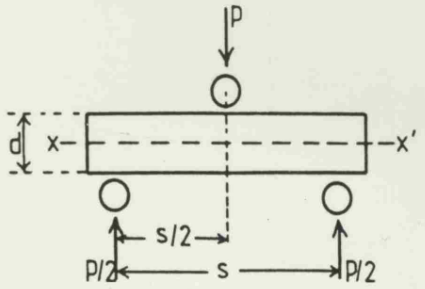

Figure A2.1 3-point bend test geometry

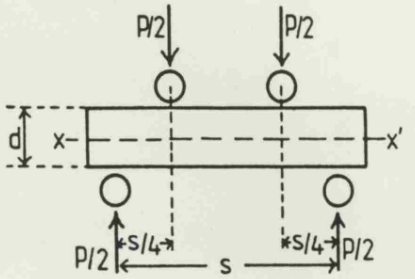

Figure A2.2 4-point bend test geometry

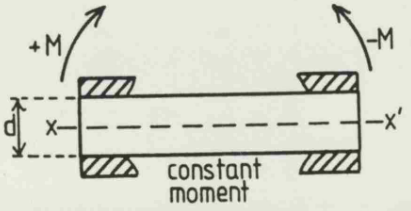

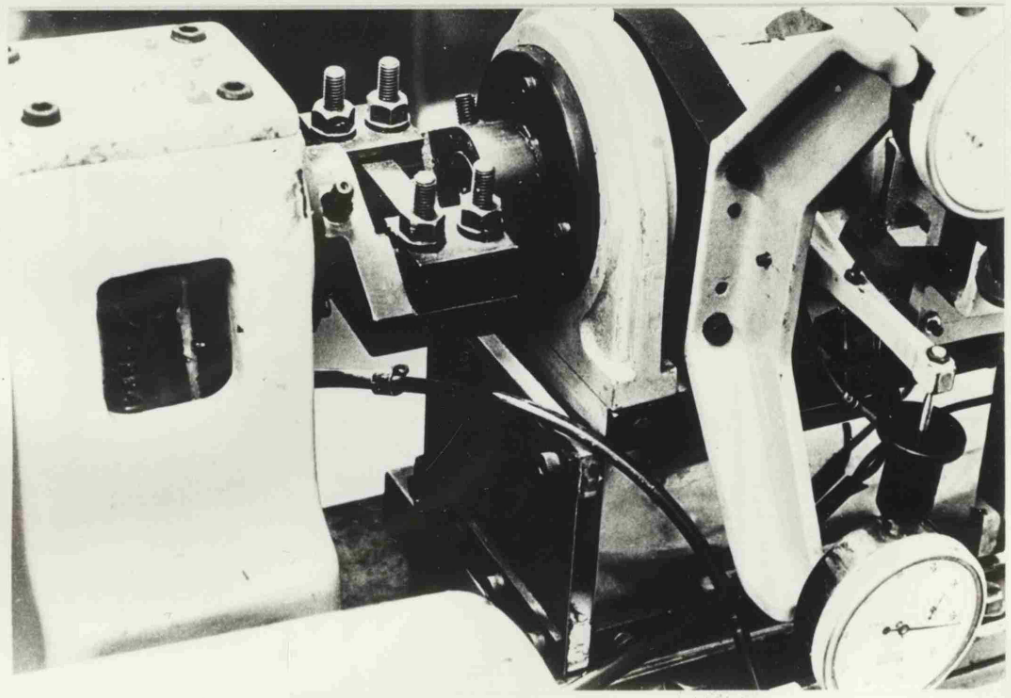

Figure A2.3 a) Avery bend test geometry

b) Avery machine

TABLE 2.1 TYPICAL FIBRE AND RESIN PROPERTIES

Property	Carbon HT-S	E-Glass	Kevlar-49	Epoxy(Code 69)
Tensile strength, GPa	2.7	1.4-2.5	2.5-2.8	41×10^{-3}
Young's Modulus, GPa	250-270(a)	70-76	130(a)	4.1-4.2
	20 (b)		6.9(b)	
Failure Strain, %	1.0	1.8-3.2	2.2-2.4	1.0-1.1
Fibre Diameter, μm	7-10	10	12	-
Relative Density	1.75-1.8	2.5-2.6	1.45	1.27
Coefficient of Thermal	-0.1— -0.5(a)	4.9	-2.0— -4.0(a)	50-60
Expansion ($\times 10^{-6}$/°C)	7-12 (b)		59-205 (b)	
Swelling Coefficient	-	-	0.06-0.09(a)	0.27
(%/% weight gain)			0.5-1.0 (b)	

(a) along fibre axis

(b) transverse to fibre axis

(Data taken from references 8,9,12,19,34,35,77)

TABLE 2.2 TYPICAL UNIDIRECTIONAL COMPOSITE PROPERTIES ($V_f \sim 0.6$)

(source references 9,77,106,120,147)

Property	Carbon (HT-S)/ Epoxy (Code 69)	Glass/Epoxy	Kevlar/Epoxy
0° tensile strength, GPa	1.62	0.92	1.31-1.40
0° tensile modulus, GPa	148	42	80
90° tensile strength, MPa	34	56	20-39
90° tensile modulus, GPa	8.2	14	5.5
ILSS, MPa	100	70	37-69
0° compressive strength, GPa	1.10		0.24-0.29

TABLE 3.1 PREPREG SPECIFICATIONS

Fibre types :	Grafil HT-S carbon fibre, 132/1.55/K10, grade SF (Courtaulds)
	Silenka E glass, 600 tex, epoxy size
	Kevlar-49 aramid fibre, 4560 denier, no fibre finish
	or twist (E.I. Du Pont de Nemours and Co.)
Resin type:	Epoxy resin, Code 69 (Fothergill and Harvey)
Resin weight, %:	Glass, 28±2.5%
	Kevlar, 40±2.5%
	Carbon, 35±2.5%
Moulded thickness:	0.25mm

TABLE 3.2 LAMINATE DENSITIES AND FIBRE VOLUME FRACTIONS

Laminate	Density, $10^3 Kgm^{-3}$	V_f
GRP	2.01(0.02)	0.64(0.02)
CFRP	1.50(0.02)	0.58(0.04)
KFRP	1.36(0.02)	0.64(0.07)

(Standard deviations in brackets)

TABLE 3.3 EFFECTIVE AVERAGE TESTING RATES FOR INSTRON 1195 WITH 0.5mm/MINUTE CROSS-HEAD SPEED ('SLOW' LOADING).

Laminate		Condition	Stress Rate, $MPas^{-1}$	Load Rate, kNs^{-1}	Strain Rate, s^{-1}
GRP	0/90	ALL	0.83	0.023	$3.4x10^{-5}$
CFRP	0/90	ALL	1.34	0.038	$1.6x10^{-5}$
KFRP	0/90	ALL	0.96	0.027	$3.0x10^{-5}$
GRP	±45°	Dried	0.53	0.015	$5.9x10^{-5}$
		65%RH	0.42	0.012	$6.6x10^{-5}$
		Boiled	0.31	0.009	$7.0x10^{-5}$
CFRP	±45°	Dried	0.60	0.017	$5.3x10^{-5}$
		65%RH	0.47	0.013	$6.2x10^{-5}$
		Boiled	0.31	0.009	$6.3x10^{-5}$
KFRP	±45°	Dried	0.18	0.005	$7.1x10^{-5}$
		65%RH	0.20	0.006	$7.2x10^{-5}$
		Boiled	0.18	0.005	$6.7x10^{-5}$

TABLE 4.1 SWELLING AS A FUNCTION OF TIME IN BOILING WATER

(Specimens:200x10mm,0/90 lay-up)

Laminate	Time in boiling water, weeks	Increase in width, %	Increase in thickness,%
CFRP	0	-	-
	4	0.030(0.051)	0.916(0.202)
	26	0.082(0.097)	0.977(0.191)
GRP	0	-	-
	4	0.033(0.051)	1.188(0.490)
	26	0.132(0.081)	1.545(0.589)
KFRP	0	-	-
	4	0.115(0.115)	3.350(1.194)
	26	0.180(0.115)	4.900(1.553)

TABLE 4.2 MOISTURE LEVELS IN LAMINATES AFTER STANDARD PRECONDITIONING TREATMENTS

Condition	Water uptake expressed as percentage increase in weight (%) and increase in weight per unit volume (Kgm^{-3})					
	CFRP		GRP		KFRP	
	%	Kgm^{-3}	%	Kgm^{-3}	%	Kgm^{-3}
'Dried'	0	0	0	0	0	0
'As-received'	0.65-0.69	9.7-10.3	0.35-0.37	7.0-7.4	2.0-2.6	26-34
65%RH	0.88-0.92	13.1-13.7	0.55-0.60	11.0-12.0	2.8-3.4	37-45
'Boiled'	1.96-2.05	29.3-30.6	1.70-1.76	34.0-35.2	4.9-5.65	65-75
23°C water after 2 years	1.64-1.69	24.5-25.2	1.19-1.22	23.8-24.4	∿5.0	∿ 66

TABLE 4.3 APPARENT DIFFUSION COEFFICIENTS

ENVIRONMENTAL EXPOSURE	APPARENT DIFFUSION COEFFICIENT, $cm^2 s^{-1}$		
	CFRP	GRP	KFRP*
23°C, water from as-received	5.49×10^{-10}	2.98×10^{-10}	6.24×10^{-9}
23°C, 65%RH from Dry	2.61×10^{-10}	2.02×10^{-10}	7.29×10^{-10}
60°C, 0%RH from 65%RH	9.01×10^{-9}	1.35×10^{-8}	2.35×10^{-8}
100°C, Boiling Water from 65%RH	2.53×10^{-8}	2.03×10^{-8}	8.17×10^{-8}

*see text

TABLE 5.1 EFFECT OF PRECONDITIONING TREATMENTS ON TENSILE PROPERTIES OF 0/90 LAMINATES. 'SLOW' LOAD-RATE (INSTRON 1195; 0.5mm/MINUTE CROSS-HEAD SPEED).

LAMINATE	CONDITION	No. OF TESTS	STRENGTH MPa	MODULUS* GPa	FAILURE STRAIN, %
GRP	Dried	8	578(42)	37.4(2.9)/21.8(1.2)	2.4(0.2)
	65%RH	8	592(39)	33.6(1.7)/22.3(0.6)	2.5(0.2)
	Boiled	8	272(11)	32.1(1.2)/21.7(1.2)	1.0(0.1)
CFRP	Dried	8	944(78)	79.4(2.7)	1.2(0.1)
	65%RH	10	932(57)	82.6(2.4)	1.1(0.1)
	Boiled	8	934(47)	83.0(4.3)	1.1(0.1)
KFRP	Dried	8	674(16)	36.8(1.3)	1.9(0.1)
	65%RH	8	711(15)	33.5(1.2)	2.2(0.2)
	Boiled	8	684(13)	32.4(1.5)	2.3(0.2)
GRP	Boiled, 3 weeks	2	305	29.2/20.7	1.3
CFRP	and	2	936	83.0	1.2
KFRP	Redried	2	618	37.0	1.8
GRP	Heated at	2	629	32.8/22.5	3.0
CFRP	100°C (Dry)	2	986	84.0	1.2
KFRP	for 3 weeks	2	680	38.0	1.9
GRP	Boiled	3	206(10)	25.0(2.6)	0.8(0.1)
CFRP	6 months	3	836(41)	85.4(5.9)	1.0(0.1)
KFRP		3	444(13)	34.9(0.9)	1.3(0.1)
GRP	Water 23°C	2	537	33.0/22.1	2.2
CFRP	2 years	2	932	83.9	1.1
KFRP		2	796	35.2	2.2

*For GRP, the pairs of moduli reported are the primary and secondary moduli (except for 6 months boiled, where only the mean overall modulus is given)
Figures in brackets are standard deviations (as appropriate).

TABLE 5.2 EFFECT OF PRECONDITIONING TREATMENTS ON TENSILE PROPERTIES OF ±45° LAMINATES. 'SLOW' LOAD-RATE (INSTRON 1195; 0.5mm/minute CROSS-HEAD SPEED).

LAMINATE	CONDITION	No. of TESTS	STRENGTH MPa	FAILURE STRAIN %
GRP	Dried	8	115(2)	1.3(0.3)
	65%RH*	8	129(5)	7.7(1.5)
	Boiled	8	97(1)	4.9(2.3); 2.2*
CFRP	Dried	8	116(2)	1.0(0.1)
	65%RH	8	125(4)	1.6(0.2)
	Boiled	8	108(2)	2.5(0.4); 2.2*
KFRP	Dried	8	69(3)	2.8(0.3)
	65%RH	8	80(2)	2.9(0.3)
	Boiled	8	59(3)	2.5(0.4); 2.2*
GRP	Boiled, 3 weeks	6	95(2)	1.8(0.2)
CFRP	and	6	99(3)	1.0(0.1)
KFRP	Redried	6	57(2)	2.3(0.2)
GRP	Boiled	3	85(2)	1.6(0.4)
CFRP	6 months	3	109(3)	2.5(0.4)
KFRP		3	42(1)	2.6(0.2)

*Initial peak in stress-strain curve at 115(3)MPa and 1.8(0.2)%strain
*Strain at peak load where different from failure strain.

No modulus values are reported because the stress/strain curves were non-linear in this orientation.

TABLE 5.3 EFFECTS OF PRECONDITIONING TREATMENTS ON TENSILE PROPERTIES OF 0/90 LAMINATES. 'FAST' LOAD-RATE (INSTRON 1332; 200 kNs^{-1} FOR CFRP, 100 kNs^{-1} for GRP and KFRP).

Laminate	Condition	No. of Tests	Strength MPa	Modulus* GPa	Failure Strain*, %
GRP	Dried	4	869(58)	25.1	3.1
	65%RH	4	875(6)	25.5	3.4
	Boiled	5	416(20)	25.5	1.6
CFRP	Dried	4	916(20)	87.6	1.1
	65%RH	7	920(41)	85.4	1.1
	Boiled	4	928(32)	78.3	1.1
KFRP	Dried	5	664(26)	44.4	1.5
	65%RH	7	724(18)	35.5	1.6
	Boiled	4	710(27)	40.3	1.8
GRP	Boiled	3	291(2)	-	-
CFRP	6 months	-	-	-	-
KFRP		-	-	-	-
GRP 90/0	65%RH	-	-		
CFRP		3	900		
KFRP		4	647(29)	-	-
GRP	0.4GPa preload boiled 3 weeks	4	409(19)	-	-
GRP	0.7GPa preload boiled 3 weeks	4	342(20)	-	-
CFRP	0.7 GPa preload boiled 3 weeks	3	889(27)	-	-
KFRP	0.6GPa preload boiled 3 weeks	3	758(2)	-	-

*Based on results from single tests.

TABLE 5.4 EFFECTS OF PRECONDITIONING TREATMENTS ON TENSILE PROPERTIES OF ±45° LAMINATES. 'FAST' LOAD-RATE (INSTRON 1332; 25kNs^{-1}).

Laminate	Condition	No.of Tests	Strength MPa	Failure Strain %
GRP	Dried	4	132(3)	-
	65%RH	4	139(2)	-
	Boiled	4	124(2)	2.0
CFRP	Dried	4	126(4)	-
	65%RH	4	142(2)	-
	Boiled	4	129(2)	-
KFRP	Dried	4	69(2)	-
	65%RH	4	91(1)	-
	Boiled	4	78(4)	2.4

TABLE 5.5 COMPARISONS OF TENSILE PROPERTIES OF ±45° LAMINATES FOR 10mm and 20mm WIDE SPECIMENS

Laminate	Condition	No. of Tests	Specimen Width mm	Tensile Strength MPa	Failure Strain %
GRP	65%RH	6	10	129(5)	7.7(1.5)
		2	20	143	8.8
GRP	100%RH	6	10	97(1)	4.9(2.3)
		2	20	98	5.2
KFRP	65%RH	6	10	80(2)	2.9(0.3)
		2	20	95	3.2
KFRP	100%RH	6	10	59(3)	2.5(0.4)
		2	20	67	4.9

TABLE 5.6 INFLUENCE OF LOAD-RATE ON TENSILE STRENGTH - SUMMARY

Laminate	Condition	Average Increase in Strength (MPa) per decade load-rate	% Increase in Strength per decade load-rate increase
GRP, 0/90	Dried	+80	9-14
	65%RH	+78	9-13
	Boiled	+40	10-15
CFRP, 0/90	Dried	- 8	-1
	65%RH	- 3	0
	Boiled	- 2	0
KFRP, 0/90	Dried	- 3	0
	65%RH	+ 4	1
	Boiled	+ 7	1
GRP, ±45°	Dried	+ 5	3-4
	65%RH	+ 3	2
	Boiled	+ 8	7-8
CFRP, ±45°	Dried	+ 3	2-3
	65%RH	+ 5	4
	Boiled	+ 6	5-6
KFRP, ±45°	Dried	0	0
	65%RH	+ 3	3-4
	Boiled	+ 5	6-9

TABLE 5.7 COMPARISON OF SPECIFIC TENSILE PROPERTIES OF LAMINATES

Material	Specific gravity	Specific tensile strength, MPa	Specific Young's modulus, GPa
0/90 GRP	2.01	295	16.7/11.1
0/90 CFRP	1.50	621	55.1
0/90 KFRP	1.36	523	24.6
±45°GRP	2.01	64	-
±45° CFRP	1.50	83	-
±45° KFRP	1.36	59	-
Steel alloy*	7.8	170	25
Al alloy*	2.8	210	25
Ti alloy*	4.5	220	26

* O H Wyatt and D Dew-Hughes, 'Metals, Ceramics and Polymers', Cambridge University Press, Cambridge, 1974.

TABLE 6.1 APPARENT INTERLAMINAR SHEAR STRENGTHS (SHORT BEAM SHEAR)

Laminate	Condition	ILSS* MPa
CFRP 0/90	Dried	40.0 (3.0)
	65%RH	51.4(6.0)
	Boiled	51.8(2.8)
GRP 0/90	Dried	51.3(2.8)
	65%RH	58.5(4.7)
	Boiled	45.4(3.7)
KFRP 0/90	Dried	22.2(2.3)
	65%RH	28.7(1.2)
	Boiled	22.1(0.6)

*Mean and Standard deviation of 10 tests for each laminate and condition.

TABLE 6.2 APPARENT FLEXURAL STRENGTHS OF 0/90 LAMINATES (65%RH)

Laminate	APPARENT FLEXURAL STRENGTH, GPa		
	3-Point Bending	4-Point Bending	Avery Flexure
CFRP	1.04(0.30)	>0.75(0.05)	0.90
GRP	0.79	0.83(0.02)	>0.79
	(0.99 for S/d = 30/1)		
KFRP	0.43	>0.40(0.01)	>0.43

Standard deviations in brackets

TABLE 6.3 APPARENT INTERLAMINAR SHEAR STRENGTH OF 0/90 LAMINATES (65%RH) IN 4-POINT BENDING (MEAN OF 4 SPECIMENS)

Laminate	Apparent ILSS, MPa (Standard Deviation)
CFRP	33.2(2.3)
GRP	>35.9(1.0)
KFRP	17.3(0.6)

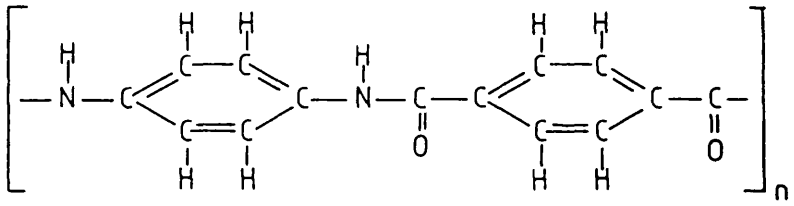

Figure 2.1a The molecular structure of Kevlar

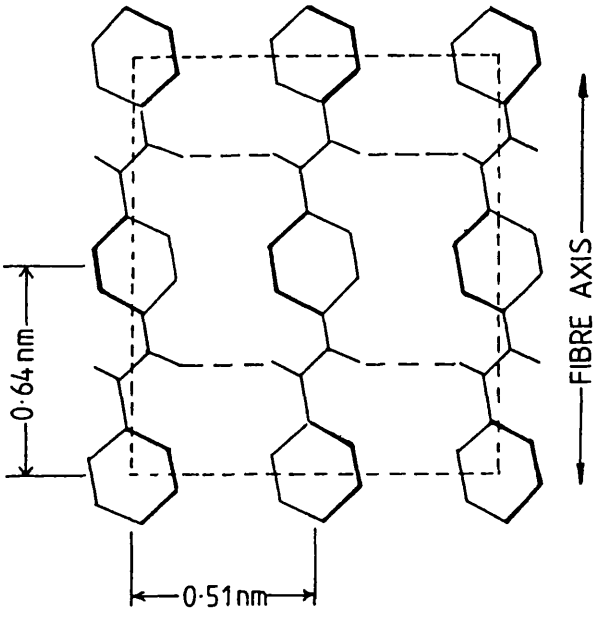

Figure 2.1b The physical structure of Kevlar.
Planar array of poly-p-phenylene terephthalamide molecules showing interchain hydrogen bonding (after Dobb et al(14)).

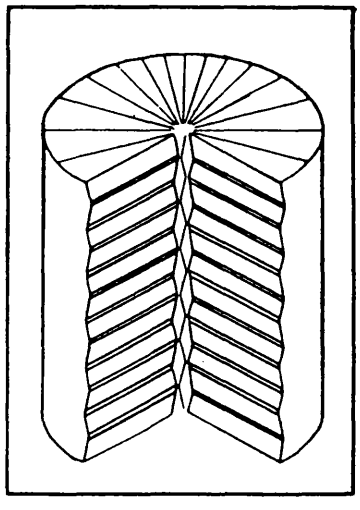

Figure 2.1c Schematic representation of the supramolecular structure of Kevlar-49 depicting the radially arranged pleated system (after Dobb et al (14)).

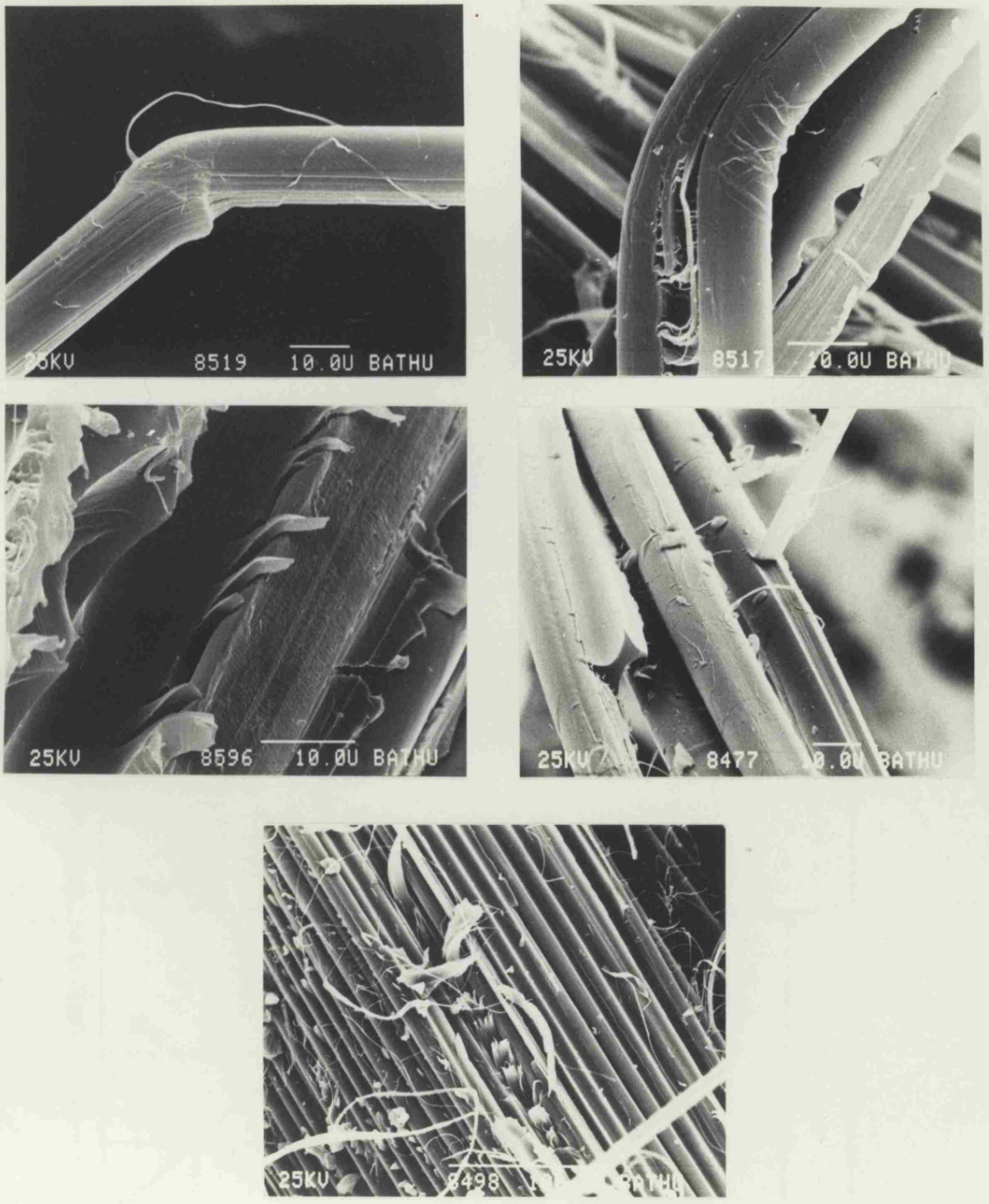

Figure 2.1 Scanning electron micrographs showing modes of damage in Kevlar fibres.

d. Fibre buckling e. Fibre buckling and splitting

f. Split fibre g. Fibre skin peeling

h. Fibre tearing

TETRAGLYCIDYL 4 4'-DIAMINO DIPHENYL METHANE (T.G.D.D.M.)

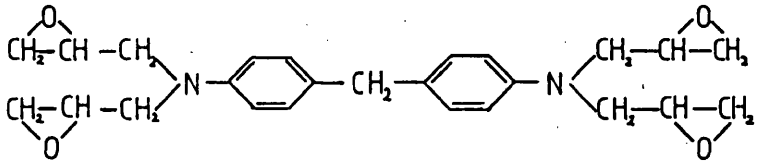

DIAMINO DIPHENYL SULPHONE (D.D.S.)

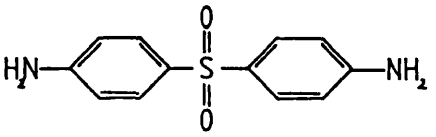

Figure 2.2 a) The chemical structure of TGDDM
b) The chemical structure of DDS

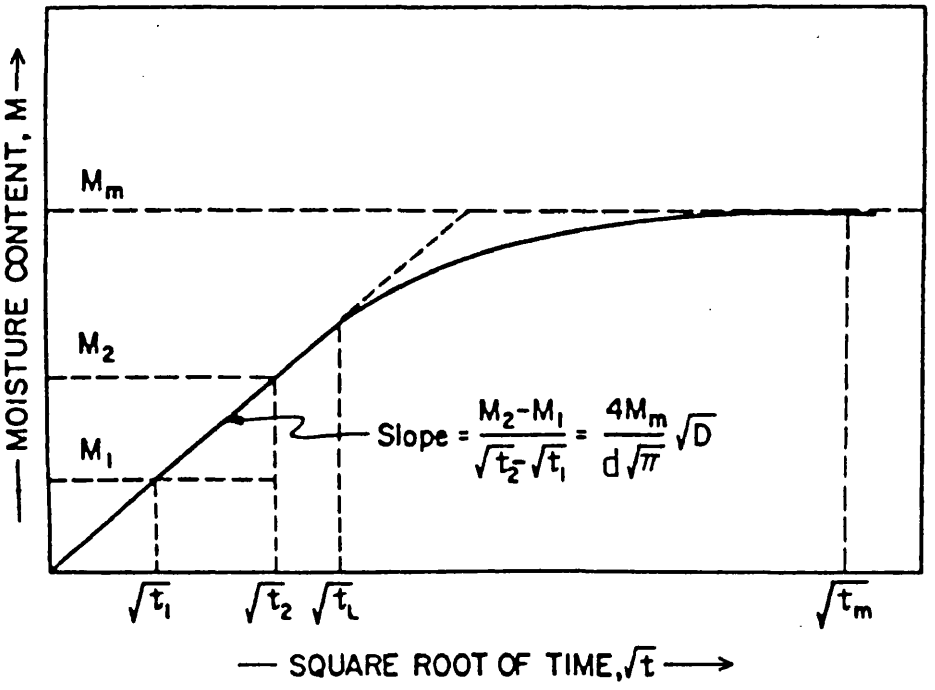

Figure 2.3 Illustration of the change in moisture content with the square root of time for Fickian diffusion. For $t < t_L$ the slope is constant (after Springer(65)).

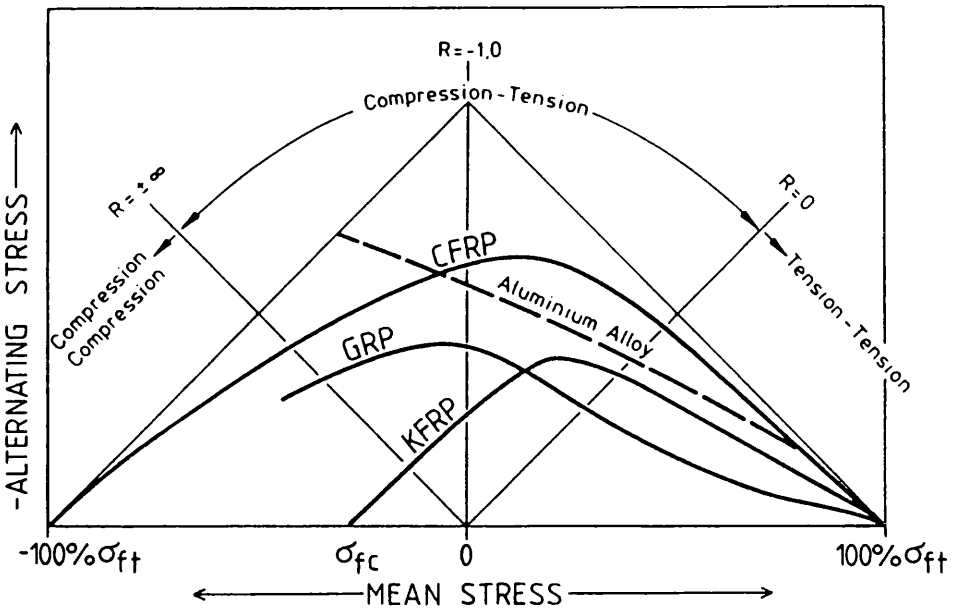

Figure 2.4 Schematic constant life curves for typical CFRP, GRP and KFRP composites and for aluminium alloy (after Gerharz(95)).

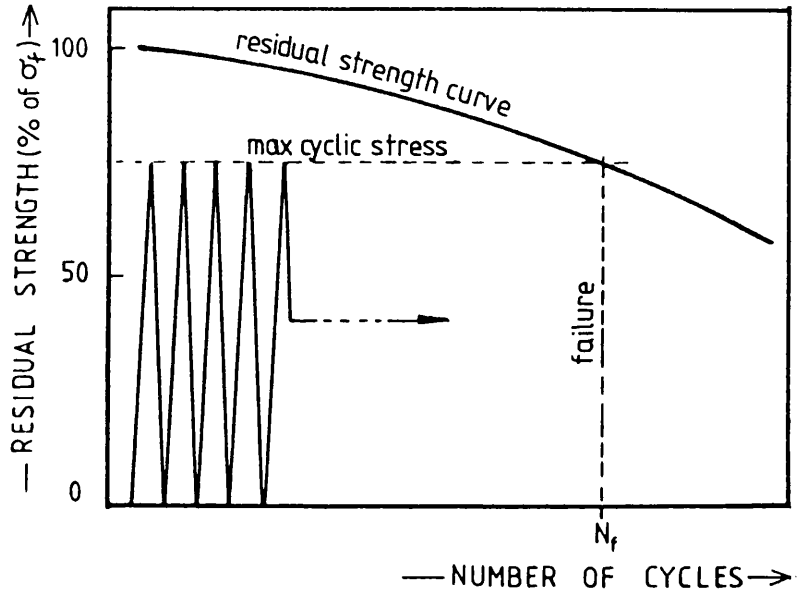

Figure 2.5 Schematic illustration of wear-out failure in fatigue.

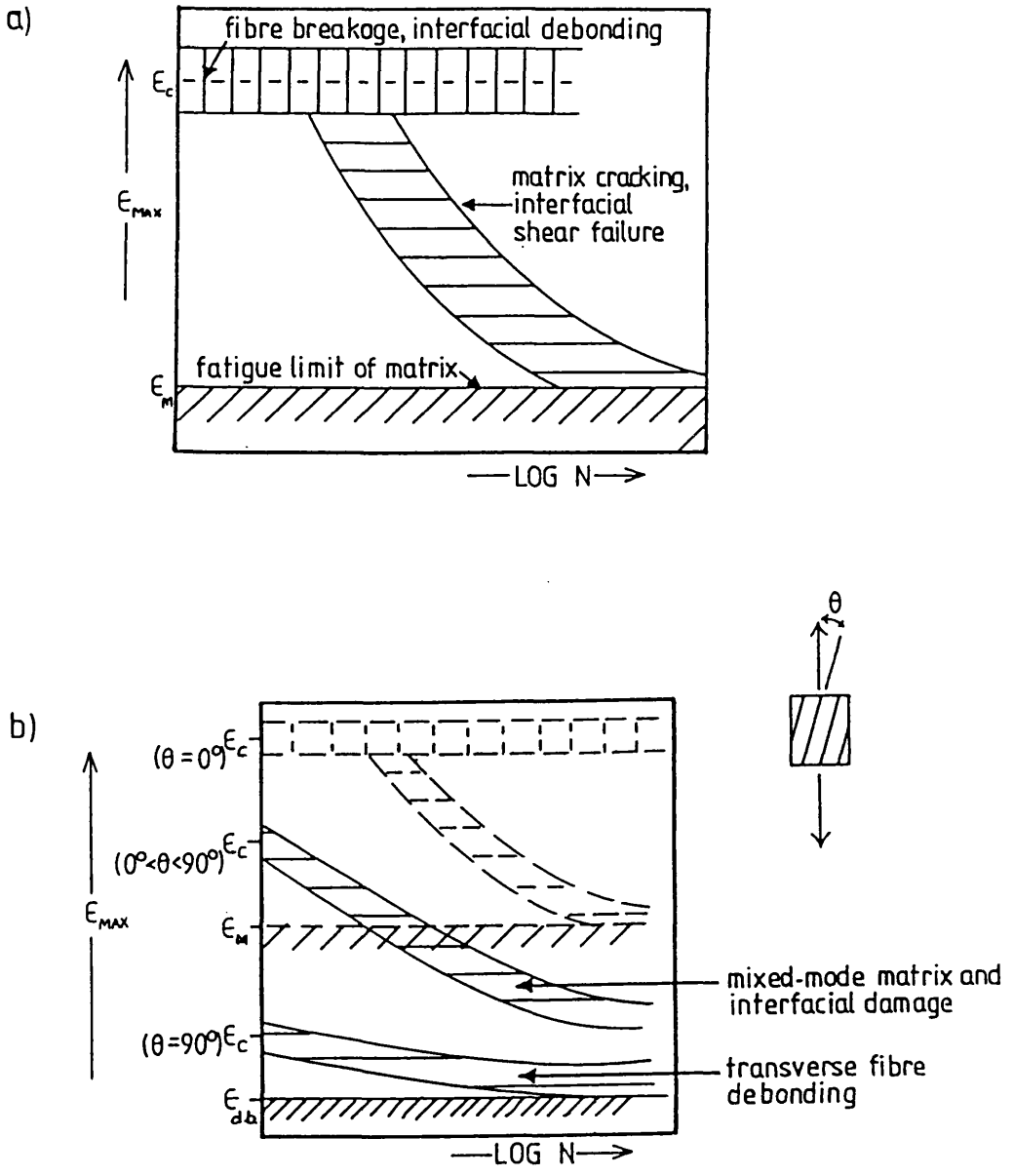

Figure 2.6 Schematic fatigue curves for unidirectional composites, after Talreja(98).

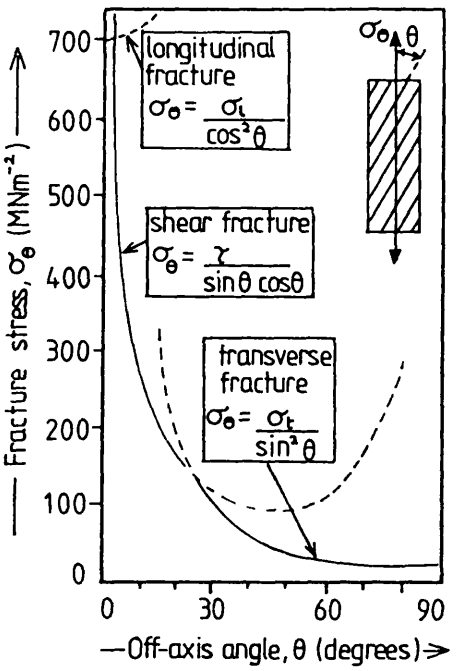

Figure 2.7 Orientation dependence of fracture strength for off-axis loading of unidirectional laminae (after Hull(9)).

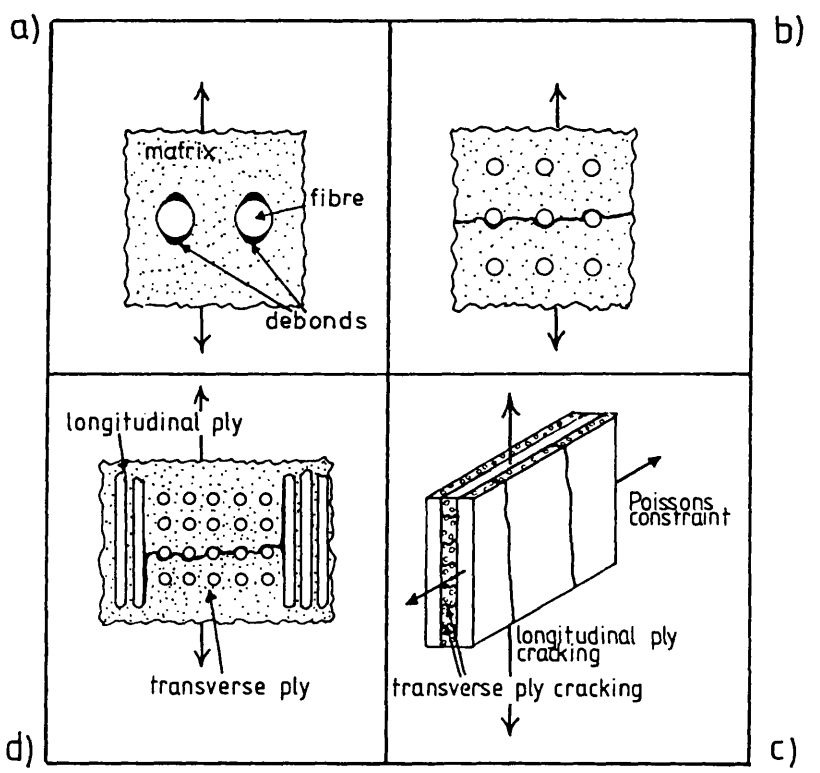

Figure 2.8 Damage modes in 0/90 laminates

a) Transverse fibre debonding
b) Transverse ply cracking
c) Saturation cracking (CDS) including longitudinal splitting
d) Delamination.

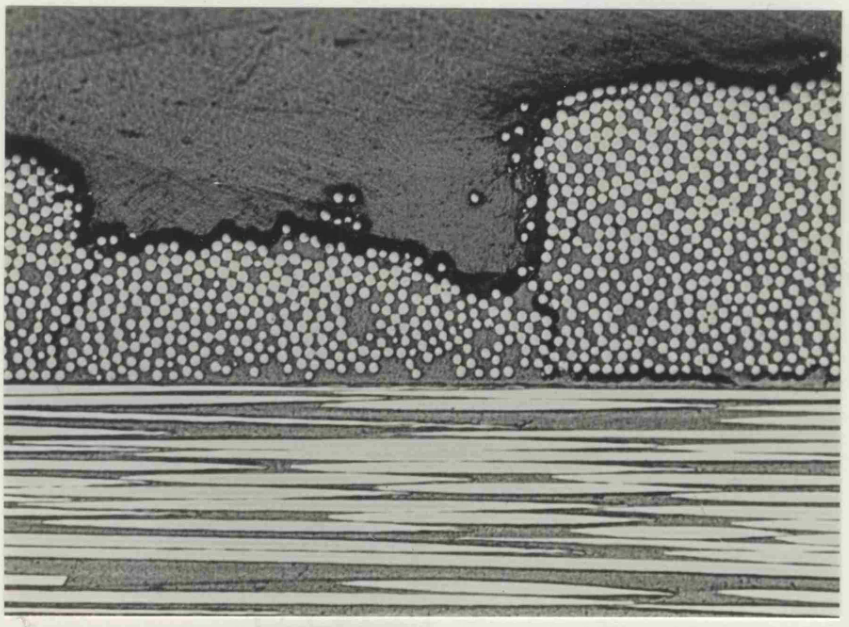

Figure 2.9 Delamination damage mode.

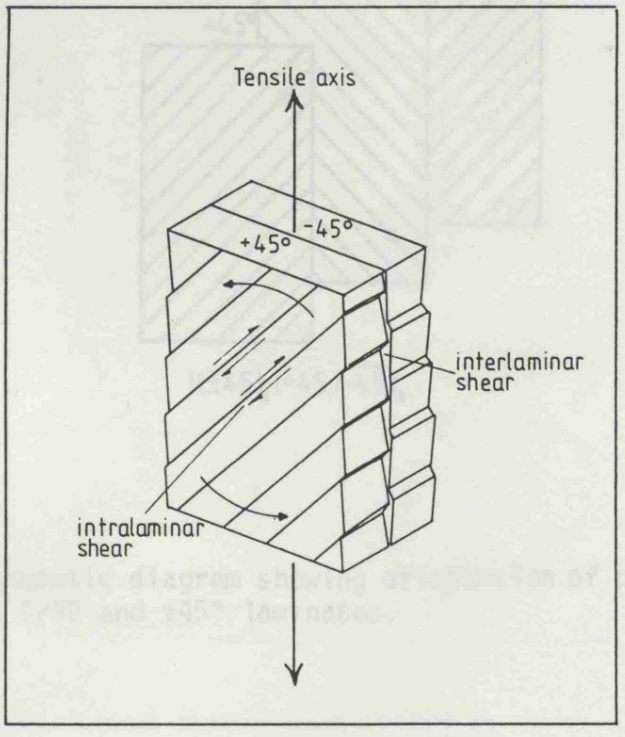

Figure 2.10 Schematic view of intralaminar and interlaminar shear associated with a tensile test on a ±45° laminate (after Hull(9)).

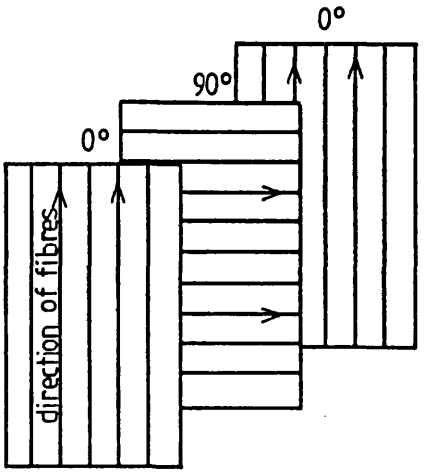

$[(0/90)_2/0/\overline{90}]_s$

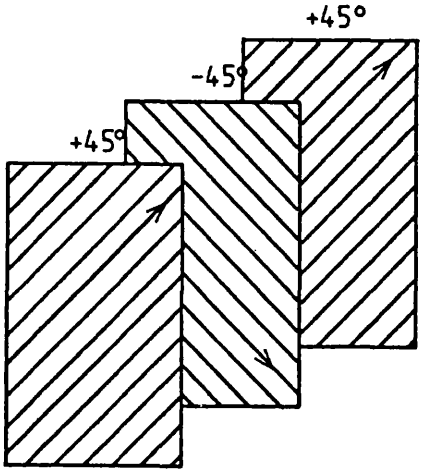

$[(\pm 45)_2/+45/-\overline{45}]_s$

Figure 3.1 Schematic diagram showing orientation of plies in 0/90 and ±45° laminates.

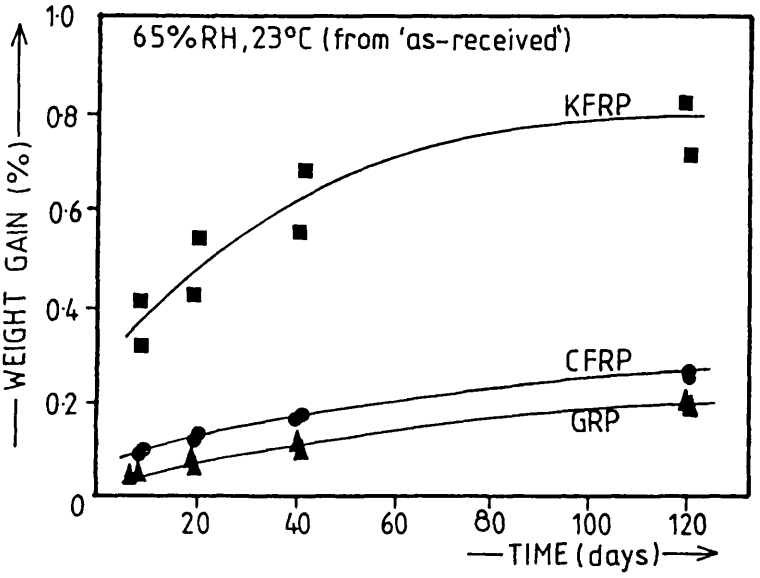

Figure 4.1 Weight gains of 'as-received' laminates exposed to 65% RH atmosphere at 23°C.

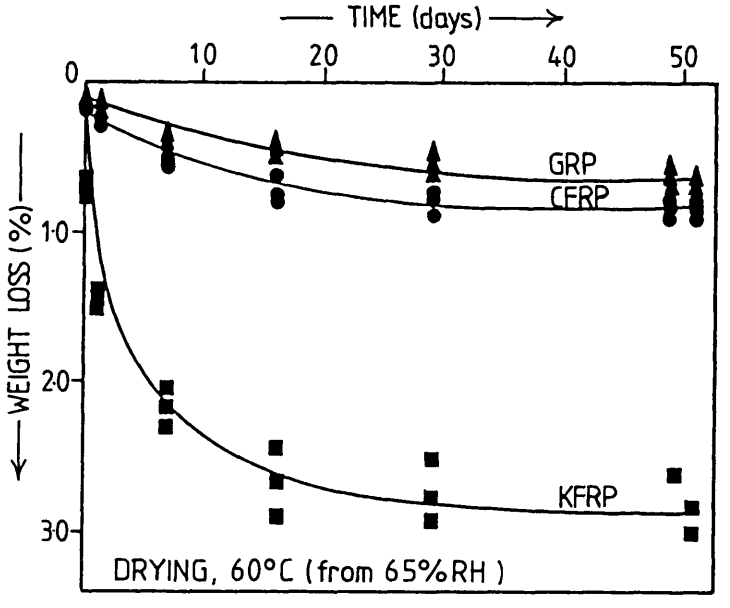

Figure 4.2 Weight losses during oven drying at 60°C. Starting condition stabilised at 65% RH.

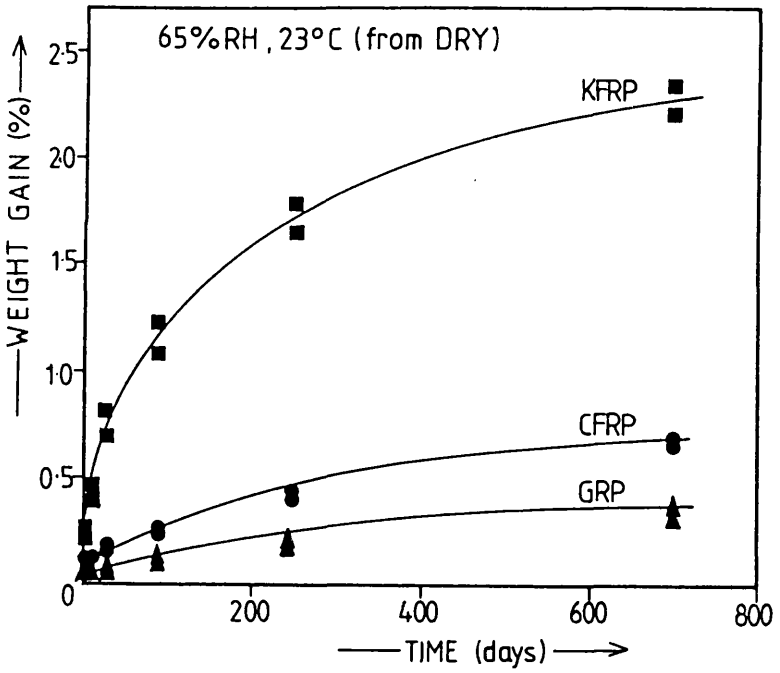

Figure 4.3 Weight gains of fully dried laminates in 65% RH atmosphere (23°C).

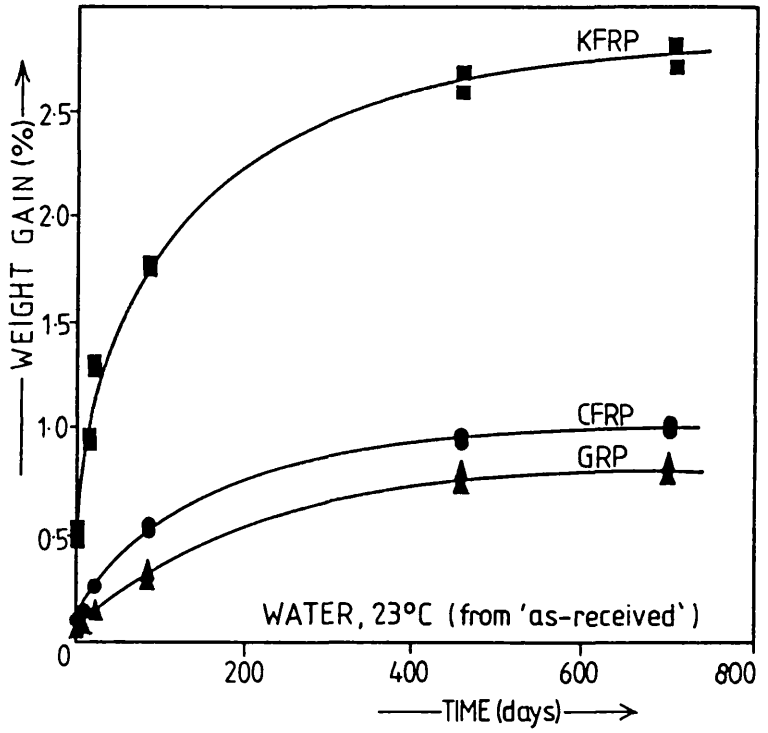

Figure 4.4 Weight gains of 'as-received' laminates in water at 23°C.

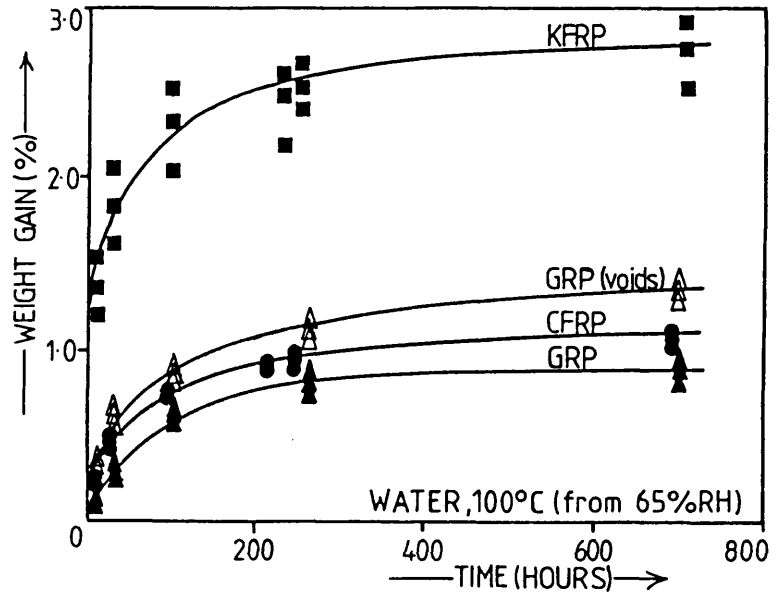

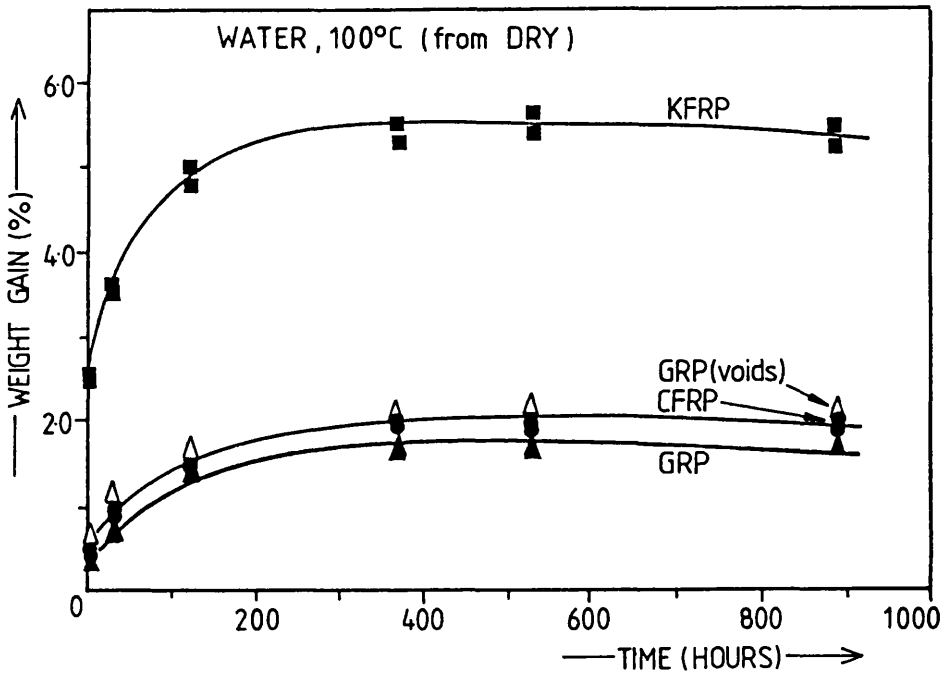

Figure 4.5 Weight gains in water at 100°C from

a) 65% RH
b) dried condition.

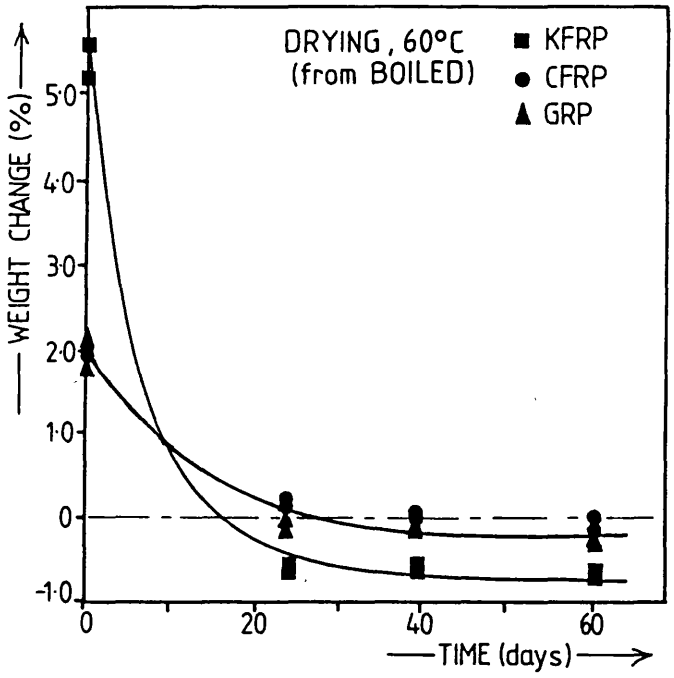

Figure 4.6 Weight losses on drying at 60°C after 5 weeks in boiling water (following Figure 4.5b).

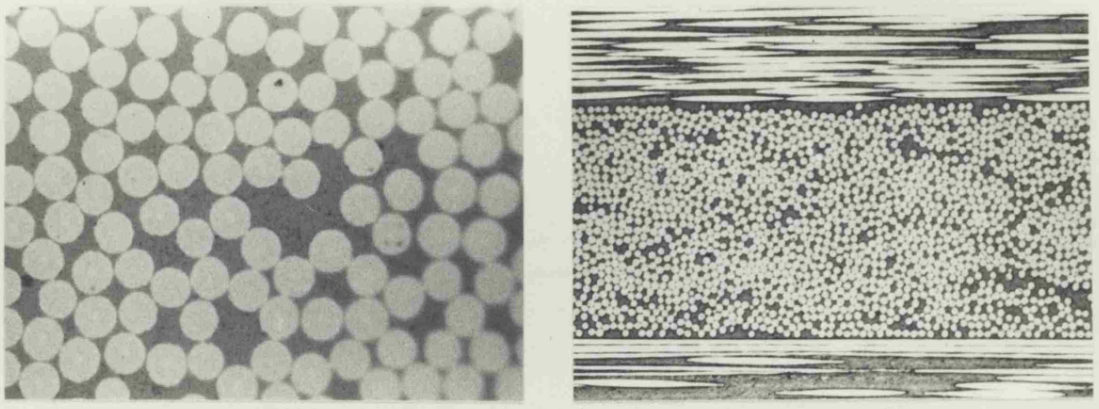

Figure 4.7 CFRP after 3 weeks in boiling water

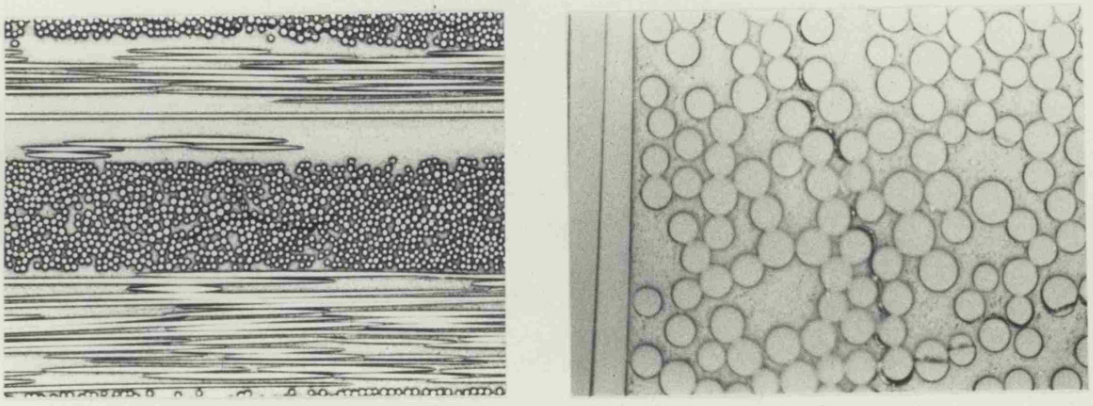

Figure 4.8 GRP after 6 months in boiling water

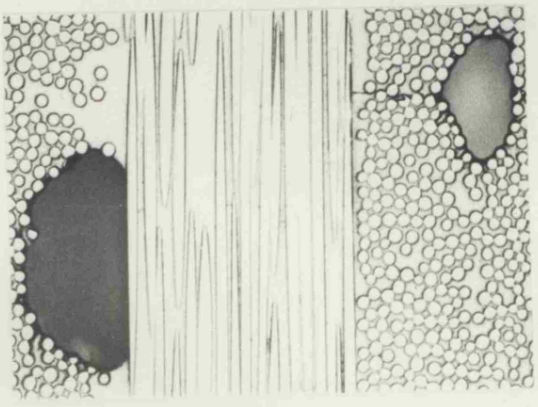

Figure 4.9 Voids in GRP

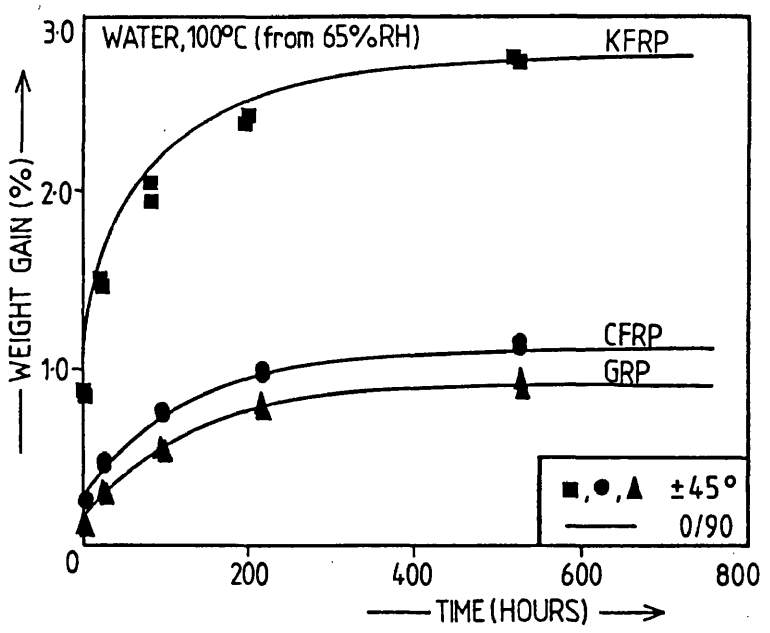

Figure 4.10 Comparison of weight gains in boiling water for 0/90 and ±45° specimens (from 65% RH).

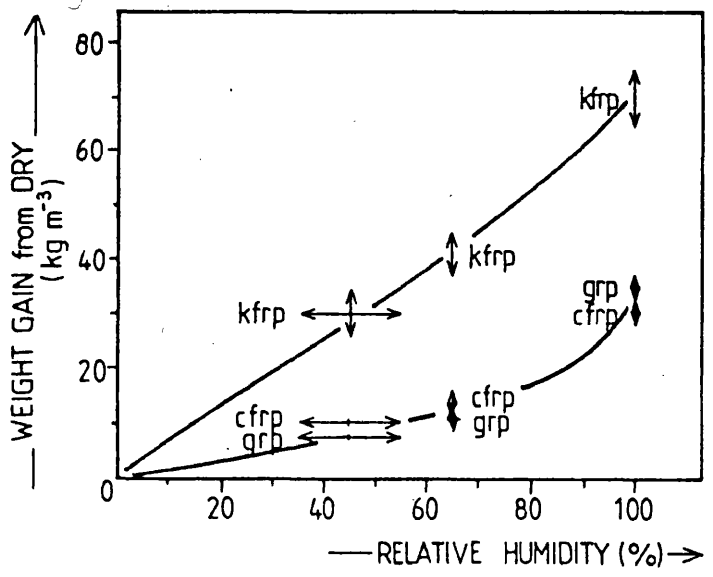

Figure 4.11 Saturation moisture absorption of the GRP, CFRP and KFRP laminates as a function of relative humidity of the conditioning environment.

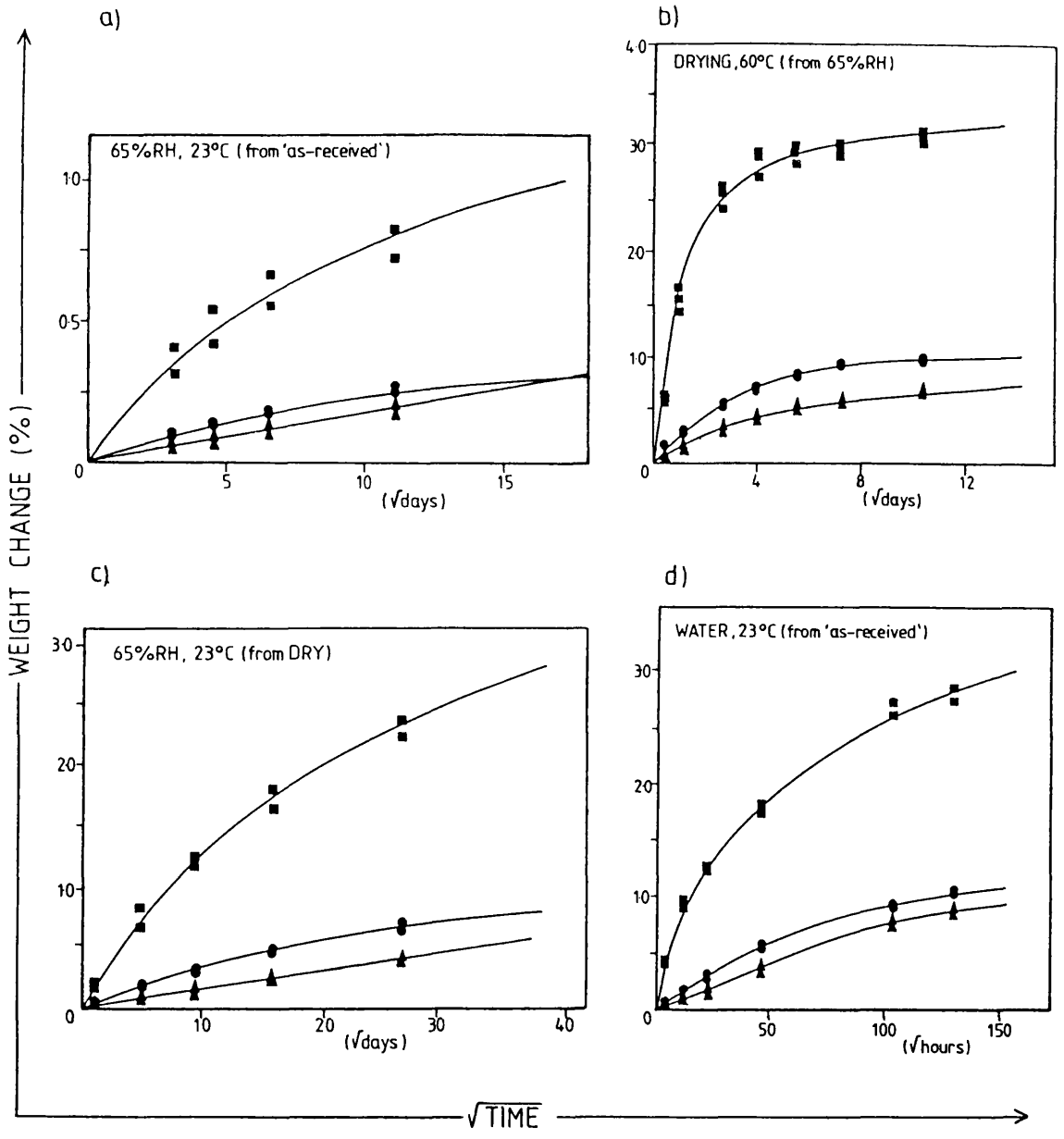

Figure 4.12 Weight changes in laminates during conditioning treatments. (Figures 4.1 to 4.5) plotted against √time.

a) 65%RH,23°C from 'as-received'
b) Drying oven, 60°C from 65%RH
c) 65%RH, 23°C, from dried
d) Water, 23°C, from 'as-received'

Symbols represent experimental points

Full lines are Ramberg-Osgood generated curves.

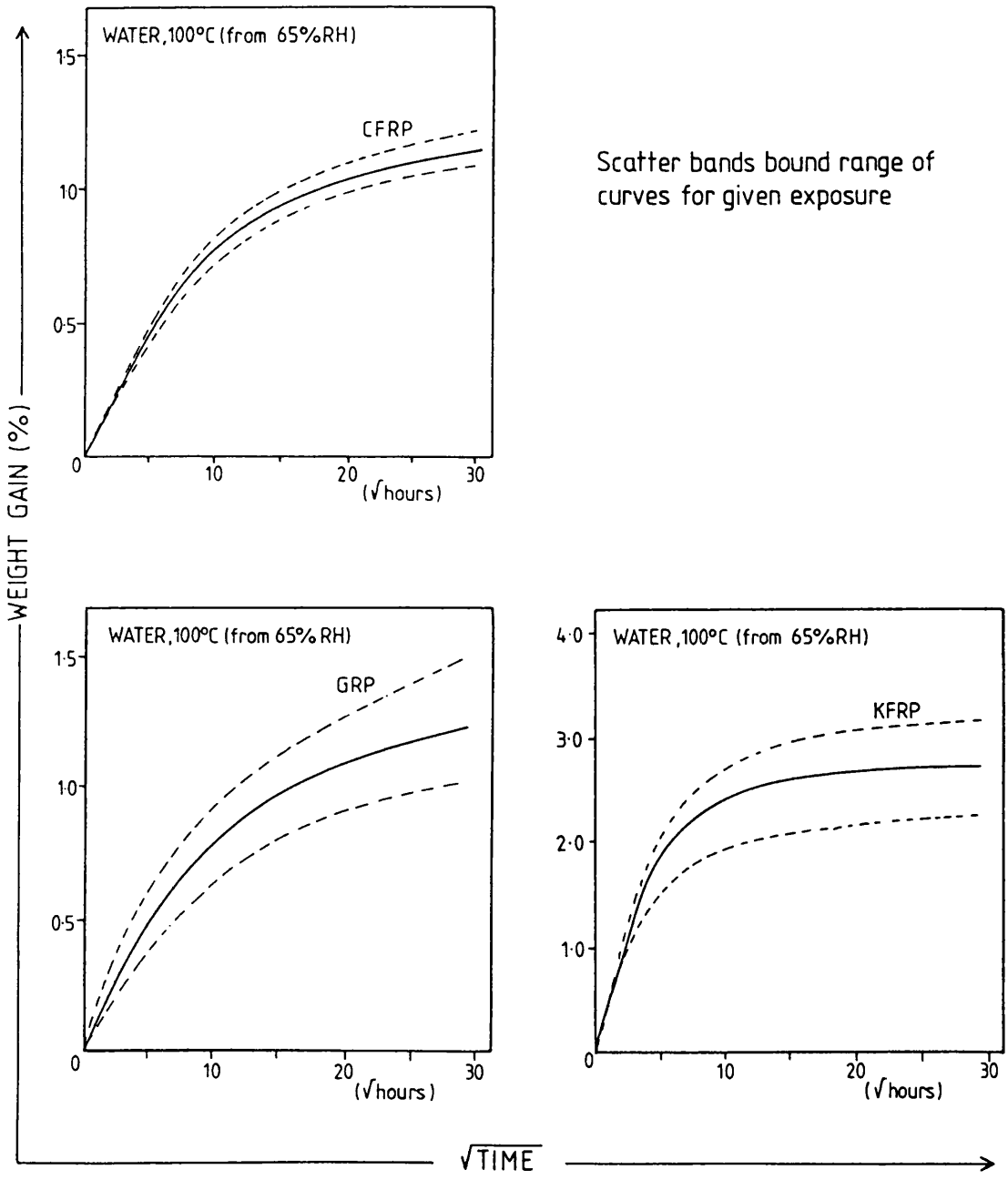

Figure 4.12 Weight changes in laminates during conditioning treatments. (Figures 4.1 to 4.5) plotted against √time.

e) Boiling water from 65%RH.

Full lines are typical Ramberg-Osgood generated curves.

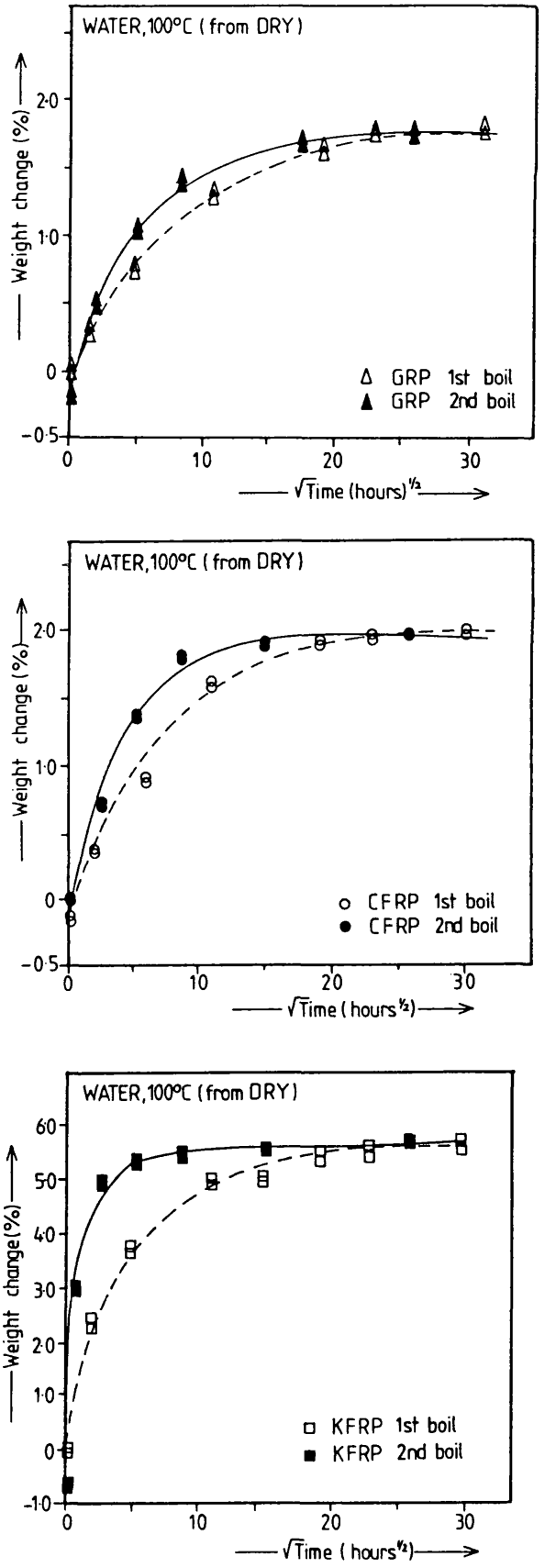

Figure 4.13 Weight gain curves for secondary exposures to boiling water, following drying from initial boiling water exposure (also shown).

a) GRP
b) CFRP
c) KFRP

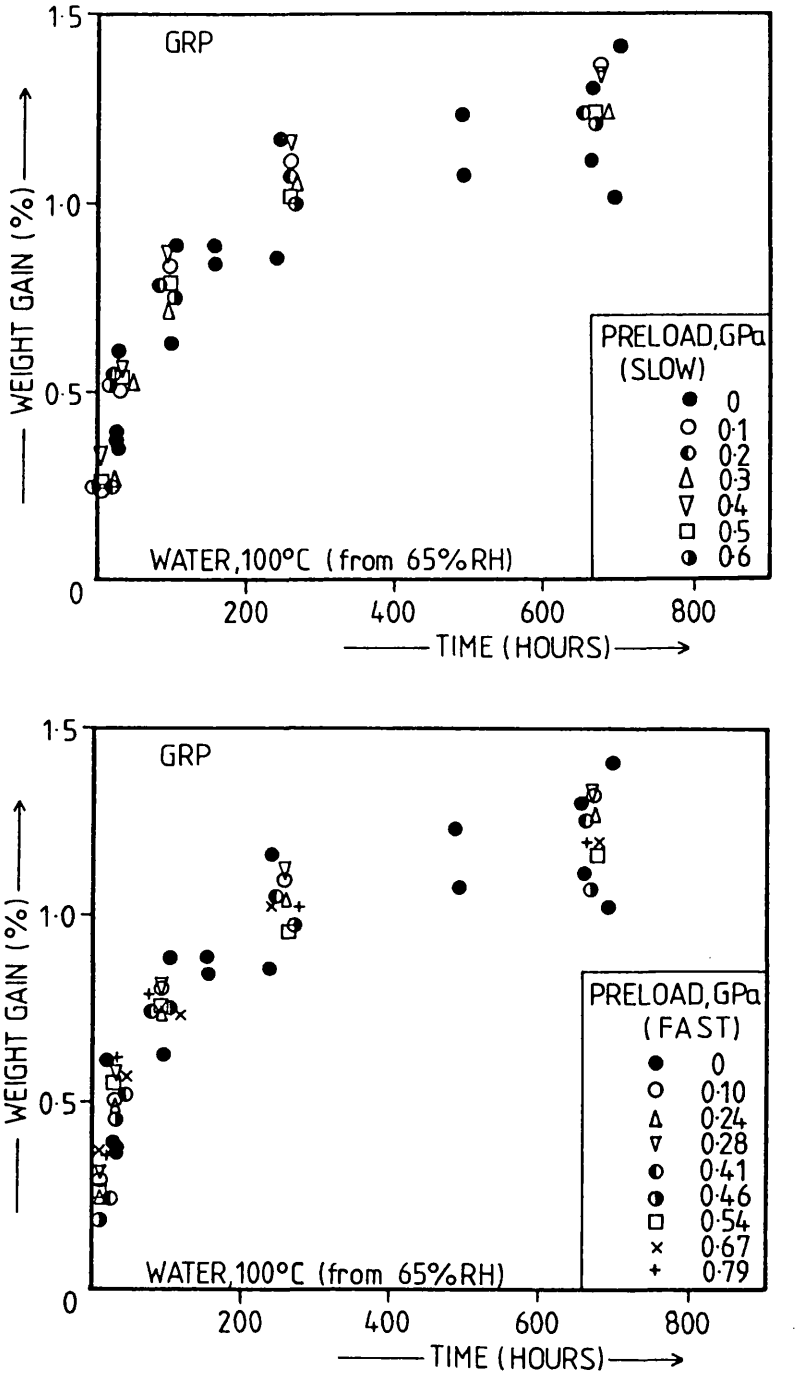

Figure 4.14 Effects of preloads on moisture absorption curves for 0/90 GRP during exposure to boiling water

a) Preloads at slow loading rate
b) Preloads at 100kNs^{-1} (fast) loading rate

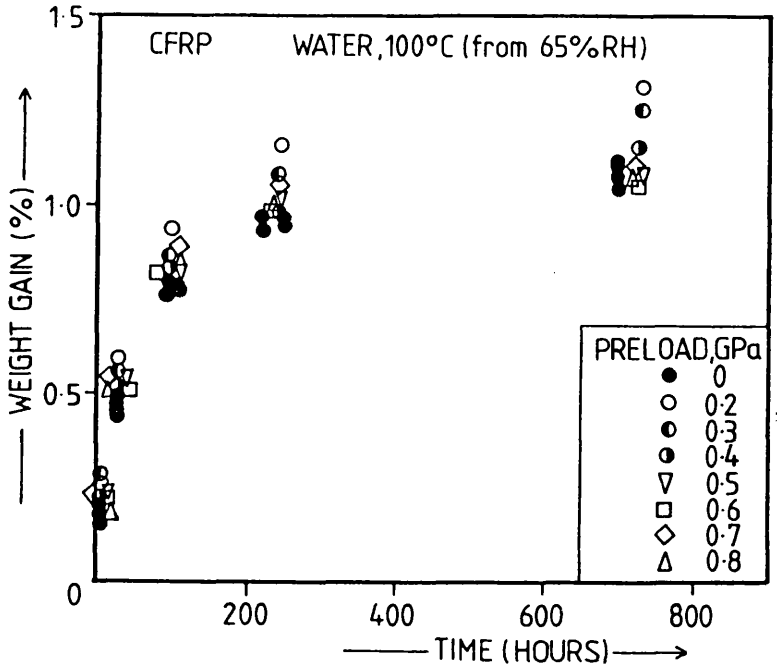

Figure 4.15 Effects of preloads on moisture absorption curves for 0/90 CFRP during exposure to boiling water.

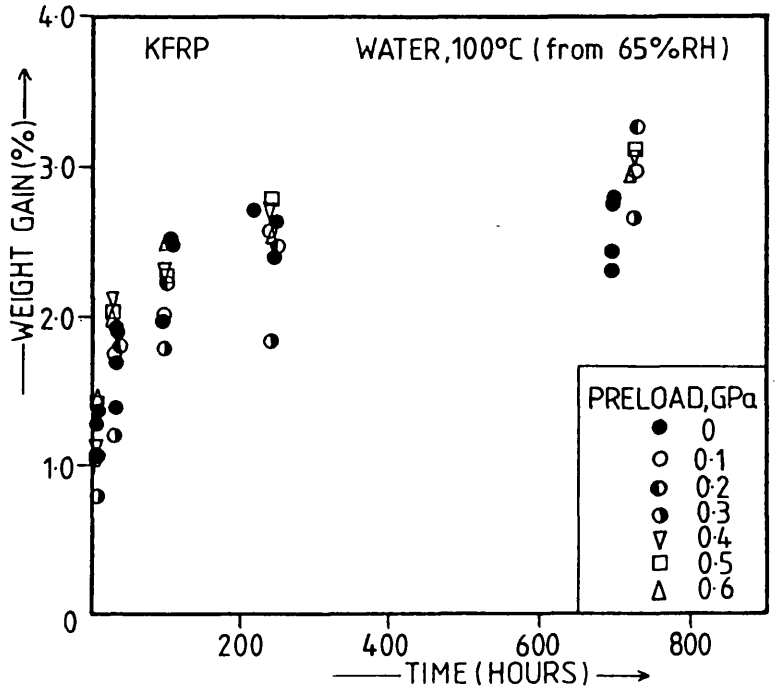

Figure 4.16 Effects of preloads on moisture absorption curves for 0/90 KFRP during exposure to boiling water.

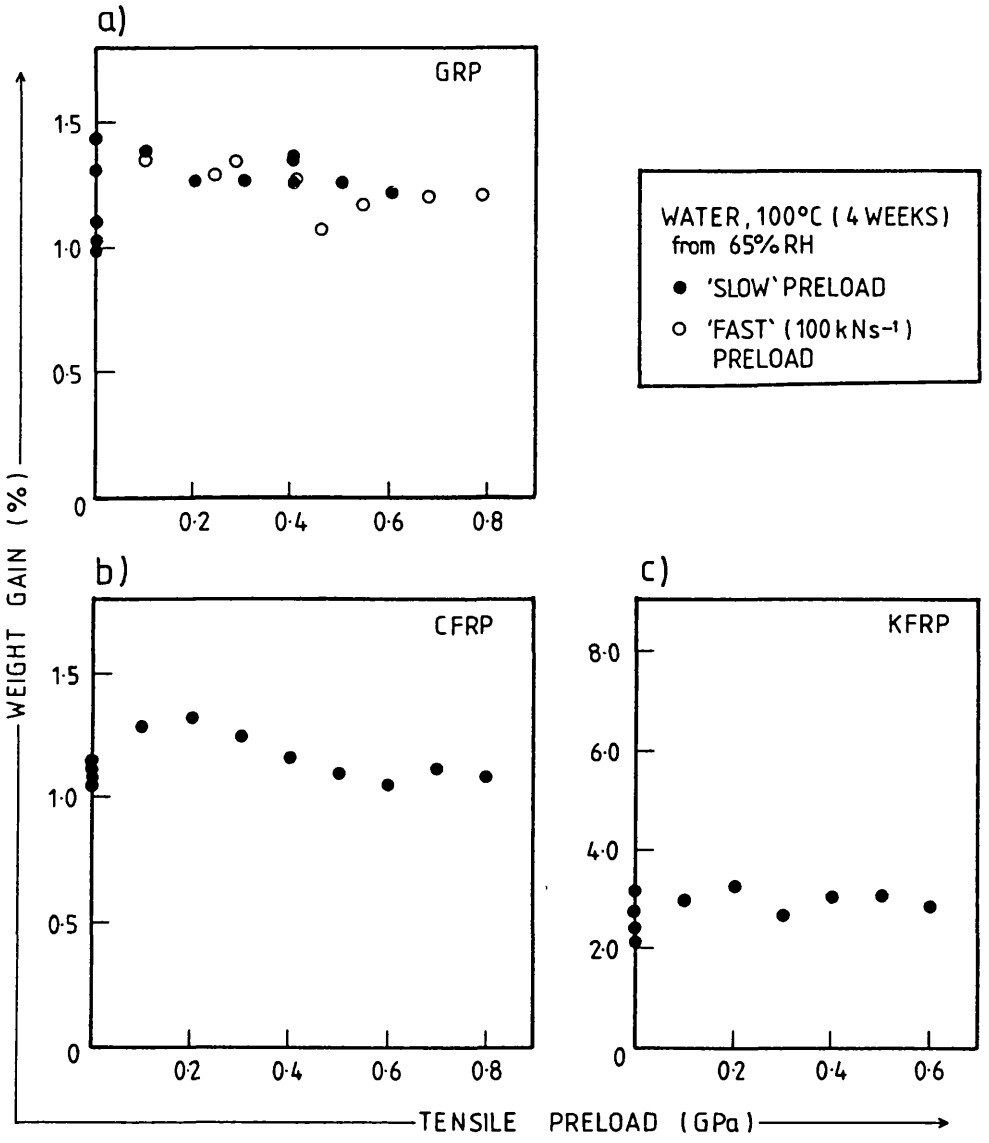

Figure 4.17 Effects of preload level on the weight gains of laminates after 4 weeks in boiling water

a) GRP
b) CFRP
c) KFRP.

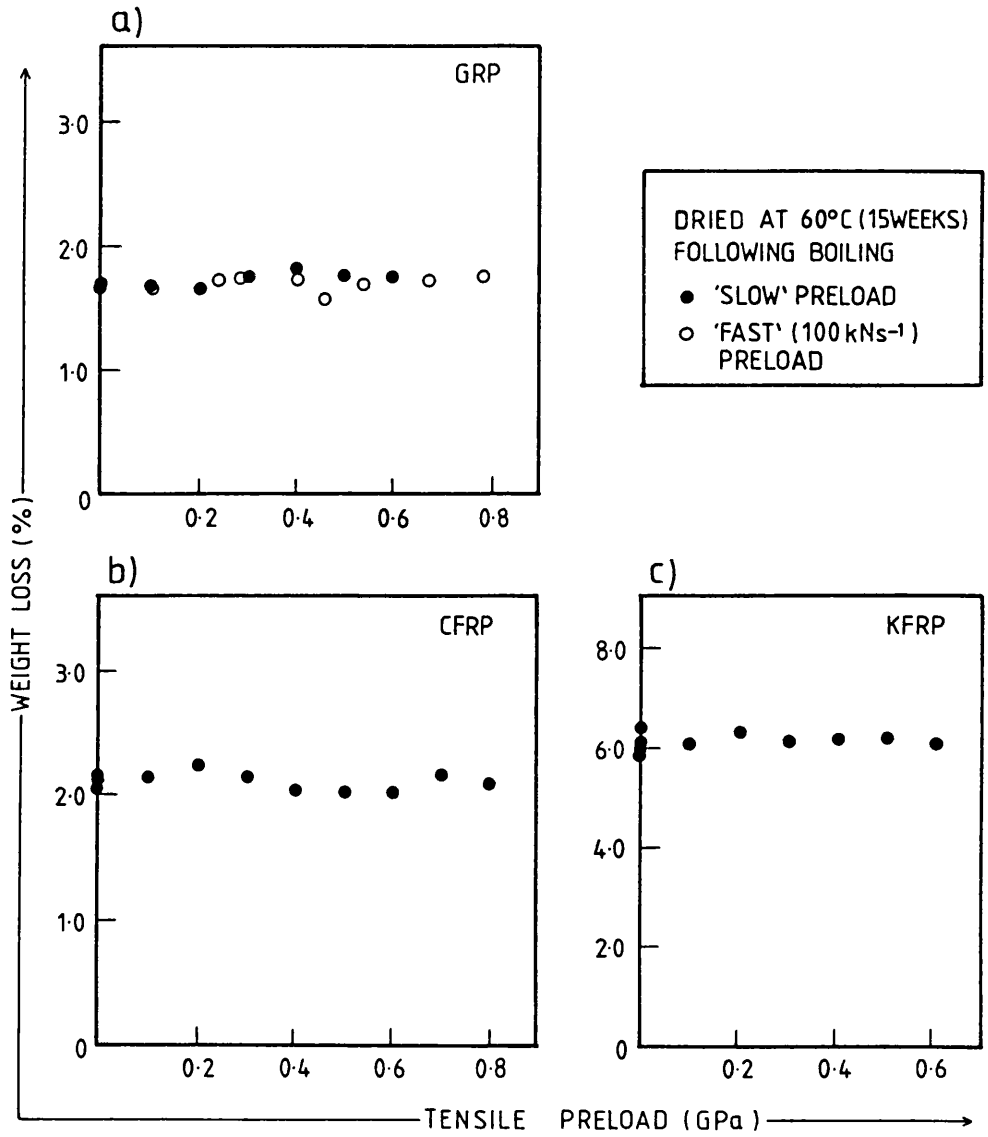

Figure 4.18 Weight losses on re-drying preloaded samples at 60°C after 4 weeks exposure to boiling water.

a) GRP
b) CFRP
c) KFRP.

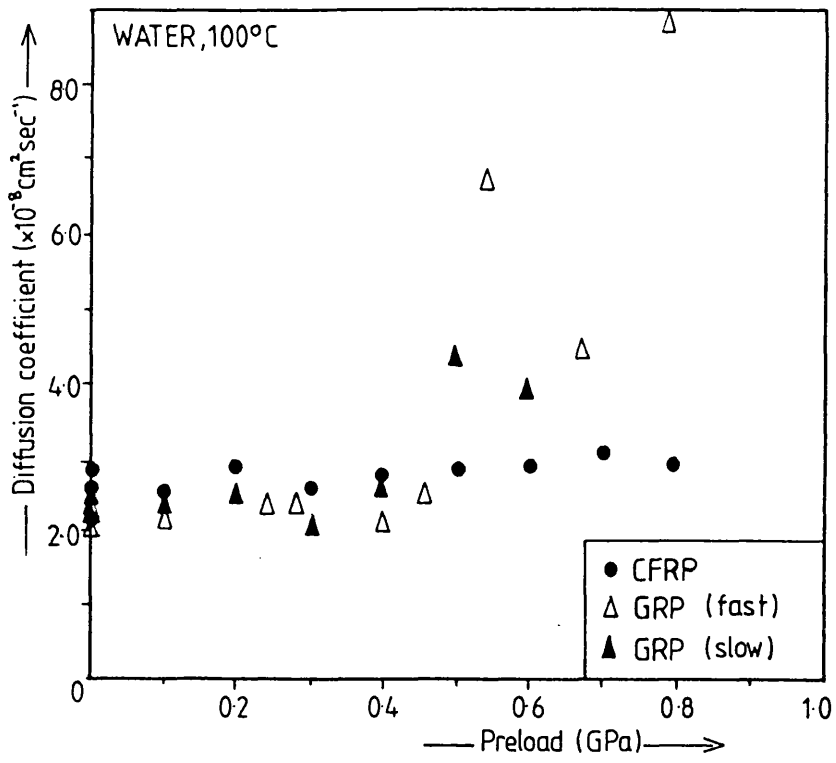

Figure 4.19 Effect of preload on the initial rates of moisture uptake for the GRP and CFRP laminates in boiling water.

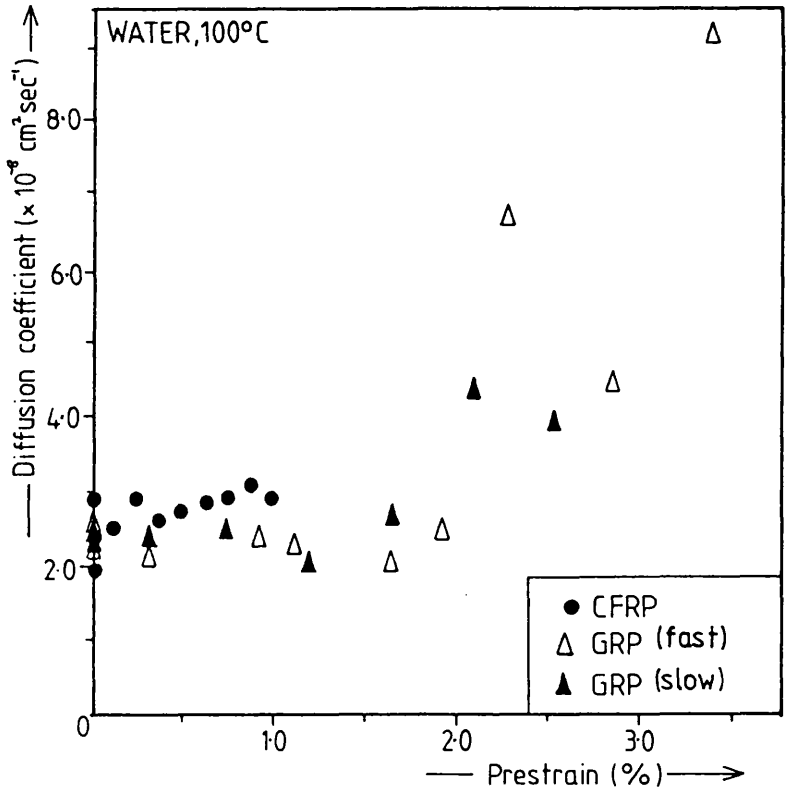

Figure 4.20 Dependency of initial moisture uptake rates of CFRP and GRP in boiling water on level of prestrain.

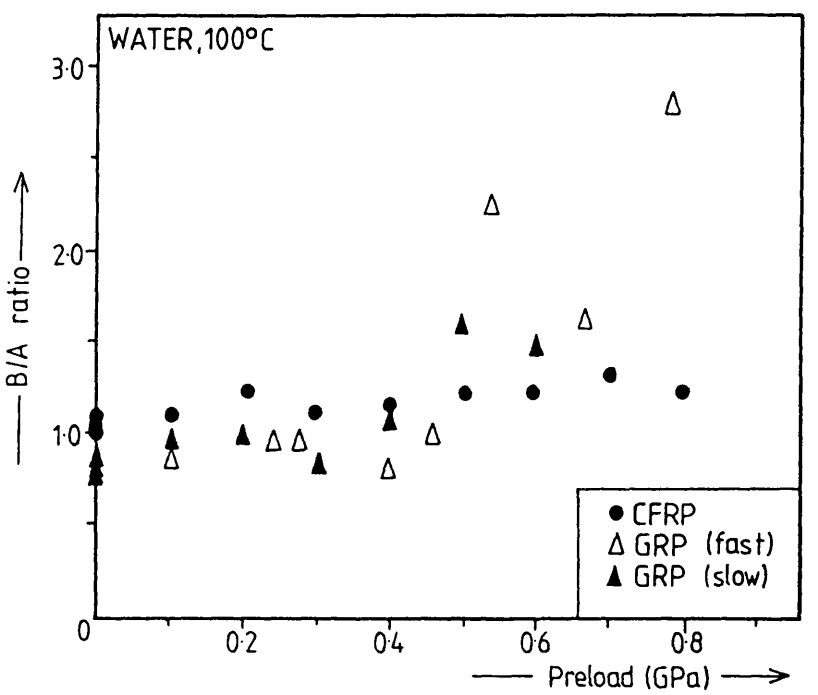

Figure 4.21 Effect of preload on the $^{B}/A$ ratio(strength of the deviation from linearity of the √time plot) for CFRP and GRP in boiling water.

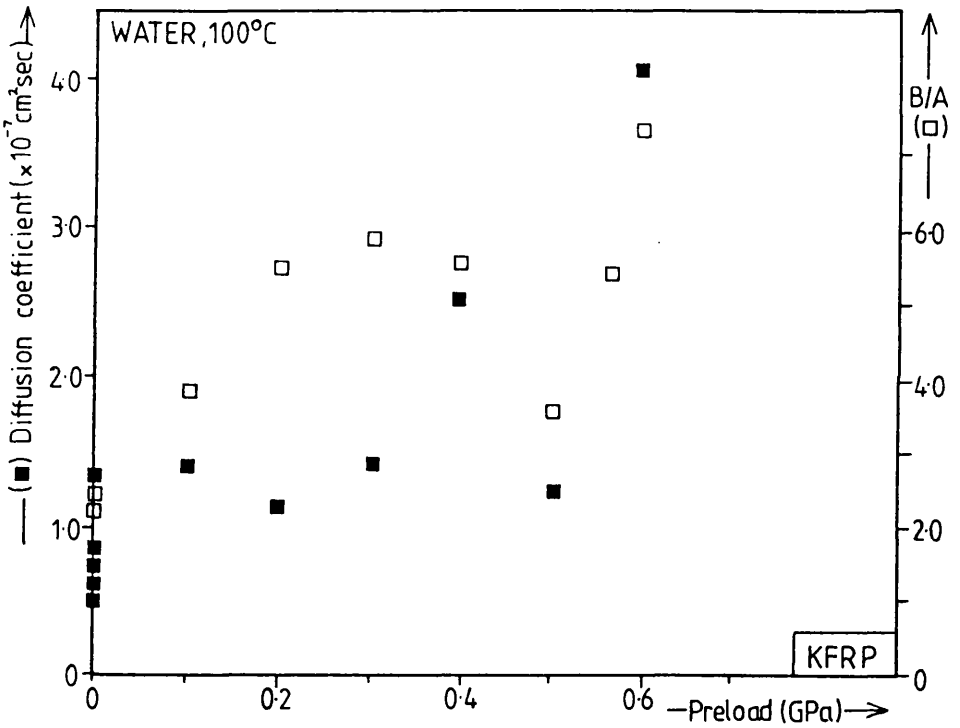

Figure 4.22 Effect of preload on the initial rates of moisture uptake and 'B/A' ratio for KFRP in boiling water.

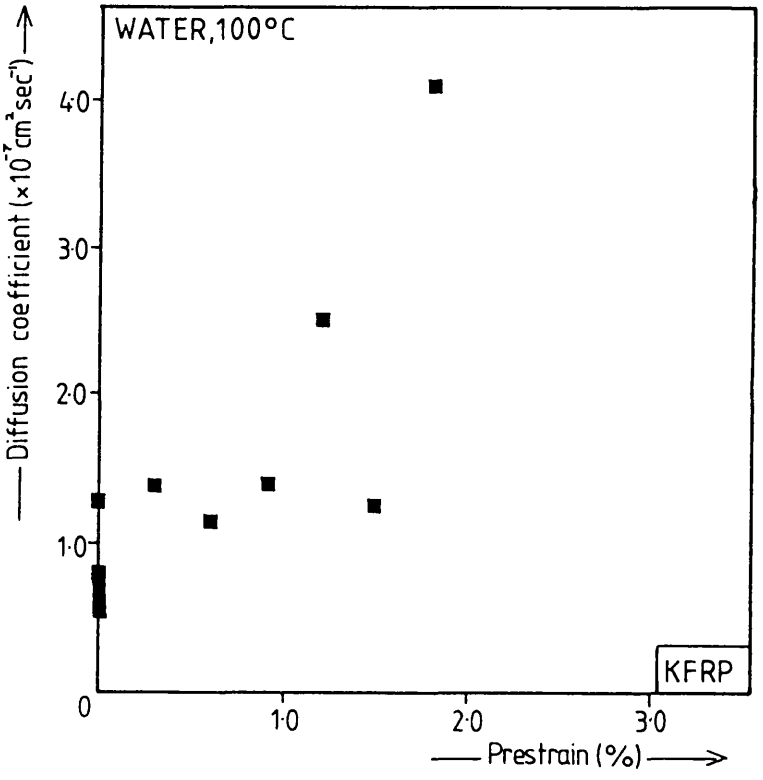

Figure 4.23 Initial rates of moisture uptake for KFRP in boiling water plotted against prestrain.

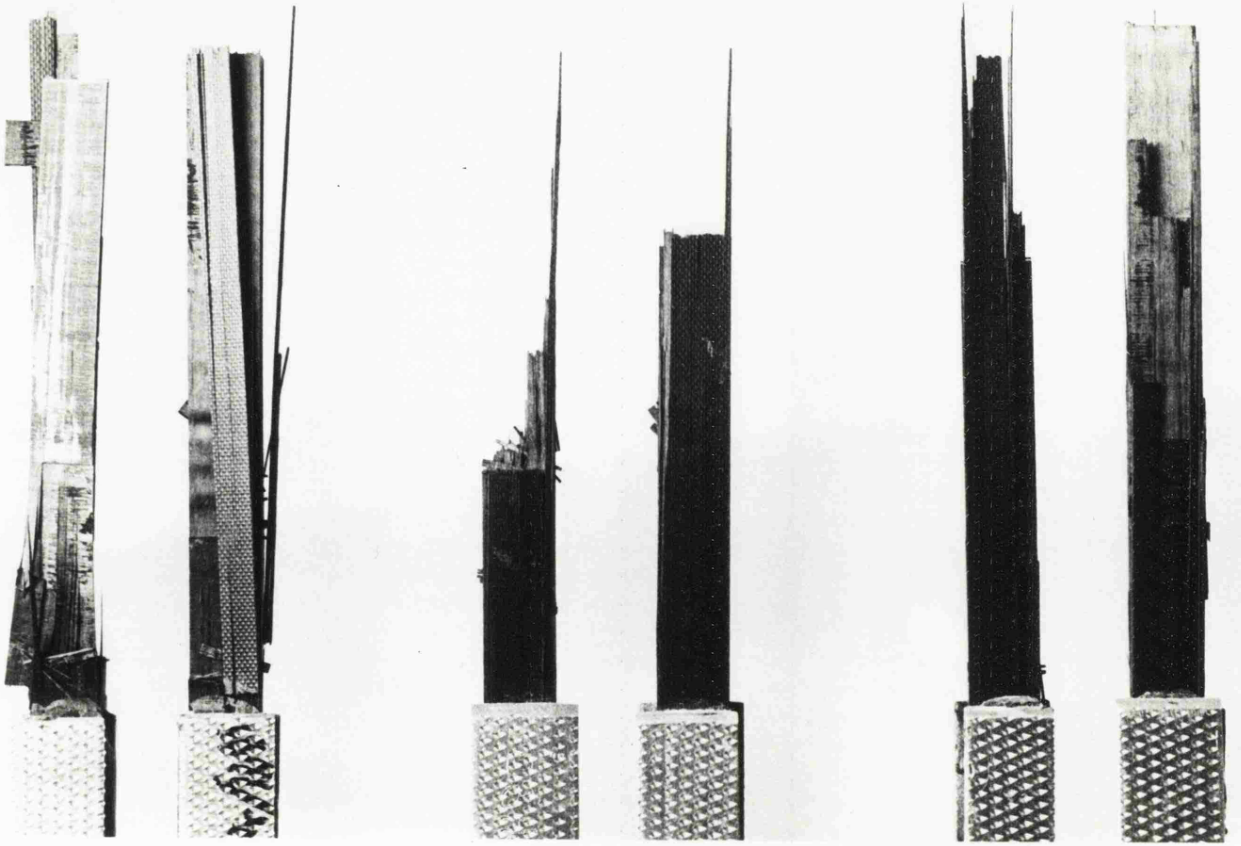

Figure 5.1 Tensile failure of 0/90 CFRP: Dried 65% Boiled

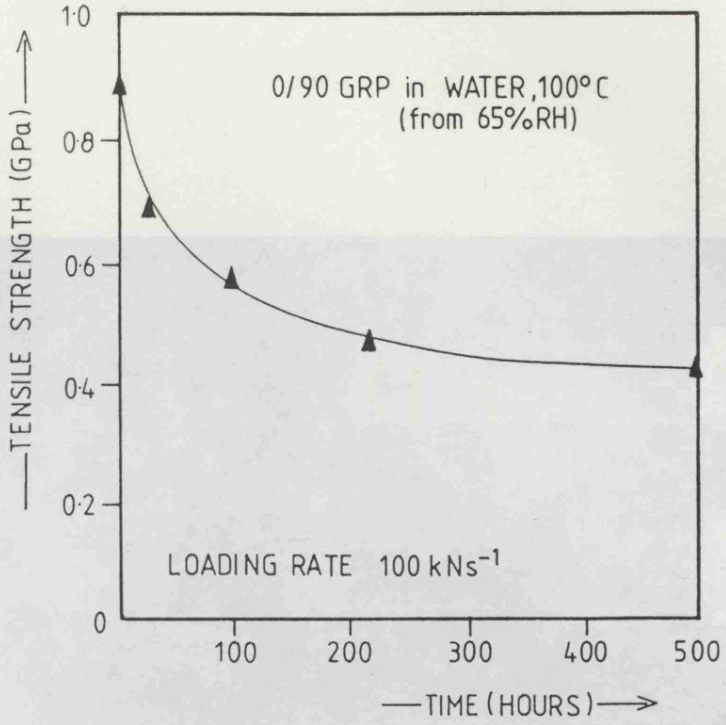

Figure 5.2 Reduction in tensile strength of 0/90 GRP as a function of time in boiling water.

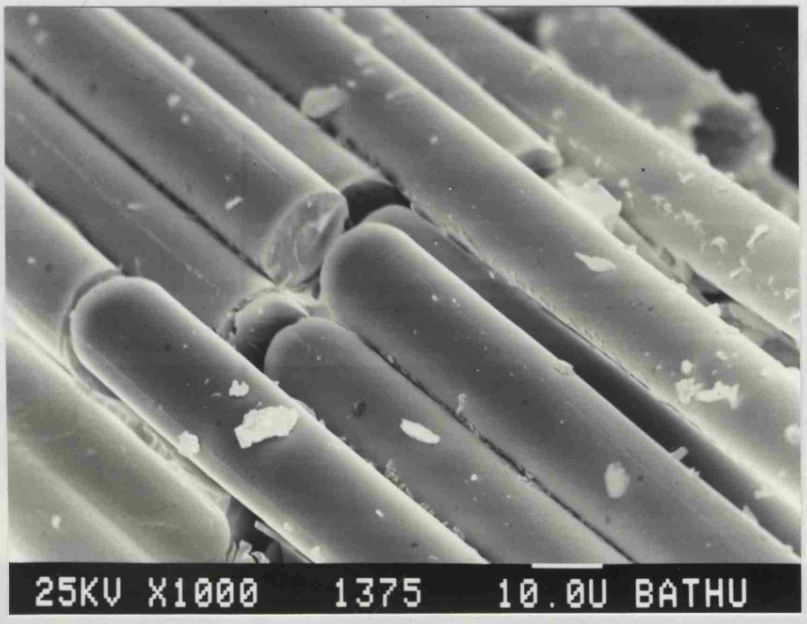

Figure 5.3 Scanning electron micrograph showing surface of glass fibres after 3 weeks in boiling water (taken from fracture surface of ±45° specimen).

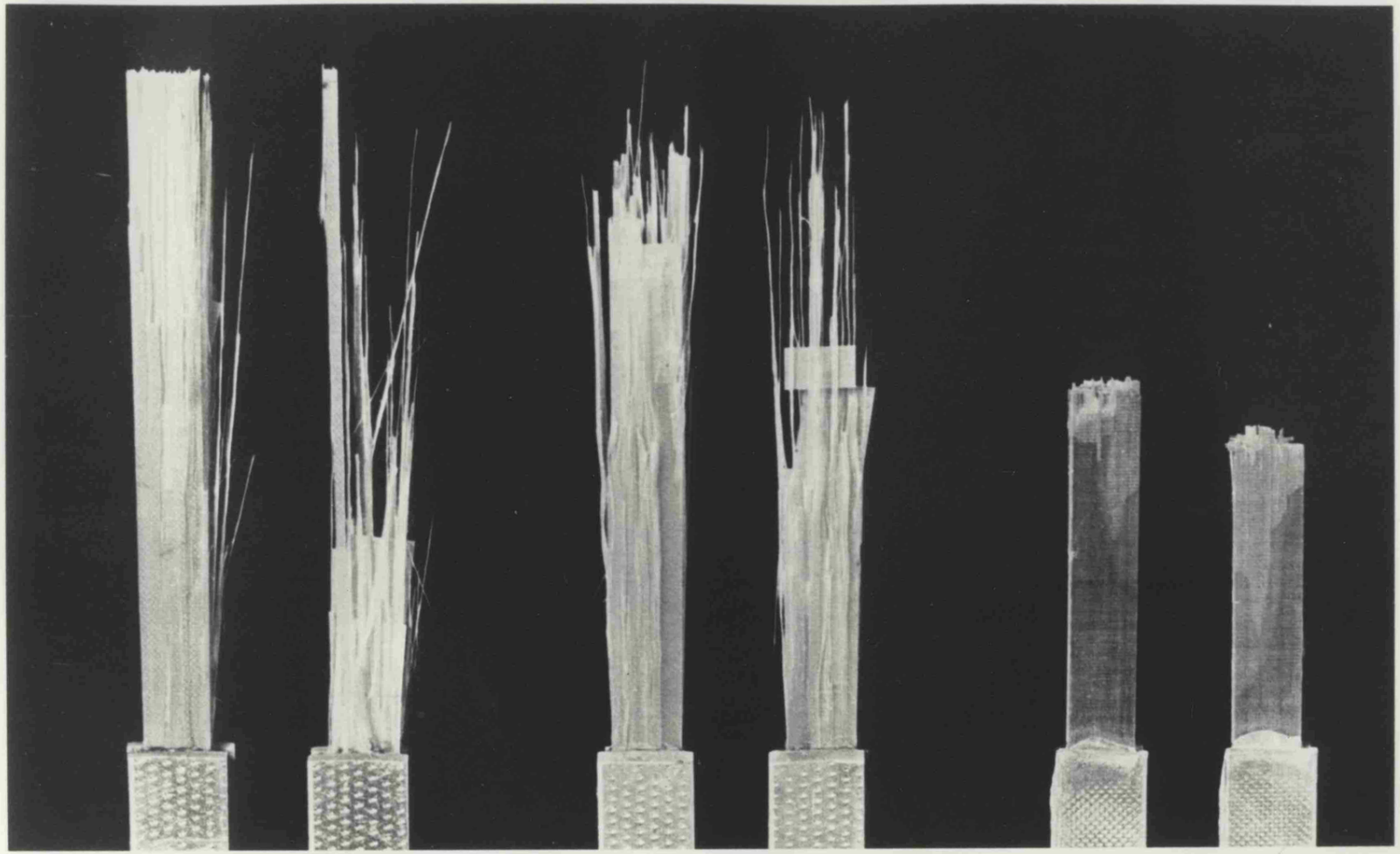

Figure 5.4 Tensile failure of 0/90 GRP: Dried 65% RH Boiled

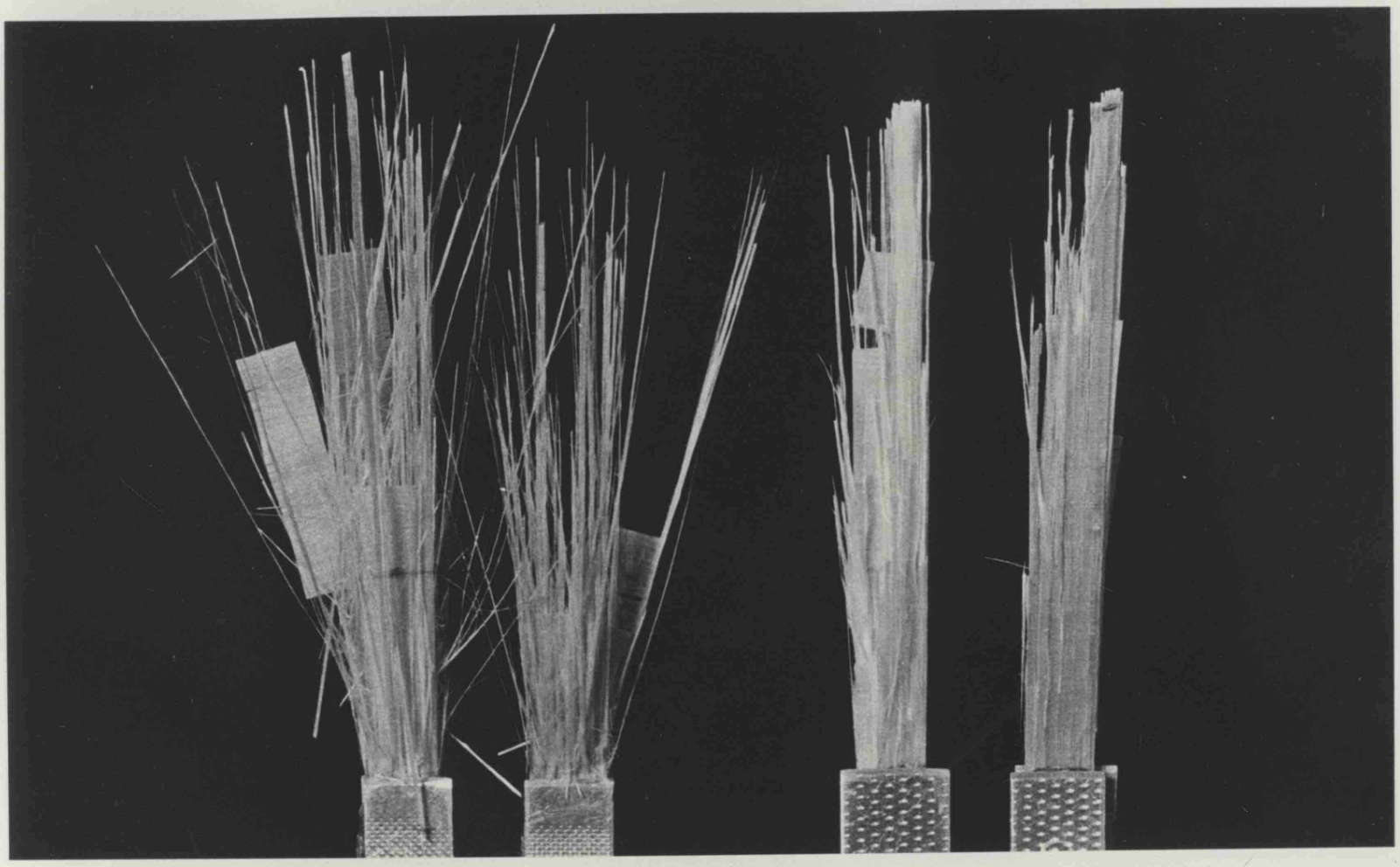

Figure 5.5 Tensile failure of 0/90 GRP: 'Fast' Loading 'Slow' Loading

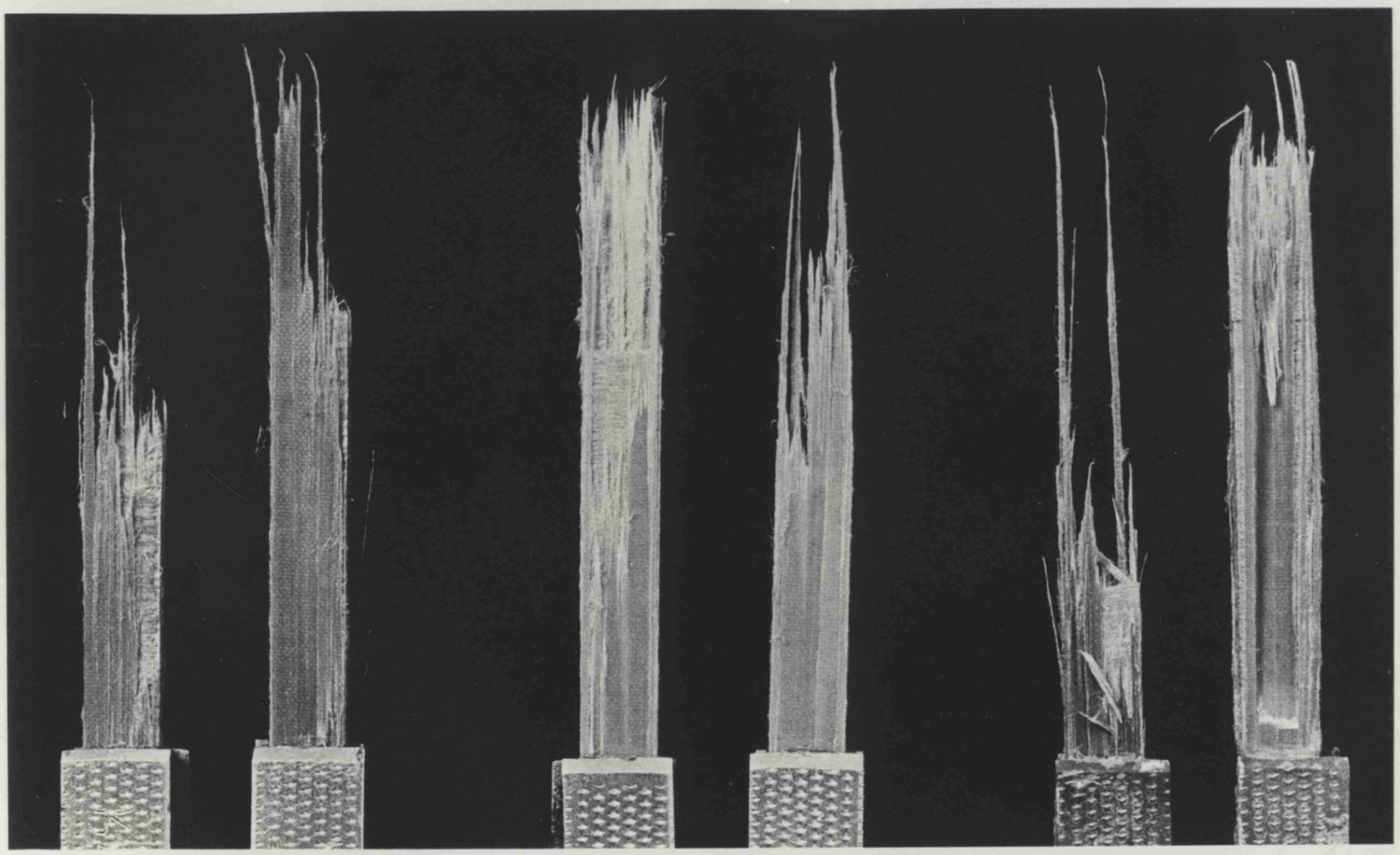

Figure 5.6 Tensile Failure of 0/90 KFRP: Dried 65% RH Boiled

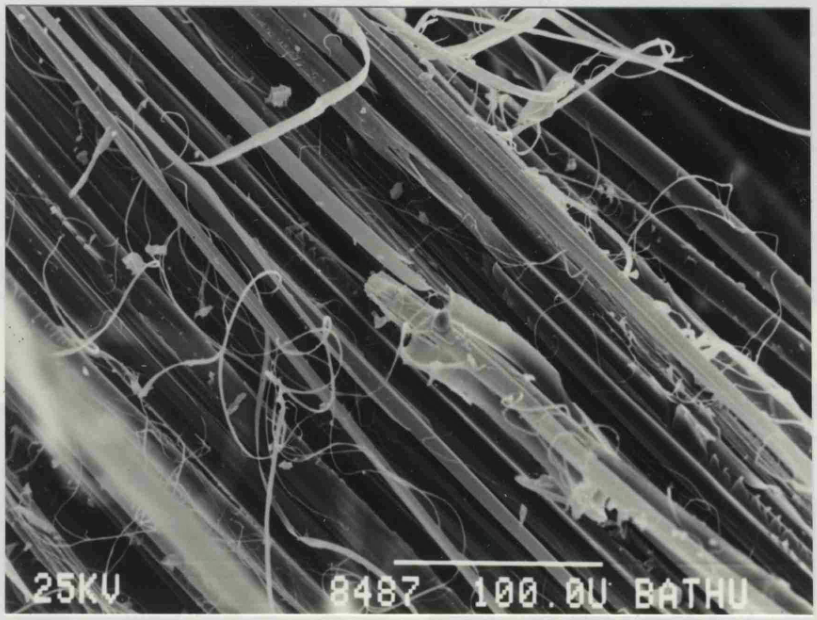

Figure 5.7 Scanning electron micrograph illustrating the extensive fibre splitting in the tensile failure surface of KFRP laminate.

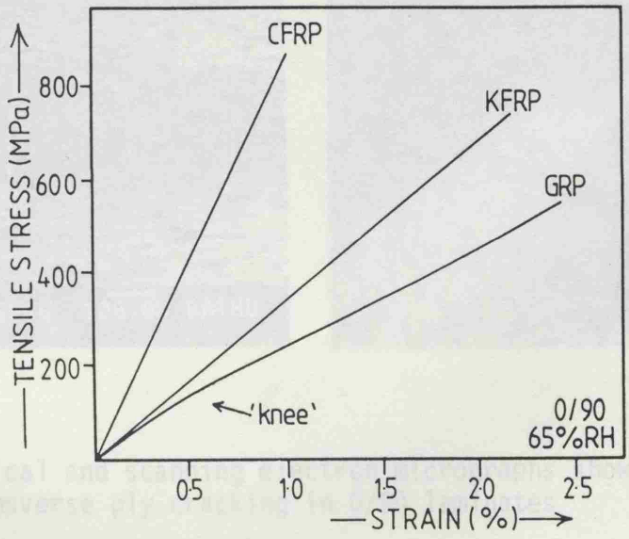

Figure 5.8 Typical tensile stress-strain curves for 0/90 laminates (65%RH).

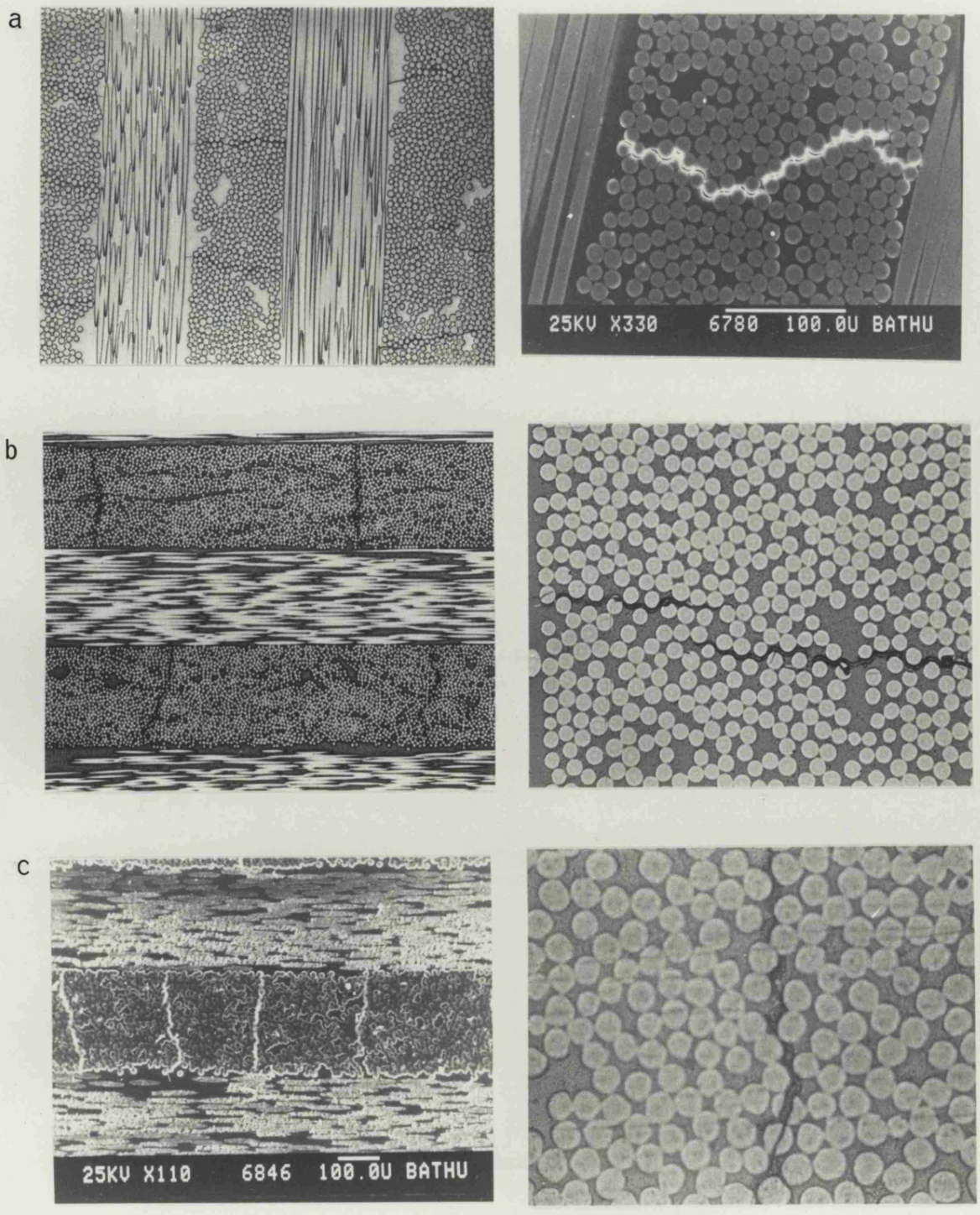

Figure 5.9 Optical and scanning electron micrographs showing transverse ply cracking in 0/90 laminates

a. GRP b. CFRP c. KFRP

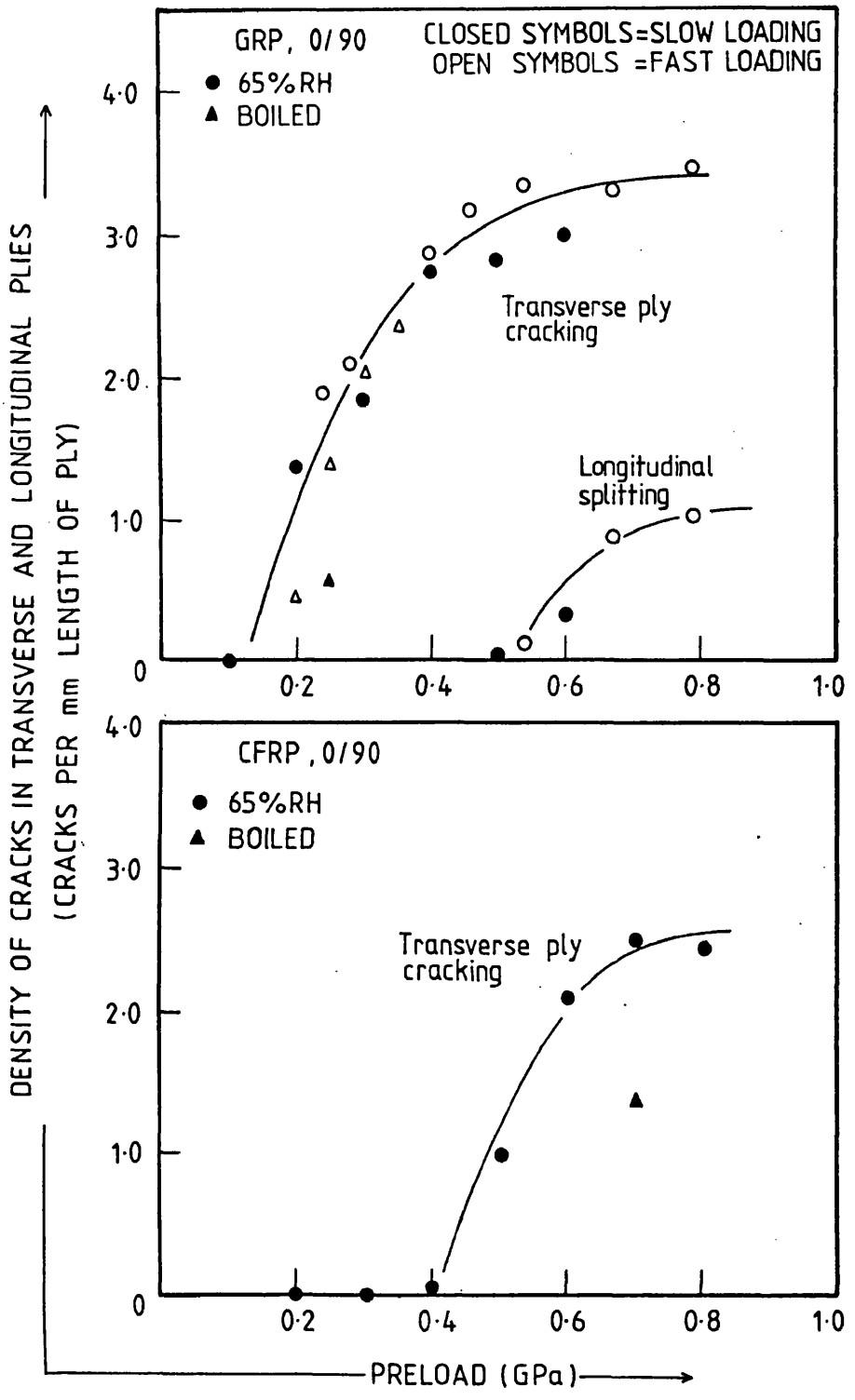

Figure 5.10 The accumulation of transverse ply cracks and longitudinal splits with increasing levels of tensile stress.

a) 0/90 GRP
b) 0/90 CFRP

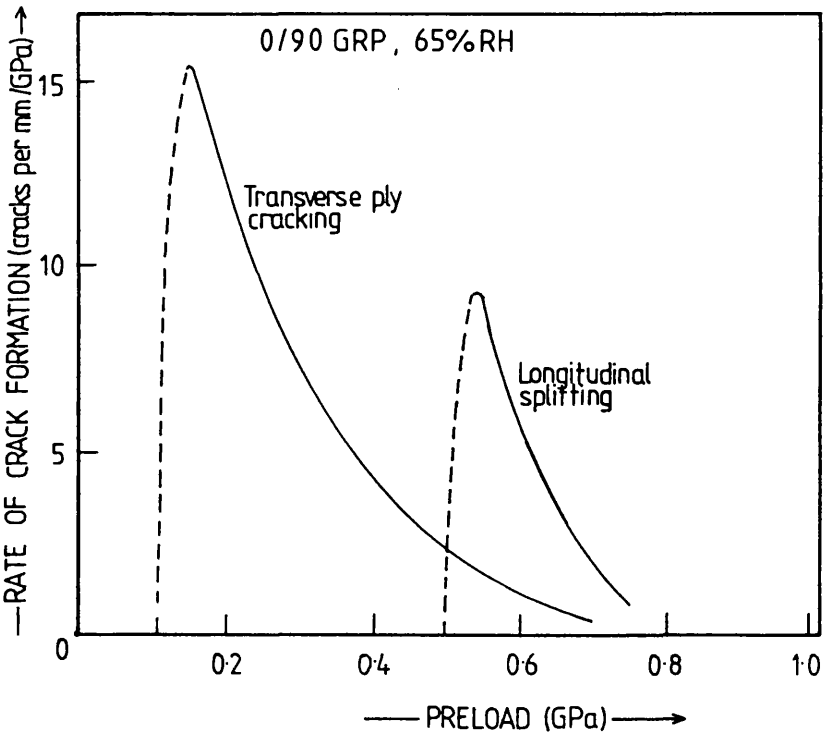

Figure 5.10 c) 0/90 GRP (rate of cracking with increasing stress).

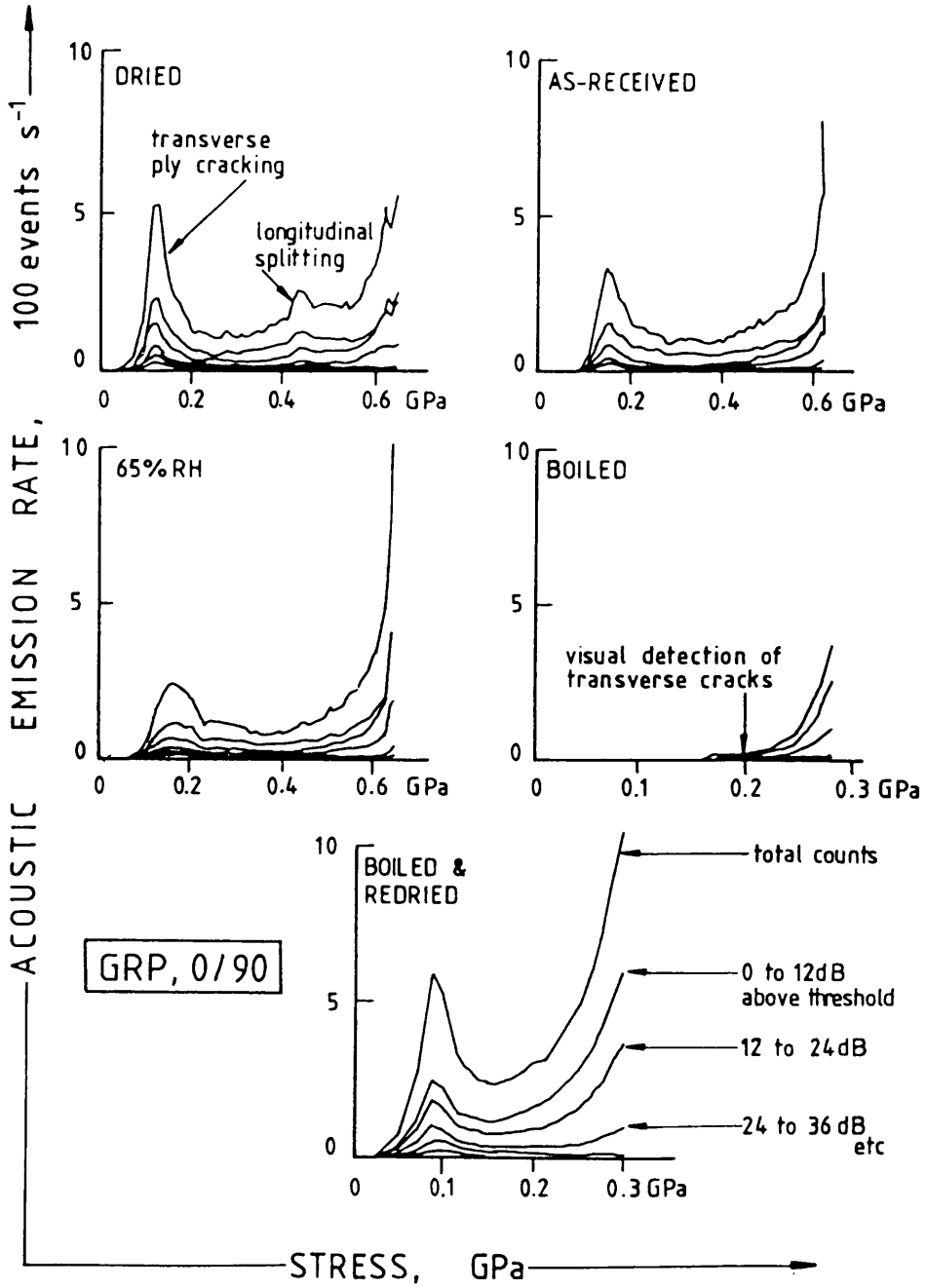

Figure 5.11 Acoustic emission versus stress curves for 0/90 GRP laminate in various preconditioned states (References P1, P4).

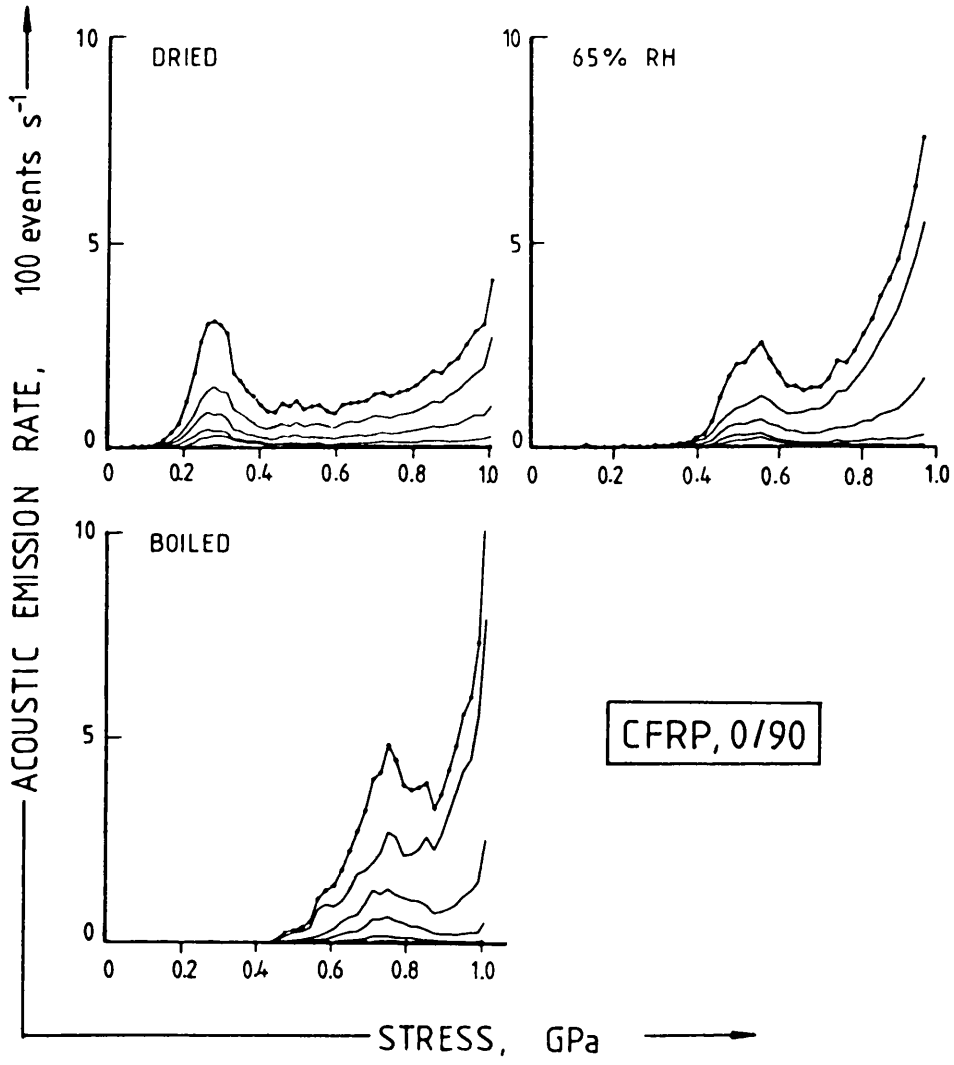

Figure 5.12 Acoustic emission versus stress curves for 0/90 CFRP laminate in various preconditioned states (References P1, P4).

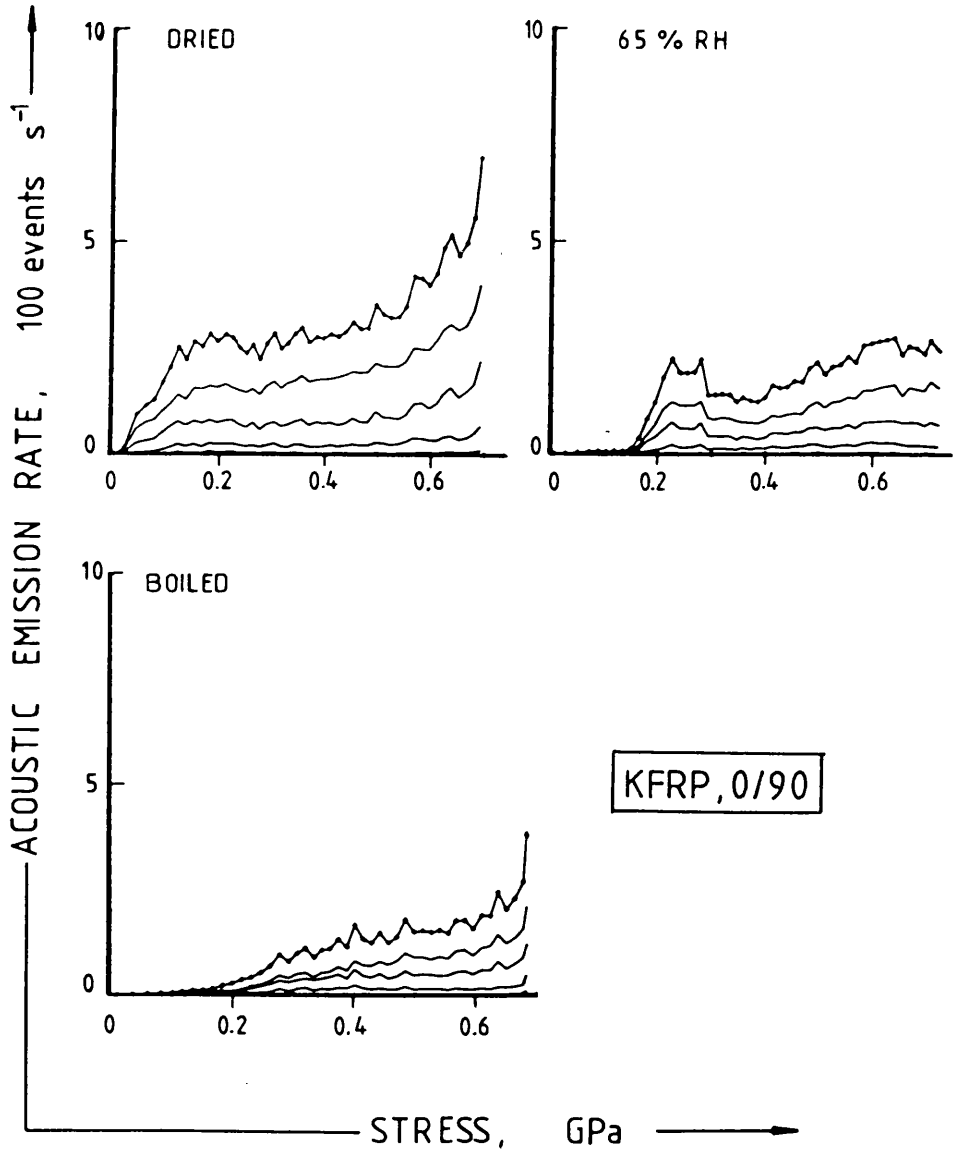

Figure 5.13 Acoustic emission versus stress curves for 0/90 KFRP laminate in various preconditioned states (References P1, P4).

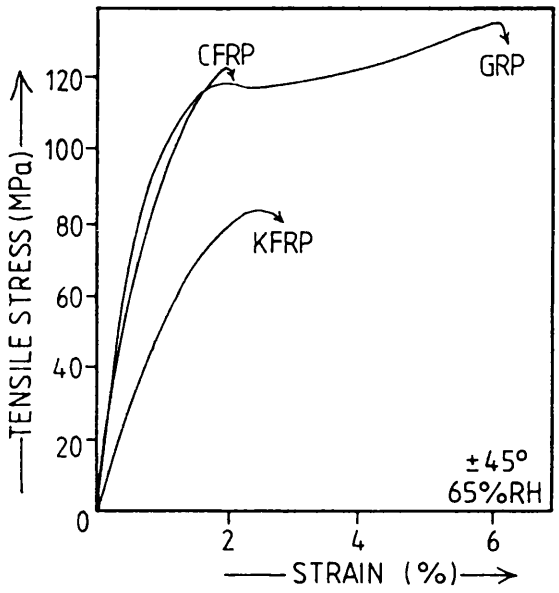

Figure 5.14 Typical tensile stress-strain curves for ±45° laminates (65% RH)

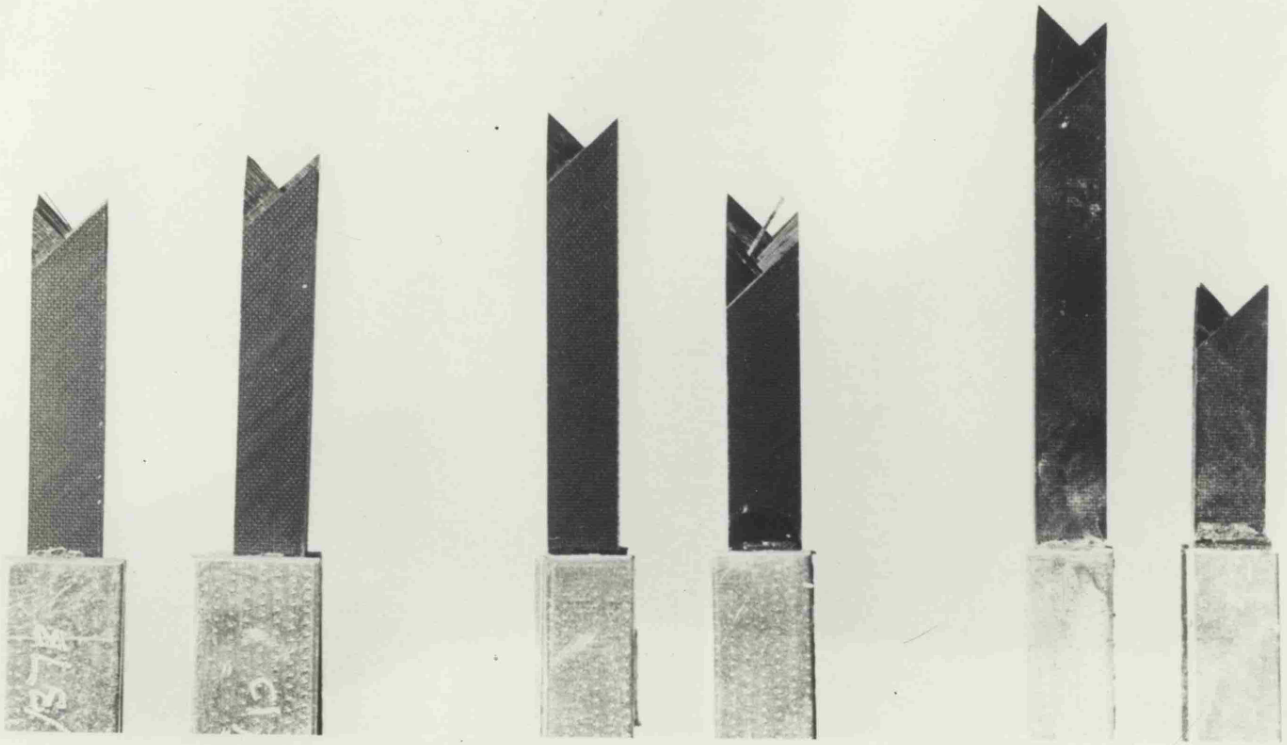

Figure 5.15 Tensile failure of ±45° CFRP: Dried 65% Boiled

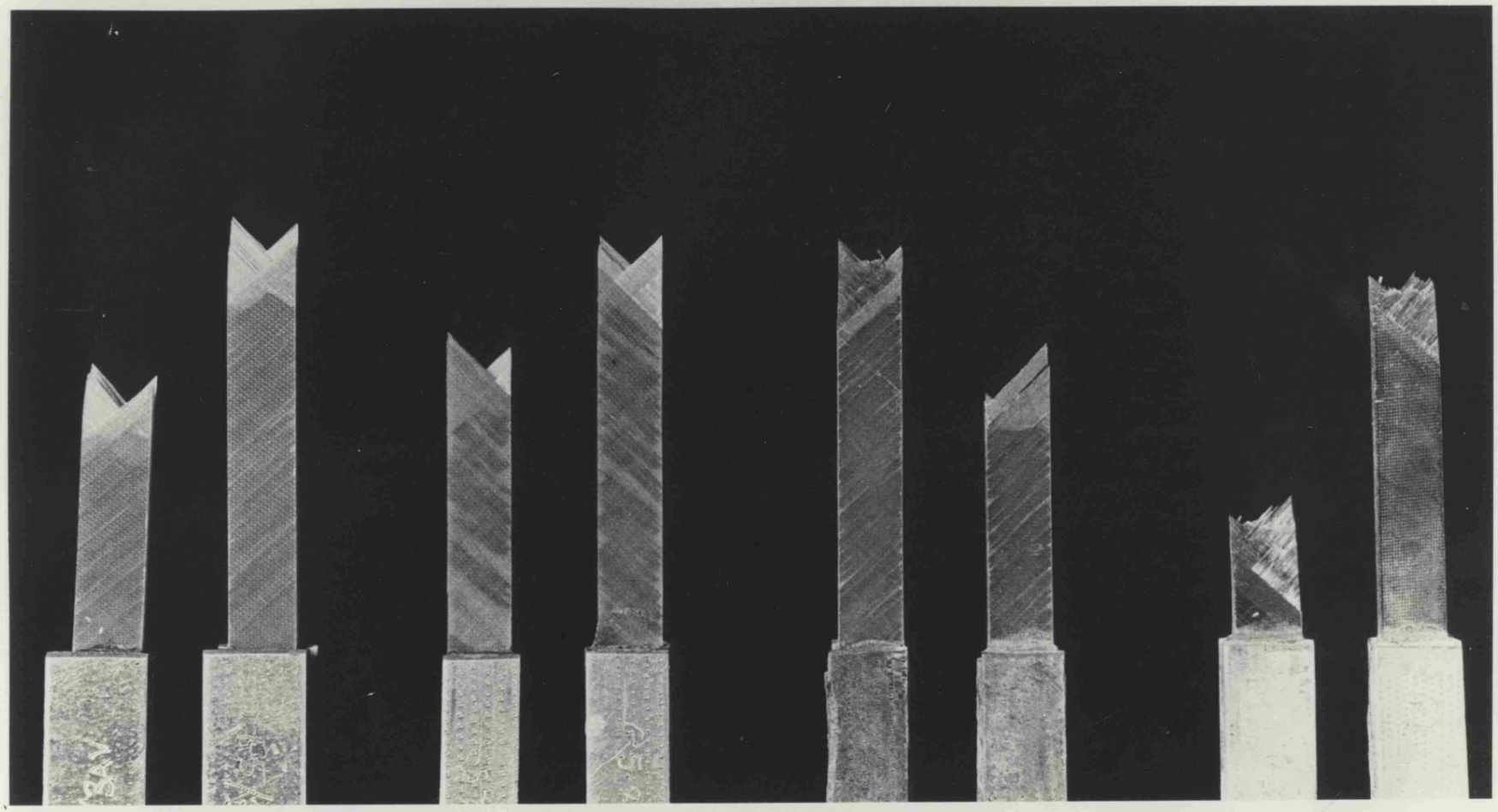

Figure 5.16 Tensile failure of ±45° GRP: Dried 65%RH Boiled(3 weeks) Boiled(6 months)

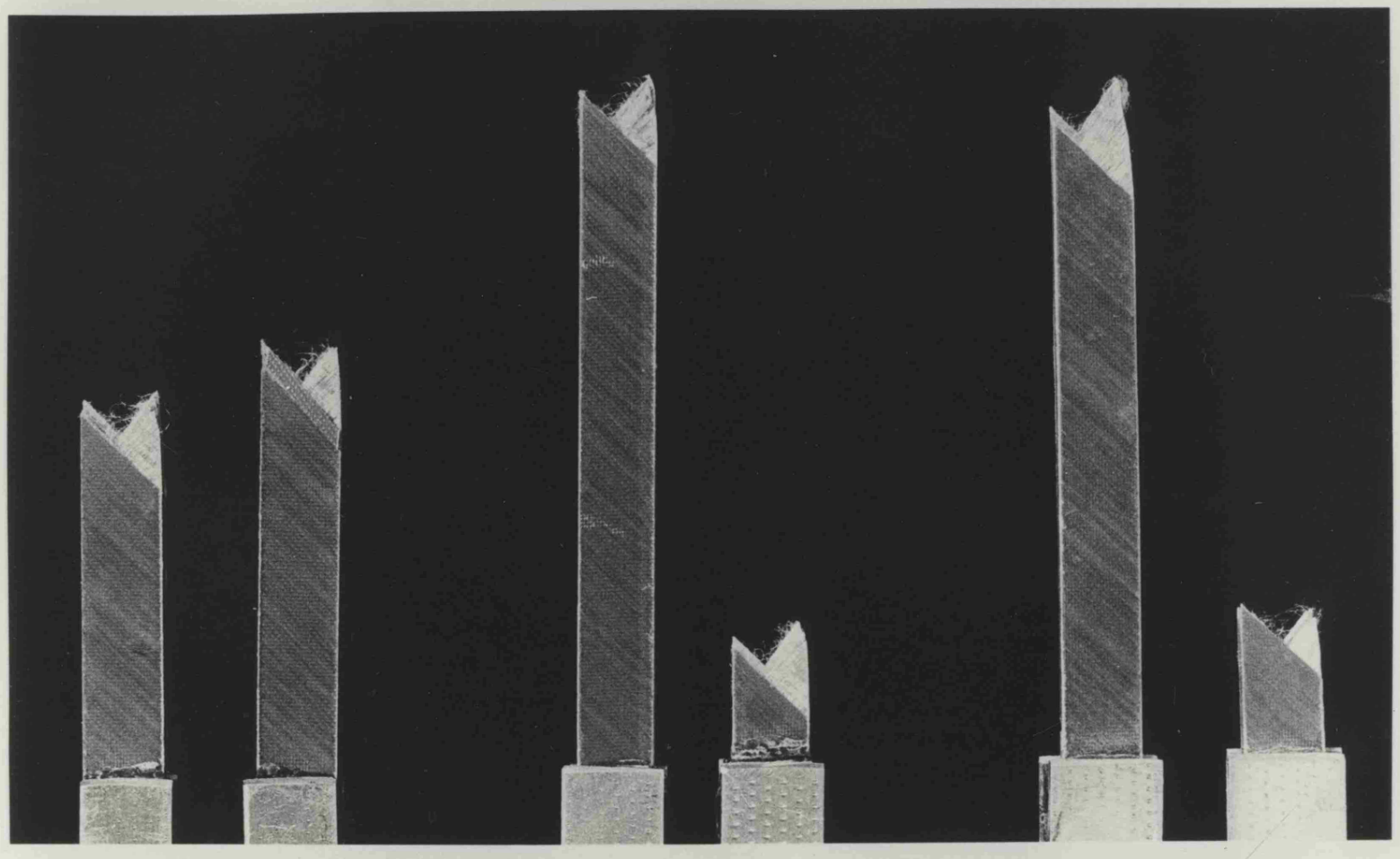

Figure 5.17 Tensile failure of ±45° KFRP: Dried 65%RH Boiled

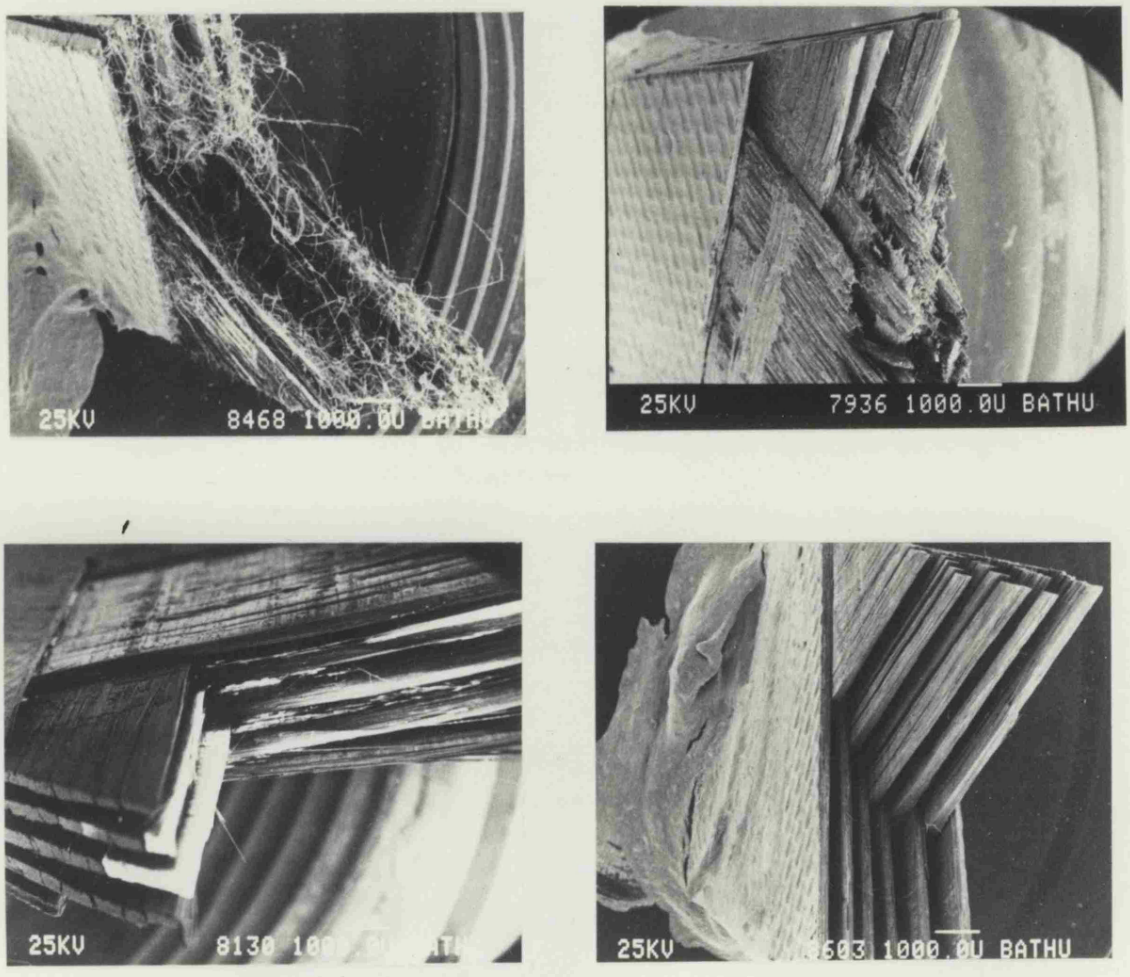

Figure 5.18 Scanning electron micrographs showing tensile fracture surfaces of ±45° laminates.

a. 65%RH KFRP
b. Boiled GRP
c. Dried GRP
d. Dried CFRP

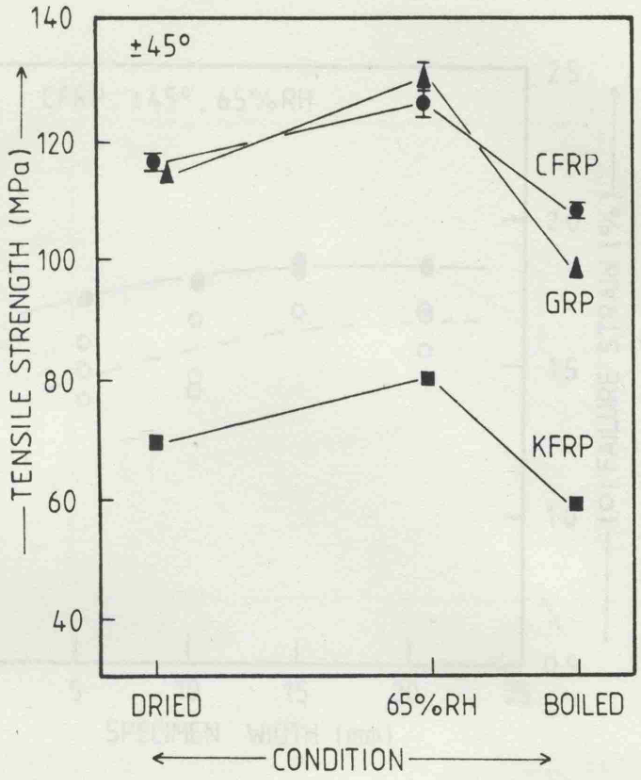

Figure 5.19 Effect of preconditioning on tensile strength of ±45° laminates.

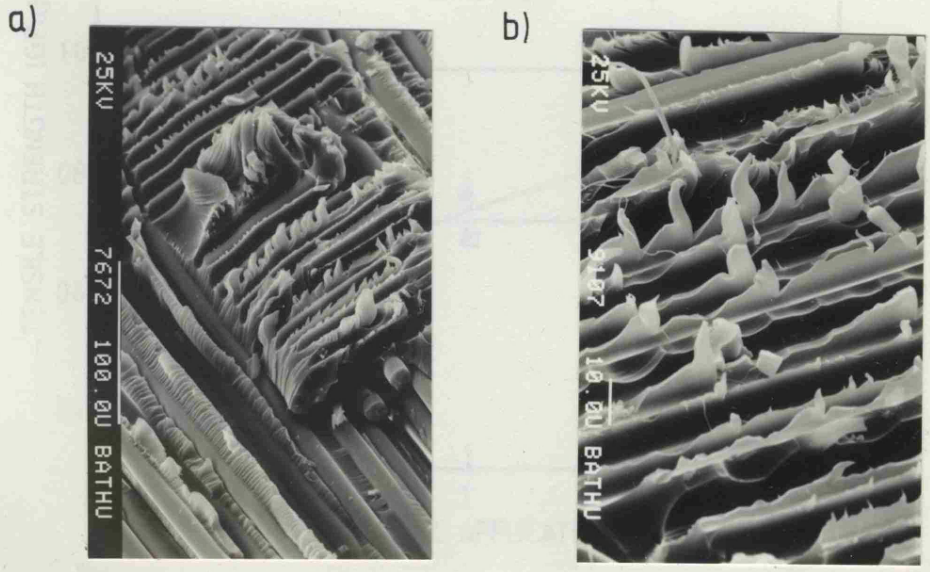

Figure 5.20 Scanning electron micrographs of ±45° fracture surfaces showing localised plastic behaviour

a) 65% RH GRP
b) Dried KFRP.

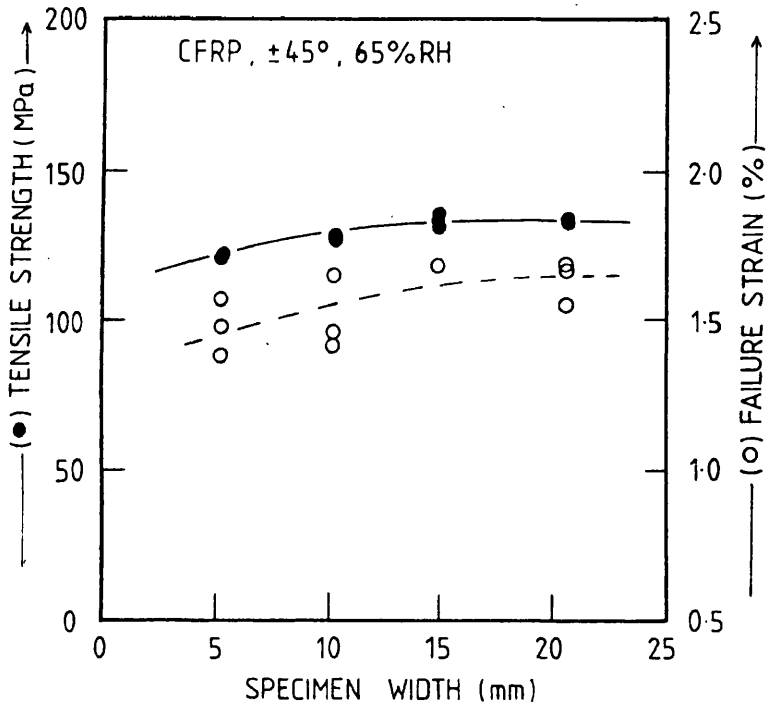

Figure 5.21 Effect of specimen width on tensile strength and failure strain of ±45° CFRP (65% RH).

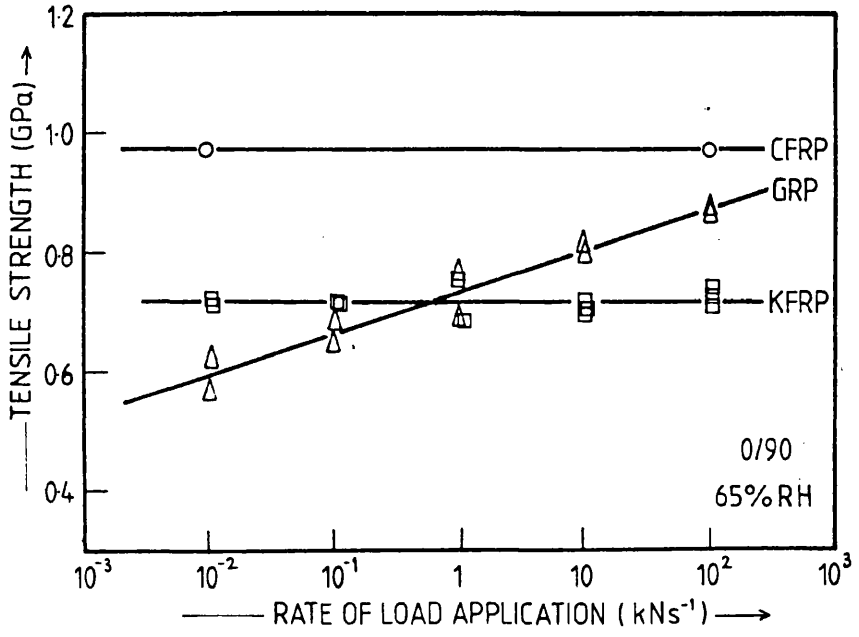

Figure 5.22 Effect of loading rate on tensile strength of 0/90 laminates (65% RH)

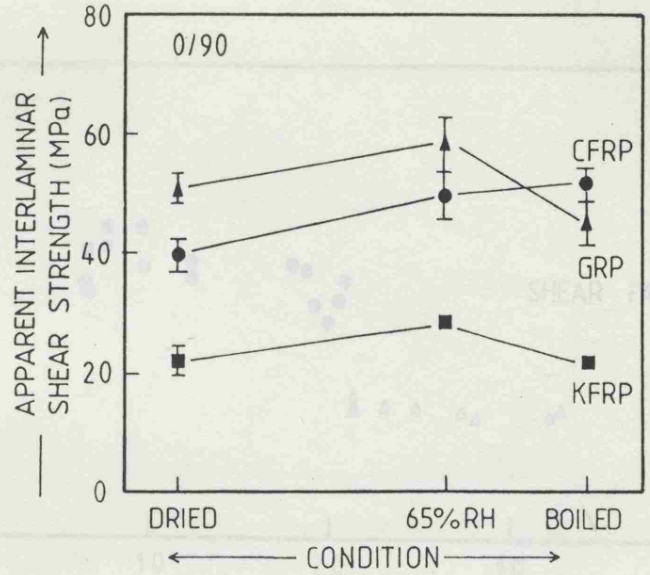

Figure 6.1 Effect of preconditioning on apparent interlaminar shear strength.

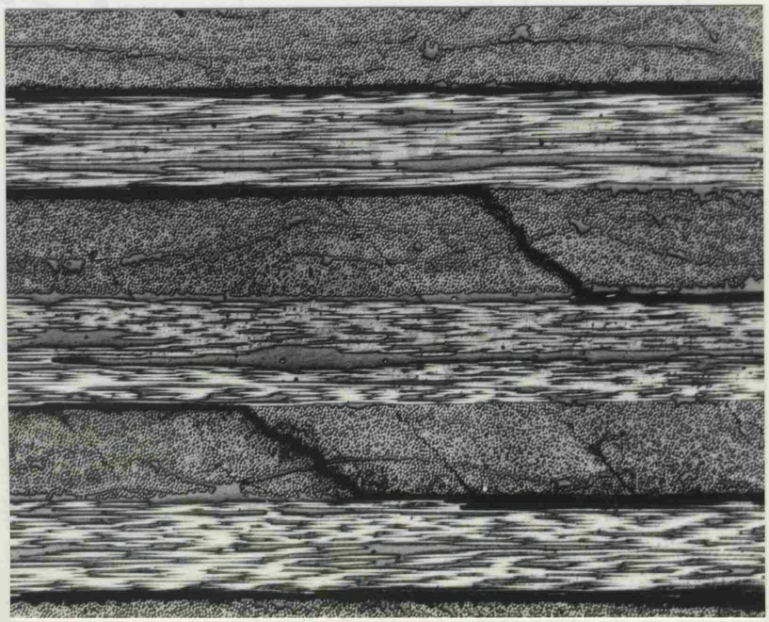

Figure 6.2 Interlaminar shear failure mode (CFRP, 65% RH), showing oblique transverse ply cracking and delamination.

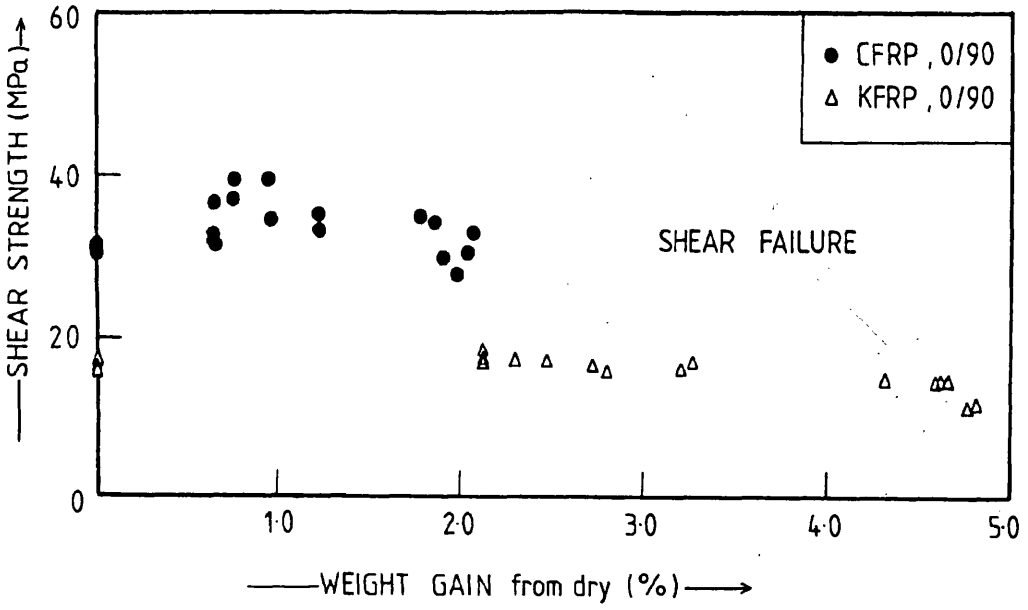

Figure 6.3 Effect of moisture content on 4-point bending strengths of CFRP and KFRP-shear failure mode.

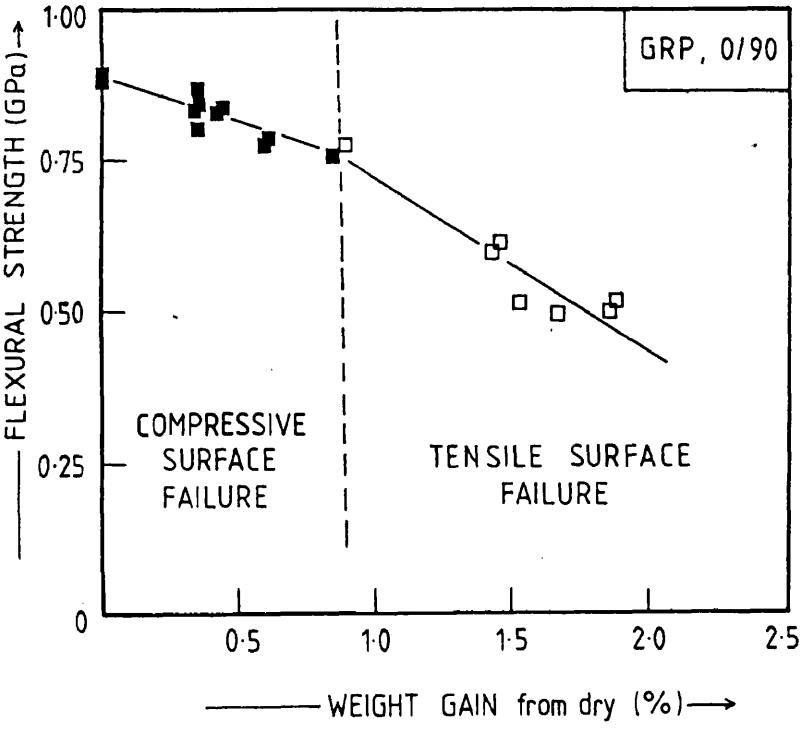

Figure 6.4 Effect of moisture content on 4-point bending strength of GRP-flexural failure mode.

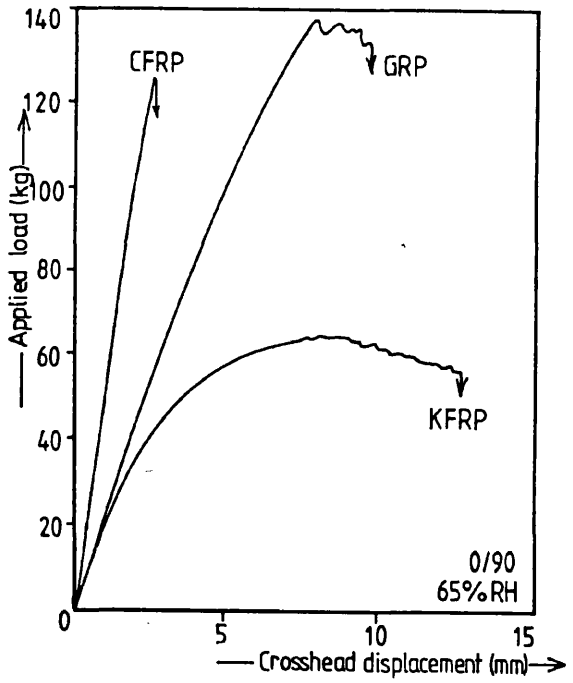

Figure 6.5 Typical load-deflection curves for the laminates in 4-point bending (65% RH).

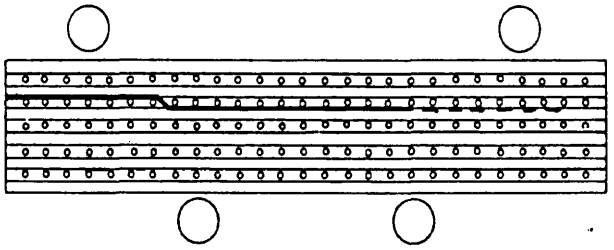

Figure 6.6 Schematic representation of shear failure mode in 4-point bending for CFRP and KFRP 0/90 laminates. Bold line highlights plane of failure.

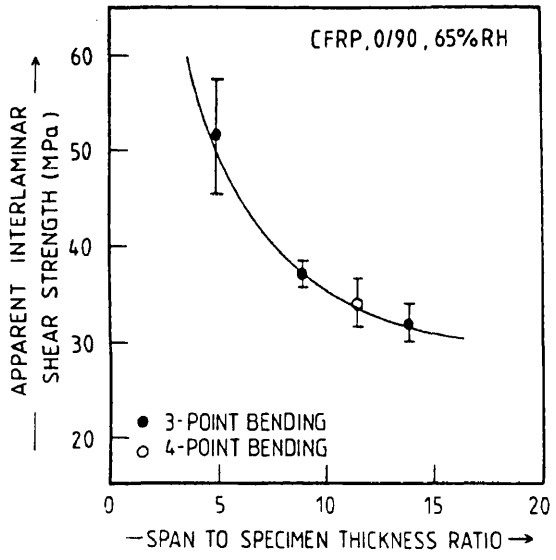

Figure 6.7 Dependence of apparent interlaminar shear strength on ratio of span to specimen thickness (CFRP, 65%RH).

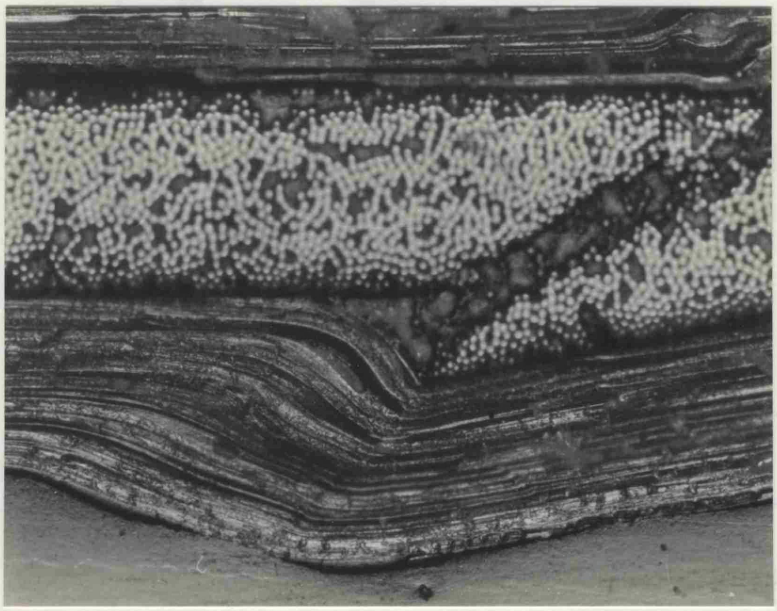

Figure 6.8 Fibre buckling under inner load point for 0/90 KFRP in four-point bending (65%RH).

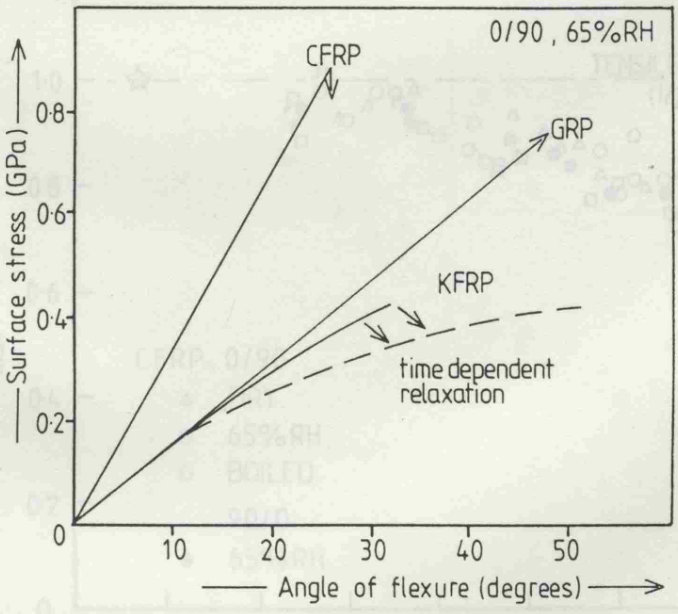

Figure 6.9 Typical load-deflection curves for the laminates in Avery flexure, highlighting the time-dependent relaxation for KFRP (65%RH).

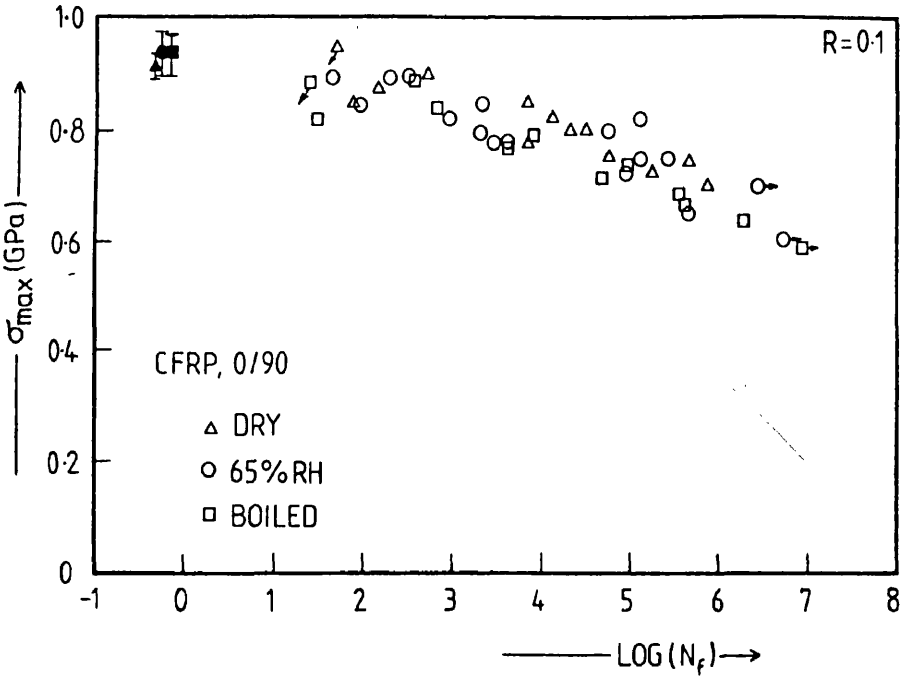

Figure 7.1a Tensile fatigue curves for 0/90 CFRP laminate showing effects of preconditioning treatments (loading rate = 200kNs^{-1}). Filled symbols represent static tensile strength measured at 200kNs^{-1}.

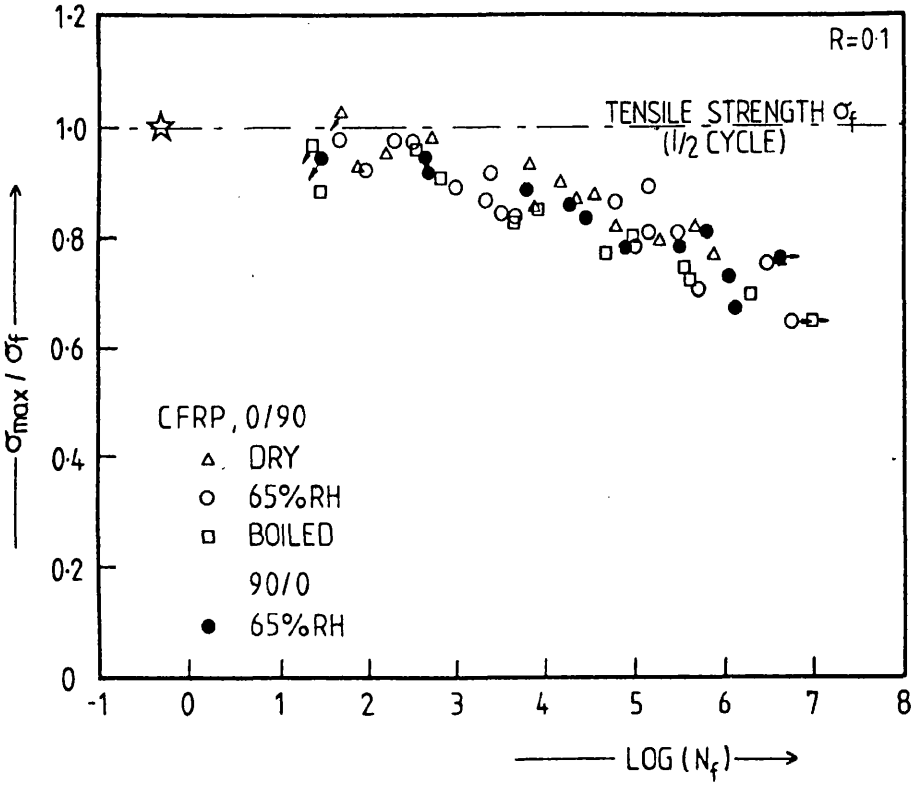

Figure 7.1b Tensile fatigue curves for 0/90 CFRP laminate normalised to static failure strengths at the same rate of loading (200kNs^{-1}). Includes fatigue data for laminate in 90/0 orientation.

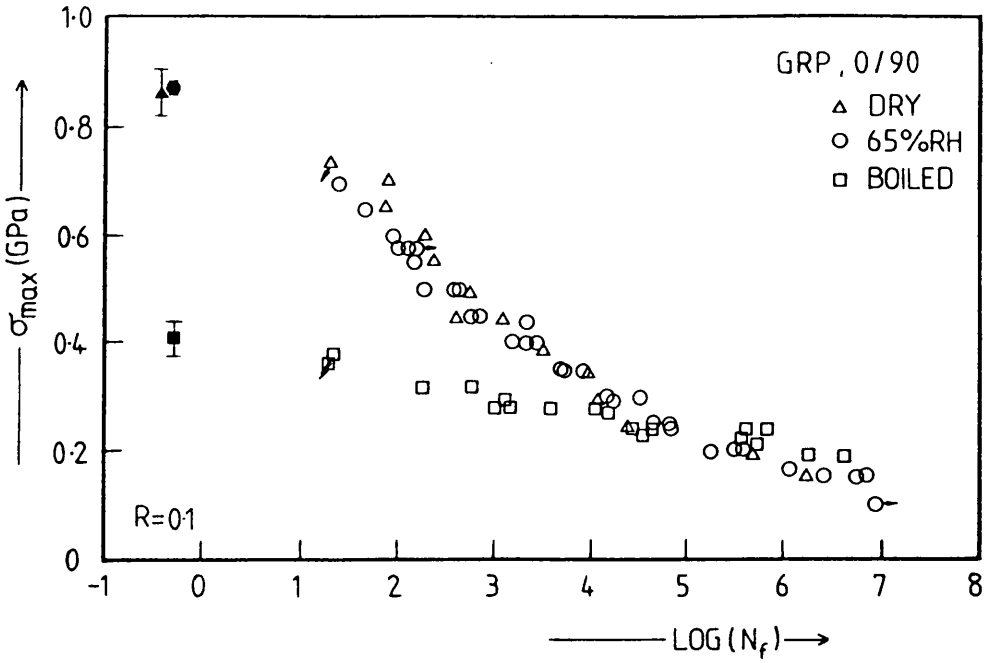

Figure 7.2a Tensile fatigue curves for 0/90 GRP laminate showing effects of preconditioning treatments (loading rate = 100kNs^{-1}). Filled symbols represent static tensile strength measured at 100kNs^{-1}.

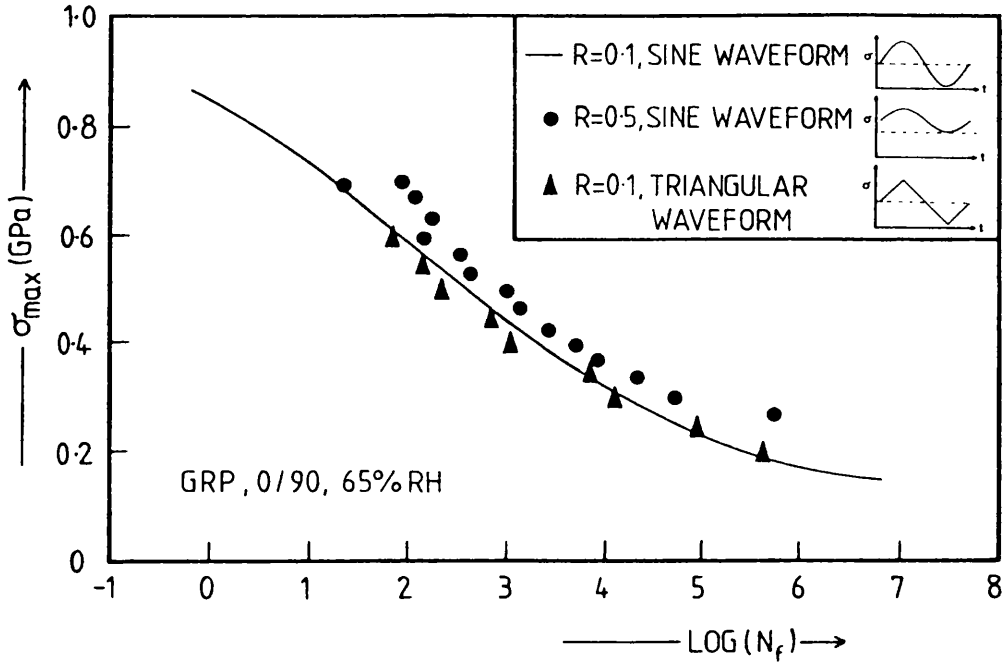

Figure 7.2b Effect of R-ratio and waveform shape on fatigue life of 0/90 GRP (65%RH).

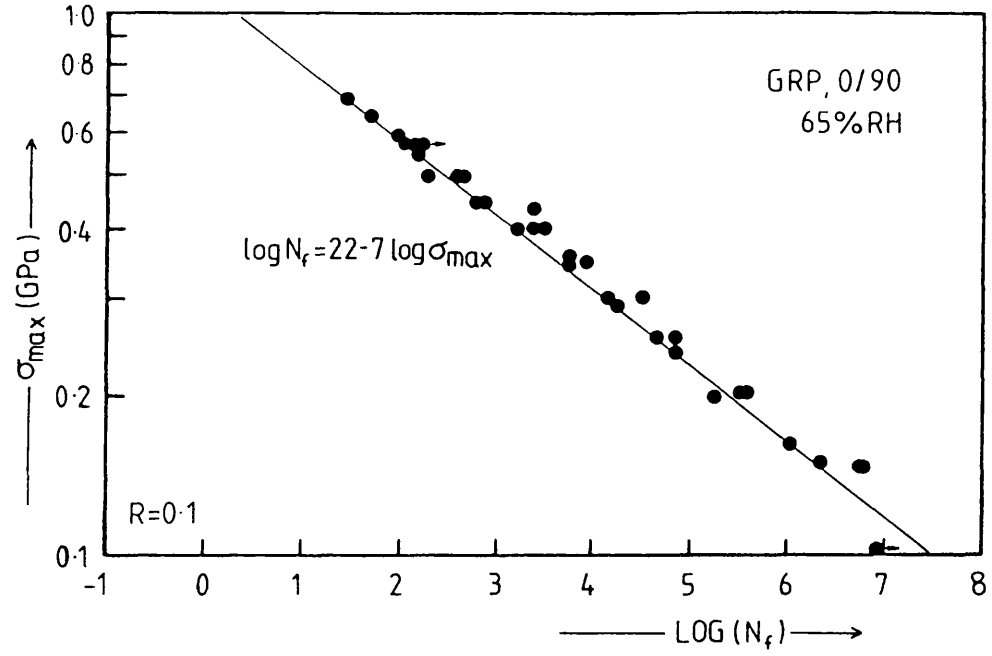

Figure 7.3 Fatigue data for 0/90 GRP (65%RH), plotted on a log-log scale.

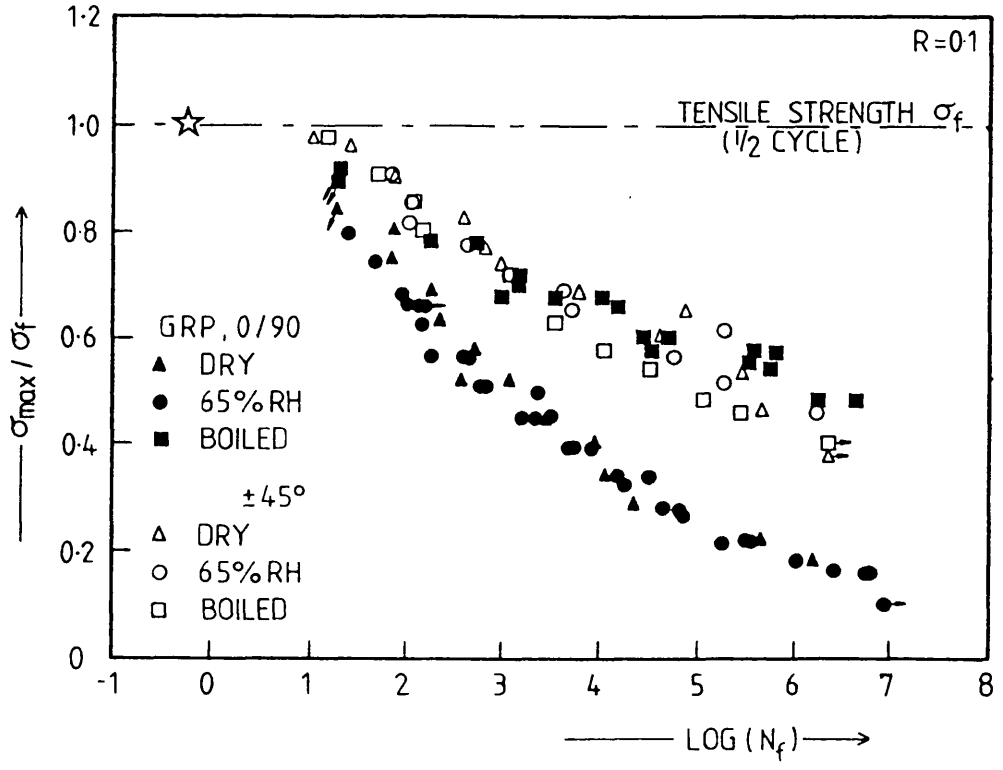

Figure 7.4 Tensile fatigue curves for 0/90 and ±45° GRP laminates normalised to static failure strengths at appropriate loading rates (100kNs^{-1} and 25kNs^{-1}).

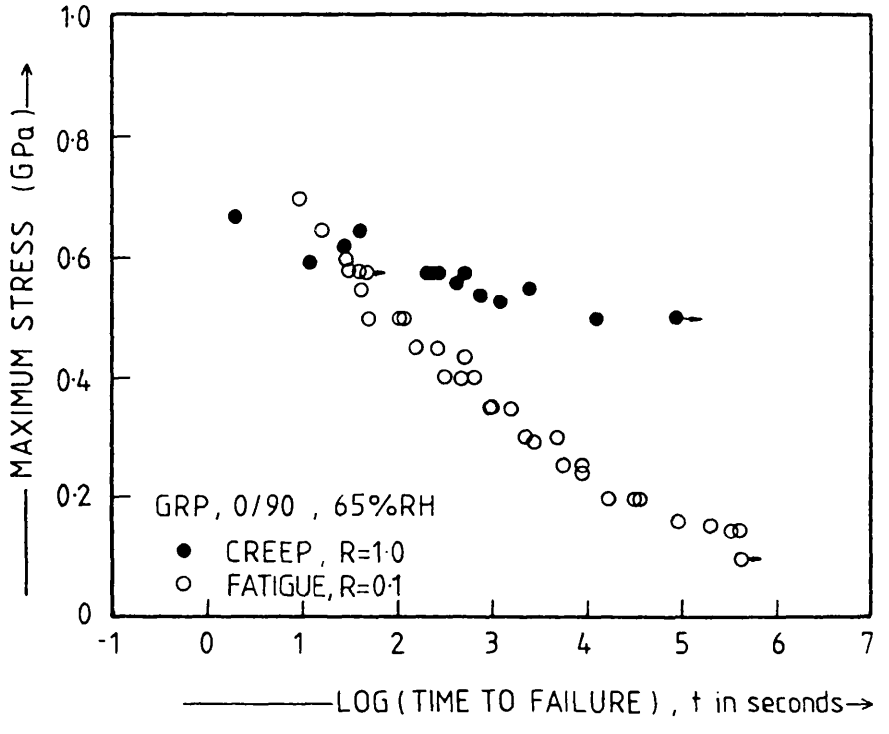

Figure 7.5 Comparison of times to failure of 0/90 GRP laminate in stress-rupture and fatigue (65%RH).

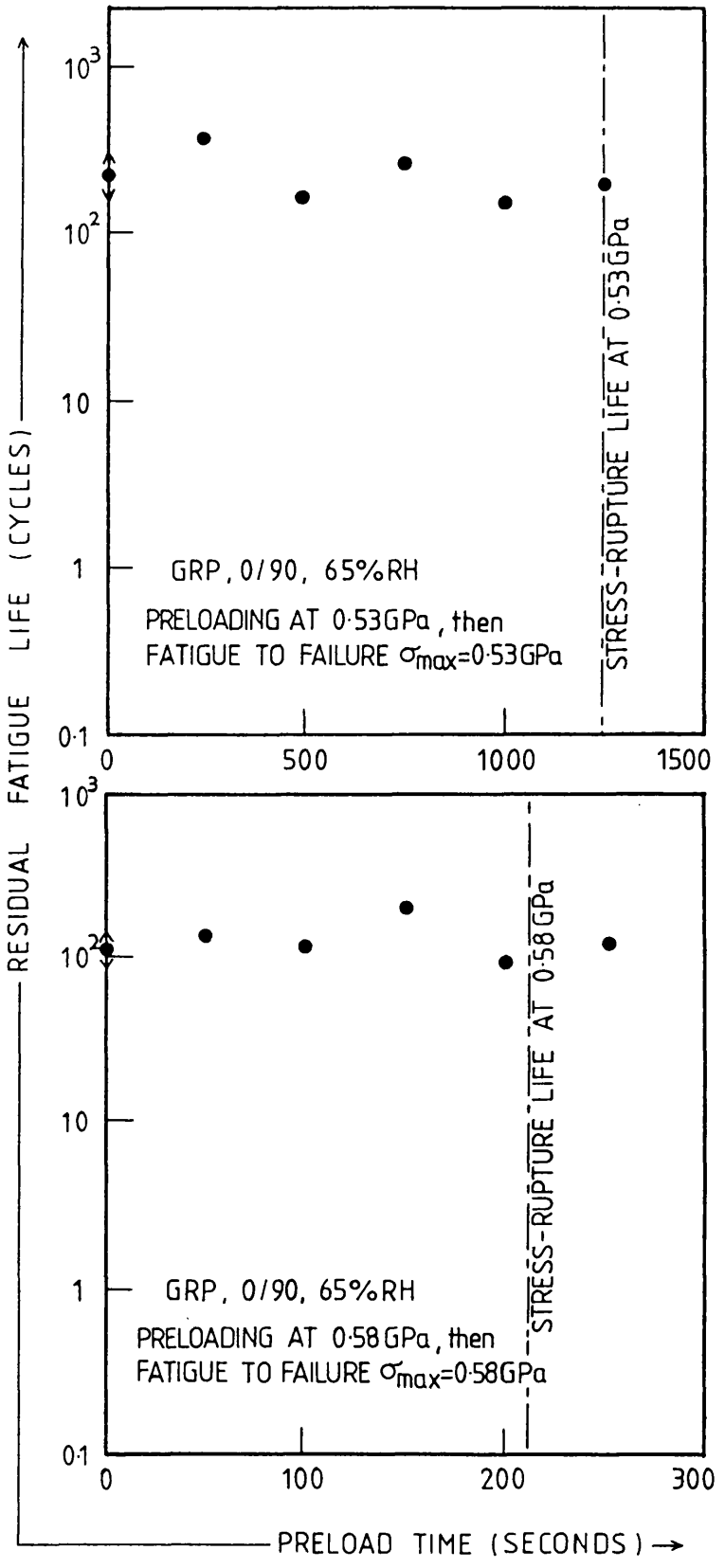

Figure 7.6a-b The effect of prior preloading for periods of time from zero to the stress-rupture life on the residual fatigue life of 0/90 GRP cycled to the same stress level (65%RH).

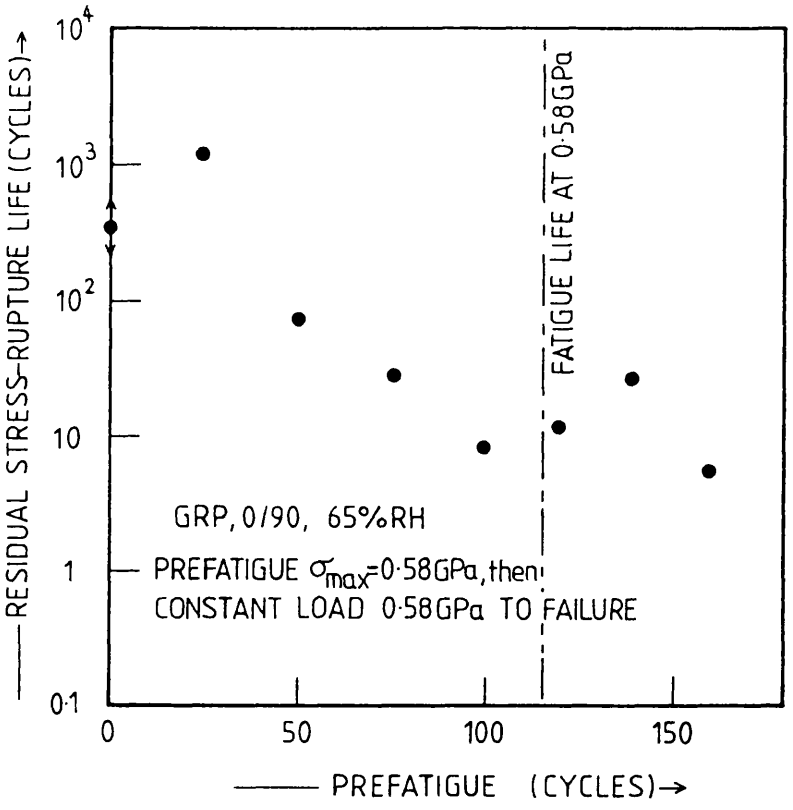

Figure 7.6c The effect of prior fatigue loading on the residual stress-rupture life (at the level of the peak cyclic stress) for 0/90 GRP (65%RH).

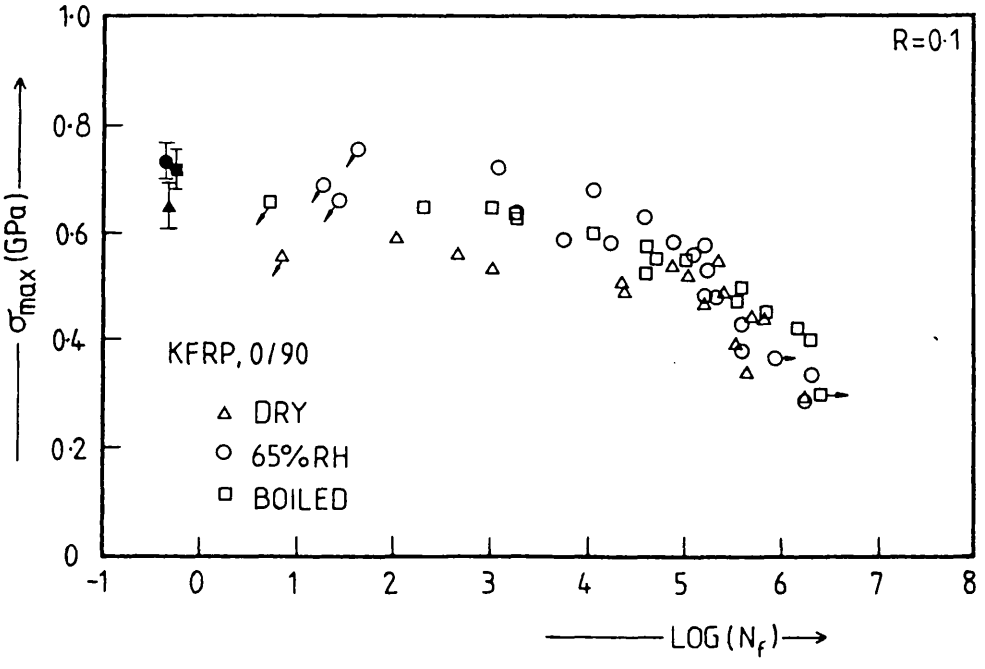

Figure 7.7a Tensile fatigue curves for 0/90 KFRP laminate showing effects of preconditioning treatments (Loading rate = 100kNs^{-1}). Filled symbols represent static tensile strengths measured at 100 kNs^{-1}

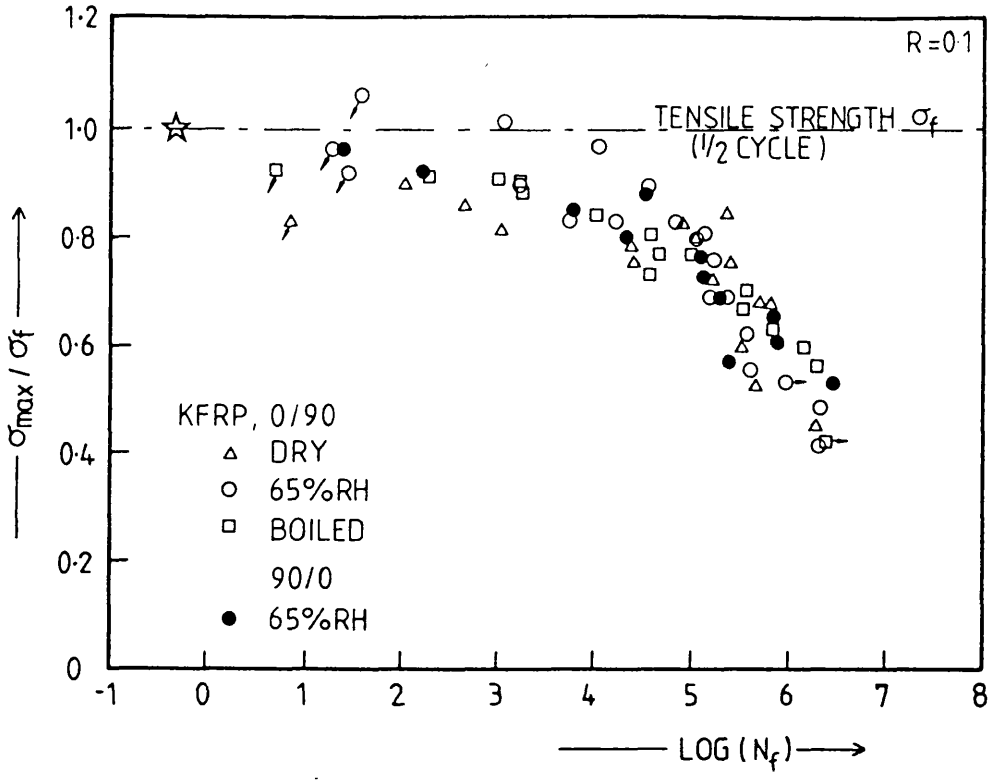

Figure 7.7b Tensile fatigue curves for 0/90 KFRP laminate normalised to static failure strengths at the same rate of loading (100kNs^{-1}). Includes data for laminate in 90/0 orientation.

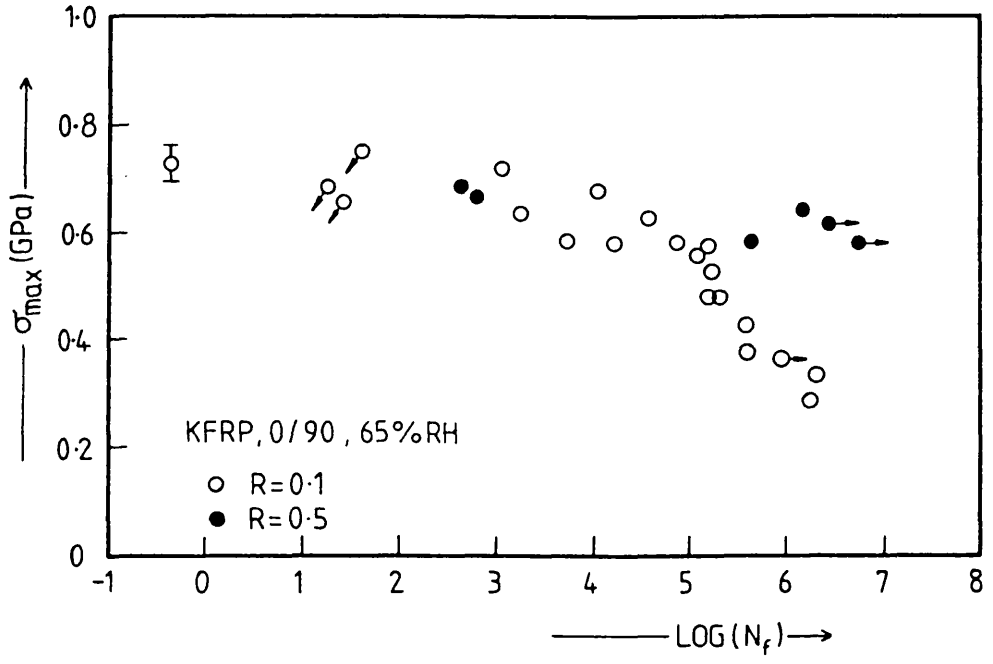

Figure 7.7c Effect of R-ratio on fatigue life of 0/90 KFRP (65%RH).

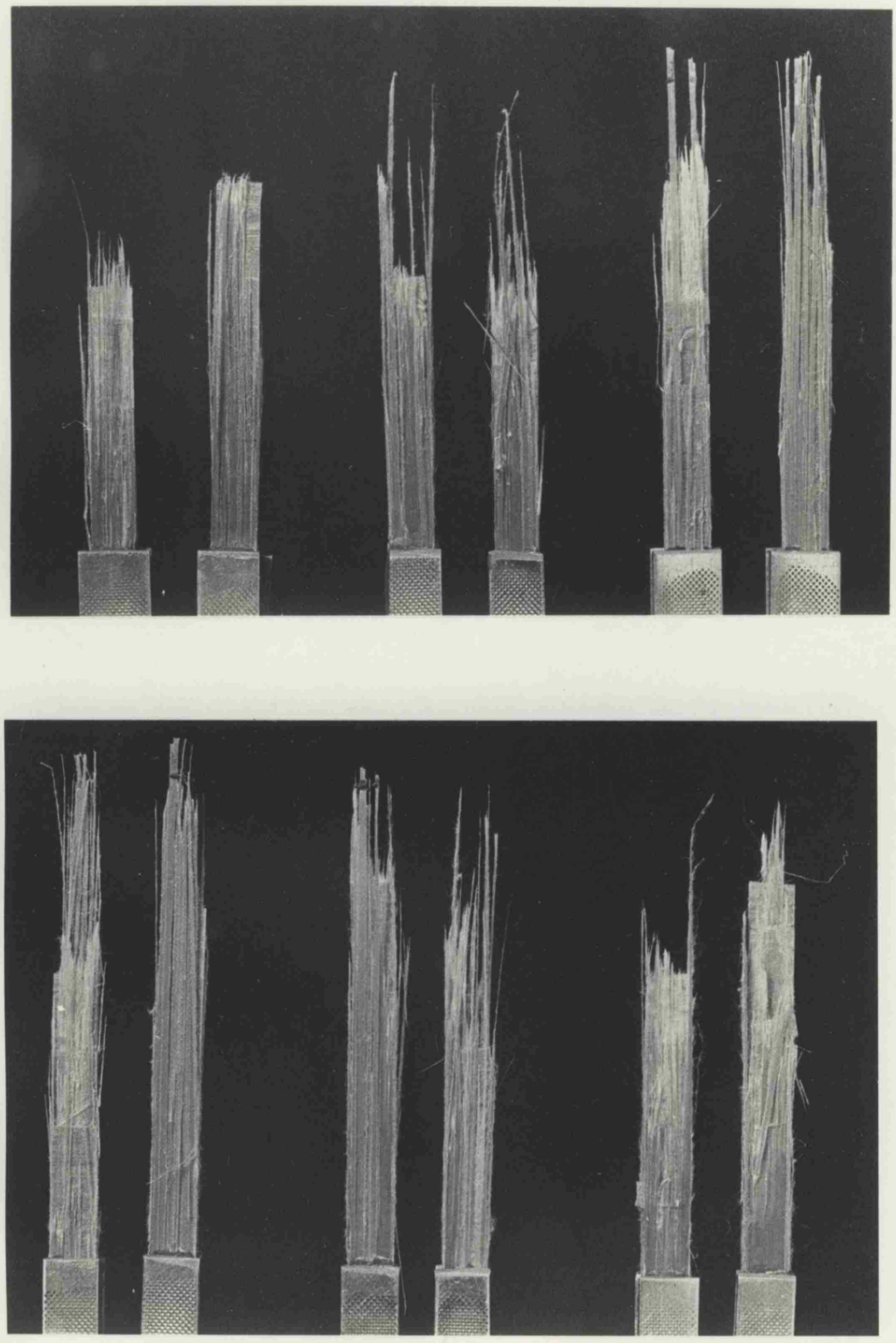

Figure 7.8 Fatigue failures of 0/90 KFRP (65% RH)

a. Effect of fatigue life (σ_{max}):

39 cycles (0.77GPa)	17,100 cycles (0.6GPa)	244,500 cycles (0.5GPa)

b. Effect of R-Ratio:

R=0.1	R=0.3	R=0.5

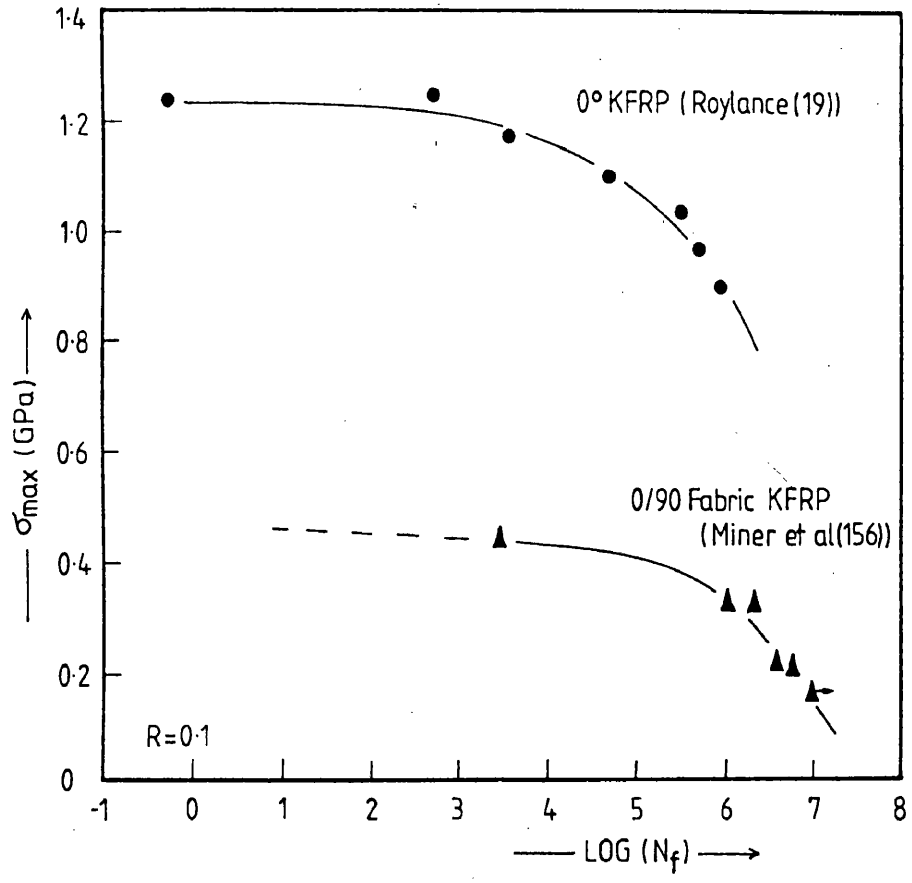

Figure 7.9 Fatigue data for KFRP reported by Roylance(19) and Miner et al(156).

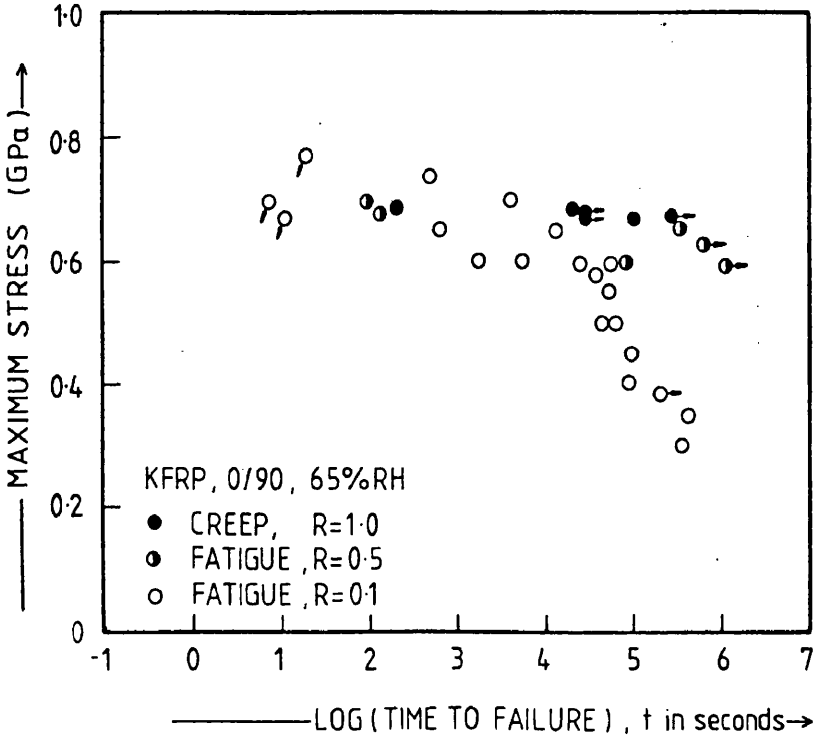

Figure 7.10 Comparison of times to failure of 0/90 KFRP laminate in stress-rupture and fatigue (65%RH).

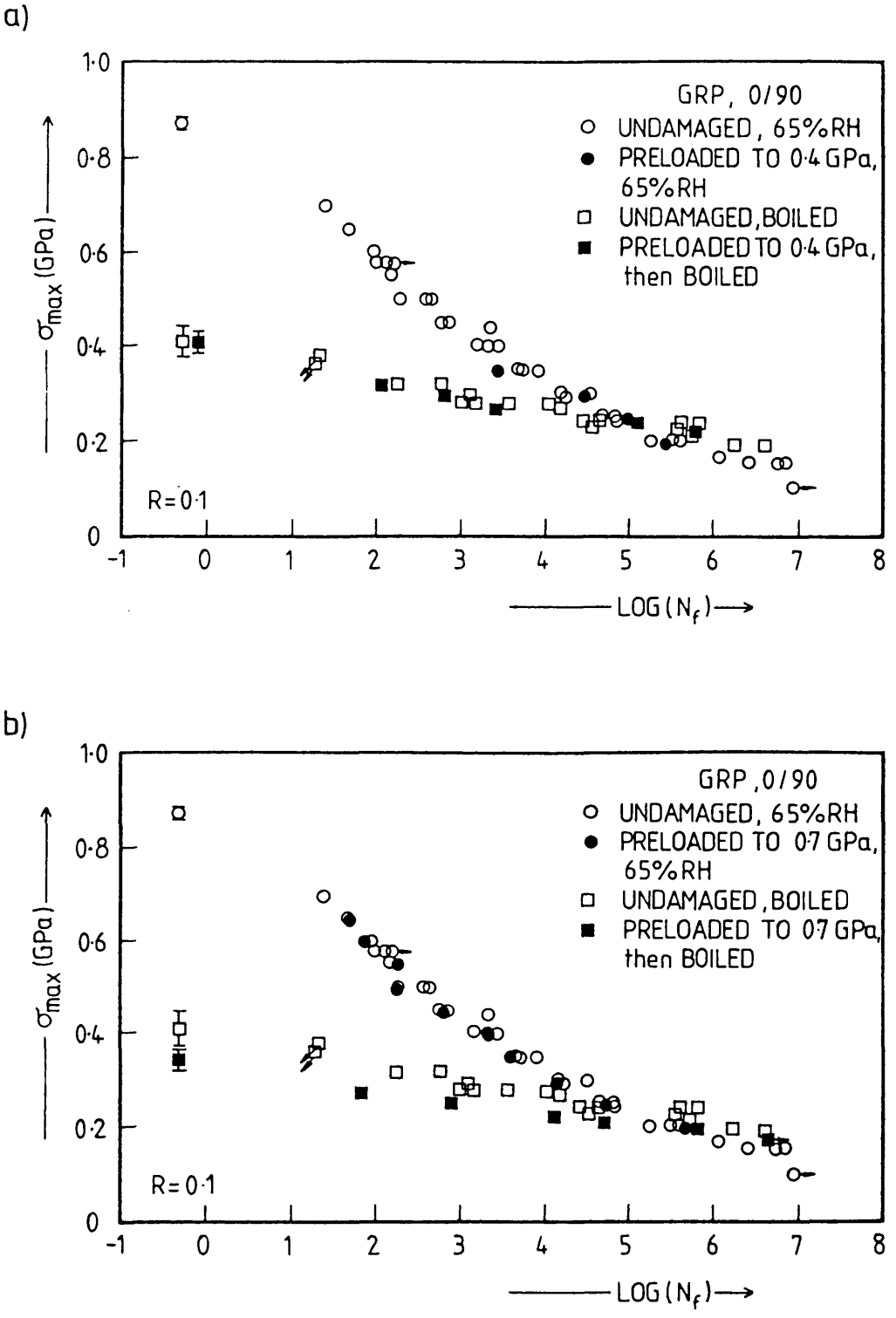

Figure 7.11 Effects of preloading and boiling in water for 3 weeks prior to fatigue testing.

a) 0/90 GRP laminate preloaded to 0.4 GPa
b) 0/90 GRP laminate preloaded to 0.7 GPa

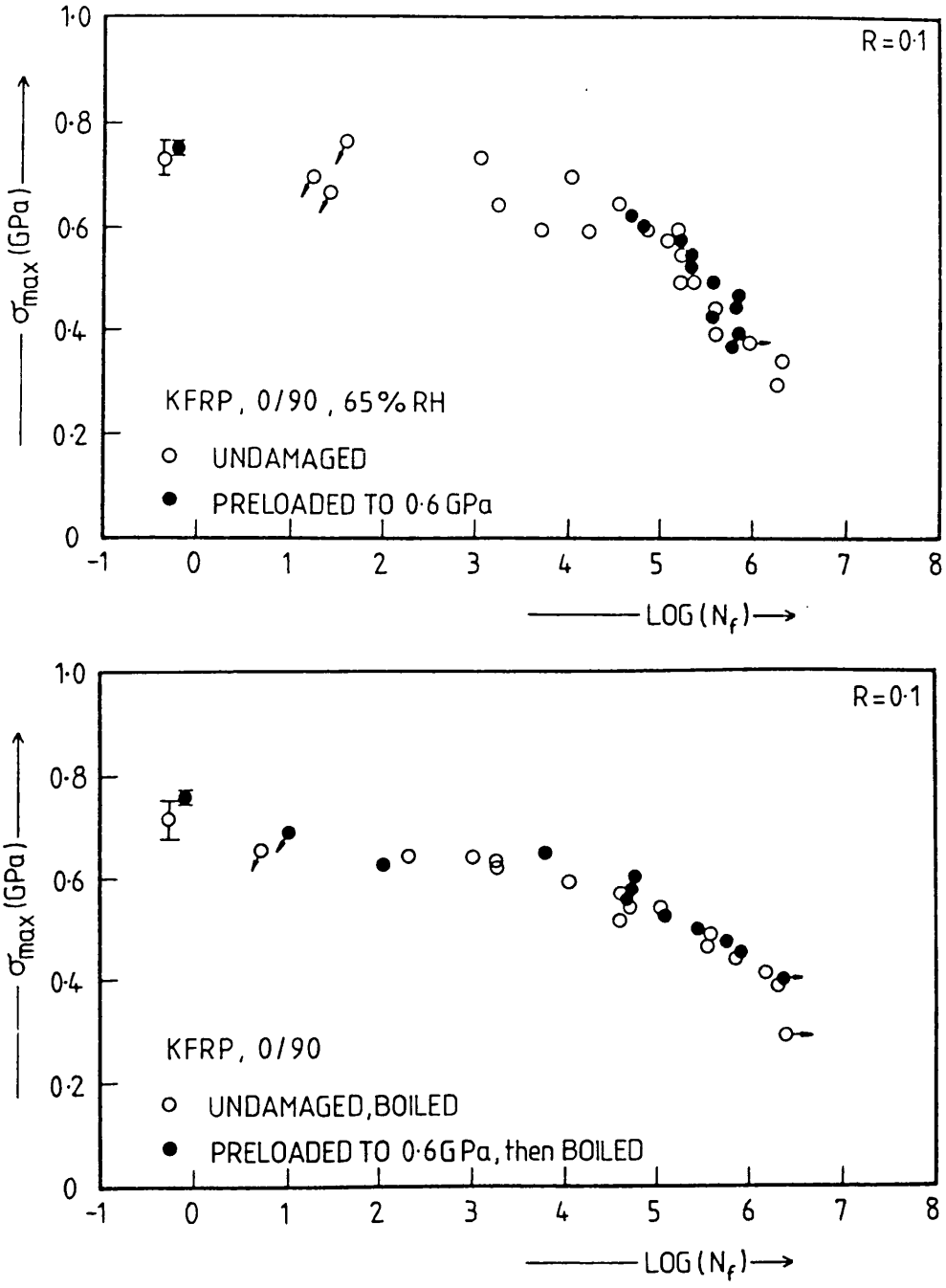

Figure 7.11 Effects of preloading and boiling in water for 3 weeks prior to fatigue testing.

c) 0/90 KFRP laminate preloaded to 0.6 GPa

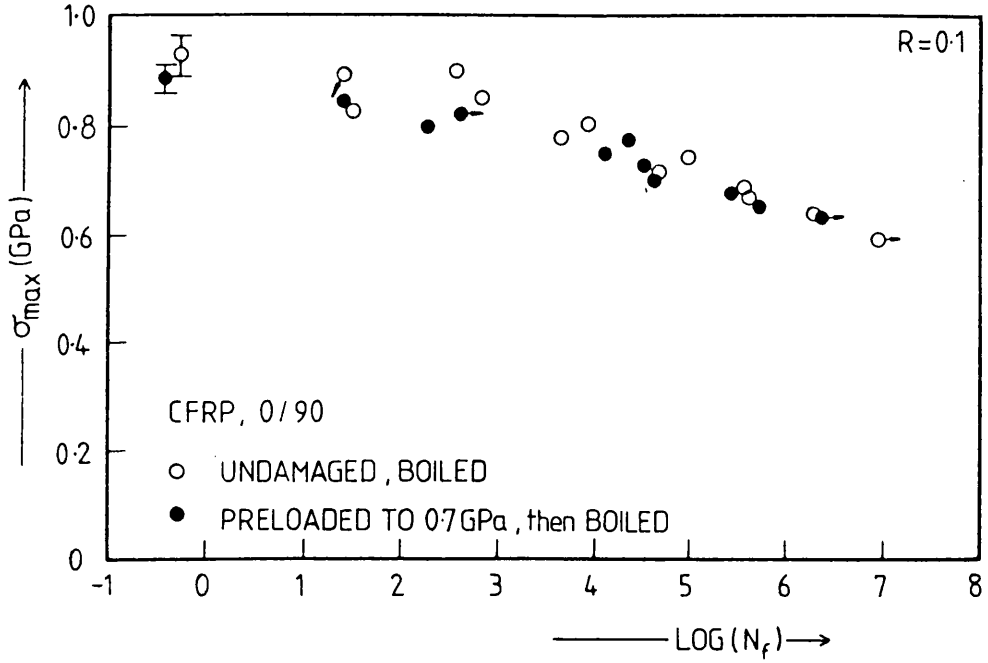

Figure 7.11 Effects of preloading and boiling in water for 3 weeks prior to fatigue testing.

d) 0/90 CFRP laminate preloaded to 0.7 GPa

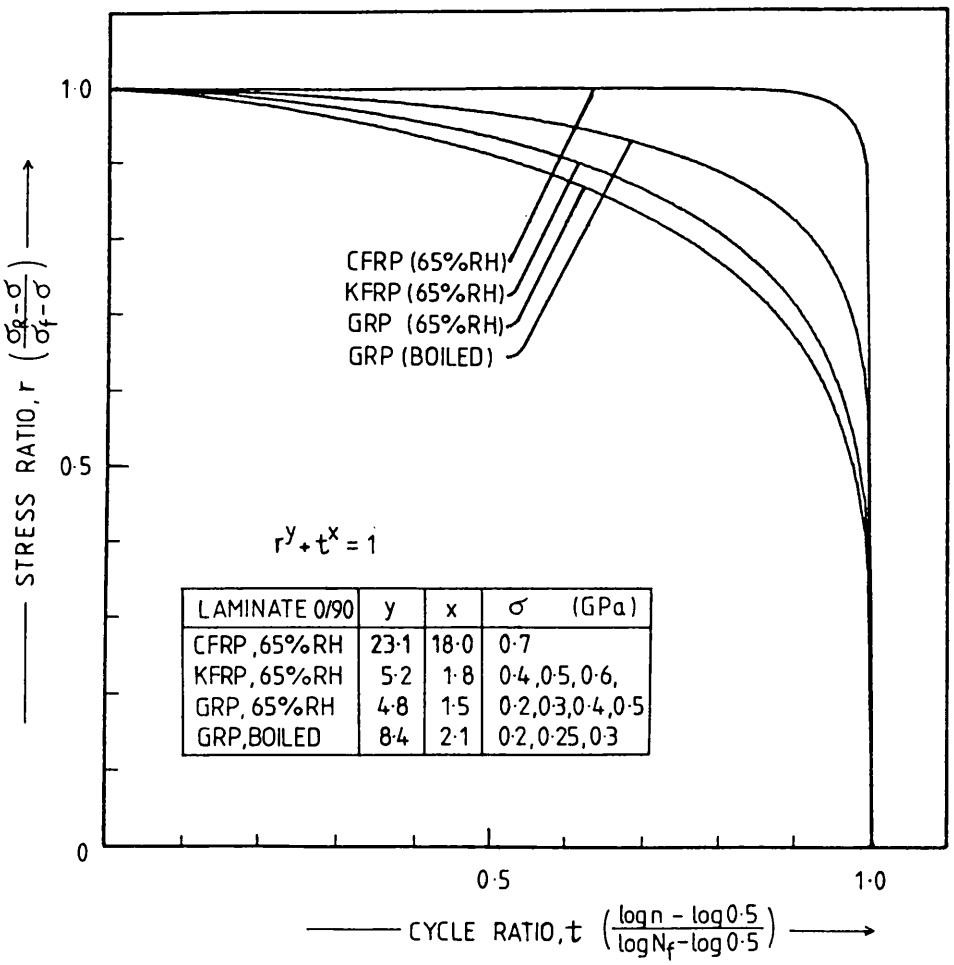

LAMINATE 0/90	y	x	σ (GPa)
CFRP, 65%RH	23·1	18·0	0·7
KFRP, 65%RH	5·2	1·8	0·4, 0·5, 0·6,
GRP, 65%RH	4·8	1·5	0·2, 0·3, 0·4, 0·5
GRP, BOILED	8·4	2·1	0·2, 0·25, 0·3

Figure 7.12 Relationships between the residual strength (σ_R) and the number of fatigue cycles endured (n) for the 0/90 laminates. In each instance, the plots of stress ratio versus cycle ratio are independent of cyclic stress level (σ) and fatigue life (N).

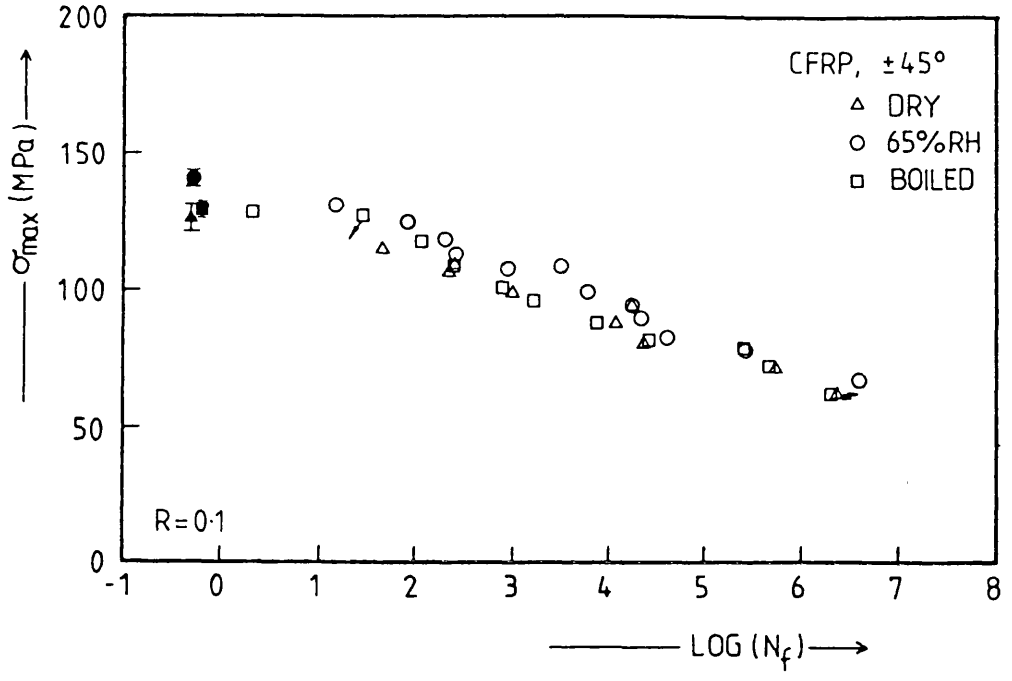

Figure 7.13 Tensile fatigue curves for CFRP laminate in ±45° orientation, showing effects of preconditioning treatments (Loading rate = 25kNs^{-1}). Filled symbols represent static tensile strengths measured at 25kNs^{-1}.

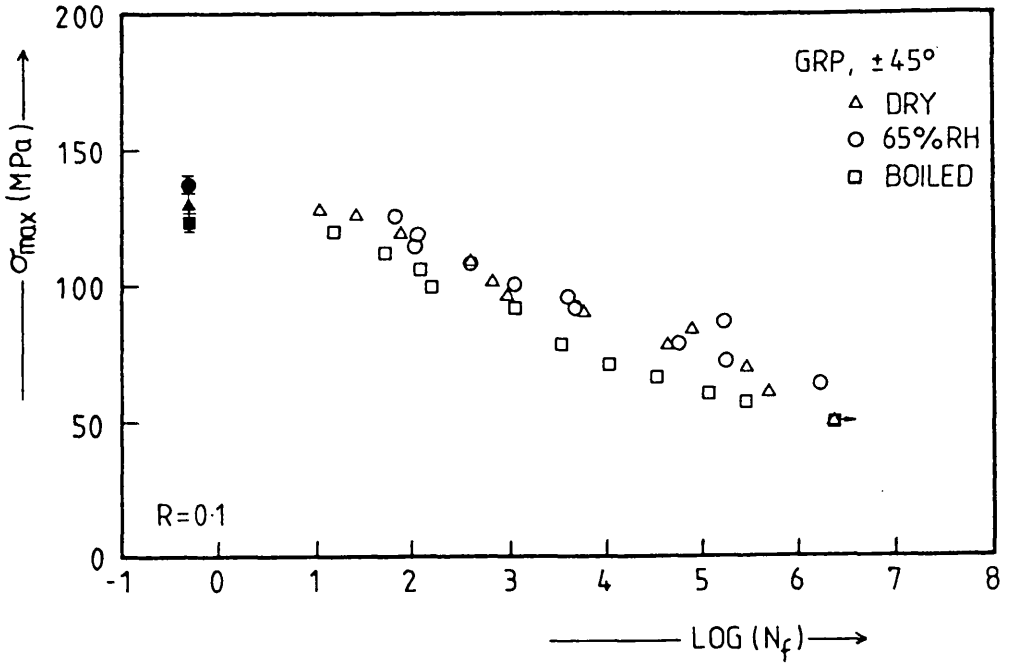

Figure 7.14 Tensile fatigue curves for ±45° GRP laminate, showing effects of preconditioning treatments (Loading rate = 25kNs^{-1}).
Filled symbols represent static tensile strengths measured at 25kNs^{-1}.

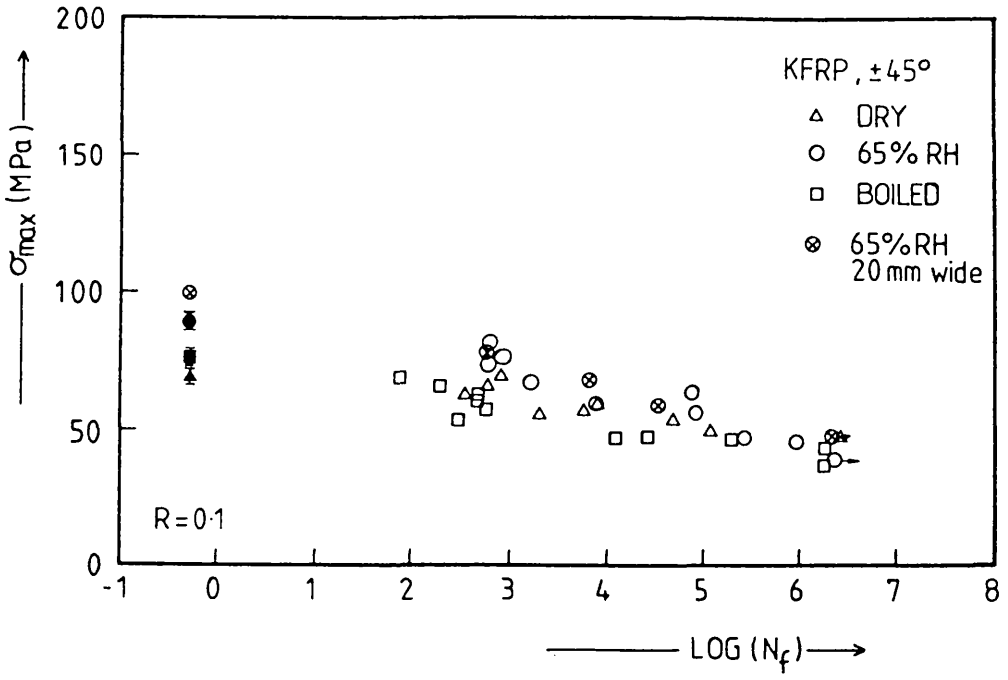

Figure 7.15 Tensile fatigue curves for ±45° KFRP laminate, showing effects of preconditioning treatments (Loading rate = 25kNs^{-1}). Filled symbols represent static tensile strengths measured at 25kNs^{-1}.

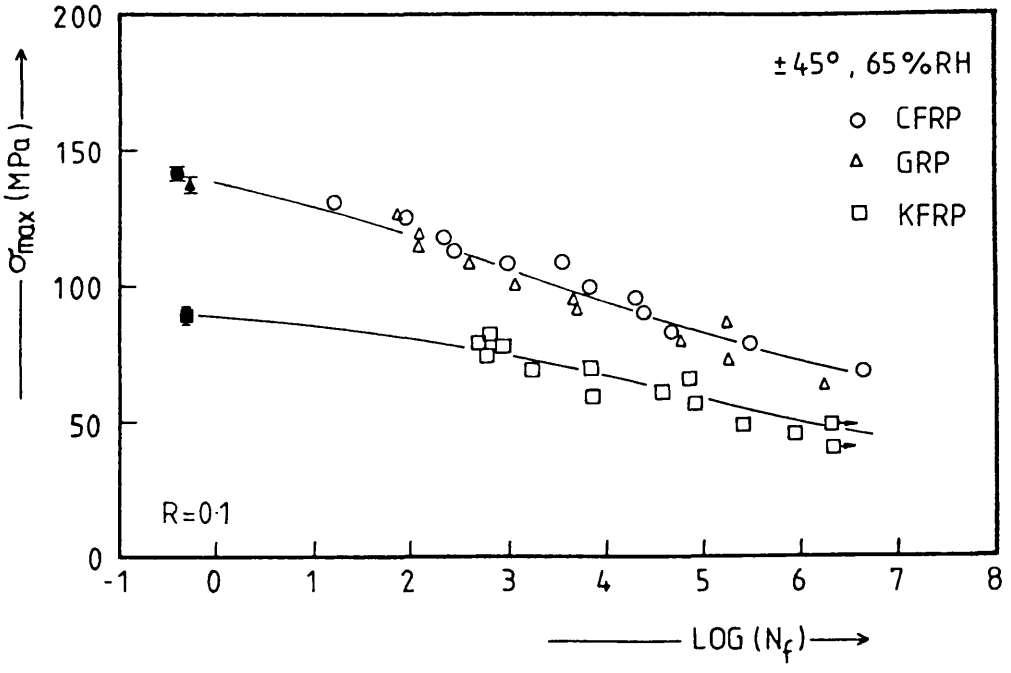

Figure 7.16 Comparison of the tensile fatigue curves for GRP, CFRP and KFRP laminates in the ±45° orientation (65%RH).

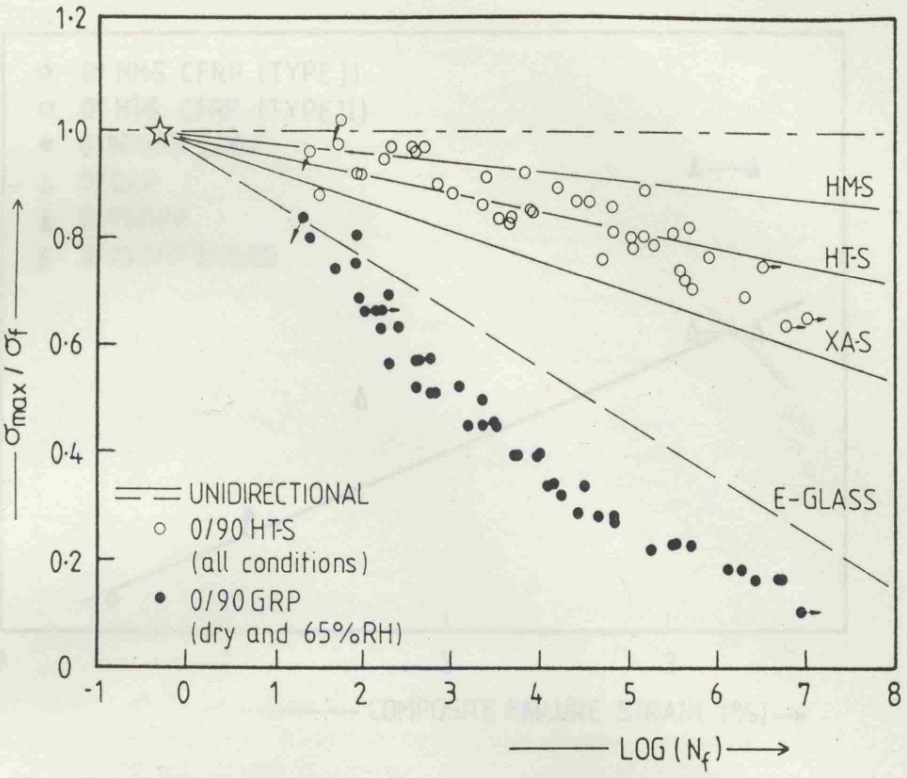

Figure 7.17 Comparison of normalised fatigue data for the 0/90 CFRP (all conditions, Figure 7.1b) and the 0/90 GRP (dry and 65% RH, Figure 7.4) with fatigue curves for unidirectional composites reinforced with HMS, HTS and XAS carbon fibres (from Sturgeon(93)) and with E-glass fibres (from Mandell (87)).

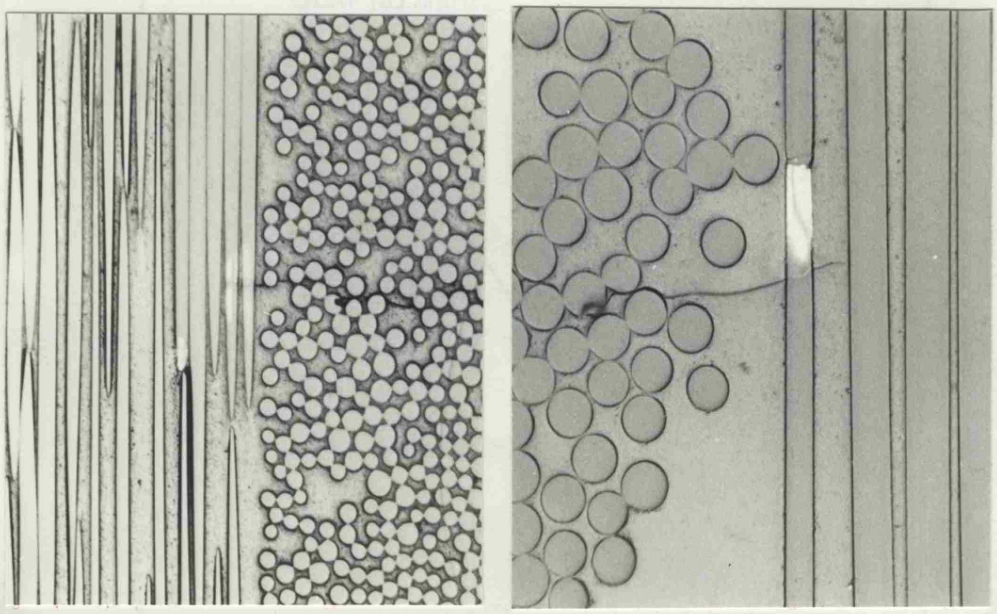

Figure 7.18 Micrographs of pre-fatigued 0/90 GRP in the 65%RH condition, showing damage induced in longitudinal plies at tips of transverse ply cracks. Specimen had sustained 10^3 cycles at a peak stress level of 0.4 GPa.

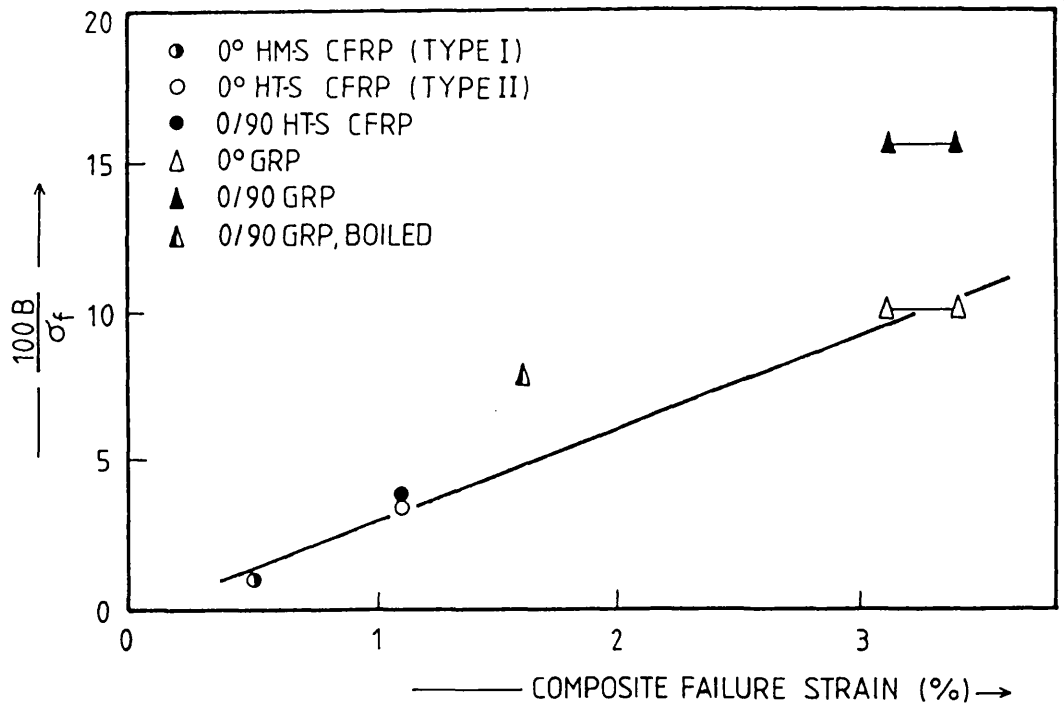

Figure 7.19 Normalised slopes to fatigue curves (B/σ_f) plotted against composite failure strain. All values are taken from Figure 7.17. Solid line indicates relationship for unidirectional composites.

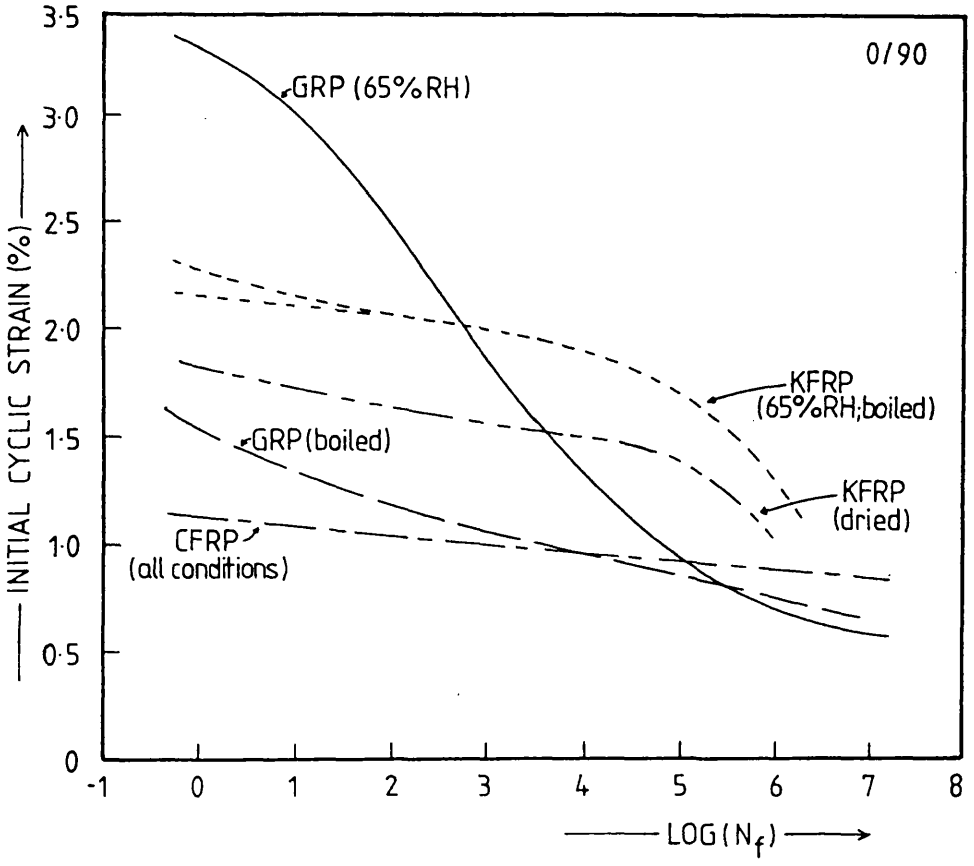

Figure 7.20 Fatigue results for the 0/90 laminates from earlier figures replotted in terms of initial cyclic strain versus log life.

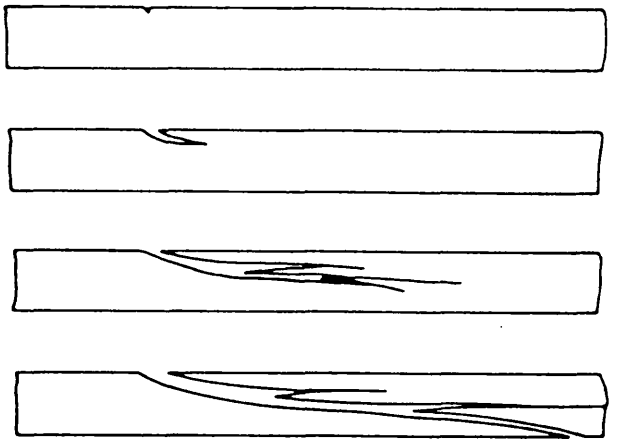

Figure 7.21 Schematic representation of simple tensile fracture development in Kevlar-49 fibres (after Konopasek and Hearle (20)).
Note the transverse dimensions are expanded for clarity: actual breaks extend over longer lengths relative to fibre diameter. Also, under fatigue loading, damage is more extensive and multiple splitting is associated with both halves of the broken fibre.

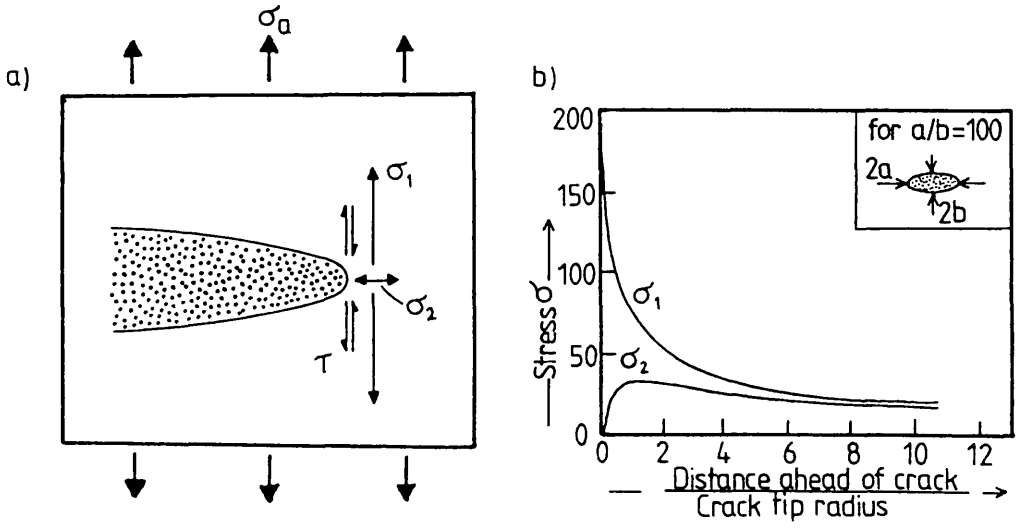

Figure 7.22 a) Schematic representation of stress system close to an elliptical crack in an elastic solid meeting a fibre interface (in response to a remotely applied uniaxial stress σ_a).

b) Tensile stress ahead of crack tip for $\sigma_a = 1$ (after Cook and Gordon (174)).

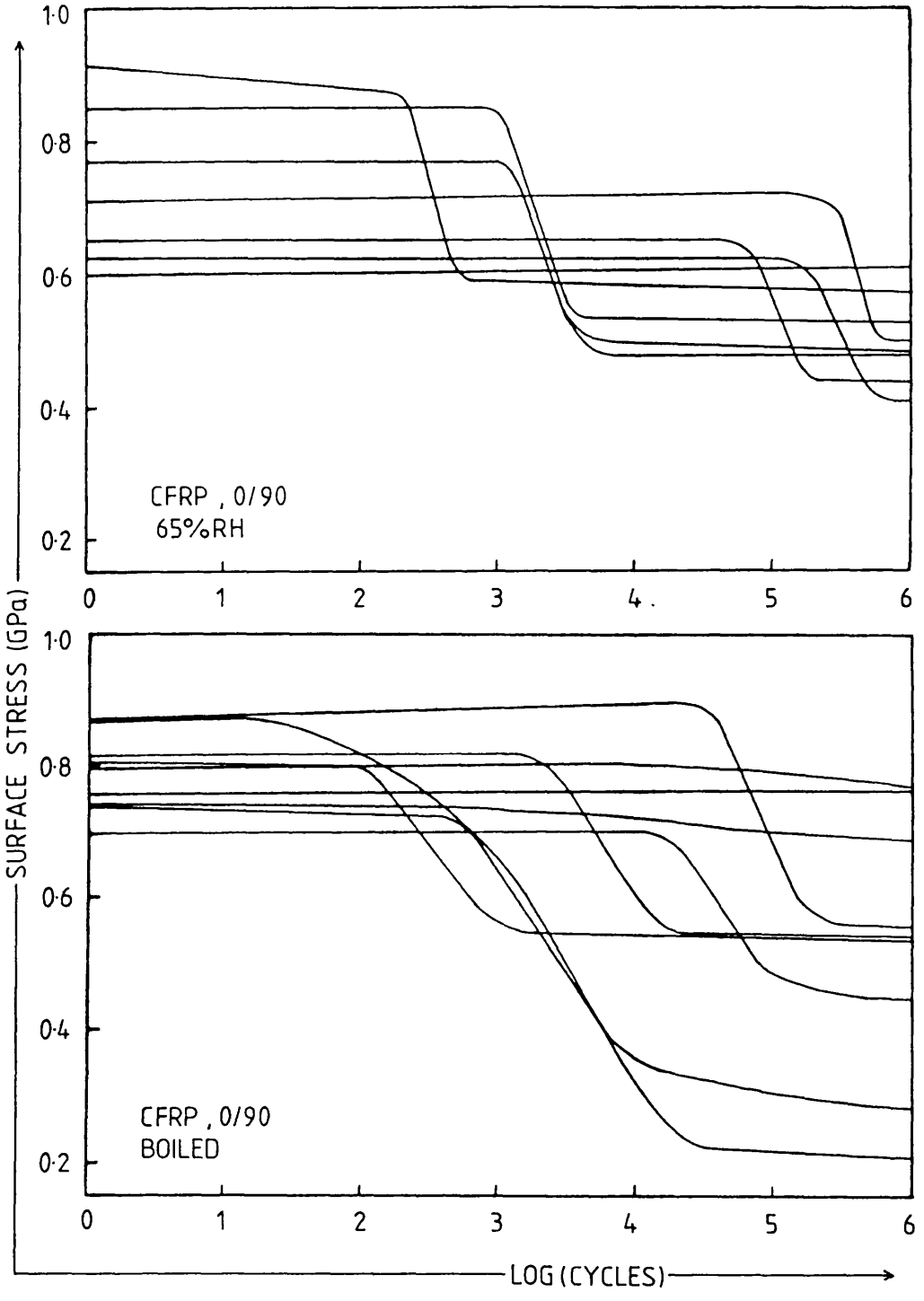

Figure 8.1 Change in flexural stiffness during cycling of 0/90 CFRP in repeated flexure.

a) 65% RH
b) Boiled.

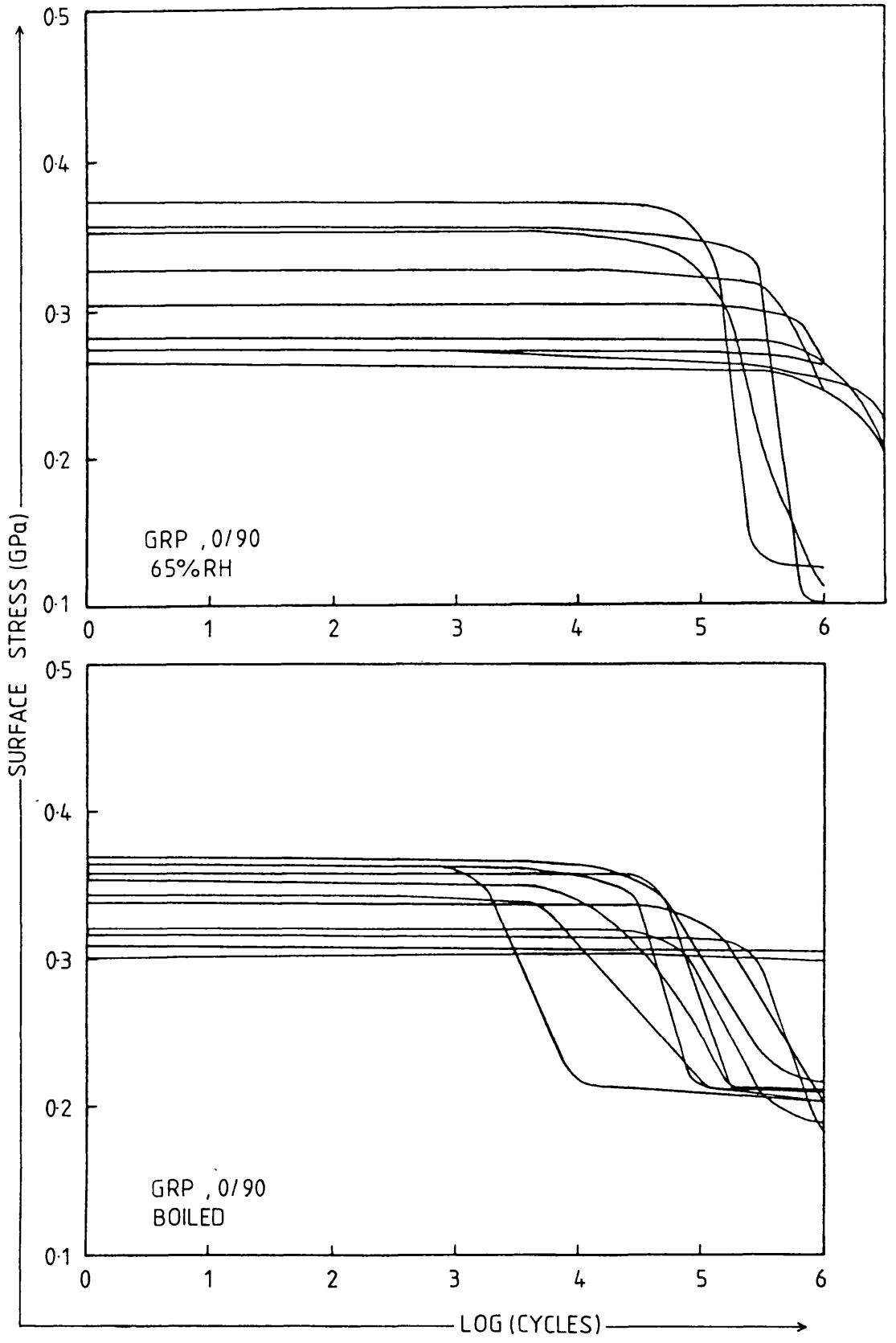

Figure 8.2 Change in stiffness during flexural cycling of 0/90 GRP.

a) 65% RH
b) Boiled

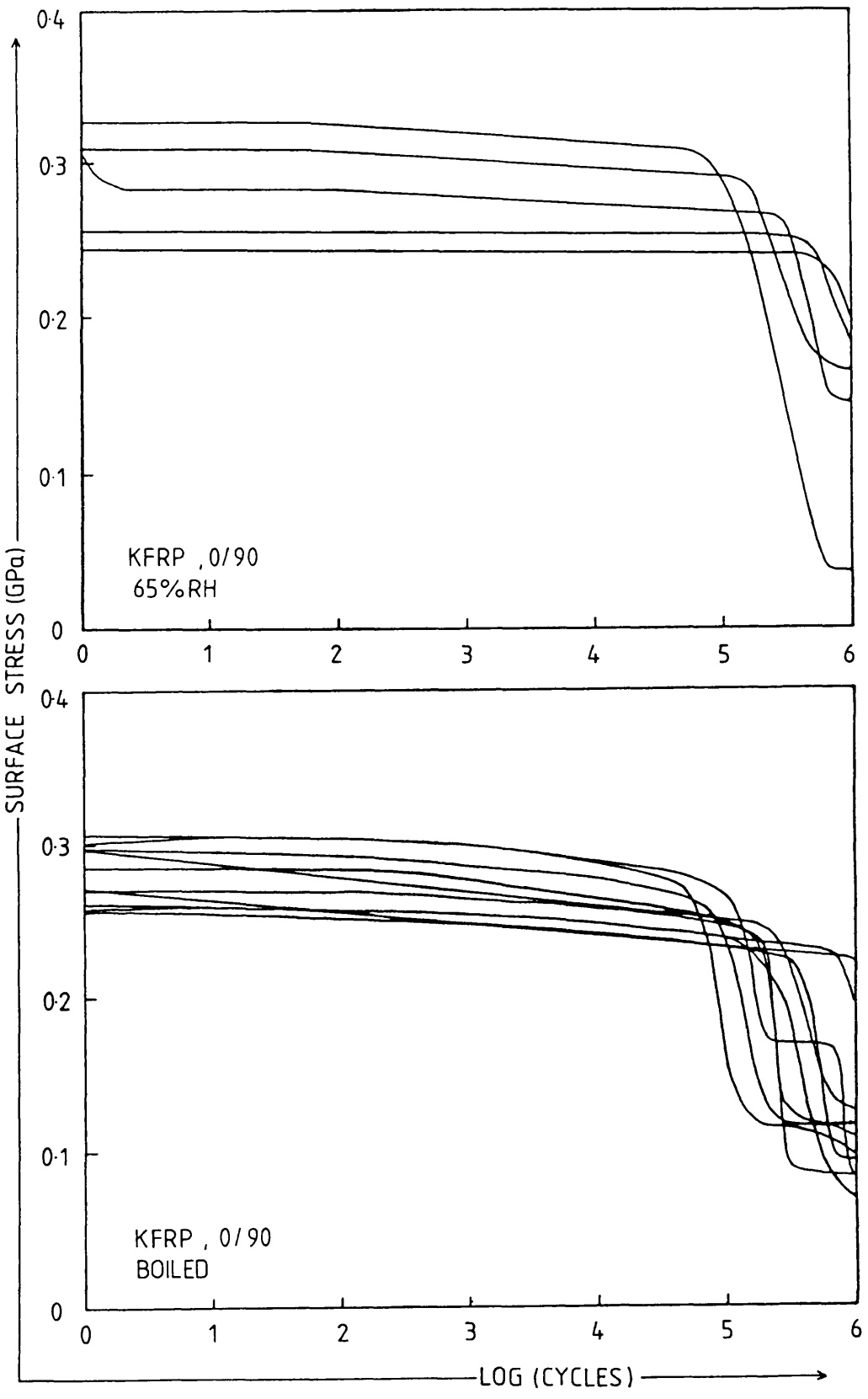

Figure 8.3 Change in stiffness during flexural cycling of 0/90 KFRP

a) 65% RH
b) Boiled.

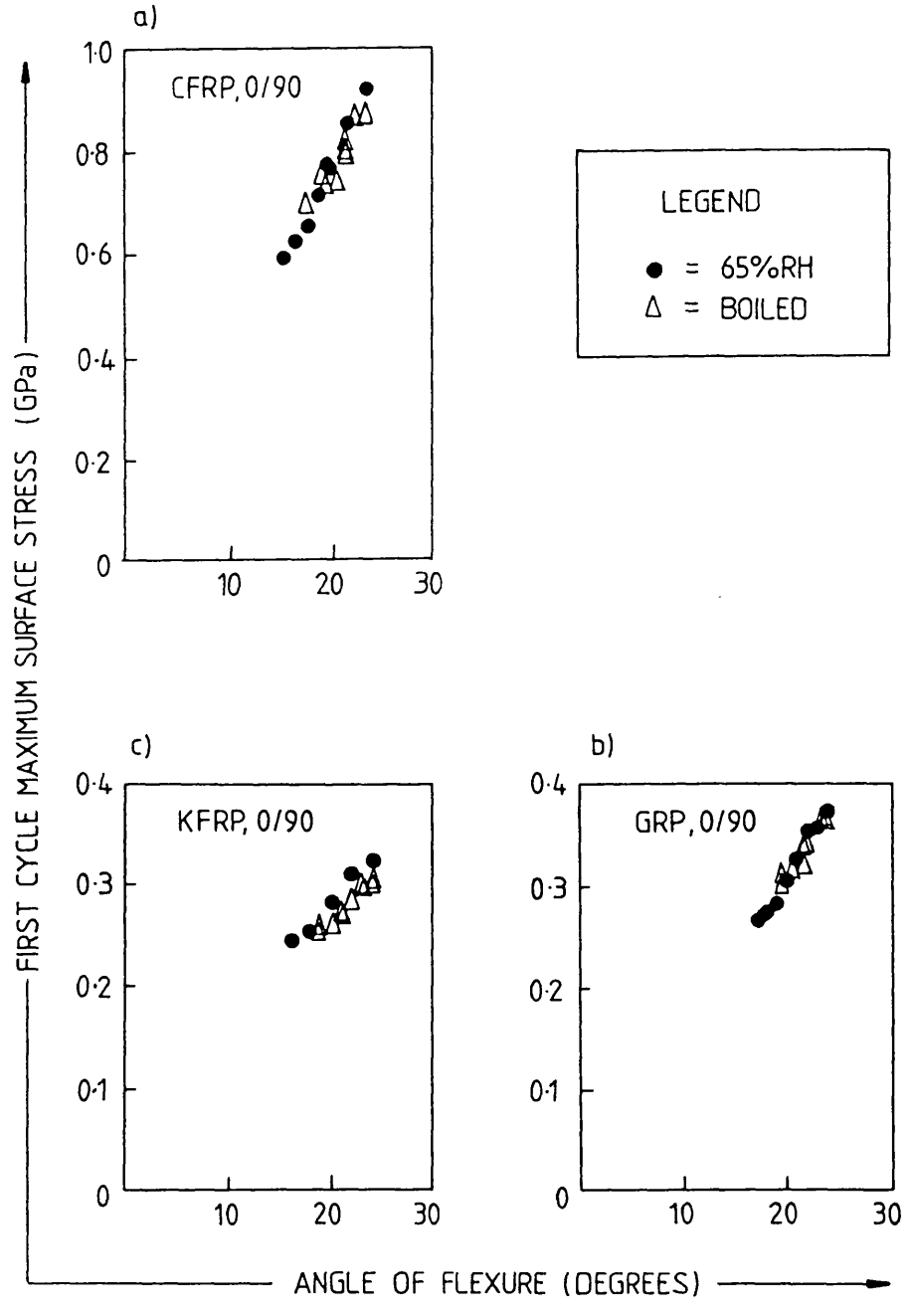

Figure 8.4 Effect of preconditioning treatments on the flexural stiffness of the 0/90 laminates.

a) CFRP
b) GRP
c) KFRP

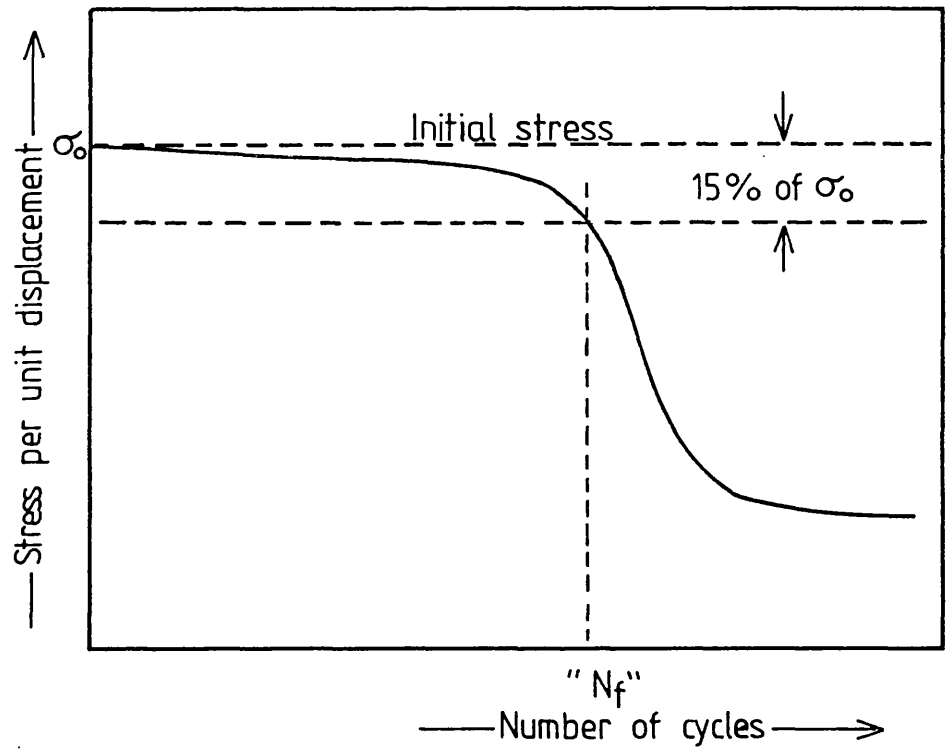

Figure 8.5 Schematic illustration of 'failure' criterion for laminates fatigue tested in flexure.

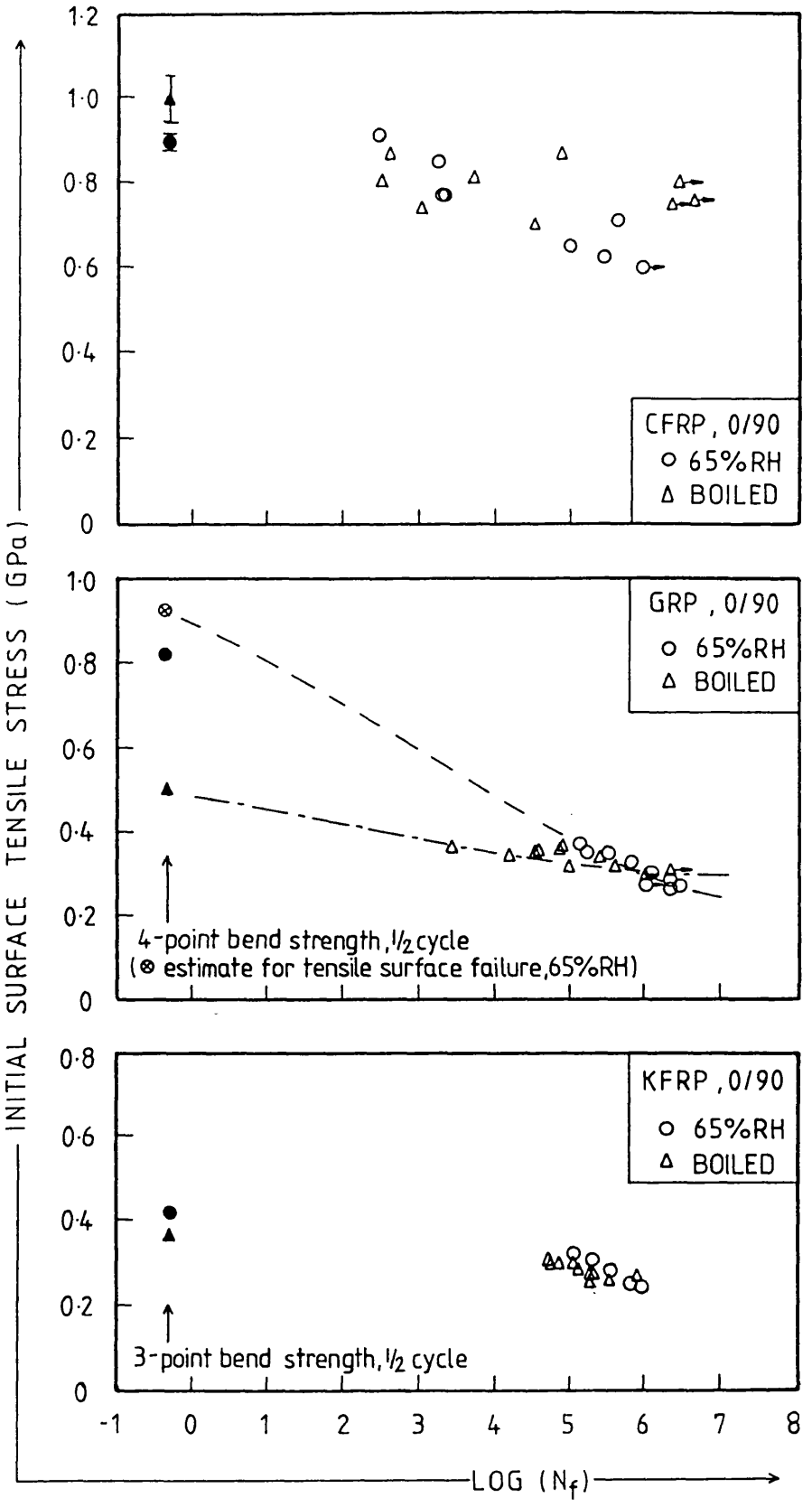

Figure 8.6 Flexural fatigue results for 0/90 laminates, showing effects of preconditioning treatments.

a) CFRP
b) GRP
c) KFRP

(only the CFRP exhibited single cycle failures in the Avery fatigue machine).

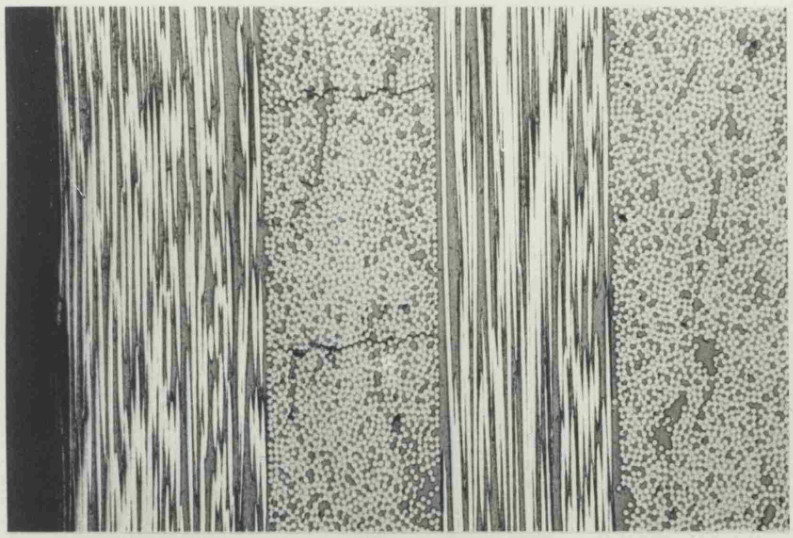

Figure 8.7 Transverse ply cracking near tensile surface of 0/90 CFRP in flexural fatigue.

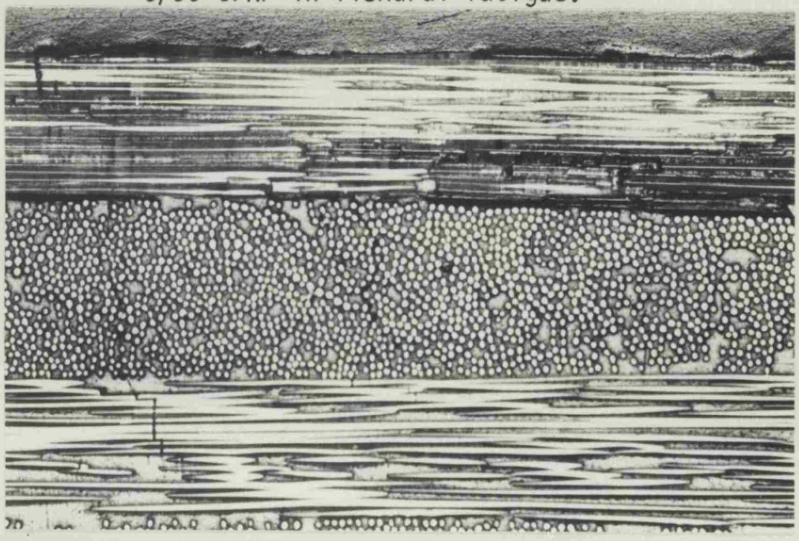

Figure 8.8 Tensile surface fatigue damage in 0/90 GRP under flexural loading.

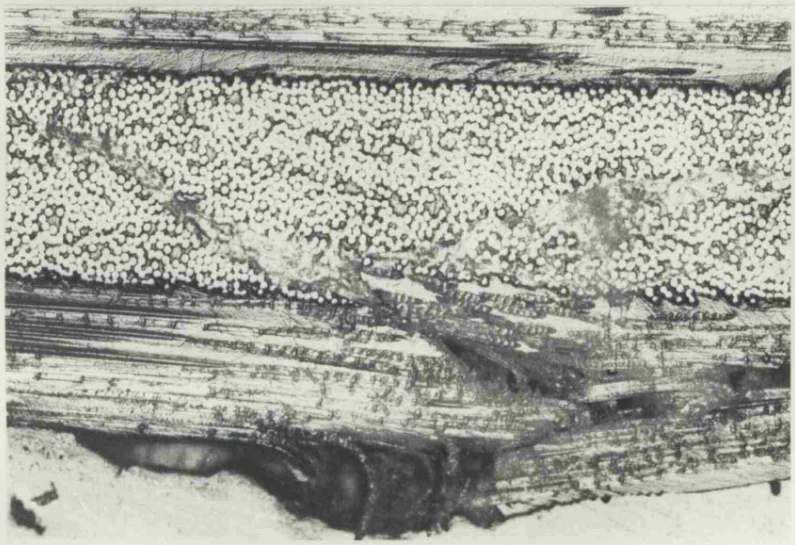

Figure 8.9 Compression surface failure of 0/90 KFRP in flexural fatigue.

Bath University Library

PHOTOCOPY APPLICATION

This form must be completed and signed for all photocopying done on Library equipment

---

Material to be Copied (If material is your own private material, write 'Private Papers')

Author and Title of Book OR *Title and Volume Number of Periodical*

Date of Publication ..... Page Numbers .....

Applicant's Name *School* *Address (External Readers only)*

Copyright Declaration

1. I have not previously been supplied with a copy of the above item.
2. I undertake that I shall not use this copy except for the purpose of research or private study.

Signature ..... Date .....

The signature **must** be the personal signature of the applicant. A stamp or the signature of an agent is **not** sufficient.

Office Use Only

Number of Prints *Total Price* *Finance Code*

Please do not Remove

26/10/88